PROCEEDINGS

OF THE

AMERICAN SOCIETY OF CIVIL ENGINEERS

VOL. 71 JUNE, 1945 No. 6

TECHNICAL PAPERS

AND

DISCUSSIONS

Published monthly, except July and August, at Prince and Lemon Streets, Lancaster, Pa., by the American Society of Civil Engineers. Editorial and General Offices at 33 West Thirty-ninth Street, New York, N. Y. Reprints from this publication may be made on condition that the full title of Paper, name of Author, page reference, and date of publication by the Society, are given.

Entered as Second-Class Matter, September 23, 1937, at the Post Office at Lancaster, Pa., under the Act of March 3, 1879. Acceptance for mailing at special rate of postage provided for in Section 1103, Act of October 3, 1917, authorized on July 5, 1918.

Subscription (if entered before January 1) $8.00 per annum. Price $1.00 per copy

Copyright, 1945, *by the* AMERICAN SOCIETY OF CIVIL ENGINEERS

Printed in the United States of America

	Published	Discussion closes
Gray, Hamilton. Simultaneous Consolidation of Contiguous Layers of Unlike Compressible Soils	Feb., 1944	
Discussion in June, Sept., 1944, June, 1945		Closed
Amster, Maurice N. Hydraulic Model Investigation of Miter Gate Operation	Mar., 1944	
Discussion in June, Sept., 1944, Mar., June, 1945		Closed
Krynine, D. P. Pressure on the Lining of Circular Tunnels in Plastic Soils	May, 1944	
Discussion in Sept., Dec., 1944, June, 1945		Closed
Foster, H. Alden. Construction of the Flow Net for Hydraulic Design	May, 1944	
Discussion in Jan., Mar., June, 1945		Closed
Wilbur, John B. Characteristic Redundants Used for Analyzing Statically Indeterminate Structures	June, 1944	
Discussion in Sept., Dec., 1944, Jan., May, June, 1945		Closed
Wilkinson, J. H. Translatory Waves in Natural Channels	June, 1944	
Discussion in Jan., Feb., June, 1945		Closed
Stewart, Ralph W. Amplified Slope Deflection	Sept., 1944	
Discussion in Nov., 1944, Feb., Mar., June, 1945		Closed
Vanoni, Vito A. Transportation of Suspended Sediment by Water	June, 1944	
Discussion in Dec., 1944, Feb., Mar., June, 1945		Closed*
Moorman, Robert B. B. Wedge-Shaped Structural Members Under Direct Stress and Bending	June, 1944	
Discussion in Oct., 1944, Jan., Mar., Apr., 1945		Closed*
Terzaghi, Karl. Stability and Stiffness of Cellular Cofferdams	Sept., 1944	
Discussion in Dec., 1944, Feb., Mar., Apr., May, June, 1945		Closed
Ahlf, August L. Design Constants for Beams with Nonsymmetrical Straight Haunches	Oct., 1944	
Discussion in Apr., June, 1945		Closed
Soucek, Edward, and Zelnick, E. W. Lock Manifold Experiments	Oct., 1944	
Discussion in Mar., Apr., May, June, 1945		Closed
Symposium: Concentration of Sewage Sludge	Oct., 1944	
Discussion in Apr., 1945		Closed*
Hickox, G. H. Evaporation from a Free Water Surface	Oct., 1944	
Discussion in Feb., Mar., Apr., May, 1945		Closed*
Bull, Anders. Stresses in the Linings of Shield-Driven Tunnels	Nov., 1944	
Discussion in Jan., Feb., May, June, 1945		Aug., 1, 1945
Johnson, Lee H., Jr. Analysis of Statically Indeterminate Structures Using Reduced Equations	Nov., 1944	
Discussion in Feb., May, June, 1945		Aug., 1, 1945
Kalinske, A. A. Conversion of Kinetic to Potential Energy in Flow Expansions	Dec., 1944	
Discussion in Feb., May, June, 1945		Aug. 1, 1945
Osgood, William R. Column Formulas	Dec., 1944	
Discussion in Feb., Mar., May, June, 1945		Aug, 1, 1945
Blanks, R. F., and Meissner, H. S. Deterioration of Concrete Dams Due to Alkali-Aggregate Reaction	Jan., 1945	Sept. 1, 1945
DeYoung, Isaac. A Plan for a Movable Dam	Feb., 1945	
Discussion in May, June, 1945		Aug. 1, 1945
Report: Organization, Financing, and Administration of Sanitary Districts: Progress Report of the Committee of the Sanitary Engineering Division	Feb., 1945	
Discussion in May, June, 1945		Aug. 1, 1945
Powell, Ralph W. Flow in a Channel of Definite Roughness	Dec., 1944	
Discussion in June, 1945		Sept. 1, 1945
Bennett, Preston T. The Effect of Blankets on Seepage Through Pervious Foundations	Jan., 1945	
Discussion in Mar., Apr., June, 1945		Sept. 1, 1945
Conkling, Harold. Utilization of Ground-Water Storage in Stream System Development	Jan., 1945	
Discussion in Mar., Apr., May, June, 1945		Sept. 1, 1945
Weiss, Camillo. Interrelation of Certain Structural Concepts	Jan., 1945	
Discussion in May, June, 1945		Aug. 1, 1945
Bakhmeteff, Boris A., and Allan, William. The Mechanism of Energy Loss in Fluid Friction	Feb., 1945	Sept. 1, 1945
Hayes, Harry. Elimination of Cross Connections in Los Angeles, Calif	Mar., 1945	
Discussion in May, 1945		Sept. 1, 1945
Eliel, Leon T. Economics of Photogrammetry	Mar., 1945	
Discussion in June, 1945		Sept. 1, 1945
Nelidov, I. M. Determination of Pressures within a Siphon Spillway	Mar., 1945	Sept. 1, 1945
Genter, A. L. Computing Coagulant Requirements in Sludge Conditioning	Mar., 1945	
Discussion in June, 1945		Sept. 1, 1945
Mullis, Ira B. Design of Roadbeds	Apr., 1945	Sept. 1, 1945
Harrold, Lloyd L. Flow from Drainage Basins Determined by Short-Term Records	Apr., 1945	Sept. 1, 1945
Camp, Thomas R. Sedimentation and the Design of Settling Tanks	Apr., 1945	Sept. 1, 1945
Stevens, J. C. Future of Lake Mead and Elephant Butte Reservoir	May, 1945	Oct. 1, 1945
Brumfield, R. C. Moving Loads on Restrained Beams and Frames	May, 1945	Oct. 1, 1945
Eichler, John Oran, and Eves, Howard W. Mathematical Examination of the Highway Transition Spiral	May, 1945	Oct. 1, 1945
Report: Water Supply Engineering: Report of the Committee of the Sanitary Engineering Division for the Two Years Ending December 31, 1944	May, 1945	Oct. 1, 1945

NOTE.—The closing dates herein published are final except when names of prospective discussers are registered for special extension of time.

* Publication of closing discussion pending.

CONTENTS FOR JUNE, 1945

PAPERS

PAGE

Effects of Radiant Heat on Reinforced-Concrete Rigid Frames.
By Milan A. Johnston 793

Structural Skew Plates.
By F. L. Ehasz 805

Correlating Flood Control and Water Supply, Los Angeles Coastal Plain.
By Finley B. Laverty 831

DISCUSSIONS

Pressure on the Lining of Circular Tunnels in Plastic Soils.
By D. P. Krynine 849

Design Constants for Beams with Nonsymmetrical Straight Haunches.
By August L. Ahlf 858

Construction of the Flow Net for Hydraulic Design.
By H. Alden Foster 863

Transportation of Suspended Sediment by Water.
By Paul F. Nemenyi 865

Characteristic Redundants Used for Analyzing Statically Indeterminate Structures.
By John B. Wilbur 875

Translatory Waves in Natural Channels.
By J. H. Wilkinson 879

Amplified Slope Deflection.
By A. A. Eremin, and Ralph W. Stewart 881

Stresses in the Linings of Shield-Driven Tunnels.
By Leon Beskin, and D. P. Krynine 885

The Effect of Blankets on Seepage through Pervious Foundations.
By Harry R. Cedergren 897

Utilization of Ground-Water Storage in Stream System Development.
By Irving B. Crosby 902

Economics of Photogrammetry.
By Raymond A. Hill, Raymond L. Moore, and Ralph S. Pearse 907

Interrelation of Certain Structural Concepts.
By Max W. Strauss 916

CONTENTS FOR JUNE, 1945 (*Continued*)

PAGE

Column Formulas.
By Leon Beskin 921

Computing Coagulant Requirements in Sludge Conditioning.
By Paul D. McNamee 926

Organization, Financing, and Administration of Sanitary Districts: Progress Report of the Committee of the Sanitary Engineering Division.
By I. Vernon Werbin 929

A Plan for a Movable Dam.
By Jay L. Southworth 931

Analysis of Statically Indeterminate Structures Using Reduced Equations.
By Jaroslav Polivka 933

Hydraulic Model Investigation of Miter Gate Operation.
By Maurice N. Amster 935

Lock Manifold Experiments.
By Ralph W. Powell, and Edward Soucek and E. W. Zelnick 941

Flow in a Channel of Definite Roughness.
By Joe W. Johnson and E. A. LeRoux 948

Simultaneous Consolidation of Contiguous Layers of Unlike Compressible Soils.
By Hamilton Gray 954

Conversion of Kinetic to Potential Energy in Flow Expansions.
By Boris A. Bakhmeteff, and E. R. Van Driest 959

Stability and Stiffness of Cellular Cofferdams.
By Robert F. Legget, D. P. Krynine, J. J. Polivka, and Karl Terzaghi 966

A list of "Current Papers and Discussions" may be found on the page preceding the table of contents

The Society is not responsible for any statement made or opinion expressed in its publications

HINTS TO AUTHORS

Those who are planning papers for submission to PROCEEDINGS *will expedite Committee action measurably by first studying the standard instructions as to style, content, and format. For reprints, address the Secretary, Committee on Publications, 33 W. 39th St., New York 18, N. Y.*

AMERICAN SOCIETY OF CIVIL ENGINEERS

Founded November 5, 1852

PAPERS

EFFECTS OF RADIANT HEAT ON REINFORCED-CONCRETE RIGID FRAMES

BY MILAN A. JOHNSTON,[1] JUN. AM. SOC. C. E.

SYNOPSIS

The reinforced-concrete rigid frame is subjected to two types of temperature stresses: (1) Those resulting from long-range, or seasonal, temperature changes, and (2) those resulting from the radiant heat of the sun.

The method of determining stresses caused by seasonal temperature changes has been well established, although designers differ in opinion as to the importance of these changes. The purpose of this paper is to present an analytical method of finding the moments at the knee and crown of a reinforced-concrete rigid frame subjected to the second type of temperature change—namely, that caused by radiant heat from the sun. In order to present numerical computations for a structure of known cross section, a two-span rigid frame highway bridge, previously designed for H-20 loading, was used. A rigid frame was selected because of the increasing popularity of this type of structure for railroad and highway grade-separation projects.

Analysis shows that the radiant-heat moment at the crown of the specific frame used is equal to 35.5% of the maximum design moment. This moment is reduced somewhat because the deck is probably elongating due to the rise in seasonal temperature on the days when radiant heat causes the greatest effect. Main longitudinal steel in the crown for the purpose of resisting the effects of a seasonal temperature drop is also available for the radiant-heat stresses.

INTRODUCTION

In the future there should be a marked increase in the number of long-span rigid frames built as a feature of superhighway grade separation. Consequently, the secondary effects of temperature will become more important in

NOTE.—Written comments are invited for immediate publication; to insure publication the last discussion should be submitted by November 1, 1945.

[1] Instr., Univ. of Minnesota, Eng. Experimental Station, Minneapolis, Minn.

their design, especially as the spans become longer. Many designers now include in their design of reinforced-concrete rigid frames the secondary effects of temperature change, shrinkage, and settlement of footings.

The present temperature specifications, whenever used in the design of indeterminate structures, refer to the axial strains caused by long-range or seasonal temperature variation. These unit strains, although not necessarily uniformly distributed over a cross section, will be symmetrical about the neutral axis as long as the difference in air temperature causes the strains. Hence, maximum axial deformations will occur roughly in half-year cycles.

Methods of analyzing the stresses due to seasonal temperature changes are well established, but the authorities responsible for design specifications among the various states differ in opinion as to the importance of these changes. (Questionnaire data collected by D. H. Pletta, and loaned to the writer, show this to be true among state highway departments.[2]) This difference of opinion is not surprising in view of the many variables present in temperature design.

For example, some designers rely on low allowable unit stress for the primary loads to provide additional safety from secondary effects. They also realize that any strains due to extreme temperature changes during the early period of the structure are modified by plastic flow. The data collected by Captain Pletta[2] showed that most of the states having mild climates, with a small mean temperature difference between January and July, either disregarded temperature changes or provided very little plus and minus temperature change from some mean value. As an exception to this, some of the states with mild climates provided nearly twice the plus and minus temperature change of states having much greater mean temperature difference between January and July.

Closely allied with seasonal temperature changes is the effect of radiant heat on rigid frames. This paper will be limited to the analysis of stresses caused by radiant heat not only to illustrate a method of analyzing a more complex type of temperature change, but to emphasize the need for more uniform seasonal temperature specifications in the milder states where radiant heat has its greatest effect.

Some work already has been done in Europe on variable temperature change in rigid frames,[3,4] but, as far as the writer knows, this is the first time such a method has been offered for publication in the United States. According to tests made by the Swiss Government on fifty reinforced-concrete rigid frames built between 1924 and 1927, variable temperature change has no damaging effects on frames properly designed and built, even though variable temperature change was neglected in the design.

The Effect of Radiant Heat

Differential temperature strain, most frequently caused by radiant heat from the sun, occurs because the temperature of the top surface of the deck

[2] "Notes on Existing Rigid Frames in the United States," by D. H. Pletta, *Journal*, A.C.I., March-April, 1938, p. 517.

[3] "Die Neuern Methoden der Festigkeitslehre und der Statik der Baukonstruktionen," by Heinrich Mueller-Breslau, 5 durchges aufl., A. Kröner, Leipzig, 1924.

[4] "Ueber das Elastische Verhaulten von Eisenbetonrahmen unter dem Einfluss Ungleicher Erwaermung," by Adolf Eppler, St.: Wittwer, 1932.

is relatively higher than that of the bottom surface. An experiment conducted in 1941 and 1942 by the Minnesota State Highway Department[5] showed that the surface temperature of a concrete slab is sometimes raised 30° F above the air temperature because of radiant heat. Investigations conducted in states with warmer year-round climates would probably show even higher relative surface temperatures. This difference in temperature tends to elongate the upper fibers and cause the deck to bulge upward. In the basic, or simply supported, beam this bowing effect causes angular rotations at the supports as shown in Fig. 1. In a rigid frame, where the ends are restrained, this end rotation is subdued by the resisting moments at the knees, causing fiber stresses in all the members. Furthermore, the bridge is subjected to these stresses in short cycles—once every clear, hot summer day.

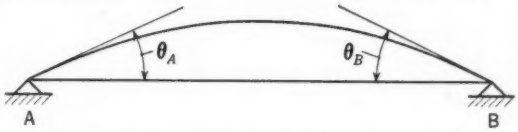

FIG. 1.—END ROTATIONS IN THE BASIC BEAM CAUSED BY THE HEAT OF RADIATION

Increase in the temperature of any surface above the air temperature depends on many factors—such as the intensity of the sun, the angle between the surface and the sun, the quantity of heat reflected back into the air, the wind velocity, etc. A theoretical calculation of the surface temperature rise necessarily must take into account so many assumptions and variables that it would not only be approximate but impracticable. Therefore, the surface temperatures used in the following analysis are taken from actual readings (original data) made on a comparable surface August 18 and 19, 1941, at Minneapolis, Minn.[6]

General Procedure and Tools of Analysis

Stresses due to strain in a statically indeterminate structure can be investigated only by the analysis of a specific structure. A rigid frame structure with two spans of 80 ft each, designed for an H-20 live loading, was selected. This particular selection was made because of the increasing popularity of this type of structure for grade-separation projects and because it was relatively long, since the magnitude of temperature stresses increases with length.

Details of the rigid frame are shown in Fig. 2. The deck has been divided into segments, each with a length Δs, for use in the angular rotation equation:

$$\theta = \sum \frac{M \, \Delta s}{E \, I} \quad \ldots\ldots\ldots\ldots\ldots\ldots\ldots\ldots (1)$$

The general procedure for finding the moments at the knee and crown due to radiant heat is as follows:

1. Find the distribution of the differential temperature strain on a cross section of the deck (a method for doing this is presented under the heading, "Numerical Example");

[5] "Temperature and Moisture Variations in Concrete Pavements," *Investigation 132*, Minnesota Dept. of Highways, Div. of Materials and Research, 1941–1942.

[6] "Heat Transmission Through Insulation as Affected by Orientation of Wall," by Frank B. Rowley and C. E. Lund, *Technical Paper No. 44*, Univ. of Minnesota Eng. Experiment Station, Minneapolis, Minn., 1943.

2. Compute the angle change caused by temperature strain for as many sections as necessary to develop an angle-change loading equation for the entire deck;

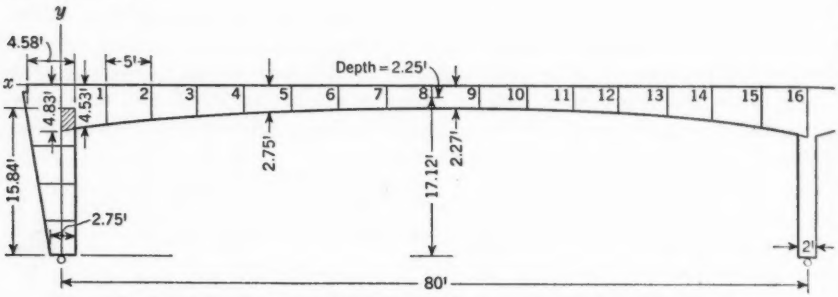

FIG. 2.—DETAILS OF THE RIGID FRAME USED IN THE NUMERICAL EXAMPLE

3. Load a 1-ft increment of deck with the angle change and compute the end rotations, assuming the deck to be simply supported;

4. Load a 1-ft increment of deck with the $\frac{M}{E\,I}$-diagram and find the end-rotation equation in terms of $M/E\,I$, assuming the deck to be simply supported;

5. Since there is no end rotation in a beam with fixed ends, equate steps 3 and 4 to find the fixed-end moment M; and

6. By the method of moment distribution, find the final or true moments in the rigid frame.

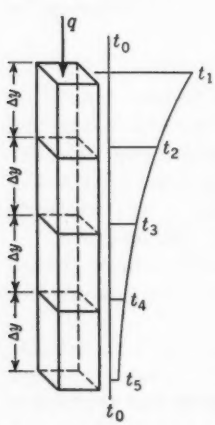

FIG. 3.—INDEPENDENT PRISM METHOD OF TRACING THE RADIANT TEMPERATURE RISE THROUGH A SLAB

Notation.—The letter symbols used in this paper conform essentially to American Standard Letter Symbols for Heat and Thermodynamics Including Heat Flow (ASA—Z10.4—1943), American Standard Letter Symbols for Mechanics of Solid Bodies (ASA—Z10.3—1942), and American Standard Letter Symbols for Mechanics, Structural Engineering and Testing Materials (ASA—Z10a—1932)—each compiled by Committees of the American Standards Association, with Society representation.

NUMERICAL EXAMPLE

Step 1. Distribution of Temperature Strains on the Cross Section of the Rigid Frame Deck.—For this step, use is made of a method of tracing heat flow through a solid body presented in 1937 by R. W. Carlson,[7] Assoc. M. Am. Soc. C. E. Mr. Carlson divides the body into independent prisms of unit cross-sectional area as shown in Fig. 3. This method was modified by the writer especially to analyze the problem of tracing temperature throughout the depth of a slab if the quantity of heat q entering at the surface

[7] "A Simple Method for the Computation of Temperatures in Concrete Structures," by Roy W. Carlson, *Journal*, A.C.I., November-December, 1937, pp. 89–102.

is known.[8] Only the general features of Mr. Carlson's method are explained in the first step, as the development of this method with subsequent numerical computations of the modified method is much too long to include in this paper.

Let t denote temperature in degrees Fahrenheit, t_0 being the initial temperature at the top surface of the slab. In Fig. 3, the subscripts 1, 2, 3, 4, and 5 denote the readings at corresponding temperature stations (spaced at depths Δy) after the first hour of radiant heat applied at the surface. Each station is considered to be the center of a volume of concrete extending halfway to each adjacent station. Since the cross-sectional area of each prism is equal to unity, the volume of the concrete (or prism) between each station is numerically equal to the distance Δy between stations.

It is assumed that the heat flow is in one direction only and that the temperatures of the deck and the air are the same at the beginning of the first hour of heat flow computations. The temperature change per hour at each station is equal to the average quantity of heat entering, and the average quantity of heat leaving, a volume during each hour. The quantity of heat entering and leaving each station depends upon the heat capacity of each volume in British Thermal Units (Btu) and the conductivity of concrete in Btu per hour per degree Fahrenheit.

The thermal diffusivity, which is the relation between heat conduction and the rate of temperature change, is equal to $\frac{k}{c\,\rho}$, in which k is the conductivity of concrete in Btu per hour per degree Fahrenheit, c is the specific heat per unit of weight, and ρ is the density of the concrete. For the numerical computations of heat flow through the slab the term $\frac{k}{c\,\rho}$ was taken as 1.00 sq ft per day.

The temperature distribution was computed for sections 1, 5, and 9 (Fig. 2), the results for sections 1 and 9 being shown in Fig. 4. The hourly surface temperatures were taken from actual readings on a concrete surface.[6] The temperature flow was computed on the basis of the method and assumptions stated previously.

Step 2. Angle Change Caused by Temperature Strain Distribution.—The strain on each fiber of the cross section is taken as equal to

$$\epsilon = \alpha\,\Delta t_f \qquad (2)$$

in which α is the coefficient of thermal expansion of concrete, and Δt_f is the temperature change of each fiber in degrees Fahrenheit. The temperature distribution shown in Fig. 4 will also represent the strain distribution multiplied by $1/\alpha$. It can be seen from these curves that the temperature or strain distribution does not vary as a straight line. Furthermore, the strains are present only in the first foot or so of the slab depth. Angle-change computations are simplified with slight error by approximating a straight-line strain distribution as shown by the heavy dashed line in Fig. 4.

[8] "The Effect of Temperature Stresses in a Reinforced Rigid Concrete Frame," by Milan A. Johnston, thesis submitted to Univ. of Minnesota, Minneapolis, Minn., in 1942 in partial fulfilment of the requirements for the degree of Master of Science, pp. 20–27.

Fig. 5(*a*) shows a single unrestrained section with temperature strains drawn in solid lines. The adjoining section is shown as a dashed line, having been rotated to touch the top and the bottom of the unrestrained section.

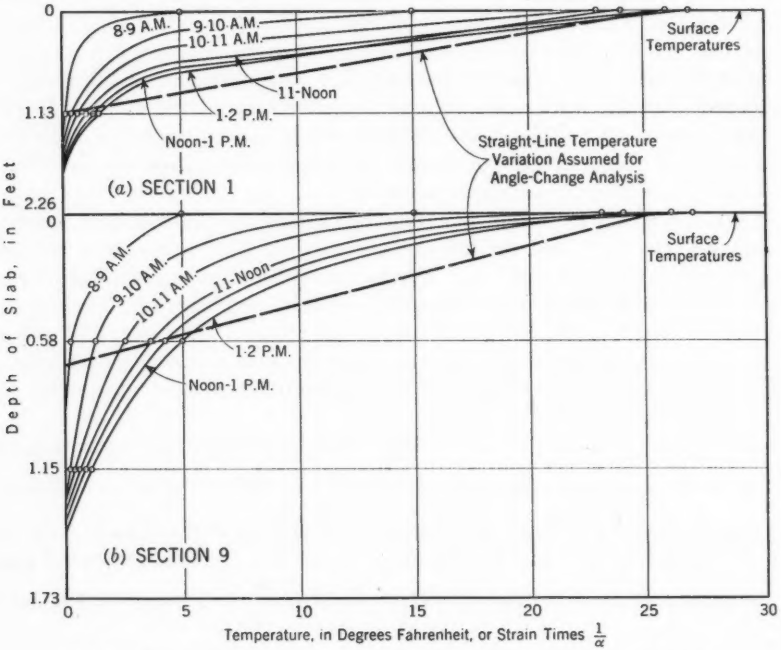

FIG. 4.—HOURLY TEMPERATURE RISE THROUGH GIVEN SECTIONS OF THE DECK, DUE TO THE HEAT OF RADIATION

Since the surfaces or adjoining sections must actually be in continuous contact, and assuming that "a plane before bending remains plane after bending," it is necessary to continue the movement of both surfaces until all the boundaries meet between top and bottom of the section. This has been done in Fig. 5(*b*).

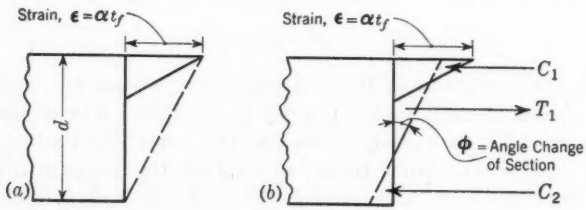

FIG. 5

The final position of the dashed line in Fig. 5(*b*) must be such that the summation of the horizontal forces and moments on the section is zero (ΣH and $\Sigma M = 0$; and also assuming that stress is proportional to strain). The movement of the surfaces to their final position (dashed line in Fig. 5(*b*)) will produce

compressive forces C_1 and C_2 and a tensile force T_1. Since an algebraic solution for the final position of the section yields cumbersome equations, a semigraphic trial solution is used. This method is shown in Table 1, numerical computation being by slide rule.

TABLE 1.—SEMIGRAPHICAL TRIAL SOLUTION FOR ANGLE CHANGES AT A GIVEN SECTION OF DECK

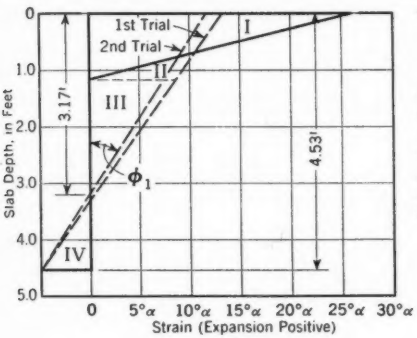

SECTION 1

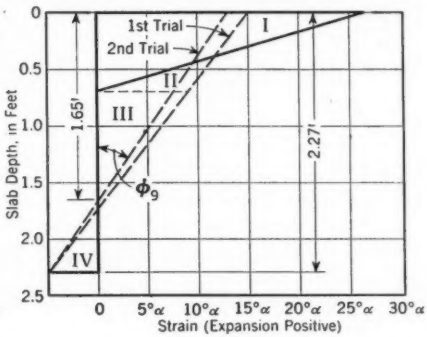

SECTION 9

Area	Section 1				Section 9			
	Computation	H	Arm	Moment	Computation	H	Arm	Moment
	First Trials							
I	13 ×0.69 ×0.5	−4.49	4.29	−19.25	11.8 ×0.40 ×0.5	−2.36	2.17	−5.13
II	8.5 ×0.47 ×0.5	2.00	3.52	7.04	9.1 ×0.30 ×0.5	1.36	1.70	2.31
III	8.5 ×2.10 ×0.5	8.92	2.69	24.00	9.1 ×1.04 ×0.5	4.73	1.25	5.91
IV	5.0 ×1.27 ×0.5	−3.18	0.42	−1.34	5.0 ×0.53 ×0.5	−1.33	0.19	−0.25
...	ΣH = 10.92 −7.67	+3.25[a]	....	....	ΣH = +6.09 −3.69	+2.40[a]	....	....
...	ΣM = +31.04 −20.59	....	....	+10.45[a]	ΣM = +8.22 −5.38	....	....	+2.84[a]
	Second Trials							
I	14.4 ×0.77 ×0.5	−5.54	4.27	−23.60	13.3 ×0.46 ×0.5	−3.06	2.14	−6.55
II	7.4 ×0.39 ×0.5	1.44	3.51	5.05	7.7 ×0.24 ×0.5	0.92	1.68	1.55
III	7.4 ×2.01 ×0.5	7.44	2.68	19.95	7.7 ×0.95 ×0.5	3.66	1.28	4.69
IV	5.0 ×1.36 ×0.5	−3.40	0.44	− 1.50	5.0 ×0.62 ×0.5	−1.55	0.217	−0.34
...	ΣH = −8.94 +8.88	−0.06[a]	....	....	ΣH = −4.61 +4.58	−0.03[a]	....	....
...	ΣM = −25.10 +25.00	....	....	− 0.10[a]	ΣM = −6.89 +6.24	....	....	−0.65[a]

[a] Unsatisfactory in the first trials but satisfactory in the second trials.

Assuming the coefficient of thermal expansion of concrete $\alpha = 0.0000065$, the angle change at the center line of section 1 of the rigid frame (see Fig. 2) is $\phi_1 = \dfrac{0.0000065 \times 11.6°}{3.17 \text{ ft} \times 12 \text{ in.}} = 0.000002$ radian; and the angle change at section 9 is $\phi_9 = \dfrac{0.0000065 \times 13°}{1.65 \text{ ft} \times 12 \text{ in.}} = 0.0000042$ radian. Similarly, the angle change at section 5 is found to be $\phi_5 = 0.0000035$ radian.

Inspection of these three sections shows that the angle change varies inversely as the depth of the section. For example, section 9 has an angle change approximately twice that of section 1 and its depth is one half of section 1. Similarly, section 5 has an angle change equal to 1.67 that of section 1, and its depth is equal to 0.606 times the depth of section 1.

Since the thickness of the deck (see Fig. 2) conforms with the parabolic equation,

$$y = \frac{(x - 40)^2}{2\,a} + 2.25 \ldots\ldots\ldots\ldots\ldots\ldots\ldots\ldots (3)$$

(in which a = a constant found from known boundary conditions = 310), it follows that the angle-change loading in this case is also parabolic. The angle-change loading for the deck is shown in Fig. 6.

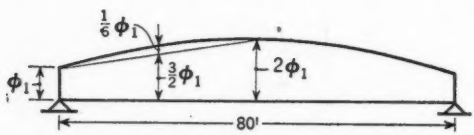

FIG. 6.—ANGLE-CHANGE LOADING OF DECK

Step 3. Computation of End Rotation in Basic Beam.—From Fig. 6, using the method of elastic weights,

$$R_e = \theta_A = \theta_B = \frac{\phi_1 + 2\,\phi_1}{2} \times \frac{L}{2} + \frac{2}{3} \times \frac{1}{6}\,\phi_1 \times \frac{L}{2}$$

$$= 40 \times 12 \left(\frac{3\,\phi_1}{2} + \frac{1}{9}\,\phi_1 \right) = 773\,\phi_1 \ldots\ldots\ldots\ldots\ldots\ldots (4)$$

in which R_e = the elastic reaction of the angle-change loading.

Step 4. Computation of End Rotation of Basic Beam Loaded with $\frac{M}{E\,I}$*-Diagram.*—Since in beams with fixed ends there can be no end rotation, it is necessary to apply moments at each end of the beam large enough to rotate the tangents back through the angles θ_A and θ_B. Since θ_A is equal to θ_B, the applied moments are equal. In this step, $\theta_A = \theta_B$ equals the elastic reactions of a beam loaded with the $\frac{M}{E\,I}$-diagram, or

$$\theta_A = \theta_B = \frac{M}{E} \sum_{0}^{40} \frac{\Delta s}{I_s} \ldots\ldots\ldots\ldots\ldots\ldots\ldots\ldots (5)$$

in which Δs = the length of each deck division for use in the summation = 60 in. The summation equation (Eq. 5) is necessary since the moment of inertia of the deck is not constant. The moment of inertia of each segment I_s is equal to

$$I_s = \frac{1}{12}\,b\,(d')^3 + A_s\,(n - 1)\,\frac{d^2_s}{4} \ldots\ldots\ldots\ldots\ldots\ldots\ldots (6)$$

in which b is assumed to be a transverse 12-in. strip of the deck; d' is the total depth of the section; A_s is the cross-section area of the steel reinforcement; $n = \frac{E_s}{E_c}$ = the ratio of the moduli of elasticity; and d_s is the distance between

compression and tension steel, assuming neutral axis of section halfway between steel bars. Values of the ratio $\Delta s/I_s$, for use in Eq. 5, are:

Segment No.	$\frac{\Delta s}{I} \times 1{,}000$
1	0.325
2	0.480
3	0.712
4	1.063
5	1.450
6	1.900
7	2.280
8	2.295
$\sum \frac{\Delta s}{I} \times 1{,}000$	10.505

Step 5. Equating Steps 3 and 4 to Find Fixed-End Moment.—Combining Eqs. 4 and 5, $\frac{M}{E} \times \frac{10.505}{1{,}000} = 773\,\phi_1$; and

$$M = \frac{773\,\phi_1 E}{0.0105} \qquad (7)$$

If $\phi_1 = 0.000002 = 2 \times 10^{-6}$ radians and $E = 3 \times 10^6$, the fixed moment for the deck is $M = \frac{773 \times 2 \times 10^{-6} \times 3 \times 10^6}{0.0105} = 450{,}000$ in-lb.

Step 6. Distribution of Fixed-End Moments.—In this step the Hardy Cross method of moment distribution is used to find the final moments at the ends of the deck of each span, the stiffness and carry-over factors for the beams of varying moments of inertia being as shown in Fig. 7.[9] Accordingly, the final resisting moments in span BC, Fig. 7 (symmetrical about the center line) are:

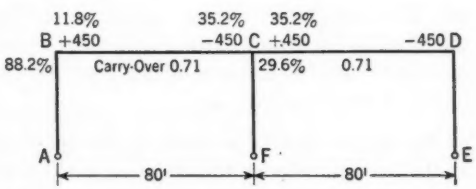

FIG. 7.—FIXED-END MOMENTS READY FOR DISTRIBUTION, SHOWING STIFFNESS FACTORS AND CARRY-OVER FACTORS

Description	End A	End B
Inch-kips	397.0	488.0
Foot-kips	33.1	40.6
Direction	Clockwise	Counterclockwise

The moment at the crown of span BC is the average of the end moments, or knee moments, plus the thrust at end B, multiplied by its arm to the center line of the deck at the crown: $\frac{33{,}100 + 40{,}600}{2} + \frac{33{,}100}{15.83} \times 1.28 = 36{,}850 + 2{,}670 = 39{,}520$ ft-lb.

[9] "Analysis of Rigid Frame Concrete Bridges," Portland Cement Assn., 11th Ed., 1936.

Interpretation of Results

The moments M_{BC} and M_{CB} at the ends of the deck, caused by radiant heat, act in a direction opposite to the primary dead-load moments and live-load moments. Therefore, radiant heat causes no serious effects at these points. At the crown, however, the radiant-heat moment of 39,520 ft-lb acts in the same direction as the primary moments. The design moment at the crown for this particular frame included the following moments:

Description	Foot-pounds
Dead load	37,120
Live load	25,340
Impact	6,200
Shrinkage and movement of footings	25,500
Temperature change (−45° F) from a mean value	17,160
Total design moment	111,320

For this frame the radiant-heat moment at the crown equals $\frac{39,520}{68,660} \times 100$ or 57.5% of the primary moments, and $\frac{39,520}{111,320} \times 100$ or 35.5% of the total design moment. This represents a moment of considerable magnitude, and one which would necessitate the provision of additional steel were it not for the compensating seasonal temperature changes. The following relationships exist between these seasonal changes and the theoretical radiant-heat moment: (*a*) The maximum design moment at the crown includes the effect of a 45° F drop in temperature; and (*b*) the remaining 56% of the radiant-heat moment and its corresponding fiber stress effect are further reduced by a seasonal temperature rise.

(*a*) *Effect of a 45° F Drop in Temperature.*—The maximum design moment at the crown includes the effect of a 45° F drop in temperature. Accordingly, in this design there is steel and compressive area to resist 17,160 ft-lb of moment which would not occur on the days when the effect of radiant heat is greatest. This material would be available for $\frac{17,160}{39,520} \times 100$ or 44% of the radiant-heat moment at the crown.

(*b*) *Effect of a Seasonal Temperature Rise.*—The remaining 56% of the radiant-heat moment and its corresponding fiber stress effect are further reduced by a seasonal temperature rise. On the days when the radiant heat causes the greatest strains, the deck is probably elongating due to the rise in seasonal temperature. In addition, the axial strains in the deck, due to the radiant heat itself, increase the length of the deck somewhat. The effects of radiant heat and axial elongation counteract each other. Exactly how much the remaining 56% or 22,000 ft-lb is reduced is difficult to evaluate since radiant-heat stresses occur in short cycles whereas seasonal temperature elongation is a long-range process. It is possible that the reduction could be from a

small amount on certain days to an amount corresponding to the maximum seasonal temperature rise. In this particular design, if one of the radiant-heat cycles occurred on the same day that the full seasonal elongation was effective, the reduction would be 17,120 ft-lb. The axial elongation accompanying the radiant-heat strain distribution is also difficult to compute because there is both elongation and contraction of the cross section as shown in Fig. 5(*b*).

Conclusions

The most definite design procedure to provide for the effects of radiant heat in a rigid frame is to include in the maximum design moment at the crown the moment due to a sizable seasonal temperature drop (−45° F or more for frames comparable in length to the one just analyzed). This should be done in states with warm climates, where radiant heat is likely to be high, even though the actual temperature drop is moderate.

The assumptions made in computing the heat flow through the slab due to radiant heat, in this paper, are on the conservative side. For example, the heat was assumed to flow in one direction only—downward into the slab. The effect that the main longitudinal steel may have on the temperature distribution was not taken into account. Temperature and shrinkage steel at right angles to the main longitudinal steel would also probably absorb some of lateral heat strain which surely exists. Practical measures, such as expansion joints in the slab itself, would relieve some of the strain. However, the magnitude of the moments that were found with the assumptions made should indicate a need for further study and discussion of this type of temperature stress. Possibly more uniform seasonal temperature change specifications will result.

Six conclusions seem reasonable on the basis of this paper:

1. The radiant-heat moments at the knee sections of the rigid frame would not affect the maximum combination of design moments as they act in a direction opposite to the dead-load and live-load moments.
2. The radiant-heat moment at the crown of the particular frame analyzed in this paper is equal to 35.5% of the maximum design moment and acts in the same direction as the dead-load and live-load moments.
3. If the maximum design moment at the crown includes the moment caused by a substantial seasonal temperature drop (45° F or more from a mean value) steel will be available for the radiant-heat stresses, as this temperature drop will not coincide with maximum radiant heat. Material was present in this design to account for 44% of the radiant-heat moment, corresponding to a 45° F drop in seasonal temperature.
4. Axial strains due to seasonal temperature rise and radiant heat itself reduce the effect of the radiant-heat moment, although it is difficult to ascertain exactly how much on any given day or radiant-heat cycle.
5. The magnitude of radiant-heat moment at the crown should warrant serious consideration of seasonal temperature specifications, particularly temperature drop, in the design of long-span reinforced-concrete rigid frames.

Acknowledgment

Material from which this paper was prepared was taken from a thesis by the writer, entitled "The Effect of Temperature Stresses in a Reinforced Rigid Concrete Frame," presented in 1942 to the University of Minnesota, at Minneapolis, in partial fulfilment of the requirements for the degree of Master of Science. Constructive criticism and guidance in the preparation of the thesis were given by Prof. C. A. Hughes, formerly of the structural department at the University of Minnesota.

AMERICAN SOCIETY OF CIVIL ENGINEERS

Founded November 5, 1852

PAPERS

STRUCTURAL SKEW PLATES

By F. L. Ehasz,[1] Jun. Am. Soc. C. E.

Synopsis

In the theory of elasticity it is sometimes feasible by means of approximate methods to obtain analyses of problems which do not lend themselves readily to exact treatment. This is true in the study of the structural behavior of plates and slabs. It is particularly valid for skew plates and slabs which, so far as the writer knows, have not been analyzed by other than approximate methods in technical literature. The object of this paper is to present a comparison of results acquired for certain skew plates by means of approximate methods involving finite differences, trigonometric series, and power series.

Introduction

Some consideration has been given by various investigators in the United States and abroad to the analysis and design of skew plates and slabs. In the field of reinforced concrete these studies have been of considerable interest and practical importance, especially in the case of highway bridge slabs that cross streams, railways, or other highways below at an oblique angle. It is common knowledge that modern traffic and speed requirements in the United States stipulate the construction of many skew structures. Whereas bridge slabs usually are provided with integral curbs and rails, which tend to make the structural behavior more complex, it is nevertheless of interest to ascertain the manner in which the more simple slabs perform. Structural engineers have been studying the skew plate, simply supported on all four sides, the clamped skew plate, and skew slabs simply supported on two sides with two free edges, in addition to the more practical bridge slabs with the integral curbs mentioned previously.

A skew plate or slab may be defined as one having the shape of a parallelogram which is not a rectangle nor a square. Some engineers designate the rectangular or square plate as a plate with a skew angle of zero. In any case, the term "degree of skew," in this paper, is defined as the angle of distortion

Note.—Written comments are invited for immediate publication; to insure publication the last discussion should be submitted by **November 1, 1945.**

[1] Asst. Engr., O. H. Ammann, Cons. Engr., New York, N. Y.

from the rectangular or square shape. This designation corresponds in general with the practice and the technical literature pertaining to other types of skew structures. As in the case of skew arches,[2] the skew effect in plates depends upon the ratio of the lengths of sides as well as on the angle of skew.

It was the purpose of the investigation upon which this paper was based to study theoretically the structural action of skew plates simply supported on all four sides, subjected to a uniformly distributed lateral load, and a clamped skew plate similarly loaded. In the course of these studies various systems of coordinates were used to determine whether the skew boundaries would lend themselves to treatment more readily by one system than by the others. It is to be observed, moreover, that, although the results reported herein pertain directly to metal plates (Poisson's ratio approximately 0.3), they can be modified easily to include other materials, such as concrete, in which case Poisson's ratio may be varied from 0.15 to 0.20.

In this work simply supported skew plates were investigated by the method of finite differences, by trigonometric series satisfying the plate equation throughout and the boundary conditions only at certain points, and by power series. A clamped skew plate was also treated by these methods. A preliminary review was made of solutions for triangular plates with a view to ascertaining the effect of the density of difference-equation networks and to determining some measure of the accuracy to be expected for similar meshes in the case of skew plates.

Previous Studies

The structural behavior of skew plates and slabs has been investigated mainly by the method of finite differences. The first publication on skew plates that has come to the writer's attention is a paper by Cecilia Vittoria Brigatti.[3] Results were obtained by difference equations for uniformly loaded skew plates simply supported and clamped, the sides being of the same length. The fundamental considerations in this work appear to be open to question.

Adolf Anzelius[4] has given some attention to a uniformly loaded skew plate, simply supported on two opposite sides and free on the other two. His solution is in the form of series involving hyperbolic and trigonometric functions, which yield an infinite system of linear equations. The method is approximate and appears to be quite cumbersome. As in other similar approaches, the accuracy of the method depends upon the number of coefficients taken in the series. Mr. Anzelius gave, qualitatively, only twisting moments for a 45° skew slab.

A summary of results obtained by difference equations for uniformly loaded skew slabs, in particular, with two opposite sides simply supported and the other

[2] "The Design and Construction of a Skew Arch," by S. C. Hollister, *Proceedings*, A.C.I., Vol. XXIV, 1928, p. 371.

[3] "Applicazione del metodo di H. Marcus al calcolo della piastra parallelogrammica," by Cecilia Vittoria Brigatti, *Ricerche di Ingegneria*, Vol. XVI, No. 2, March–April, 1938, p. 42.

[4] "Über die elastische Deformation parallelogrammförmiger Platten," by Adolf Anzelius, *Der Bauingenieur*, Vol. 20, No. 35–36, September, 1939, p. 478.

two edges free, has been abstracted from the doctoral work of Helmut Vogt[5] and promulgated in a paper[6] by the same author. Professor Vogt has given particular attention to the arrangement of the reinforcement in bridge slabs. Brief mention was made of skew slabs simply supported on four sides and uniformly loaded.

Studies of skew slabs by means of difference equations have also been made by V. P. Jensen,[7] M. Am. Soc. C. E. Uniformly loaded skew slabs simply supported on four sides, and similarly loaded skew slabs simply supported on two opposite edges and free on the other two sides, were analyzed by use of difference equations developed in a form readily applicable to networks made up of lines parallel to the sides, regardless of the degree of skew. In these slabs the ratio of the length of the long side to that of the short span was kept nearly constant and equal to a value of 2.0. Poisson's ratio was taken to be 0.2. Particular attention was given by Professor Jensen to a simple-span slab bridge with curbs and a 45° skew. The method of obtaining influence surfaces by means of difference equations as recommended by Nathan Newmark,[7] Assoc. M. Am. Soc. C. E., proved to be useful in these studies. Also, Professor Jensen considered the effectiveness of reinforcement for various arrangements of the main and transverse steel.

Ordinary Theory of Plates

Notation.—The letter symbols in this paper are identified in the text, or by diagram, where they first appear and, for convenience of reference, are assembled alphabetically in the Appendix.

Assumptions and Limitations.—In the ordinary theory of plates several simplifying assumptions are made, resulting in concomitant limitations. As a matter of convenience the plate is considered to be horizontal, homogeneous, elastic, isotropic, uniform in thickness, and subjected to lateral loads only. In addition to being uniform, the thickness must be small compared with the lateral dimensions. The deflections and the energy of deformation in the medium-thick plate are not affected by the vertical stresses (tensions, compressions, and shears) as they are in the case of thick plates. Likewise, the energy due to shortening and stretching of the middle surface may be neglected, which is tantamount to stating that the deflections are small relative to the thickness of the plate. This work of deformation, naturally, must be considered in the theory of thin plates. It is taken for granted, furthermore, that Hooke's law applies to the horizontal strains. In the theory of beams, it will be recalled, plane cross sections before bending are assumed to remain plane after bending. Similarly, in the ordinary theory of plates, straight lines normal to the middle surface of the plate before bending remain straight and normal after bending. Analogous to the concept of straight-line variation of tensile and

[5] "Beitrag zur Berechnung schiefwinkliger Platten, nebst Anwendung bei der Berechnung und Anordnung der Bewehrung schiefwinkliger Brückenbauwerke," by Helmut Vogt, Dissertation, Technische Hochschule, Hannover, 1940.

[6] "Die Berechnung schiefwinkliger Platten und plattenartiger Brückensysteme," by Helmut Vogt, *Beton und Eisen*, Vol. 39, No. 17, September, 1940, pp. 243–245.

[7] "Analyses of Skew Slabs," by V. P. Jensen, *Bulletin No. 332*, Univ. of Illinois Eng. Experiment Station, Urbana, Ill., September, 1941.

compressive stresses in the cross section of the beam, there follows in the case of the plate the postulation that horizontal unit stresses (tensions, compressions, and shears) in vertical sections are distributed linearly.

Fundamental Differential Equations.—The derivation of the differential equations for the ordinary theory of plates in Cartesian coordinates has been given by various writers in the technical literature[8,9,10,11] and therefore will not be given in this paper. It is pertinent, however, to outline the basic equations for later reference.

The bending and twisting moments in the distorted plate (see Fig. 1) are given by the expressions

$$M_x = -N\left(\frac{\partial^2 w}{\partial x^2} + \mu\frac{\partial^2 w}{\partial y^2}\right) \quad \ldots\ldots(1a)$$

$$M_y = -N\left(\frac{\partial^2 w}{\partial y^2} + \mu\frac{\partial^2 w}{\partial x^2}\right) \quad \ldots\ldots(1b)$$

and

$$M_{xy} = -(1-\mu)N\frac{\partial^2 w}{\partial x\,\partial y} \quad \ldots\ldots(1c)$$

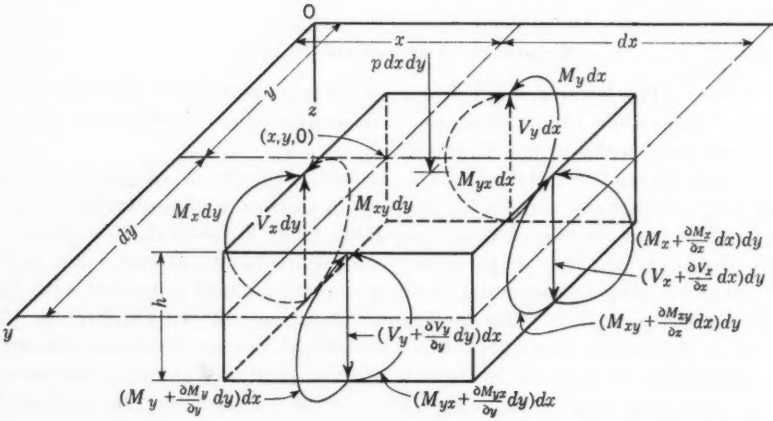

FIG. 1.—RECTANGULAR ELEMENT OF A PLATE (THE DIRECTIONS SHOWN ARE POSITIVE)

in which w designates the deflection, μ is Poisson's ratio for the material, and N, the flexural rigidity, is a function of the modulus of elasticity, E, of the material, the plate thickness, h, and Poisson's ratio, as is manifested from the equation

$$N = \frac{E\,h^3}{12\,(1-\mu^2)} \quad \ldots\ldots(2)$$

[8] "Theory of Plates and Shells," by S. Timoshenko, 1st Ed., McGraw-Hill Book Co., Inc., New York and London, 1940, p. 85.

[9] "An Introduction to the Theory of Elasticity for Engineers and Physicists," by R. V. Southwell, Oxford Univ. Press, 1936, p. 228.

[10] "Die elastischen Platten," by A. Nadai, Julius Springer, Berlin, 1925, p. 18.

[11] "Die Theorie elastischer Gewebe und ihre Anwendung auf die Berechnung biegsamer Platten," by H. Marcus, 2d Ed., Julius Springer, Berlin, 1932.

The Lagrange equation for the flexure of plates produced by a uniformly distributed lateral load p may be shown to be

$$\frac{\partial^4 w}{\partial x^4} + 2\frac{\partial^4 w}{\partial x^2 \partial y^2} + \frac{\partial^4 w}{\partial y^4} = \frac{p}{N} \quad \ldots\ldots (3)$$

or

$$\nabla^4 w = \nabla^2 \nabla^2 w = \frac{p}{N} \quad \ldots\ldots (4)$$

in which

$$\nabla^2 = \frac{\partial^2}{\partial x^2} + \frac{\partial^2}{\partial y^2} \quad \ldots\ldots (5)$$

is the Laplace operator. From Eqs. 1 it is clear that the moment sum is expressible in the form

$$M_x + M_y = -(1 + \mu) N \nabla^2 w \quad \ldots\ldots (6)$$

The vertical shears are given by the equations

$$V_x = -N\frac{\partial}{\partial x}\nabla^2 w \quad \ldots\ldots (7a)$$

and

$$V_y = -N\frac{\partial}{\partial y}\nabla^2 w \quad \ldots\ldots (7b)$$

Maximum stresses, occurring at the surface, are

$$\sigma_x = \pm\frac{6 M_x}{h^2} \quad \ldots\ldots (8a)$$

$$\sigma_y = \pm\frac{6 M_y}{h^2} \quad \ldots\ldots (8b)$$

and

$$\tau_{xy} = \pm\frac{6 M_{xy}}{h^2} \quad \ldots\ldots (8c)$$

From the shears and the twisting moments it is possible to deduce the vertical reactions

$$R_x = V_x + \frac{\partial M_{xy}}{\partial y} = -N\left[\frac{\partial^3 w}{\partial x^3} + (2 - \mu)\frac{\partial^3 w}{\partial x \partial y^2}\right] \quad \ldots\ldots (9a)$$

and

$$R_y = V_y + \frac{\partial M_{xy}}{\partial x} = -N\left[\frac{\partial^3 w}{\partial y^3} + (2 - \mu)\frac{\partial^3 w}{\partial x^2 \partial y}\right] \quad \ldots\ldots (9b)$$

These reactions are defined in the same manner as the vertical shears.

Polar Coordinates.—The differential equations for the bending of plates may be readily placed into polar form by some simple transformations. It will be necessary later to use the concept of average curvature at a point of the distorted plate and, consequently, it is introduced here. Curvatures in the xz-plane and the yz-plane are

$$\frac{1}{r_x} = \frac{\partial}{\partial x}\left(\frac{\partial w}{\partial x}\right) = \frac{\partial^2 w}{\partial x^2} \quad \ldots\ldots (10a)$$

and

$$\frac{1}{r_y} = \frac{\partial}{\partial y}\left(\frac{\partial w}{\partial y}\right) = \frac{\partial^2 w}{\partial y^2} \quad \ldots\ldots\ldots\ldots\ldots\ldots\ldots\ldots (10b)$$

respectively. It can be shown that at the same point the sum of the curvatures in any two perpendicular directions n and t is equal to the sum of Eqs. 10 or, symbolically,

$$\frac{1}{r_n} + \frac{1}{r_t} = \frac{\partial^2 w}{\partial n^2} + \frac{\partial^2 w}{\partial t^2} = \frac{1}{r_x} + \frac{1}{r_y} = \frac{\partial^2 w}{\partial x^2} + \frac{\partial^2 w}{\partial y^2} \quad \ldots\ldots\ldots\ldots (11)$$

r_n and r_t are defined in a manner similar to r_x and r_y. The invariant sum defined by Eq. 11 has been designated as the average curvature of the plate's

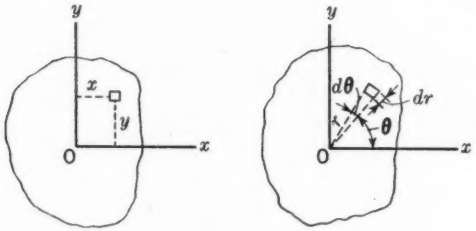

FIG. 2.—TRANSFORMATION TO POLAR COORDINATES

surface at a point. Transformation from Cartesian to polar coordinates (see Fig. 2) yields the result

$$\nabla^2 w = \frac{\partial^2 w}{\partial r^2} + \frac{1}{r}\frac{\partial w}{\partial r} + \frac{1}{r^2}\frac{\partial^2 w}{\partial \theta^2} \quad \ldots\ldots\ldots\ldots\ldots\ldots (12a)$$

By repetition of this operation it is possible to obtain the Lagrange plate equation in the form

$$\nabla^2\nabla^2 w = \left(\frac{\partial^2}{\partial r^2} + \frac{1}{r}\frac{\partial}{\partial r} + \frac{1}{r^2}\frac{\partial^2}{\partial \theta^2}\right)\left(\frac{\partial^2 w}{\partial r^2} + \frac{1}{r}\frac{\partial w}{\partial r} + \frac{1}{r^2}\frac{\partial^2 w}{\partial \theta^2}\right) = \frac{p}{N} \ldots (12b)$$

Eqs. 12 will be used subsequently in the approximate trigonometric-series solution for a skew plate.

From simple transformation equations, expressions for moments in polar form may be deduced by stipulating that the x-axis coincides with the radius r. If t is the direction (tangential) perpendicular to the radial direction r, M_r and M_t are the moments per unit length acting in sections perpendicular to r and t, respectively. These moments and the corresponding twisting moments, M_{rt}, may be shown to be

$$M_r = -N\left[\frac{\partial^2 w}{\partial r^2} + \mu\left(\frac{1}{r}\frac{\partial w}{\partial r} + \frac{1}{r^2}\frac{\partial^2 w}{\partial \theta^2}\right)\right] \quad \ldots\ldots\ldots\ldots (13a)$$

$$M_t = -N\left(\mu\frac{\partial^2 w}{\partial r^2} + \frac{1}{r}\frac{\partial w}{\partial r} + \frac{1}{r^2}\frac{\partial^2 w}{\partial \theta^2}\right) \quad \ldots\ldots\ldots\ldots\ldots (13b)$$

and

$$M_{rt} = -(1-\mu)\,N\left(\frac{1}{r}\frac{\partial^2 w}{\partial r\,\partial\theta} - \frac{1}{r^2}\frac{\partial w}{\partial\theta}\right) = -(1-\mu)\,N\frac{\partial}{\partial r}\left(\frac{1}{r}\frac{\partial w}{\partial\theta}\right) \ldots (13c)$$

It is possible to obtain a power series in quadrilinear form that would yield an approximate solution of skew plate problems. Since this procedure would have entailed considerably more work than a similar series approach in Cartesian form, solutions were not sought by quadrilinear coordinates. In this work the power-series approach, useful for attacking a wide variety of plate problems, was dealt with only in Cartesian coordinates and was applied to a few plate problems which were treated also by other methods.

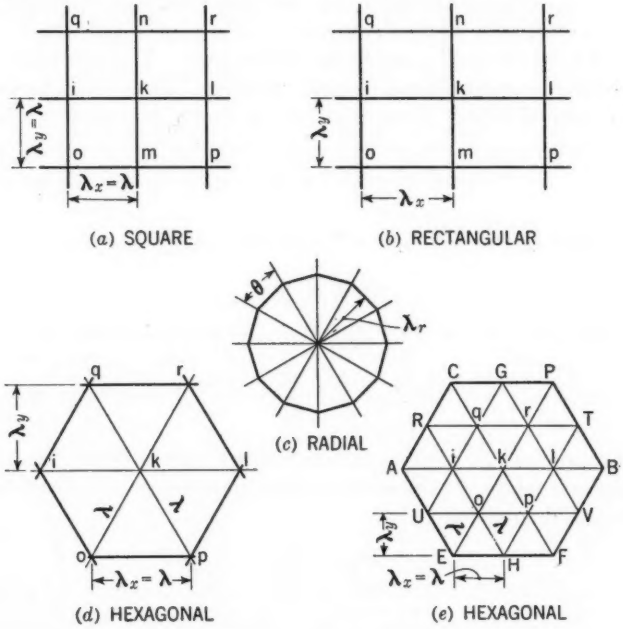

FIG. 3.—TYPES OF NETWORKS FOR DIFFERENCE EQUATIONS

Difference Equations.—By means of difference equations it is possible to obtain approximate solutions for many plate problems which cannot be treated easily by exact methods. Skew plates and slabs fall into this category. Many writers have applied this method to plate problems.[8–17] Since finite squares, rectangles, and triangles (hexagons) (see Fig. 3) are used in the formation of

[12] "Bestemmelse af Spaendinger i Plader ved anvendelse af Differensligninger," by N. S. Nielsen, Kopenhagen, 1920.

[13] "Die elastischen Platten," by A. Nadai, Julius Springer, Berlin, 1925, p. 205.

[14] "The Calculation of Flat Plates by the Elastic Web Method," by Joseph A. Wise, *Proceedings*, A.C.I., 1928, p. 408.

[15] "Design of Reinforced Concrete Slabs," by Joseph A. Wise, *ibid.*, 1929, p. 712.

[16] "Analysis of Plate Examples by Difference Methods and the Superposition Principle," by D. L. Holl, *Journal of Applied Mechanics, Transactions*, A.S.M.E., Vol. 58, September, 1936, p. A-81.

[17] "Cantilever Plate with Concentrated Edge Load," by D. L. Holl, *ibid.*, Vol. 59, March, 1937, p. A-8.

difference-equation networks, rather than the corresponding infinitesimal elements associated with differential equations, only approximate results are obtained. The approximations become better as the elements become smaller. An attempt was made in this investigation to ascertain the effect of the density of the networks for triangular plates as well as skew plates.

The procedure for the method of finite differences as presented by H. Marcus,[11] M. Am. Soc. C. E., was followed throughout this work. According to Mr. Marcus, the elastic web is said to consist of a network of elastic strings attached to the edges of the plate in such a way as to conform with the boundary conditions of the actual plate or slab. In the case of a plate that supports a concentrated load, it is desirous to arrange a network that has a point of intersection at the position of the load. If the load is uniformly distributed, it is replaced by a statically equipollent system of concentrated forces applied at the intersection points contiguous to the loaded area. The difference equations relating the deflections of the web usually yield a system of simultaneous linear equations in normal form. A function of the moment sum can be written

$$\bar{M} = -N\left(\frac{\partial^2 w}{\partial x^2} + \frac{\partial^2 w}{\partial y^2}\right) \ldots\ldots\ldots\ldots\ldots\ldots (14)$$

From Eqs. 4 and 14 the equation of the elastic surface becomes

$$\nabla^2 \bar{M} = -p \ldots\ldots\ldots\ldots\ldots\ldots\ldots\ldots (15)$$

The sum of the moments in the x-direction and the y-direction is

$$M_x + M_y = -N(1+\mu)\left(\frac{\partial^2 w}{\partial x^2} + \frac{\partial^2 w}{\partial y^2}\right) = (1+\mu)\,\bar{M} \ldots\ldots (16)$$

The deflections, $\bar{w}$, of a membrane subjected only to fiber stresses parallel to the surface, are related to the horizontal component, S, of the surface stresses by the differential equation

$$\nabla^2 \bar{w} = \frac{\partial^2 \bar{w}}{\partial x^2} + \frac{\partial^2 \bar{w}}{\partial y^2} = -\frac{p}{S} \ldots\ldots\ldots\ldots\ldots\ldots (17)$$

Manifestly, S must be constant over the entire membrane because of conditions of static equilibrium. If $S = 1$, comparison of Eqs. 15 and 17 suggests the theorem:[16]

> "The deflection of a membrane subjected to loads proportional to those on a given plate may be considered as the sum of the principal moments of the actual plate."

Similar to the procedure in the case of beams, it is possible to derive another theorem:

> "A second membrane may be loaded with elastic weights proportional to these moment sums and, subject to appropriate boundary conditions, the deflections of the latter membrane will be proportional to the deflections of the actual plate under the given loading system."

The elastic weights in the second theorem are actually $\frac{\bar{M}}{N}$.

It is obvious that the solution of the plate problem is manifested by the equations

$$\nabla^2 \bar{M} = -p \quad \ldots\ldots\ldots\ldots\ldots\ldots\ldots\ldots (18a)$$

and

$$\nabla^2 w = -\frac{\bar{M}}{N} \quad \ldots\ldots\ldots\ldots\ldots\ldots\ldots\ldots (18b)$$

By analogy and equilibrium considerations one may obtain the relations

$$\bar{M}_k = S_1 \bar{w}_k \quad \ldots\ldots\ldots\ldots\ldots\ldots\ldots\ldots (19)$$

in which S_1 is the quantity S referred to the first membrane, and

$$w_k = \bar{z}_k \frac{S_1 S_2}{N} \quad \ldots\ldots\ldots\ldots\ldots\ldots\ldots\ldots (20)$$

in which $\bar{z}_k$ designates the deflection of the nodal point k in the second membrane. Equations relating the web deflections for the square mesh may be written as follows:

$$4\,\bar{w}_k - (\bar{w}_i + \bar{w}_l + \bar{w}_m + \bar{w}_n) = \frac{p_k \lambda^2}{S_1} \quad \ldots\ldots\ldots\ldots (21a)$$

and

$$4\,\bar{z}_k - (\bar{z}_i + \bar{z}_l + \bar{z}_m + \bar{z}_n) = \frac{\bar{M}_k \lambda^2}{S_1 S_2} \quad \ldots\ldots\ldots\ldots (21b)$$

in which the subscripts refer to the points in Fig. 3(*a*). For the hexagonal network, the following expressions apply (see Figs. 3(*d*) and 3(*e*)):

$$4\,\bar{w}_k - \frac{2}{3}(\bar{w}_i + \bar{w}_l + \bar{w}_o + \bar{w}_p + \bar{w}_q + \bar{w}_r) = \frac{p_k \lambda^2}{S_1} \quad \ldots\ldots\ldots (22a)$$

and

$$4\,\bar{z}_k - \frac{2}{3}(\bar{z}_i + \bar{z}_l + \bar{z}_o + \bar{z}_p + \bar{z}_q + \bar{z}_r) = \bar{M}_k \frac{\lambda^2}{S_1 S_2} \quad \ldots\ldots\ldots (22b)$$

From the simultaneous linear equations the values of $\bar{w}_k$ and $\bar{z}_k$ are obtained. Once these are found the $\bar{M}_k$-functions and deflections of the actual plate result from Eqs. 19 and 20.

Bending moments and twisting moments in the case of rectangular meshes (see Fig. 3(*b*)) are given by the expressions[18]

$$M_x = S_1 S_2 \left[\frac{2\,\bar{z}_k - \bar{z}_i - \bar{z}_l}{\lambda^2_x} + \mu \frac{2\,\bar{z}_k - \bar{z}_m - \bar{z}_n}{\lambda^2_y} \right] \quad \ldots\ldots\ldots (23a)$$

$$M_y = S_1 S_2 \left[\frac{2\,\bar{z}_k - \bar{z}_m - \bar{z}_n}{\lambda^2_y} + \mu \frac{2\,\bar{z}_k - \bar{z}_i - \bar{z}_l}{\lambda^2_x} \right] \quad \ldots\ldots\ldots (23b)$$

and

$$M_{xy} = (1 - \mu)\, S_1 S_2 \left[\frac{(\bar{z}_p + \bar{z}_q) - (\bar{z}_o + \bar{z}_r)}{4\,\lambda_x \lambda_y} \right] \quad \ldots\ldots\ldots (23c)$$

[18] "Die Theorie elastischer Gewebe und ihre Anwendung auf die Berechnung biegsamer Platten," by H. Marcus, 2d Ed., Julius Springer, Berlin, 1932, p. 18.

values of λ being defined in Fig. 3. The vertical shearing forces are to be found from the equations

$$V_x = S_1 \frac{\partial \bar{w}}{\partial x} = \frac{S_1}{2\,\lambda_x} (\bar{w}_l - \bar{w}_i) \quad \ldots\ldots (24a)$$

and

$$V_y = S_1 \frac{\partial \bar{w}}{\partial y} = \frac{S_1}{2\,\lambda_y} (\bar{w}_n - \bar{w}_m) \quad \ldots\ldots (24b)$$

Bending moments in the directions 1, 2, and 3 (in which $M_2 = M_x$ and directions 1 and 3 are $-60°$ and $+60°$, respectively) may be obtained from the following:

$$M_{1k} = (1 - \mu)\, S_1\, S_2 \frac{2\,\bar{z}_k - \bar{z}_p - \bar{z}_q}{(\lambda_y \sec \alpha)^2} + \mu\, S_1\, \bar{w}_k \quad \ldots\ldots (25a)$$

$$M_{2k} = (1 - \mu)\, S_1\, S_2 \frac{2\,\bar{z}_k - \bar{z}_i - \bar{z}_l}{\lambda^2_x} + \mu\, S_1\, \bar{w}_k \quad \ldots\ldots (25b)$$

and

$$M_{3k} = (1 - \mu)\, S_1\, S_2 \frac{2\,\bar{z}_k - \bar{z}_o - \bar{z}_r}{(\lambda_y \sec \alpha)^2} + \mu\, S_1\, \bar{w}_k \quad \ldots\ldots (25c)$$

in which $2\,\alpha$ equals $60°$. Vertical shearing forces are given by the terms

$$V_{1k} = S_1 \frac{\bar{w}_p - \bar{w}_q}{2\,\lambda_y \sec \alpha} \quad \ldots\ldots (26a)$$

$$V_{2k} = S_1 \frac{\bar{w}_l - \bar{w}_i}{2\,\lambda_x} \quad \ldots\ldots (26b)$$

and

$$V_{3k} = S_1 \frac{\bar{w}_r - \bar{w}_o}{2\,\lambda_y \sec \alpha} \quad \ldots\ldots (26c)$$

The twisting moments result from the expression (see Fig. 4(*a*)):

$$M_{xy} = -(1 - \mu)\, N \frac{\partial^2 w}{\partial x\, \partial y} = (1 - \mu) \frac{S_1\, S_2}{2\,\lambda_x\, \lambda_y} [(\bar{z}_p + \bar{z}_q) - (\bar{z}_o + \bar{z}_r)] \quad \ldots (27)$$

As stated previously, $M_x = M_2$. In order to find M_y, it is possible to use the simple equation (from Eq. 16):

$$M_y = (1 + \mu)\, \bar{M} - M_x \quad \ldots\ldots (28)$$

The maximum and minimum bending moments may be shown to be

$$M_{\max} = \frac{M_x + M_y}{2} + \frac{1}{2} \sqrt{(M_x - M_y)^2 + 4\, M^2_{xy}} \quad \ldots\ldots (29a)$$

and

$$M_{\min} = \frac{M_x + M_y}{2} - \frac{1}{2} \sqrt{(M_x - M_y)^2 + 4\, M^2_{xy}} \quad \ldots\ldots (29b)$$

The maximum value of the twisting moment is

$$M_t = \frac{1}{2} \sqrt{(M_x - M_y)^2 + 4\, M^2_{xy}} \quad \ldots\ldots (30)$$

To obtain the trajectories of the principal moments (see Fig. 2(*b*)), use is made of the equation

$$\tan 2\theta = \frac{2 M_{xy}}{M_x - M_y} \quad \ldots\ldots\ldots\ldots\ldots\ldots\ldots\ldots (31)$$

Preliminary Survey of Triangular Plates

A brief preliminary study of the effect of density of difference-equation networks on certain deflections and moments was made for the equilateral triangular plate, the 30°–60°–90° triangular plate, and an isosceles triangular plate having a right angle, all plates being simply supported and subjected to a uniformly distributed load. Comparison with published results obtained by more exact methods indicated that a relatively small number of nodal points gives values that are in fair agreement with those of the more accurate solutions. This is especially true in the case of bending moments. In general, moments and deflections for points nearer the center of gravity of the plates showed better agreement than those for points nearer the boundaries. Net works considered involved from two to twenty-one coefficients. Because of lack of space, however, detailed observations for triangular plates are not given herein.

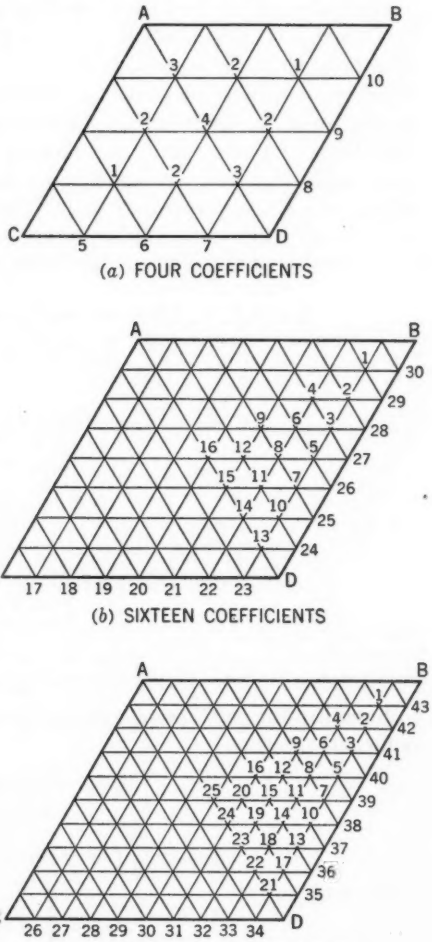

FIG. 4.—NETWORKS FOR 30° SKEW PLATES (AB = AC = 2 *c*)

Simply Supported 30° Skew Plate with Equal Sides Subjected to a Uniformly Distributed Load

Analysis by Method of Finite Differences.—The most convenient network for the analysis of a 30° skew plate by the difference-equation method is a triangular (hexagonal) arrangement formed by drawing lines parallel to the sides and the shorter diagonal of the plate (see Figs. 3(*d*) and 4). To determine the effect of the mesh intervals on the results for deflections and moments in the case of the uniformly loaded,

simply supported, 30° skew plate having equal sides (length = 2 c), three networks of varying density ($\lambda = c/2, c/4, c/5$) were analyzed by this method.

The difference equations relating the $\bar{w}$-values and $\bar{z}$-values at the intersections of the lines forming the networks result in a system of simultaneous linear equations. The number of those equations depends upon the number of intersection points or nodal points. In the particular plate under consideration, there is symmetry about both diagonals and, consequently, only one quarter of the plate need be analyzed.

If the length of the sides is divided into four parts ($\lambda = c/2$), it is apparent that four nodal points result (some of them are repeated), and, therefore, four simultaneous linear equations must be written and four coefficients are to be found. For $\lambda = c/4$ and $\lambda = c/5$, sixteen and twenty-five equations, respectively, must be written. As stated previously, the equations relating the deflections of the membranes involved in this method are usually in normal form, and they may be solved conveniently by the "Doolittle Method" of solving simultaneous equations.[19] The boundary conditions for the membranes associated with simply supported plates are indicated in Table 1. It is to be noted that the relations given for $\bar{z}$ in this table are also valid for $\bar{w}$.

TABLE 1.—BOUNDARY CONDITIONS FOR SKEW PLATES

Condition	(a) SQUARE MESH		(b) HEXAGONAL MESH	
	$\bar{z}_s$	$\bar{z}_q$	$\bar{z}_u$	$\bar{z}_R$
Simply supported edge	$\bar{z}_i = \bar{z}_n = 0$	$-\bar{z}_k$	$\bar{z}_i = \bar{z}_q = 0$	$-\bar{z}_k$
Clamped edge	$\bar{z}_i = \bar{z}_n = 0$	$+\bar{z}_k$	$\bar{z}_i = \bar{z}_q = 0$	$+\bar{z}_k$

Substitution in Eqs. 22 gives the following equations for the sixteen-coefficient solution—

$$\left.\begin{aligned} 4\,\bar{w}_1 - \frac{2}{3}(2\,\bar{w}_2) &= \frac{p\,\lambda^2}{S_1} \\ 4\,\bar{w}_2 - \frac{2}{3}(\bar{w}_1 + \bar{w}_2 + \bar{w}^3 + \bar{w}_4) &= \frac{p\,\lambda^2}{S_1} \end{aligned}\right\} \quad \ldots\ldots\ldots\ldots (32)$$

—etc.; and

$$\left.\begin{aligned} 4\,\bar{z}_1 - \frac{2}{3}(2\,\bar{z}_2) &= \bar{w}_1\frac{\lambda^2}{S_2} \\ 4\,\bar{z}_2 - \frac{2}{3}(\bar{z}_1 + \bar{z}_2 + \bar{z}_3 + \bar{z}_4) &= \bar{w}_2\frac{\lambda^2}{S_2} \end{aligned}\right\} \quad \ldots\ldots\ldots\ldots (33)$$

[19] "Application of the Theory of Least Squares to the Adjustment of Triangulation," by Oscar S. Adams, *Special Publication No. 28*, U. S. Coast and Geodetic Survey, Government Printing Office, Washington, D. C., 1915.

etc. Eqs. 32 and 33 may be put into the form given in Table 2. The last two columns in this table are the terms that appear on the right side of Eqs. 32 and 33. Hence, it is to be remembered that after each numerical value in these

TABLE 2.—NORMAL FORM OF DIFFERENCE EQUATIONS, EQUAL-SIDED, 30° SKEW PLATE; UNIFORMLY DISTRIBUTED LOAD, SIMPLY SUPPORTED

Coefficient No.:																$\frac{p\lambda^2}{S_1} = A$	$\frac{p\lambda^4}{S_1 S_2} = B$
1	2	3	4	5	6	7	8	9	10	11	12	13	14	15	16		
3	−1															−0.750000	−0.463973
−1	5	−1	−1													−1.500000	−1.658843
	−1	6	−1	−1	−1											−1.500000	−2.192174
	−1	−1	3		−1											−0.750000	−1.462041
		−1		6	−1	−1	−1									−1.500000	−2.523863
		−1	−1	−1	5		−1	−1								−1.500000	−3.796233
				−1		6	−1		−1	−1						−1.500000	−2.636190
				−1	−1	−1	6	−1		−1	−1					−1.500000	−4.268592
					−1		−1	3			−1					−0.750000	−2.411222
						−1			6	−1		−1	−1			−1.500000	−2.469393
						−1	−1		−1	6	−1		−1	−1		−1.500000	−4.305309
							−1	−1		−1	5			−1	−1	−1.500000	−5.277498
									−1			3	−0.5			−0.750000	−0.915260
									−1	−1		−0.5	3	−0.5		−0.750000	−1.897150
										−1	−1		−0.5	3	−0.5	−0.750000	−2.567936
											−1			−0.5	1.50	−0.375000	−1.401323

TABLE 3.—SOLUTION OF EQS. 32 AND 33 WITH REFERENCE TO TABLE 2

Point number:	$\bar{w}$	$\bar{z}$	Point number:	$\bar{w}$	$\bar{z}$
1	0.618631 A	0.811050 B	9	3.214962 A	8.697569 B
2	1.105895 A	1.969178 B	10	1.646262 A	3.956232 B
3	1.461449 A	3.107640 B	11	2.870206 A	7.690210 B
4	1.949388 A	4.268346 B	12	3.518332 A	9.904091 B
5	1.682575 A	3.949917 B	13	1.220346 A	2.718592 B
6	2.530822 A	6.266184 B	14	2.529533 A	6.568515 B
7	1.757560 A	4.290623 B	15	3.423915 A	9.605294 B
8	2.845728 A	7.511201 B	16	3.736860 A	10.738709 B

two columns (Table 2) there are actually an equal sign and zero, since a minus sign precedes each one. The "Doolittle Method" was adopted for simultaneous equations that happened to occur in normal form.[19]

The solution yields the values for $\bar{w}_1$, $\bar{w}_2$, $\bar{z}_1$, $\bar{z}_2$, etc., given in Table 3, in which, to simplify typography,

$$A = \frac{p\lambda^2}{S_1} \qquad (34a)$$

and

$$B = \frac{p\lambda^4}{S_1 S_2} \qquad (34b)$$

When all the $\bar{w}$-coefficients and $\bar{z}$-coefficients are found, it is an easy matter to obtain the deflections and moments. These are indicated for the sixteen-coefficient solution in Table 4. It is necessary to refer to Figs. 3(d) and 4(b) in the preparation and interpretation of these results. Similar analyses were made for the uniformly loaded, simply supported, 30° skew plate or slab, having equal sides, by utilizing four-coefficient and twenty-five-coefficient difference-equation networks (see Figs. 4(a) and 4(c)).

Table 5 affords a comparison of the moments and deflections at the center of the equal-sided, uniformly loaded, simply supported, 30° skew plate for

TABLE 4.—UNIFORMLY LOADED, SIMPLY SUPPORTED, 30° SKEW PLATE HAVING EQUAL SIDES

(Sixteen Coefficients, $\lambda = c/4$ and $\mu = 0.3$)

Point	Deflection $\frac{w\,N}{p\,c^4}$	Moments								Degrees, θ
		$\frac{M_1}{p\,\lambda^2}$	$\frac{M_2}{p\,\lambda^2}$	$\frac{M_3}{p\,\lambda^2}$	$\frac{M_x}{p\,\lambda^2}$	$\frac{M_y}{p\,\lambda^2}$	$\frac{M_{xy}}{p\,\lambda^2}$	$\frac{M_{max}}{p\,\lambda^2}$	$\frac{M_{min}}{p\,\lambda^2}$	
1	0.003168	1.321059	−0.057366	−0.057366	−0.057366	0.861586	−0.795830	1.321057	0.516837	30
2	0.007692	1.710194	0.100776	0.345535	0.100776	1.336888	−0.787882	1.720206	−0.282542	26
3	0.012139	1.801289	0.402802	0.645765	0.402802	1.497082	−0.667139	1.812749	0.087135	25.5
4	0.016673	2.209804	0.795747	0.795747	0.795747	1.738457	−0.816402	2.209804	0.324400	30
5	0.015429	1.648328	0.776816	0.855873	0.776816	1.410532	−0.457522	1.650204	0.537145	27.5
6	0.024477	2.380634	1.268258	1.286222	1.268258	2.021811	−0.631856	2.380698	0.909369	29.5
7	0.016760	1.276270	1.150963	0.999806	1.150963	1.133735	−0.159615	1.302199	0.982499	−43.5
8	0.029341	2.277665	1.671594	1.599924	1.671594	2.027852	−0.391292	2.279652	1.419794	33
9	0.033975	2.625404	1.821893	1.821893	1.821893	2.357588	−0.463905	2.625396	1.554056	30
10	0.015454	0.649457	1.436043	1.126153	1.436043	0.704098	0.275219	1.527981	0.612163	18
11	0.030040	1.925130	1.900214	1.771555	1.900214	1.831054	−0.088666	1.960806	1.770462	−34.5
12	0.038688	2.605217	2.146290	2.109223	2.146290	2.427542	−0.286360	2.605942	1.967889	32
13	0.010620	−0.425828	1.402770	1.402770	1.402770	0.183680	1.055736	2.012292	−0.425842	30
14	0.025658	1.328061	1.802272	1.802272	1.802272	1.487121	0.273784	1.960338	1.328054	30
15	0.037521	2.359530	2.158576	2.158576	2.158576	2.292514	−0.116020	2.359507	2.091583	30
16	0.041948	2.707839	2.289523	2.289523	2.289523	2.568395	−0.241513	2.707833	2.150086	30
17	0	....	....	....	0	0	−0.655560	0.655560	−0.655560	45
18	0	....	....	....	0	0	−0.936099	0.936099	−0.936099	45
19	0	....	....	....	0	0	−0.920203	0.920203	−0.920203	45
20	0	....	....	....	0	0	−0.680801	0.680801	−0.680801	45
21	0	....	....	....	0	0	−0.275388	0.275388	−0.275388	45
22	0	....	....	....	0	0	0.270284	0.270284	−0.270284	45
23	0	....	....	....	0	0	1.000367	1.000367	−1.000367	45
24	0	....	....	....	0.866348	−0.866348	0.500184	1.000367	−1.000367	15
25	0	....	....	....	0.234074	−0.234074	0.135142	0.270284	−0.270284	15
26	0	....	....	....	−0.238494	0.238494	−0.137694	0.275388	−0.275388	15
27	0	....	....	....	−0.589594	0.589594	−0.340401	0.680801	−0.680801	15
28	0	....	....	....	−0.796923	0.796923	−0.460101	0.920203	−0.920203	15
29	0	....	....	....	−0.810690	0.810690	−0.468049	0.936099	−0.936099	15
30	0	....	....	....	−0.567735	0.567735	−0.327780	0.655560	−0.655560	15

TABLE 5.—COMPARISON OF MOMENTS AND DEFLECTIONS AT THE CENTER OF THE UNIFORMLY LOADED, SIMPLY SUPPORTED, 30° SKEW PLATE FOR DIFFERENT NETWORKS

Description	Twenty-five coefficients	Sixteen coefficients	Four coefficients
λ	$c/5$	$c/4$	$c/2$
Moments:			
M_1	0.169566 $p\,c^2$	0.169240 $p\,c^2$	0.166256 $p\,c^2$
M_2	0.142812 $p\,c^2$	0.143095 $p\,c^2$	0.146451 $p\,c^2$
M_3	0.142812 $p\,c^2$	0.143095 $p\,c^2$	0.146451 $p\,c^2$
M_x	0.142812 $p\,c^2$	0.143095 $p\,c^2$	0.146451 $p\,c^2$
M_y	0.160650 $p\,c^2$	0.160524 $p\,c^2$	0.159654 $p\,c^2$
M_{xy}	−0.015446 $p\,c^2$	−0.015095 $p\,c^2$	−0.011434 $p\,c^2$
Deflections:			
w	0.041583 $p\,c^4/N$	0.041948 $p\,c^4/N$	0.045291 $p\,c^4/N$

three different networks. It is seen that the moments M_1, M_2, M_3, M_x, and M_y are in fairly good agreement even in the four-coefficient case. The twisting moments, M_{xy}, are in fair agreement only for the sixteen-coefficient and twenty-

five-coefficient solutions. The deflections at the center of the plate agree fairly well again only for the sixteen-coefficient and twenty-five-coefficient cases.

Solutions in Trigonometric Series.—Another approximate method for determining deflections and moments in a plate is one in which the deflection function is set up in the form of a trigonometric series, satisfying the plate equation. This series contains a set of arbitrary constants that can be computed in such a manner as to satisfy the boundary conditions at an arbitrary number of points. The degree of approximation, naturally, depends upon the number of points selected on the boundary, but it has been found that in many cases a relatively small number of points is sufficient to give fairly reliable results. There is reason to believe that the use of approximate methods is justified, since the assumptions made in theories are very seldom entirely true in practice.

The approximate determination of the stress function for the prismatic bar in torsion and the deflection function in a clamped square plate has been indicated by J. Barta.[20] These problems had been solved previously by more exact methods, and the agreement found by Mr. Barta was fairly good.

The trigonometric-series approach may be used quite readily in the solution of both simply supported and clamped skew plates. Both of these cases are

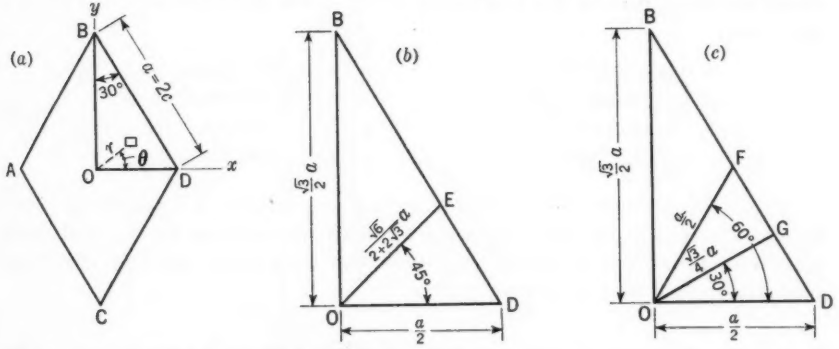

FIG. 5.—DIAGRAMS FOR TRIGONOMETRIC-SERIES ANALYSES OF SKEW PLATES (AB = AC = BD = CD)

treated for a 30° skew in this paper. It is to be noted (see Fig. 5) that a new set of Cartesian-coordinate axes is chosen in order to take advantage of symmetry.

In Fig. 5(*c*) it is seen that the number of points chosen along the entire boundary is 12. It is sufficient, therefore, to satisfy the boundary conditions at points B, D, F, and G. Because of symmetry, the assumed deflection function is taken to be

$$w = \frac{p\,r^4}{64\,N} + a_0 + r^2\,a_2 \cos 2\theta + r^2\,c_2 + r^4\,a_4 \cos 4\theta + r^4\,c_4 \cos 2\theta + r^6\,a_6 \cos 6\theta + r^6\,c_6 \cos 4\theta + r^8\,c_8 \cos 6\theta \ldots\ldots\ldots\ldots (35)$$

[20] "Über die näherungsweise Lösung einiger zweidimensionaler Elastizitätsaufgaben," by J. Barta, *Zeitschrift für Angewandte Mathematik und Mechanik*, Vol. 17, No. 3, 1937, pp. 184–185.

The boundary conditions for a simply supported edge (length of side = a) are: $w = 0$; and

$$\nabla^2 w = \frac{\partial^2 w}{\partial x^2} + \frac{\partial^2 w}{\partial y^2} = 0 \quad \ldots\ldots (36)$$

which, in polar form, becomes Eq. 12a equated to zero.

From Eqs. 35, 36, and 12a it is clear that, at the boundary points, the following relations must be valid:

$$w = \frac{p\,r^4}{64\,N} + a_0 + r^2\,a_2 \cos 2\,\theta + r^2\,c_2 + r^4\,a_4 \cos 4\,\theta + r^4\,c_4 \cos 2\,\theta + r^6\,a_6 \cos 6\,\theta + r^6\,c_6 \cos 4\,\theta + r^8\,c_8 \cos 6\,\theta = 0 \quad \ldots\ldots (37a)$$

and

$$\nabla^2 w = \frac{p\,r^2}{4\,N} + 4\,c_2 + 12\,r^2\,c_4 \cos 2\,\theta + 20\,r^4\,c_6 \cos 4\,\theta + 28\,r^6\,c_8 \cos 6\,\theta = 0 \quad \ldots\ldots (37b)$$

It may be shown easily that the assumed deflection function (Eq. 35) satisfies the plate formula, Eq. 4.

By substituting the values of r and θ for points B, D, F, and G in Eqs. 37, and allowing a and its powers to equal unity, it is possible to obtain eight simultaneous equations, the solution of which yields the values of the arbitrary constants:

$$\left.\begin{array}{ll} a_0 = 0.0027059329\,p/N & c_4 = 0.0057873004\,p/N \\ a_2 = -\,0.0038678560\,p/N & a_6 = 0.0041150544\,p/N \\ c_2 = -\,0.0148808677\,p/N & c_6 = -\,0.0138895211\,p/N \\ a_4 = 0.0131565067\,p/N & c_8 = -\,0.0068034953\,p/N \end{array}\right\} \quad \ldots (38)$$

These values, multiplied by the corresponding powers of a (length of side), may be inserted in Eq. 35 to give the approximate solution for the deflection function. From the resulting expression the maximum value of deflection may be obtained by letting $r = 0$:

$$w_{max} = 0.0432949264\,\frac{p\,c^4}{N} \quad \ldots\ldots (39a)$$

in which $a = 2\,c$. The corresponding value obtained by the method of finite differences is

$$w_{max} = 0.041583\,\frac{p\,c^4}{N} \quad \ldots\ldots (39b)$$

which indicates a difference of about 4%, based upon the difference-equation value.

From Eqs. 13 and 35, expressions may be deduced which, for the center of the plate ($r = 0$ and $\theta = 0$), reduce to:

$$M_r = -\,2\,N\,[a_2 + c_2 + \mu\,(c_2 - a_2)] \quad \ldots\ldots (40a)$$

and

$$M_t = -\,2\,N\,[\mu\,(a_2 + c_2) - a_2 + c_2] \quad \ldots\ldots (40b)$$

At the center of the plate these moments are found to be

$$M_r = 0.1764210176\, p\, c^2 \ldots\ldots\ldots\ldots\ldots\ldots (41a)$$

and

$$M_t = 0.1331010304\, p\, c^2 \ldots\ldots\ldots\ldots\ldots\ldots (41b)$$

which compare fairly well with the corresponding difference-equation moments

$$M_r = 0.169566\, p\, c^2 \ldots\ldots\ldots\ldots\ldots\ldots (42a)$$

and

$$M_t = 0.133894\, p\, c^2 \ldots\ldots\ldots\ldots\ldots\ldots (42b)$$

The differences based upon the difference-equation values for these radial and tangential moments are 4% and 0.6%, respectively. The agreement for the deflections and moments in this case is fairly good.

Power-Series Method.—Several power-series approaches may be found for the approximate solution of plate problems. One of these is presented in this paper, whereas others studied in the investigation are given in a more detailed report filed in the Engineering Societies Library.[20a] In the detailed report plates with unequal sides are also treated.

In the case of the uniformly loaded, simply supported, 30° skew plate having equal sides, it is desirable to establish a set of Cartesian-coordinate axes as shown in Fig. 6(*a*). This enables one to take advantage of the symmetry

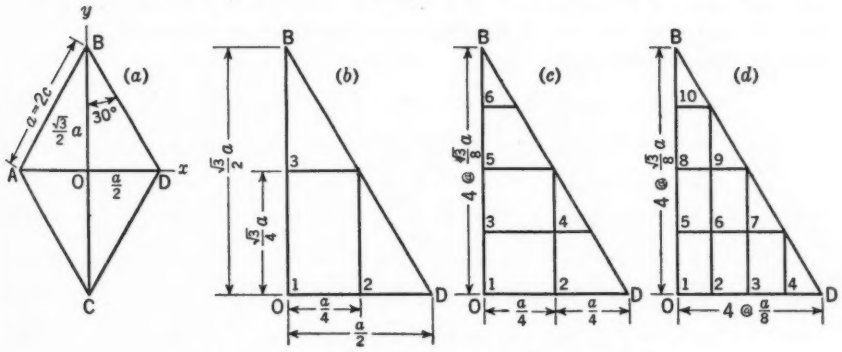

FIG. 6.—POWER-SERIES NETWORKS FOR SKEW PLATES

prevailing about both axes. The deflection function may be written in the form

$$w = \frac{p}{N}\left(y + \sqrt{3}\,x + \frac{\sqrt{3}}{2}a\right)\left(y - \sqrt{3}\,x - \frac{\sqrt{3}}{2}a\right)\left(y + \sqrt{3}\,x - \frac{\sqrt{3}}{2}a\right) \times \left(y - \sqrt{3}\,x + \frac{\sqrt{3}}{2}a\right) \sum_{m=0,2,\ldots}^{\infty} \sum_{n=0,2,\ldots}^{\infty} C_{m,n} \left(\frac{x}{a}\right)^m \left(\frac{y}{a}\right)^n \ldots\ldots (43)$$

Since Eq. 43 involves the product of expressions for the sides, it is apparent that one of the boundary conditions, $w = 0$, is already satisfied.

[20a] 29 West 39th St., New York. N. Y

Other conditions to be imposed on Eq. 43 are that $\nabla^4 w = \frac{p}{N}$ (Eq. 4) throughout the entire plate, and that $\nabla^2 w = 0$ (see Eq. 36) along the boundary.

It is to be expected that an approximate solution of the deflection function should result, if Eqs. 4 and 36 are satisfied only at certain points within the plate and certain other points along the boundary, respectively. One particular case involving points B, D, and E, along the boundary, and points 1, 2, 4, and 5 (see Fig. 6(*c*)) yielded the following values for the center of the plate ($a = 2\,c$):

$$w = 0.045007\,\frac{p\,c^4}{N} \quad \ldots\ldots (44)$$

$$M_x = 0.196316\,p\,c^2 \quad \ldots\ldots (45a)$$

and

$$M_y = 0.110744\,p\,c^2 \quad \ldots\ldots (45b)$$

which are about 8%, 16%, and 17% different from the corresponding difference-equation values.

Clamped 30° Skew Plate with Equal Sides Subjected to a Uniformly Distributed Load

Analysis by Method of Finite Differences.—In solving the problem of the clamped plate, it is convenient to relate the membrane deflections in such a manner that only one set of simultaneous equations need be solved. From Eqs. 19, 22*b*, and Fig. 3(*e*),

$$4\,\bar{z}_k - 2/3\,(\bar{z}_i + \bar{z}_l + \bar{z}_o + \bar{z}_p + \bar{z}_q + \bar{z}_r) = \bar{w}_k\,\lambda^2/S_2 \quad \ldots\ldots (46a)$$

$$4\,\bar{z}_i - 2/3\,(\bar{z}_A + \bar{z}_k + \bar{z}_R + \bar{z}_q + \bar{z}_U + \bar{z}_o) = \bar{w}_i\,\lambda^2/S_2 \quad \ldots\ldots (46b)$$

$$4\,\bar{z}_l - 2/3\,(\bar{z}_k + \bar{z}_B + \bar{z}_r + \bar{z}_T + \bar{z}_p + \bar{z}_V) = \bar{w}_l\,\lambda^2/S_2 \quad \ldots\ldots (46c)$$

$$4\,\bar{z}_q - 2/3\,(\bar{z}_R + \bar{z}_r + \bar{z}_C + \bar{z}_G + \bar{z}_i + \bar{z}_k) = \bar{w}_q\,\lambda^2/S_2 \quad \ldots\ldots (46d)$$

$$4\,\bar{z}_r - 2/3\,(\bar{z}_q + \bar{z}_T + \bar{z}_G + \bar{z}_D + \bar{z}_k + \bar{z}_l) = \bar{w}_r\,\lambda^2/S_2 \quad \ldots\ldots (46e)$$

$$4\,\bar{z}_o - 2/3\,(\bar{z}_U + \bar{z}_p + \bar{z}_i + \bar{z}_k + \bar{z}_E + \bar{z}_H) = \bar{w}_o\,\lambda^2/S_2 \quad \ldots\ldots (46f)$$

$$4\,\bar{z}_p - 2/3\,(\bar{z}_o + \bar{z}_V + \bar{z}_k + \bar{z}_l + \bar{z}_H + \bar{z}_F) = \bar{w}_p\,\lambda^2/S_2 \quad \ldots\ldots (46g)$$

From Eqs. 22*a* and 46 the more convenient form is found as follows:

$$42\,\bar{z}_k - 10\,(\bar{z}_i + \bar{z}_l + \bar{z}_o + \bar{z}_p + \bar{z}_q + \bar{z}_r) + (\bar{z}_A + \bar{z}_B + \bar{z}_C + \bar{z}_D + \bar{z}_E + \bar{z}_F) + 2\,(\bar{z}_R + \bar{z}_T + \bar{z}_U + \bar{z}_V + \bar{z}_G + \bar{z}_H) = \frac{9}{4}\,\frac{p\,\lambda^4}{S_1\,S_2} \quad \ldots\ldots (47)$$

For this particular clamped plate, sixteen coefficients were used (see Fig. 4(*b*)). Table 6 contains the deflections and moments at the intersection points of the network and at certain boundary points.

Solutions in Trigonometric Series.—The trigonometric-series approach, as mentioned previously, applies to the clamped skew plate as well as to the simply supported case. Again, a plate having a 30° skew is selected, the sides being clamped and the lengths equal to a. The assumed function for the deflections

must satisfy the plate formula, Eq. 4, throughout the entire plate and the boundary conditions, as before, are to be met at an arbitrary number of points (twelve in this case).

TABLE 6.—UNIFORMLY LOADED, CLAMPED, 30° SKEW PLATE HAVING EQUAL SIDES

(Sixteen Coefficients, $\lambda = c/4$ and $\mu = 0.3$)

Point	Deflection, $\frac{w\,N}{p\,c^4}$	Moments		
		$\frac{M_x}{p\,\lambda^2}$	$\frac{M_y}{p\,\lambda^2}$	$\frac{M_{xy}}{p\,\lambda^2}$
1	0.000440	−0.084288	0.075654	−0.138513
2	0.001339	−0.226305	0.209767	−0.156285
3	0.002410	−0.369557	0.201683	−0.073520
4	0.003919	0.107912	0.488398	−0.329509
5	0.003291	−0.431873	0.089358	0.061223
6	0.006665	0.277831	0.720474	−0.260080
7	0.003664	−0.362506	−0.060125	0.208976
8	0.008551	0.458341	0.744322	−0.119157
9	0.010656	0.939737	1.699625	−0.244719
10	0.003240	−0.177311	−0.216376	0.347719
11	0.008760	0.585401	0.611740	0.054672
12	0.012802	0.958844	1.123920	−0.131579
13	0.001782	−0.082983	−0.527702	0.385134
14	0.006963	0.524883	0.390833	0.202693
15	0.012224	0.958416	0.989663	−0.027060
16	0.014384	1.112409	1.250479	−0.119571
17	0	−0.045034	−0.150112	0
18	0	−0.182127	−0.607089	0
19	0	−0.383836	−1.279452	0
20	0	−0.583738	−1.945795	0
21	0	−0.712181	−2.373603	0
22	0	−0.706964	−2.356548	0
23	0	−0.514224	−1.714081	0
24	0	−1.414117	−0.814189	0.519550
25	0	−1.944152	−1.119360	0.714287
26	0	−1.958497	−1.127620	0.719557
27	0	−1.605281	−0.924252	0.589784
28	0	−1.055548	−0.607740	0.387811
29	0	−0.500849	−0.288367	0.184013
30	0	−0.123842	−0.071303	0.045500

Boundary conditions at points B, D, F, and G (see Fig. 5(*c*)), which must be satisfied are: $w = 0$; $\partial w/\partial r = 0$; and $\partial w/\partial \theta = 0$.

Because of symmetry the deflection function may be put in the form

$$w = \frac{p\,r^4}{64\,N} + a_0 + r^2\,a_2 \cos 2\,\theta + r^2\,c_2 + r^4\,a_4 \cos 4\,\theta + r^4\,c_4 \cos 2\,\theta + r^6\,a_6 \cos 6\,\theta + r^6\,c_6 \cos 4\,\theta + r^8\,a_8 \cos 8\,\theta + r^8\,c_8 \cos 6\,\theta + r^{10}\,c_{10} \cos 8\,\theta \quad \ldots\ldots\ldots\ldots\ldots\ldots (48)$$

Differentiation of Eq. 48 results in

$$\frac{\partial w}{\partial r} = \frac{p\,r^3}{16\,N} + 2\,r\,a_2 \cos 2\,\theta + 2\,r\,c_2 + 4\,r^3\,a_4 \cos 4\,\theta + 4\,r^3\,c_4 \cos 2\,\theta + 6\,r^5\,a_6 \cos 6\,\theta + 6\,r^5\,c_6 \cos 4\,\theta + 8\,r^7\,a_8 \cos 8\,\theta + 8\,r^7\,c_8 \cos 6\,\theta + 10\,r^9\,c_{10} \cos 8\,\theta \quad \ldots\ldots\ldots (49a)$$

and

$$\frac{\partial w}{\partial \theta} = -2r^2 a_2 \sin 2\theta - 4r^4 a_4 \sin 4\theta - 2r^4 c_4 \sin 2\theta - 6r^6 a_6 \sin 6\theta - 4r^6 c_6 \sin 4\theta - 8r^8 a_8 \sin 8\theta - 6r^8 c_8 \sin 6\theta - 8r^{10} c_{10} \sin 8\theta \quad \ldots\ldots (49b)$$

By substituting values of r and θ for points B, D, F, and G (see Fig. 5(c)) and setting a equal to unity, it is feasible to derive ten simultaneous equations, the solution of which gives the values

$$\left.\begin{array}{ll} a_0 = 0.0007979061\, p/N & a_6 = -0.0168885960\, p/N \\ a_2 = -0.0022057884\, p/N & c_6 = -0.0493657788\, p/N \\ c_2 = -0.0065078196\, p/N & a_8 = 0.0177867736\, p/N \\ a_4 = 0.0128847660\, p/N & c_8 = 0.0297909016\, p/N \\ c_4 = 0.0057365111\, p/N & c_{10} = 0.0276254724\, p/N \end{array}\right\} \ldots (50)$$

These values, it must be remembered, are to be multiplied by appropriate powers of a before they are inserted in Eq. 48 to give the approximate solution for the deflection function. The maximum deflection for this plate occurs at the center ($r = 0$), and its value is found to be

$$w_{\max} = 0.0127664976 \frac{p c^4}{N} \quad \ldots\ldots (51a)$$

The corresponding value obtained by means of difference equations is

$$w_{\max} = 0.014384 \frac{p c^4}{N} \quad \ldots\ldots (51b)$$

which indicates a difference of about 11% based on the latter value. Referring to Eqs. 13, it is possible to deduce expressions for the radial and tangential moments, which for the center of the plate ($r = 0$ and $\theta = 0$) reduce to the same form as that found for the simply supported plate, Eqs. 40, except that the values of the constants are different. Substitution of the values obtained for a_2 and c_2 in Eqs. 40 gives:

$$M_r = 0.0800337388\, p c^2 \quad \ldots\ldots (52a)$$

and

$$M_t = 0.0553289088\, p c^2 \quad \ldots\ldots (52b)$$

The corresponding difference-equation values are

$$M_r = 0.082470\, p c^2 \quad \ldots\ldots (53a)$$

and

$$M_t = 0.065211\, p c^2 \quad \ldots\ldots (53b)$$

indicating, for the radial and tangential moments at the center, a difference of about 3% and 15%, respectively, based on the difference-equation moments. Obviously, in the case of the clamped plate, the boundary conditions should be satisfied for a greater number of points (for the same degree of approximation) than in the case of the simply supported skew plate.

For the equal-sided clamped 30° skew plate with the boundary conditions being satisfied at only eight points along the entire boundary (see Fig. 5(*b*)), the results are naturally less reliable than those obtained when twelve points are taken into consideration.

The maximum deflection of the plate obtained by the trigonometric-series approach for this case (eight boundary points considered) is approximately 17% too low based on the difference-equation result. The difference between the radial and tangential moments as obtained by the trigonometric and difference-equation methods average about 20%. Clearly, the degree of approximation in this case is not satisfactory.

Power-Series Method.—The clamped 30° skew plate having equal sides and subjected to a uniformly distributed load may also be analyzed by power-series methods. The deflection function may be written in the form (see Fig. 6),

$$w = \frac{p}{a^4 N}\left(y + \sqrt{3}\,x + \frac{\sqrt{3}}{2}a\right)^2\left(y - \sqrt{3}\,x - \frac{\sqrt{3}}{2}a\right)^2\left(y + \sqrt{3}\,x - \frac{\sqrt{3}}{2}a\right)^2 \times \left(y - \sqrt{3}\,x + \frac{\sqrt{3}}{2}a\right)^2 \sum_{m=0,2,4,\ldots}^{\infty} \sum_{n=0,2,4,\ldots}^{\infty} C_{m,n}\left(\frac{x}{a}\right)^m\left(\frac{y}{a}\right)^n \quad \ldots(54)$$

from which it is apparent that the boundary conditions $w = 0$, $\partial w/\partial x = 0$, and $\partial w/\partial y = 0$ are valid. The plate formula, Eq. 4, must also be satisfied. By doing this for only a certain number of interior points, it is possible to solve the problem approximately. It is convenient to select the number of points to correspond to the number of constants, $C_{m,n}$, chosen for the series; in this manner one obtains as many equations as there are unknowns in the series. Eq. 4 may be satisfied for a larger number of points by normalizing the resulting equations. This process yields a system of linear equations in normal form (symmetry about the diagonal) which may easily be solved by the Doolittle Method.[19]

Six points are now selected within the plate (see Fig. 6(*c*)) and, correspondingly, six coefficients are taken in the power series. Obviously, from symmetry, these are $C_{0,0}$, $C_{2,0}$, $C_{0,2}$, $C_{4,0}$, $C_{2,2}$, $C_{0,4}$. From Eq. 54, by a few simple operations, one may derive the differential equation presented (for compactness) in Table 7.

Substitution of values of x and y in Table 7 for the six points gives rise to a system of equations, the solution of which yields the values

$$C_{0,0} = 2.6184138565 \times 10^{-3} \qquad C_{4,0} = 20.1633240889 \times 10^{-3}$$
$$C_{2,0} = 11.8165756479 \times 10^{-3} \qquad C_{2,2} = -10.3051787620 \times 10^{-3}$$
$$C_{0,2} = -2.6453532509 \times 10^{-3} \qquad C_{0,4} = -1.1029769807 \times 10^{-3}$$

The maximum deflection of the plate is found to be

$$w_{max} = 0.0008284825\,\frac{p\,a^4}{N} \quad \ldots(55a)$$

which is about 7.8% less than the difference-equation value—

$$w_{max} = 0.000899\,\frac{p\,a^4}{N} \quad \ldots(55b)$$

From Eqs. 1 and 54 it is possible to determine the bending moments at the center of the plate

$$M_x = 0.084732\, p\, c^2 \quad \ldots\ldots (56a)$$

and

$$M_y = 0.051492\, p\, c^2 \quad \ldots\ldots (56b)$$

TABLE 7.—DIFFERENTIAL EQUATION DERIVED FROM EQ. 54, WITH $a = 1$

$$\frac{N}{p}\nabla^4 w =$$

$$+ 864\, C_{0,0} - 135\, C_{2,0} - 81\, C_{0,2} + \frac{243}{32} C_{4,0} + \frac{81}{32} C_{2,2} + \frac{243}{32} C_{0,4}$$
$$+ x^2 \left(-27{,}648\, C_{0,0} + 11{,}340\, C_{2,0} + 1{,}620\, C_{0,2} - \frac{3{,}807}{2} C_{4,0} - \frac{567}{2} C_{2,2} - \frac{243}{2} C_{0,4}\right)$$
$$+ x^4 (124{,}416\, C_{0,0} - 132{,}624\, C_{2,0} - 9{,}072\, C_{0,2} + 51{,}921\, C_{4,0} + 3{,}807\, C_{2,2} + 729\, C_{0,4})$$
$$+ x^6 (385{,}344\, C_{2,0} + 15{,}552\, C_{0,2} - 401{,}976\, C_{4,0} - 17{,}496\, C_{2,2} - 1{,}944\, C_{0,4})$$
$$+ x^8 (924{,}696\, C_{4,0} + 26{,}568\, C_{2,2} + 1{,}944\, C_{0,4})$$
$$+ y^2 \left(324\, C_{2,0} + 2{,}268\, C_{0,2} - \frac{81}{2} C_{4,0} - \frac{405}{2} C_{2,2} - \frac{1{,}701}{2} C_{0,4}\right)$$
$$+ y^4 (1{,}536\, C_{0,0} - 144\, C_{2,0} - 3{,}312\, C_{0,2} + 81\, C_{4,0} + 567\, C_{2,2} + 7{,}209\, C_{0,4})$$
$$+ y^6 (-64\, C_{2,0} + 3{,}648\, C_{0,2} - 72\, C_{4,0} - 456\, C_{2,2} - 12{,}456\, C_{0,4})$$
$$+ y^8 (24\, C_{4,0} + 72\, C_{2,2} + 8{,}856\, C_{0,4})$$
$$+ x^2 y^2 (-27{,}648\, C_{0,0} + 11{,}232\, C_{2,0} - 18{,}144\, C_{0,2} + 3{,}402\, C_{4,0} + 14{,}094\, C_{2,2} + 11{,}178\, C_{0,4})$$
$$+ x^2 y^4 (12{,}480\, C_{2,0} - 20{,}160\, C_{0,2} + 1{,}080\, C_{4,0} + 11{,}160\, C_{2,2} + 5{,}400\, C_{0,4})$$
$$+ x^2 y^6 (-2{,}976\, C_{4,0} + 8{,}352\, C_{2,2} - 26{,}784\, C_{0,4})$$
$$+ x^4 y^2 (-146{,}880\, C_{2,0} + 77{,}760\, C_{0,2} + 50{,}760\, C_{4,0} - 113{,}400\, C_{2,2} - 48{,}600\, C_{0,4})$$
$$+ x^4 y^4 (70{,}800\, C_{4,0} - 104{,}400\, C_{2,2} + 32{,}400\, C_{0,4})$$
$$+ x^6 y^2 (-476{,}064\, C_{4,0} + 282{,}528\, C_{2,2} + 69{,}984\, C_{0,4})$$
$$= 1$$

These are about 3% and 21% different from the corresponding difference-equation values.

SUMMARY AND CONCLUSIONS

In this paper a theoretical study of uniformly loaded, simply supported, and clamped skew plates has been made by means of approximate methods. No exact solution of skew plate problems has come to the attention of the writer, and consequently comparisons were made between approximate methods.

A survey was made of a few systems of coordinates in order to ascertain their convenience in the treatment of triangular and skew plates. The trilinear and quadrilinear systems appear to have no particular advantages, except possibly as regards the question of symmetry. Both seem to require more effort than the Cartesian-coordinate system in the solution of the same problems. The trilinear system has been suggested by an investigator who solved plate problems that have also been analyzed by Cartesian coordinates. The quadrilinear system, in the case of power-series methods, would definitely involve more work. Polar-coordinate equations, on the other hand, have been very useful in the trigonometric-series solutions.

From a preliminary survey of triangular plates and a more extensive investigation of the uniformly loaded, simply supported, 30° skew plate having equal sides, a measure of the reliability of difference-equation results for various

densities of networks was obtained. In general, it may be stated that a relatively small number of nodal points gives values which are in fair agreement with those of more dense and, hence, more accurate networks. This is especially true in the case of bending moments. More specifically, in this connection, the following observations are noteworthy:

(1) In the case of simply supported equilateral, triangular plates, subjected to uniformly distributed loads, reasonably good results are obtainable by the method of finite differences even for a relatively small number of coefficients—say, five. The maximum deflection given by the five-coefficient solution and the eight-coefficient solution varied from the exact solution by 2.7% and 1.2%, respectively.

(2) A comparison of deflections at certain points of the simply supported, 30°-60°-90° plate subjected to a uniformly distributed load obtained by networks having three and twenty-one nodal points showed a difference of about 6% or 7%.

(3) For the simply supported isosceles, right triangular plate subjected to a uniformly distributed load, the deflections as obtained by A. Nadai's approximation and a difference-equation network having twelve coefficients are in fair agreement at points near the center of gravity of the plate, but nearer the boundaries there is considerable disagreement.

(4) A comparison of bending moments and twisting moments at similar points of the uniformly loaded, simply supported, 30° skew plate (equal sides) obtained by the four-coefficient solution and the sixteen-coefficient solution indicated reasonably good agreement. At one pair of corresponding points the results agreed well within 1%. Two other pairs, for which a comparison was made, showed a maximum difference of about 5% for bending moments, whereas the twisting moments varied by about 10% in one case and by about 22% in the other. The deflections differed by about 8% or 9% for the three points investigated.

(5) At the center of the uniformly loaded, simply supported, 30° skew plate having equal sides, the bending moments and deflections resulting from the networks having twenty-five and sixteen coefficients agreed well within 1%. The corresponding twisting moments differed by only 2%.

(6) A similar comparison (see conclusion (5)) between these results as obtained by the twenty-five-coefficient and the four-coefficient solutions showed good agreement (within 3%) for the bending moments. The twisting moments and deflections at the center differed by 19% and 9%, respectively.

The uniformly loaded, simply supported, 30° skew plate with equal sides was analyzed by the trigonometric-series and power-series methods, as well as by the difference-equation method, and certain deflections and moments were compared. The following comparisons may be enumerated:

(*a*) The maximum deflection given by the trigonometric-series method for this case (eight coefficients) differs by about 4% from the difference-equation

value. At the center of the plate, the radial and tangential moments differ by 4% and 0.6%, respectively, for these same two methods. The agreement here is seen to be good.

(*b*) At the center of the plate, the deflection, w, and the moments M_x and M_y, as obtained by the method using power series (only three terms and seven points considered), differed by 8%, 16%, and 17%, respectively, from the corresponding difference-equation values. By increasing the number of terms in the series and the number of points for which the conditions are satisfied, it would appear to be possible to increase the accuracy.

The clamped 30° skew plate with equal sides, subjected to a uniformly distributed load, was studied by similar methods, and the following observations were made:

(*A*) A difference of 11% was found between the maximum deflections as obtained by trigonometric series (ten coefficients) and by difference equations. The radial and tangential moments at the center differed (for these two methods) by about 3% and 15%, respectively.

(*B*) The values for the maximum deflection as obtained by power series (six coefficients) and difference equations differed by 7.8%. The moments M_x and M_y differed by 3% and 21%, respectively.

Structural action of skew plates and slabs in the region of corners was not treated. Singularities prevailing in these sections probably necessitate the use of more rigorous, mathematical methods.

Acknowledgment

The source of the material for this paper was a thesis by the writer, entitled "A Theoretical Study of Skew Plates," presented to Lehigh University, Bethlehem, Pa., in June, 1941, in partial fulfilment of the requirements for the degree of Doctor of Philosophy.

This investigation was conducted under the general supervision of Hale Sutherland, M. Am. Soc. C. E., Director of the Fritz Engineering Laboratory of Lehigh University, while the writer served as Instructor in Theoretical and Applied Mechanics at the University of Illinois, Urbana, Ill. The suggestions and criticisms of Professors Newmark and Jensen, previously mentioned, are gratefully acknowledged.

APPENDIX

Notation

The following letter symbols conform essentially to American Standard Letter Symbols for Mechanics, Structural Engineering and Testing Materials (ASA—Z10a—1932) prepared by a Committee of the American Standards

Association, with Society representation, and approved by the Association in 1932:

A = a substitution coefficient in Table 2;
a = a horizontal dimension of plate (for example, see Fig. 5);
a_n = a coefficient in a trigonometric series;
B = a substitution coefficient in Table 2;
C = coefficient; $C_{m,n}$ = a coefficient in a power series;
c = a horizontal dimension of a plate (for example, see Fig. 5);
c_n = a coefficient in a trigonometric series;
E = the modulus of elasticity of a material in tension and compression;
G = the modulus of elasticity of a material in shear;
h = thickness of plate;
M = moment (positive directions shown in Fig. 1):

- M_x, M_y = bending moments per unit of length in sections perpendicular to the x-axis and the y-axis, respectively;
- M_{xy} = twisting moment per unit of length in sections perpendicular to the x-axis;
- M_r, M_t = bending moments per unit of length in sections perpendicular to radial and tangential directions (positive when producing compression in the top fibers of a plate);
- $M_{r,t}$ = twisting moments per unit of length in sections perpendicular to radial directions;
- M_1, M_2, M_3 = bending moments per unit of length in sections perpendicular to directions 1, 2, and 3, respectively;
- M_t = maximum value of a twisting moment (Eq. 30);

$\bar{M}$ = a function of the moment sum (Eq. 14); $\bar{M}_k$ = value of $\bar{M}$ at the nodal point k (Eq. 19);
N = flexural rigidity of the plate (Eq. 2);
n = a direction in any given plane, perpendicular to direction t (n = "normal" and t = "tangential");
p = uniformly distributed lateral unit load;
R = reactions; R_x and R_y = vertical reaction per unit of length in sections normal to the x-axis and the y-axis, respectively;
r = radius = polar coordinate with angular displacement θ; r_x, r_y = radii of curvature of the middle surface of a plate in planes parallel to the xz-plane and the yz-plane, respectively;
S = horizontal component of the surface stresses; S_1 = S referred to the first membrane, etc. (Eq. 19);
t = a direction perpendicular to n;
u = displacement in the x-direction;
V = vertical shear:

- V_x, V_y = vertical shear per unit of length in sections normal to the x-axis and the y-axis, respectively;

V_{1k} = vertical shear referring to the nodal point k and the plane 1;

v = displacement in the y-direction;

w = displacement in the z-direction; $\bar{w}$ = deflection of first membrane ($\bar{w}_k$ = values of $\bar{w}$ referred to the nodal point k);

x = distances in the x-direction;

y = distances in the y-direction;

z = distances in the z-direction ($\bar{z}_k$ = the deflection of the nodal point k in the second membrane);

θ = angular displacement; polar coordinate with the radius r;

λ = intervals in difference-equation networks (see, for example, Fig. 3), subscripts x and y referring to respective axes;

μ = Poisson's ratio (lateral contraction to longitudinal elongation);

σ = bending stress; σ_x, σ_y = normal components of bending stress in the x-direction and the y-direction, respectively;

τ = shear stress; τ_{xy}, τ_{xz}, τ_{yz} = shearing components of stress, the first subscript in each case indicating the axis to which the plane (in which the stress is acting) is normal, and the second subscript indicating the direction of the shearing stress;

∇ = the Laplace operator.

AMERICAN SOCIETY OF CIVIL ENGINEERS

Founded November 5, 1852

PAPERS

CORRELATING FLOOD CONTROL AND WATER SUPPLY, LOS ANGELES COASTAL PLAIN

BY FINLEY B. LAVERTY,[1] M. AM. SOC. C. E.

SYNOPSIS

Depletion of ground-water supplies by the heavy draft of new war industries has reemphasized the importance of water conservation in Los Angeles County, California, and other arid sections of western United States. The scope of this paper is limited to a description of the use of flood control reservoirs to supplement normal surface water supplies as well as underground storage; a description of development of, and a presentation of data obtained from, extensive off-stream flood water spreading grounds used to replenish ground water by percolation; and data gathered on the quality of flood waters.

Flood control works in Los Angeles County consist of three principal types —dams, channels, and water spreading grounds. Each of these takes a part in the water supply of the Los Angeles Coastal Plain. Since its inception as a State District in 1916, Los Angeles County Flood Control District has carried on a program of development of flood control and water conservation works. At present this system includes 18 dams and 18 debris basins, controlling 447 sq miles of mountain watershed; 226 miles of permanently or temporarily improved flood channels; about 2,500 check dams; and 7 water spreading grounds located adjacent to some of these channels.

It is unusual to operate reservoirs for both flood control and water conservation. Yet this dual function is necessary—first, to cope with the intense storms which frequently occur in the Los Angeles area making flood control of prime importance during the storm season; and second, to meet the demands of a high degree of agricultural development in a naturally arid region by conserving water which would otherwise waste to the ocean. Consequently, the reservoirs are operated primarily for flood regulation during the period of the greatest likelihood of severe storms, which is from December into March. During this period regulated releases often increase contributions to ground

NOTE.—Written comments are invited for immediate publication; to insure publication the last discussion should be submitted by **November 1, 1945.**

[1] Chf. Hydr. Engr., Los Angeles County Flood Control Dist., Los Angeles, Calif.

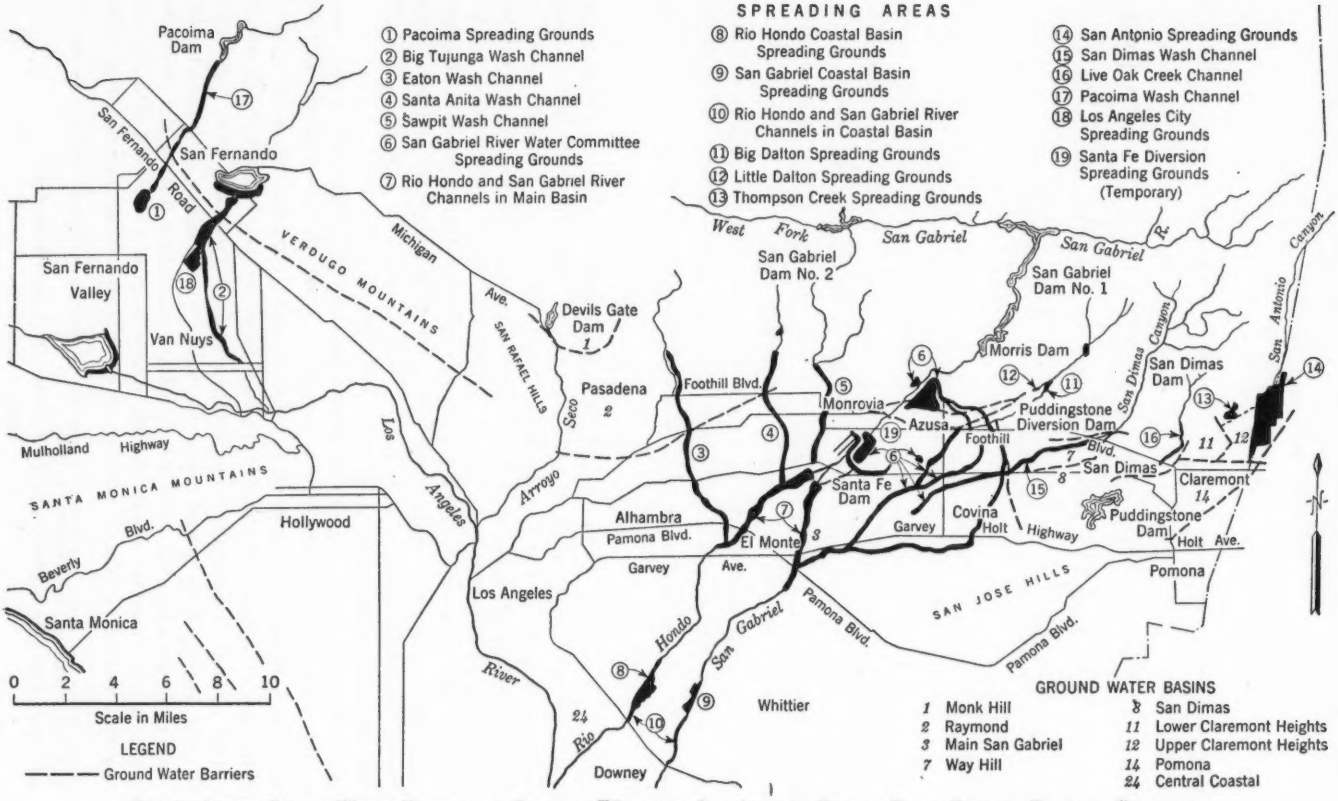

FIG. 1.—DAMS, GROUND-WATER BASINS, AND SPREADING GROUNDS, LOS ANGELES COUNTY FLOOD CONTROL DISTRICT, CALIFORNIA

water from stream-bed percolation; and off-stream spreading grounds are operated whenever the quantity of water stored and the probable period between storms warrant constructing temporary diversion dams in natural river beds, or operating permanent diversion works in improved channels. After the middle of March, flood control regulating capacity is gradually encroached on until the middle of April when all available surplus stream flow is stored. This accumulated storage is used for direct domestic and agricultural supply. Any additional reservoir water is put into underground storage by percolation in channels and spreading grounds. In this manner the cycle is completed and the reservoirs are ready for flood regulation prior to the next storm season.

Pertinent data relative to the principal mountain reservoirs (Fig. 1), listed from west to east, are presented in Table 1. These data show that for years

TABLE 1.—MOUNTAIN RESERVOIRS OF THE LOS ANGELES COUNTY FLOOD CONTROL DISTRICT

Item No.	Dam	Drainage area (sq miles)[a]	Reservoir capacity to spillway	Annual Runoff			Maximum 24-hr runoff of record
				Maximum	Minimum	Average[b]	
	(1)	(2)	(3)	(4)	(5)	(6)	(7)
1	Pacoima	27.8	4,840	38,000	630	8,090 (26)	6,120
2	Tujunga	81.4	4,240	76,400	800	19,600 (41)	24,870
3	Devils Gate	31.9	2,500	37,600[c]	80[c]	7,640[c](29)	7,420
4	Eaton	9.5	630	14,000[c]	62[c]	1,930[c](25)	1,590
5	Santa Anita	10.8	700	17,800	771	4,300 (26)	3,400
6	Sawpit	3.3	320	2,970	107	1,050 (12)	820
	San Gabriel—						
7	Dam No. 1	202.0	44,030	410,000	9,630	130,000 (48)	74,830
8	Dam No. 2	40.4	10,500	61,300	6,080	30,200 (8)	16,010
9	Big Dalton	4.5	950	3,270	41	1,000 (14)	890
10	San Dimas	16.2	1,070	12,500	485	3,680 (14)	3,400
11	Live Oak	2.3	230	818	0	325 (9)	310
12	Thompson Creek	3.7	610	1,100	0.3	228 (10)	570

[a] Except in Col. 2, all units are in acre-feet. [b] Averages are for the number of years shown in parentheses.
[c] Does not include the Pasadena Water Department diversion to direct use above the reservoir.

of plentiful water supply the storage capacity of the reservoirs is relatively small. This emphasizes the importance of utilizing the large underground reservoirs in the alluvial filled valleys below. The tabulation also shows that very little of the peak flows of severe storms can be detained for spreading.

This paper will set forth: (1) Examples of direct use of flood waters conserved in the reservoirs; (2) water spreading practices in this area, and some of the problems encountered, together with percolation rates under various conditions; and (3) water analysis data based on samples taken from flood waters.

DIRECT USE OF STORED FLOOD WATERS

Practically all of the reservoirs listed in Table 1 serve to increase the supply of water furnished by these streams for direct domestic or agricultural use. A few of these uses will be described (see also Fig. 1).

Pacoima reservoir, controlling a drainage area of 27.8 sq miles in the western portion of the Sierra Madre, lies above valuable agricultural and residential areas in the San Fernando Valley. Annually, 1,000 to 2,000 acre-ft

of the stored flood waters are released to the stream and picked up by downstream diversions for irrigation of several hundred acres of citrus groves. Since the stream above the reservoir is dry in the late summer and fall months, this supply is of large value to the ranches which would otherwise have as their only local supply a very limited ground-water basin. Additional stored flood waters are percolated in the spreading areas downstream.

Devils Gate Dam controls a mountain drainage area of 31.9 sq miles including principally the Arroyo Seco northwest of Pasadena. Here the reservoir area is owned by the City of Pasadena which has constructed galleries under, and wells adjacent to, the reservoir bed for the purpose of extracting an urban water supply. The storage in the reservoir is the primary means of supplying the galleries. These galleries had functioned well for several decades prior to the forest fire and subsequent mud flows in the fall and winter of 1933–1934, but the organic matter carried by these mud flows so increased the carbon dioxide content that the reduced amount of water percolating to the galleries has since been useless. Recently the District has conducted sluicing operations, using stream flow to scour the overburden from the reservoir bed. Results indicate that further sluicing, particularly with the aid of improved facilities, will succeed in regaining this source of water supply.

San Dimas Dam, Puddingstone Diversion Dam, and Puddingstone reservoir offer the most complete conservation system so far constructed for direct water supply. Flood flows originating in the 19 sq miles of San Dimas Canyon are regulated by San Dimas reservoir and Puddingstone Diversion reservoir and diverted through a 2.7 mile concrete channel (capacity 3,500 cu ft per sec) into Puddingstone reservoir. This entire storage may be utilized for irrigating 2,700 acres which constitute one of the most productive citrus areas in Los Angeles County. This system made it possible to conserve the entire runoff of the heavy storm of March, 1938, amounting to 9,365 acre-ft, and also that of the storm of January, 1943, amounting to 6,835 acre-ft. This salvage created an asset worth at least $15 an acre-ft for irrigation use. Puddingstone reservoir has a capacity to spillway of 17,900 acre-ft. Subsequent use of this stored water in lieu of pumping has aided ground-water basins Nos. 7 and 8 (Fig. 1) to regain sufficient storage to cope with withdrawals during dry years. The rise in water table underlying this agricultural area, since 1938, has ranged from 65 to 175 ft.

San Gabriel Canyon flows are regulated by the Flood Control District's Dams No. 1 and No. 2, and by Morris Dam which creates a 36,000 acre-ft water conservation reservoir (owned by the Metropolitan Water District of Southern California). The flows from this and near-by tributary areas will eventually be controlled by the Santa Fe and Whittier Narrows reservoirs as part of the flood control program of the United States Engineer Department. The reservoir system in the San Gabriel Canyon mountain drainage area of 210 sq miles also furnishes the means of conserving the most important local source of water supply in Los Angeles County. The first 135 cu ft per sec of normal flow is allocated to direct diversion for irrigation of citrus lands. Of this flow 90 cu ft per sec also forms a steady winter-time source of power generation which seldom falls below 30 cu ft per sec during the summer months.

The remainder of the flows which can be salvaged (Table 1) are available (*a*) for storage as direct water supply, or (*b*) through the medium of pumping from underground basins after storing in these basins by means of channel and off-stream spreading ground percolation. Subsequent discussion will deal specifically with spreading on the San Gabriel River.

Water Conservation by Spreading

Extensive spreading ground development was first undertaken in Los Angeles County in 1906 at the mouth of San Antonio Canyon. Since then, the District has developed 1,300 acres, and other agencies 765 acres, of percolating area utilizing one or more methods.

General methods of water spreading practiced in Southern California are (1) the ditch and furrow method, (2) the basin method, and (3) percolation of regulated flows in natural stream beds. All three have modifications or variations, and often are used in conjunction with each other.

(*1*) *The Ditch and Furrow Method.*—This is generally used in areas of very rough or sloping terrain, where the water at times may have a heavy silt content. Canals and ditches are laid out roughly on contours with sufficient slope to prevent deposit of the suspended material, yet flat enough to prevent scour of the waterways. Due to variation of soils across the spreading area, the proper slope is often quite difficult to determine, yet may be corrected after construction by installation of check gates.

A modification of this method is to install main canals, as broad as possible and with shallow depth, from which smaller ditches at regular intervals lead the water out and spread it over the ground, much in the same manner as flood irrigation. Water not absorbed by the flooded area flows to the next lower main distribution canal by which it is again distributed to a series of smaller ditches and their flooding area.

Advantages of the ditch method and its variations are the low costs of maintenance and operation when the works are once correctly installed. When so constructed that the main channels may be flushed, this method will handle a greater silt content than any other type. An objection to this system is that the percentage of the total spreading grounds in direct contact with the water is very low, usually not more than 10% or 12% as compared with 75% or 80% for basins.

(*2*) *The Basin Method.*—In its simplest form this involves the construction of dikes or small dams at regular intervals across the abandoned natural channels on a debris cone or former river-bed areas outside of controlled channels. The water is led into the upper basin by means of a canal and from succeeding basins, as each fills, it spills to the next; or the canal may extend past and feed basins on each side. From the last basin the waste water is returned to the flood channel. The upper basins may serve as desilting ponds and prevent excessive silt from being deposited in the lower ponds. During recent years the basin method has been used predominantly due to its economic use of land.

(*3*) *Stream Channel Spreading.*—In some form this method is practiced on most major streams in Southern California. All of these streams are subject

FIG. 2.—INITIAL TEMPORARY DEVELOPMENT OF RIO HONDO COASTAL BASIN SPREADING GROUNDS UTILIZING BASIN AND CANAL SYSTEM

to flash flows of short duration, but of comparatively high rate. On the lower valley areas this condition results in a broad, flat, sandy bed which is dry during the summer months and during most winter months normally has a surface flow covering but a small portion of its area.

For several years conservation associations and county agencies have diverted the streams in these areas and spread them by various systems. Where the stream channels are composed of materials that tend to consolidate and seal off, the stream bed is broken up by tractors dragging cultivators or plows. In flat sandy stretches, the stream is diverted into plowed furrows. Temporary basins are also constructed by furrowing machines on these flood plains. In these ways water from a narrow meandering channel may be made to cover a considerable portion of a wide wash.

In Practice.—The general procedure followed in selecting spreading areas involves an initial study of ground-water use and supply. From these data and measurements of stream-flow percolation under existing conditions, the quantity of water which it would be desirable to handle in off-stream spreading grounds is determined. The possible locations of the spreading areas relative to geologic features of the ground-water basin concerned, ground-water level range, and general soil characteristics which would indicate the precolating capacity are studied. Promising areas are checked to depths of 30 ft or more by test holes to reveal the presence of clay lenses and other soil conditions which would have an important effect on the long-time spreading rate.

Following study of these data, if a local water supply of a few cubic feet per second is available, a small sample basin is often tested for a period of several weeks to obtain further data on percolation rates. When the most suitable set of conditions has been ascertained, the ground is purchased and developed on a temporary basis—that is, with wooden intake, canal and basin structures, and a temporary sand dam for diversion from the stream. This development is operated full scale until the data derived warrant revision or replacement of the structures.

An initial 40-acre temporary development at the Rio Hondo Coastal Basin spreading grounds, constructed in 1938, is illustrated in Figs. 2 and 3. The canal is controlled by a 25 ft wide 5-bay flashboard intake faced with a 20 ft wide 4-bay flashboard sluiceway which governs the head available for the canal and enables discharge for river percolation as well as sluicing of sand from the forebay. At all drops or outlets flow gages or recording gages are installed. The canal can handle a flow of 200 cu ft per sec (to care for additional development). The cost of developing this area was approximately $10,000; the water conserved is worth at least $10 an acre-ft in the ground.

It is estimated that the cost of spreading, including the wooden structures (retired on a 10-yr basis), interest, maintenance, and operation, amounts to less than $5 per acre-ft of water spread. With several hundred acres of coastal basin spreading grounds completely developed, the cost might be as little as $3 per acre-ft for conservation of the long-time average available flow which would otherwise waste to the ocean. (Cost of retirement of land was not included in these unit charges as the value is not impaired.) This average flow is calculated to amount to a minimum of 10,000 acre-ft annually.

Fig. 2.—Initial Temporary Development of Rio Hondo Coastal Basin Spreading Grounds Utilizing Basin and Canal System

Adjacent to these spreading grounds the Rio Hondo channel has been intensively developed (Fig. 4). This is a typical example of the coverage which may be obtained by the use of a large plow and occasional checks to

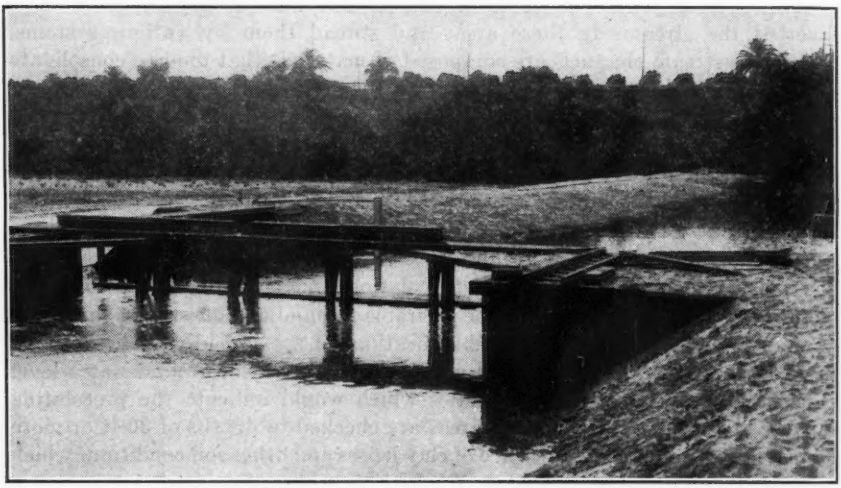

(*a*) Canal Intake, Sluiceway, and Temporary Diversion Dam

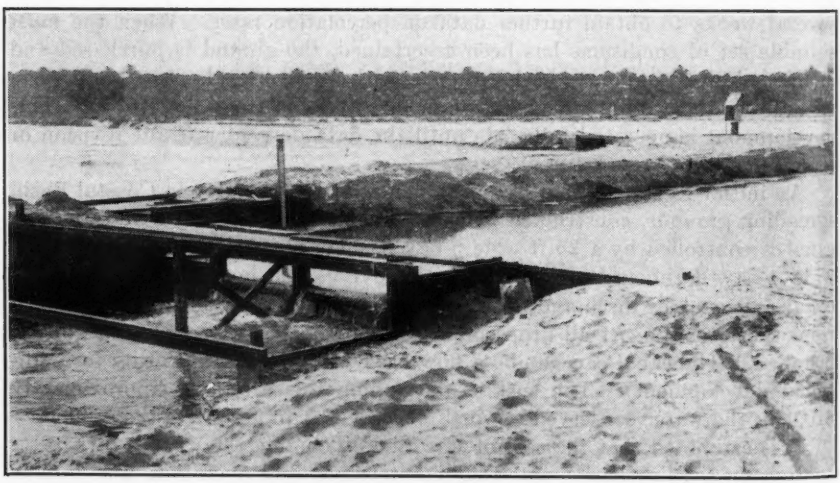

(*b*) Check-Drop No. 2, Turnout No. 2 in the Main Canal

FIG. 3.—SPREADING GROUNDS, RIO HONDO COASTAL BASIN, AUSUGT 3, 1938

redistribute the flow. Of course, it is only practical to set up this type of intensive river spreading for regulated flows to be released after the storm season. The work performed is also instrumental in spreading the next

season's storm flows until low water channels have been created again. The equipment used was a specially constructed plow capable of making a furrow from $2\frac{1}{2}$ to 3 ft deep and was drawn by a 70 or 80 hp tractor. The check levees

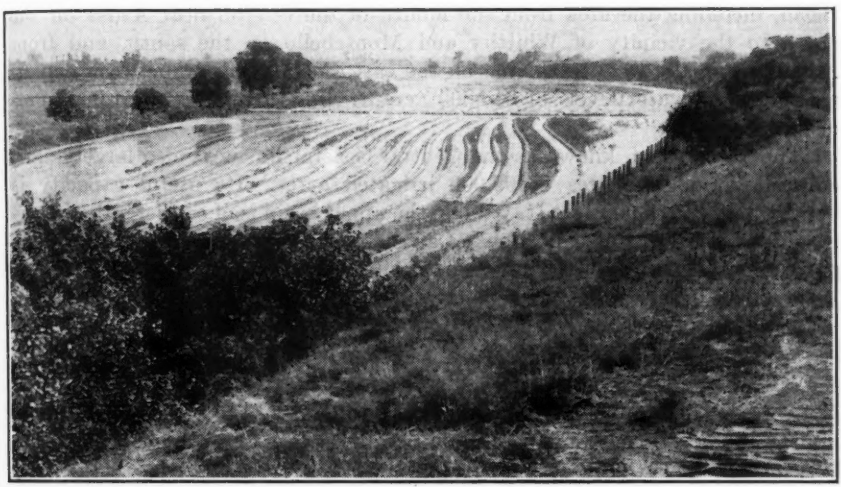

(*a*) Plowed Ditches Designed to Give Complete Channel Coverage, July, 1940

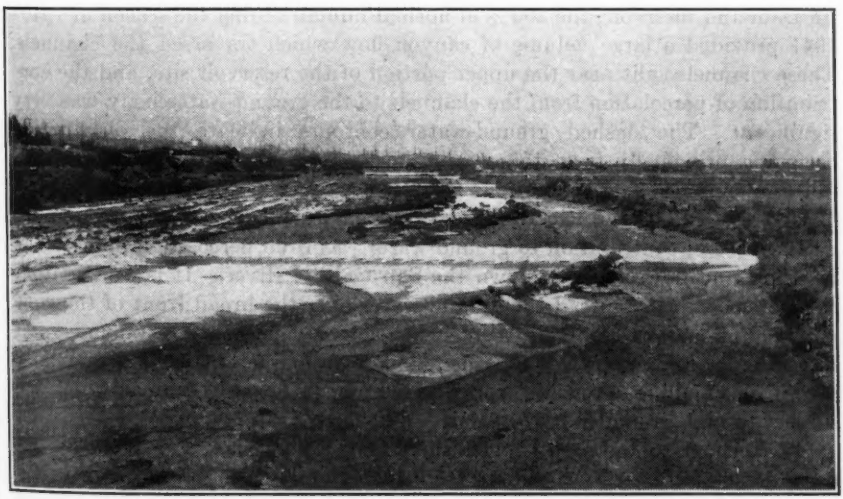

(*b*) Check Barriers Erected by Bulldozers to Increase Channel Coverage, April, 1942

FIG. 4.—RIO HONDO CHANNEL ADJACENT TO SPREADING GROUNDS

were constructed by bulldozer. One hundred ten acres developed in this manner percolated approximately 150 cu ft per sec, with rather high ground water.

Some Spreading Problems.—Intensive study has been given to both useful and economic means of conserving San Gabriel Canyon flows for use in the two principal ground-water basins over which the river and its distributary, the Rio Hondo, flow (see Fig. 1, basins 3 and 24). The upper, known as the Main Basin, including the area from the mouth of the canyon near Azusa on the north to the vicinity of Whittier and Montebello on the south, and from Alhambra on the west to Covina on the east, has a capacity between experienced ground-water levels of 615,000 acre-ft. It is overlain by 61,000 acres of irrigated land.

The lower basin, known as the Central Coastal Basin, is also largely agricultural, having an area of 99,000 irrigated acres. Its useful capacity is approximately 275,000 acre-ft. While the upper basin is of consistently porous material typical of upper portions of a detrital cone, the lower basin contains porous material in only the upper five miles along the courses of the rivers. The balance is overlain by clay strata which controls an intermittently artesian pressure supply.

Replenishment of the Main Basin is accomplished readily by percolation in the stream channels and the normal spreading which will automatically occur in Santa Fe reservoir. Percolation of flows in the Main Basin has supplied interesting data relative to the distribution of ground water dependent on the location of percolation.

Fig. 5 shows the course of the San Gabriel River and its distributary, the Rio Hondo, through the Main Basin. Prior to the construction of the Santa Fe Dam and reservoir, the 200% of normal rainfall during the season of 1940–1941 provided a large volume of canyon flow which traversed the channels. These channels split near the upper portion of the reservoir site, and the contribution of percolation from the channels to the ground-water body was very significant. The dashed ground-water contours indicate the distribution occurring principally from this stream-bed percolation. In comparison, the full line contours show conditions following the 160% normal rainfall season of 1942–1943 when the Rio Hondo was cut off from percolation and the principal source of contribution to ground water was from percolation in Santa Fe reservoir and flows released down the San Gabriel River. It is evident that the latter condition spread the ground water over the broad front of the cone making full use of available storage instead of concentrating ground-water ridges under the channels. Knowledge of such characteristics is particularly helpful in handling spreading works in relation to developed areas which are subject to high ground-water difficulties.

In contrast to the easily replenished Main Basin, the Coastal Basin has been depleted to such an extent that, in certain areas, sea-water intrusion threatens the quality of its supply. Hence, it is in this basin that the Flood Control District has developed its primary off-stream spreading works. The works now developed in the upper portion of this basin (Fig. 1, spreading areas 8, 9, and 10) consist of 240 acres adjacent to the San Gabriel River and Rio Hondo, a portion of which has been operated since 1938. Operations have included test runs to determine the characteristics of the spreading

grounds as well as routine use between winter storms and percolation of flows stored in reservoirs during spring months.

Valuable data have been gained relative to percolation of water under varying ground-water conditions. The principal factors determined have been percolation rates, relation of shape of spreading grounds to outlying areas, effect of depth of water in basins, and effect of ground-water mound. Rates obtained have varied from initial values of 9 cu ft per sec per wetted acre to final values under high ground-water conditions of 0.9 cu ft per sec per wetted acre, the latter having held constant for many weeks of continuous spreading.

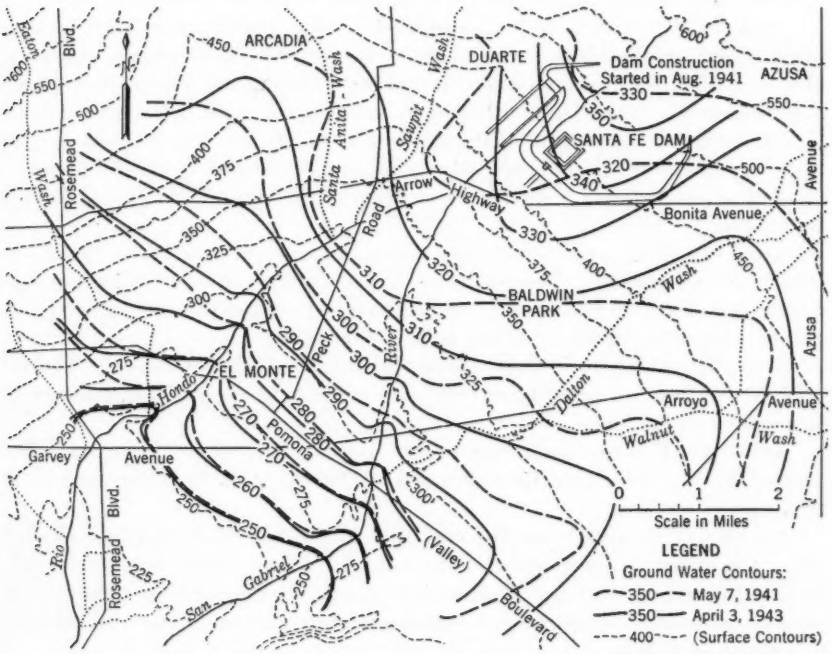

FIG. 5.—COMPARISON OF GROUND-WATER LEVELS AT SANTA FE DAM AND VICINITY

When the normal water table is less than 25 ft from the surface it has been found that spreading quickly builds a water mound up to the surface of the spreading basins. Consequently the water percolated in these basins, which would normally descend vertically to a low water table, can only move away from the spreading area at its periphery. This indicates the value of elongated spreading grounds. Fortunately, the best natural sites are the natural stream benches of these rivers. Consequently, the most inexpensive land is often the best shaped and situated area for spreading.

Tests for effect of various depths of impounded water in basins, relative to percolation rates, indicate that when the percolating water has a free escape, surface depth has little effect. However, when ground water is in contact

with the water in the basin, an increase in the depth from an average of 1 ft to an average of 2 ft may increase the percolation rate as much as 20%.

Ground-water mound—that is, the tendency of the underground water surface to build up to a higher elevation immediately under the stream bed or spreading area—is probably the most important factor governing percolation rate in porous soil. Tests along the San Gabriel River have indicated that, when the normal water table is less than 20 ft from the ground surface, continuous percolation will result in the mound reaching the stream surface within a period of a few days and thereafter will reduce the percolation rate. Hence, the economy of creating water supply in underground storage at any location may be affected largely by the normal depth to ground water.

Data on Percolation Rates.—Obviously, each spreading ground location offers benefits and problems which can be ascertained only from trial operation. Hence, a concise summary of percolation rates obtained at the several spreading grounds which the District has operated, together with pertinent comparative material at each location, should be useful. In Table 2, these are given for seven spreading grounds and three additional locations at which temporary tests were conducted. A further description of the areas in Fig. 1 and Table 2 is as follows:

Area 14.—This area is on both sides of San Antonio Wash below the mouth of the canyon. The soil (Col. 8) is a coarse sand containing a large proportion of gravel and stones. Subsurface exploration revealed gravel, and gravel containing boulders, as far as the water table.

Area 11.—This area is at the mouth of the Big Dalton Canyon. The soil (Col. 8) is a porous, gravelly, sandy loam containing a variable proportion of large and small stones.

Area 12.—This area is at the mouth of the Little Dalton Canyon. The acres (Col. 3) are only partly developed. The soil (Col. 8) is the same as in area 11.

Area 6.—This area is on the east side of the San Gabriel River channel below the mouth of the canyon. The soil (Col. 8) is a coarse micaceous sand, such as that found west and southwest of Azusa, containing large quantities of stones. Subsurface exploration revealed gravel and gravel mixed with boulders to a depth of 255 ft.

Area 9.—This area is on the west side of the San Gabriel River channel. In the gross area of 94 acres (Col. 3) only 73 acres have been developed. The soil (Col. 8) is a medium textured, friable, micaceous sand containing a proportion of fine sand and silt in the subsoil. Subsurface exploration in the upper area revealed: Sand from the surface to 10 ft, sand and gravel to 70 ft, clay to 80 ft, and sand and gravel to 120 ft; and in the lower area: Soil and sand from the surface to 7 ft, sand and gravel to 8.5 ft, fine silty sand to 12.5 ft, and silty sand to 14 ft.

Area 8.—This area is on the east side of the Rio Hondo channel. Of the 309 acres gross area (Col. 3), only 160 acres are developed. The maximum initial percolation rate at the apex of the ground-water mound (Col. 5) was 2.0 whereas the maximum initial rate for the area was 9.0. The soil (Col. 8) is a light-textured, micaceous, friable, fine, sandy soil containing stratified

TABLE 2.—DATA FROM DEVELOPED SPREADING GROUNDS AND TEST AREAS, LOS ANGELES COUNTY FLOOD CONTROL DISTRICT

Area No. (see Fig. 1)	Spreading grounds	Type[a] (B, D or O)	Area (Acres)		Percolation Rate[b]		Average seasonal capacity (cu ft per sec)	Soil type (U.D.S.A. Classification)	Depth to Water Table, in Feet	
			Gross	Wetted	Maximum	Minimum			From	To
	(1)	(2)	(3)	(4)	(5)	(6)	(7)	(8)	(9)	(10)
14	San Antonio	B, D	771	137	4.5	1.5	300	Tujunga stony sand	100	270
11	Big Dalton	D	30	9	6.0	1.1	15	Hanford stony sandy loam	18	139
12	Little Dalton	B	16	2.0	5.4[c]	....	10	Hanford stony sandy loam	18	139
6	Canyon Basin	D	500	62	1.6[c]	....	100	Hanford fine sand	1	160
9	San Gabriel Coastal Basin:									
	Upper area	B	94	54	2.5[d]	1.0[d]	75	Hanford sand	20	73
	Lower area				4.0	1.8				
8	Rio Hondo Coastal Basin	B	309	150	2.0[d]	0.9[d]	164	Hanford fine sandy loam	12	72
1	Pacoima:									
	Silty flows	B, D	174.6	80	....	0.8	60	Hanford fine sandy loam	196	260
	Cultivated area, clear water					1.9	145			
19	San Gabriel Valley, Santa Fe Diversion[e]									
	San Gabriel Cone (Upstream Area):									
	(a) Basin in old overflow channel—									
	Before blasting with dynamite	B	....	0.92	1.5[f]	0.7[f]	....	River wash	124	144
	After blasting with dynamite	B	....	0.81	4.0[c]	....	....			
	(b) Off-channel contour basins	B	....	12.75	5.0	3.8	58.6			
19	San Gabriel Cone (brush land in downstream area)	O	....	1.07	2.4[c]	....	2.6	Tujunga stony sand	55	90
19	South side of Rio Hondo (still farther downstream)									
	Natural river bed (3 days)	B	....	0.51	3.8	2.7	1.6	Hanford sandy loam	45	49
	Cultivated surface (9 days)				7.5	3.8	3.1			

[a] B = basin type, D = ditch type, and O = shallow overflow type. [b] Maximum initial rates (Col. 5) and minimum rates after an extended run (Col. 6) are given in cubic feet per second per wetted acre (Col. 4). [c] Mean percolation rate for the area. [d] Apex of ground-water mound at the level of the basin beds. [e] Temporary testing grounds. [f] 1.5 in Col. 5 is the mean value for a month with clear-water flow and 0.7 in Col. 6 is the mean value for a month following silty storm flows.

deposits of sand, silt, and gravel in the subsoil. Subsurface exploration revealed alternate strata of sand and gravel with 2-ft layers of clay at depths of 58 ft and 115 ft.

Area 1.—This area is on both sides of Pacoima Wash. The percolation rates (Col. 6) and the capacities (Col. 7) are averages of 26 days of silty flows and 16 days of clear-water flows, the latter on cultivated basins. The soil (Col. 8) is the same as area 8 except in the south half of the east side. This part is Hanford gravelly sandy loam, a coarse, sandy loam with a large percentage of granitic gravel. Subsurface exploration revealed that underlying the recent alluvium, at depths of 10 ft to 20 ft, is a less permeable surface of weathered old alluvium. Beneath this material there is sand and gravel with a 20-ft layer of clay at a depth of 220 ft.

Area 19.—In the upstream part of the San Gabriel Cone, Area 19, the river wash (Col. 8) was composed of undifferentiated alluvial deposits. It was generally very coarse and stony soil, the finer material having been washed away. Subsurface explorations revealed sand, gravel, and boulders to a depth of 260 ft. To blast the overflow channel, thirty holes were driven 10 ft apart and 3 ft deep. Each hole was charged with six $\frac{7}{8}$-in. sticks of 40% dynamite which formed craters 3 ft deep. The off-channel contour basins were interconnected to permit the circulation of water. A shutdown of two hours resulted in a 15% reduction (to 85% of 5.0) in the percolation rate for these off-channel basins. The rate of 3.8 is the average for 72 days.

In the downstream part of the San Gabriel Cone, Area 19, the soil (Col. 8) differs from the upstream part in that there is a scarcity of gravel and stones on the surface. Subsurface exploration revealed a medium gravel to a depth of 200 ft.

In the farthest downstream area on the south side of Rio Hondo (Area 19), the soil (Col. 8) is a brown, friable, micaceous, sandy loam, open and porous. There is a 6-ft layer of such soil, underlain with sand and gravel.

The area data emphasize the economic use of land by the basin method. Spreading areas 6, 11, and 14 (Fig. 1) were set aside as spreading grounds when land was relatively cheap. Equipment for development was scarce and hence "ditch" spreading solved the problem of conserving the flows available at that time.

San Antonio spreading grounds (Fig. 1, spreading area 14) is an unusual layout. It lies at the apex of the cone immediately below the canyon of the same name. The tributary uncontrolled watershed of some 30 sq miles rises to an elevation of 10,000 ft. A large portion of the runoff results from melting snow and is therefore often prolonged into the late spring—a condition which makes spreading without reservoir control and storage quite practicable.

In order to cope with storm conditions, basins have been constructed on the east side of the stream, into which flows up to 400 cu ft per sec of sand and silt-laden water can be diverted, stored, partially desilted, and circulated for percolation. These are used but a short period for flash flows, after which the water characteristically clears rapidly. When the solid content has reduced to 0.5% or less, the water is turned into the ditch and basin system on the west side of the stream. These spreading grounds have absorbed prac-

tically all of the dry season flows and a maximum of 26,630 acre-ft, which was 93% of the total runoff during the 200% of normal rainfall season of 1940–1941. They are practically the sole source of supply, other than direct rainfall, for ground-water basins 11, 12, and 14 (Fig. 1) which are covered by citrus ranches.

Table 2 shows that percolation rates in terms of cubic feet per second per wetted acre vary widely with location. Maximum initial rates under low ground-water conditions are quite high for all locations because these locations are on recent alluvial cones or in river beds.

Areas 8 and 9, already discussed in some detail, were recently developed where land available for spreading is limited and land costs are high. During 1933 Area 1 was developed as a model canal and ditch system. Later experience gained from test basins indicated the probability of better economic use of the area. Hence, half of the grounds have been completed recently as a canal-basin layout. The rates shown in Table 2 were obtained during the transition and despite the old alluvium noted at shallow depths, it appears that the average rate will be increased to 2 cu ft per sec per wetted acre for even slightly silty flows. The ditch system wetted area was 12% of the acreage while the basin system covers 80%.

Extended periods of spreading bring into play factors such as clay lenses, control of finer sands, spreading of silty flows, and rising ground water. A study of the surface soil type, log of subsurface materials, and depth to water table emphasizes these characteristics.

Under Area 19 data are tabulated for temporary test spreading grounds (1) on coarse porous stony soil; (2) on brush land containing considerable gravel; and (3) on an area in which sand predominates.

(1) On the stony soil the initial test was in a well-sealed overflow channel in the San Gabriel River. Sealing had been by deposit of silt between the rocks and by calciferous cementation. The blasting experiment was undertaken primarily to break up this sealing. Its effect was pronounced.

Later tests on the same type of stony soil were conducted on an off-channel area of approximately 15 acres. Many years previous, this area had been a portion of the river bed during major floods, but was not sealed by either silt or calciferous deposits. Clear water was diverted to contour basins which spilled from one to the next, thereby providing slow circulation through the basins. As long as the test continued uninterrupted, the water sank at the rate of 10 ft a day. This unusually high rate continued for several weeks until the shutdown of the regulating dam upstream dried up the basins temporarily, although the soil did not have a chance to dry out. When the basins were filled a few hours later, the percolation rate had reduced approximately 15%. A similar sequence has been noted on several other spreading areas having considerably finer soil.

(2) Tests on brush land were undertaken to compare with percolation rates on barren areas which have been scoured by stream flow. Water was sunk by sheet overflow and from still ponds as compared with the basins described under (1). Although the base soil was somewhat finer, it is believed that the

lack of circulation as well as the fines introduced by growth of vegetation were the principal factors in giving a reduced percolation rate. Experience on several soil types and with water almost clear or slightly silty has indicated a definite benefit from pond velocities as low as 0.05 ft per sec. In addition to carrying fine particles through the basins, even this slow movement discourages the concentration of algae and the scum it leaves on basin beds.

(3) Tests on a quite sandy soil in the flood area of a natural river bed gave an opportunity to check the relation of percolation through the natural crust formed by a small amount of silt and calciferous action, and that through the same ground after cultivation. Although the differential found was more pronounced than has been experienced in larger scale operation, nevertheless the trend was the same.

Comparative Water Analyses

It is pertinent to compare the qualities of the supply available from local mountain and valley storm waters with other sources of water supply available to the Los Angeles Basin. Table 3 presents such a comparison through the medium of samples from storm and after-storm flows, which were taken during the storm seasons from 1932 to 1934. The data were gathered as a cooperative project of the Sanitary Group of the Los Angeles Section of the American Society of Civil Engineers and the Flood Control District. Laboratory facilities arranged by R. F. Goudey, M. Am. Soc. C. E., were an important contribution in analyzing the flood waters.

Despite the fact that it has been several years since the data were obtained, it is believed that the values on other supplies are representative with the exception of the water which the Metropolitan Water District is furnishing the Coastal Plain from its Colorado River source. Although study of the data reveals many interesting comparisons, those that are perhaps the most significant will be mentioned.

The pH-value of the local mountain and valley flood water averages about 7.6, which is comparable to other supplies. Chlorides are all within the drinking water range and generally average the same as other available supplies. The total hardness is less or not greater than the average local supply.

Nitrites and nitrates are generally lower than free ammonia, showing that there is nitrogen that needs to be oxidized in order to have stable water. However, most samples show sufficient dissolved oxygen to accomplish this oxidation. Organic nitrogen was generally equal to or less than that in aqueduct water. The higher values were from the upper Los Angeles River—that is, valley water having its source in farming lands.

The comparison of dissolved oxygen and oxygen demand as shown by B.O.D. from 21 mountain water samples shows only 5 with excess B.O.D., and only 1 of the 5 was from an after-storm flow, indicating further evidence of the stability of the water. The majority of mountain water samples compare well with those from the High Sierras brought in by the Owens River aqueduct.

Color and turbidity, and suspended solids furnish the prime difference between storm waters and other supplies. The after-storm flows are generally

better in respect to these factors and reservoir storage readily corrects the excess derived from storm flows.

The greater part of the total solids is comprised of suspended solids. The analysis divided suspended solids into the subdivisions of quickly falling solids

TABLE 3.—COMPARISON OF LOCAL STORM WATERS WITH OTHER SOURCES OF WATER SUPPLY AVAILABLE TO THE LOS ANGELES BASIN

Description	(a) Los Angeles Area[a]				(b) Other Sources					
	Mountain Water		Valley Water		Mono Basin snow water	Aqueduct	Los Angeles River Gallery (Crystal Springs)	Lomita Plant No. 2 (well)	Experiments on Sewage Reclamation[b]	
	During storm	After storm	During storm	After storm					Raw	Final
(1)	(2)	(3)	(4)	(5)	(6)	(7)	(8)	(9)	(10)	(11)
Flow Range (Cu Ft per Sec)										
Minimum	65	50	35	40	....	....	....	....	....	....
Maximum	1,550	2,700	10,000	700	....	....	....	....	....	....
Potential of hydrogen (pH)	7.8[c]	7.9[c]	7.4[c]	....[d]	8.0	8.0	7.2	8.0	7.2	7.2
Parts per Million, by Weight:										
HCO_3	90	125	96	158	10	200	205	270	320	240
CO_3	0[c]	0[c]	0	0	0	10	0	0	0	0
SO_4	28	18	58	93	2	23	115	0	125	125
Cl	24	11	26	36	0	22	30	10	85	85
Ca	32[c]	37[c]	35[c]	57	5	24	74	27	86	86
Mg	0.2[c]	8.2[c]	9[c]	9.0	3	9	25	14	30	30
Total hardness	80[c]	127[c]	126[c]	177	25	96	285	124	340	340
NO_2	0.01	0.01	0.04	0.05	0	....	0	0	0	3
NO_3	0.50	0.75	0.48	0.82	0	....	4.0	0	0	4.7
NH_3	1.82	1.02	1.23	0.46	0	0	0.4	0.8	21	11
Organic nitrogen	2.80	1.50	3.82	0.68	0.4	4.0	....	2.1	28	4.0
Dissolved Oxygen (D.O.)	6.6	6.8	6.0	8.6	9.0	8.2	7.0	7.1	0	4.0
Biochemical oxygen demand (B.O.D.)	5.6	3.7	12.4	4.9	0.1	2.0	0.2	7.1	300	4.9
Color Range—										
Minimum	150	5	60	....[d]	5	20	0	70	....	33
Maximum	600	75	800	....[d]						
Turbidity Range—										
Minimum	320	25	410	50	0	5	0	0	....	10
Maximum	500	3,800	5,000	4,500						
Total Solids Range—										
Minimum	1,530	15	2,160	407	....	....	....	....	....	....
Maximum	17,594	2,039	30,985	10,015	....	....	....	....	....	....
Suspended Solids Range—										
Minimum	1,210	12	2,060	200	....	....	....	....	....	....
Maximum	17,420	1,794	30,550	9,500	....	....	....	....	....	....
Organic and Volatile Solids Range—										
Minimum	190	0	86	63	....	....	....	....	....	....
Maximum	697	260	1,885	840	....	....	....	....	....	....
Number of samples	9	12	29	8	....	....	....	....	....	....

[a] Average of total samples (see last line) except as otherwise noted. [b] Los Angeles experiments under the direction of R. F. Goudey. [c] Average computed from less than the total number of samples. [d] Not run by the laboratory.

and those remaining in suspension. The division was found to be at a size of approximately 25 microns. The data from this division indicate that more than 50% of the suspended solids might be classed as quickly falling—that is, those which would drop immediately upon contacting relatively still water.

Although the copious rainfall since 1936 has filled many of the ground-water basins in the Los Angeles area nearly to capacity, the importance of maintaining these supplies through artificial replenishment is emphasized by recent war-industry draft and the fact that approximately 75% of the water supply of the area is derived from this source and direct mountain stream flow.

It is hoped that this paper will stimulate interest in the presentation of further data on many phases of this work.

Acknowledgments

The writer is indebted to L. W. Jordan, Assoc. M. Am. Soc. C. E., for assistance in assembling and checking data, and to Paul Baumann, M. Am. Soc. C. E., for review of material presented herein. Lt. Col. H. E. Hedger, M. Am. Soc. C. E., is Chief Engineer of the Flood Control District (on leave with the Armed Forces). M. E. Salsbury, M. Am. Soc. C. E., is Acting Chief Engineer, and Mr. Baumann is Assistant Chief Engineer in charge of the work described in this paper; the writer directs the operation of reservoirs and the layout, testing, and operation of conservation works, and Mr. Jordan supervises office and field work on ground-water and spreading studies, and conservation operations.

AMERICAN SOCIETY OF CIVIL ENGINEERS

Founded November 5, 1852

DISCUSSIONS

PRESSURE ON THE LINING OF CIRCULAR TUNNELS IN PLASTIC SOILS

Discussion

BY D. P. KRYNINE

D. P. KRYNINE,[11] M. AM. SOC. C. E.[11a]—The possibility of the transfer of the weight of the overburden above a tunnel to the adjacent earth or rock mass is evident from the simple analogy shown in Fig. 13. If body A (weight W) is pressed between two plates B, it will not fall, provided the force of friction between body A and plates B balances the weight W. A system of shearing stresses acting upward is created in body A. Presumably, this system of shearing stresses extends into plates B. Another set of shearing stresses is created in plates B to balance the former system and to transmit the weight W to the earth. This analogy corresponds to the case of a tunnel in rock which may be in equilibrium without lining, or to the case of holes pierced in a masonry wall.

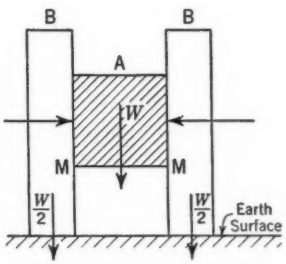

FIG. 13.—FRICTION ANALOGY

If friction between body A and plates B still exists but is not strong enough to prevent body A from falling, an upward force F, with a value less than W, may support body A in equilibrium. In this case, a system of shearing stresses with a resultant $W - F$ is set up in body A. Shearing stresses in plates B transmit part of the weight $W - F$ of body A to the earth. This situation corresponds to that in a tunnel provided with lining or to the redistribution of the weight of grain in a bin. The force F is analogous to the pressure absorbed by the lining of a tunnel or by the bottom of a bin, respectively, whereas the balance of the weight $W - F$ is transmitted to the mass surrounding the tunnel or to the walls of the bin, respectively. Secondary forces and stresses

NOTE.—This paper by D. P. Krynine, M. Am. Soc. C. E., was published in May, 1944, *Proceedings*. Discussion on this paper has appeared in *Proceedings*, as follows: September, 1944, by M. A. Drucker; and December, 1944, by John M. Bird.

[11] Research Associate in Soil Mechanics, Dept. of Civ. Eng., Yale Univ., New Haven, Conn.

[11a] Received by the Secretary April 25, 1945.

are introduced into the mass during construction of a tunnel so that the analogy of Fig. 13 may be complicated or altered.

Two extreme cases of circular tunnels in plastic soils are: (*a*) Circular holes in plastic rocks such as granite or basalt, when no lining is required because of the high shearing strength of the rock material; and (*b*) circular tunnels in plastic organic silt of restricted shearing strength of the Lincoln Tunnel type. Circular tunnels in weak plastic rocks or in plastic clays are classified between the two limits.

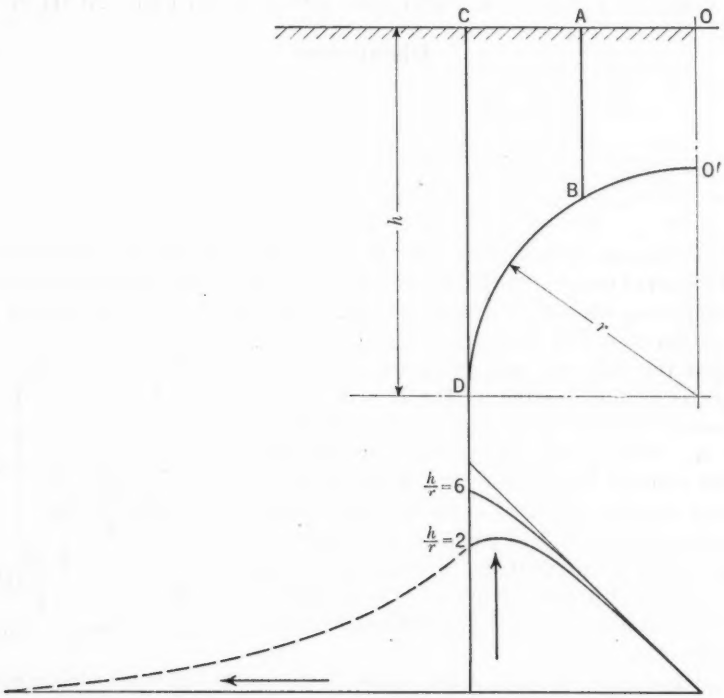

FIG. 14.—SHEAR DIAGRAM FOR THE CASE OF A TUNNEL IN ROCK

Shear Diagram for the Case of a Tunnel in Rock.—Fig. 14 represents a circular hole in rock, the radius of the hole being r and the height of the overburden above the level of the sides (haunches) being h. Because of symmetry, there is no vertical shearing stress along the center line OO′. The weight of the part of the overburden AOO′B, separated from the remainder of the mass by section AB, is carried by that section in cantilever action. The average shearing stress (in tons per square foot) acting along section AB equals area AOO′B (in square feet), divided by ordinate AB (in feet) and multiplied by the unit weight of the rock material (in tons per cubic foot). The shear diagram, at the bottom of Fig. 14, has been plotted for a shallow tunnel ($h/r = 2$) and a rather deep tunnel ($h/r = 6$). For plotting purposes, the weight of the rock material has been assumed at 1 ton per cu ft, the vertical scale of shearing

stresses (tons per square foot) being the same as that of horizontal distances (in feet). To use this diagram, the ordinates must be multipled by the actual unit weight of the rock material (in tons per cubic foot), and due correction must be introduced for the actual ratio of the vertical and horizontal scales. From Fig. 14 it is evident that the average shearing stress at the sides (haunches) of a tunnel in rock without lining cannot be larger than $r\,\gamma$, in which r is the radius of the tunnel in feet and γ is the unit weight of rock material in tons (or in pounds) per cubic foot. Assume that the maximum shear on some oblique plane may be twice the vertical shear; then it may be concluded, as an example, that a circular tunnel ($r = 30$ ft) would stand without lining at any depth in rock weighing 160 lb per cu ft, if the shearing strength of that rock is $2 \times 30 \times 160 = 9{,}600$ lb per sq ft, or about 66 lb per sq in. Although the diagram in Fig. 14 shows that the average shearing stress at the sides (haunches) of a tunnel in rock, without lining, increases only slightly with the depth of the tunnel, geological conditions, such as fissures or cleavage planes, may change the foregoing computations substantially.

In a semi-infinite mass, of rock or of earth, there is a certain ratio between the horizontal and vertical pressures which is assumed constant. It is termed "coefficient of pressure at rest" and is often designated by the symbol K_o. As soon as a tunnel is constructed, the value of K_o next to the tunnel (and, theoretically, throughout the entire rock mass) decreases. The coefficient of pressure at rest preserves its original value K_o only at an infinite distance from the tunnel. Thus, the mass tends to move toward the tunnel; hence, the horizontal shearing stresses acting against the impending movement of the mass are directed from the tunnel. Shearing stresses in the overburden COO′D (Fig. 14) itself obviously act in the same direction (shown by an arrow in Fig. 14). Since there is no horizontal shear at infinity, the diagram of shearing stresses beyond the sides (haunches) of the tunnel must have the shape indicated by the dashed lines in Fig. 14. The shape of the shear-stress diagram for deep tunnels suggests the possibility that the maximum average shear may occur somewhere beyond the sides (to the left of the haunches in Fig. 14). It is needless to add, however, that both Figs. 14 and 15 are considered simple freehand sketches and that no attempt has been made to correlate Fig.14 with Fig. 15. Both of these illustrations are intended to furnish qualitative pictures of corresponding phenomena only.

The shear diagram in Fig. 14 refers to both horizontal and vertical stresses. It may be concluded that the weight of the rock mass close to the boundary is relieved by shearing stresses not only above the tunnel but also on both sides of the tunnel; and nowhere close to that boundary is the mass overloaded. To determine what part of the mass takes care of the relieved weight, the pattern of principal stresses around the tunnel must be considered.

Principal Stresses Around a Tunnel in Rock.—Before the construction of the tunnel, the principal stresses run vertically (the major principal stress) and horizontally (the minor principal stress). This original pattern is shown in Fig. 15(*a*). Since the piercing of a circular hole originates shears both vertically and horizontally, the directions of principal stresses change. However, a major principal stress (for instance, that emanating from point 2, Fig. 15(*b*)),

after being distorted by the shearing stresses, tends to return to its original vertical line, reaching the line at an infinite depth below the hole. This is necessarily so, since at an infinite depth the hole exerts no influence. Since the major principal stress above and below the hole is distorted in two opposite directions, the shearing stresses above and below the tunnel act in opposite directions. Thus, the relieved weight close to the boundary of the mass is transmitted to that part below the sides (haunches) of the tunnel.

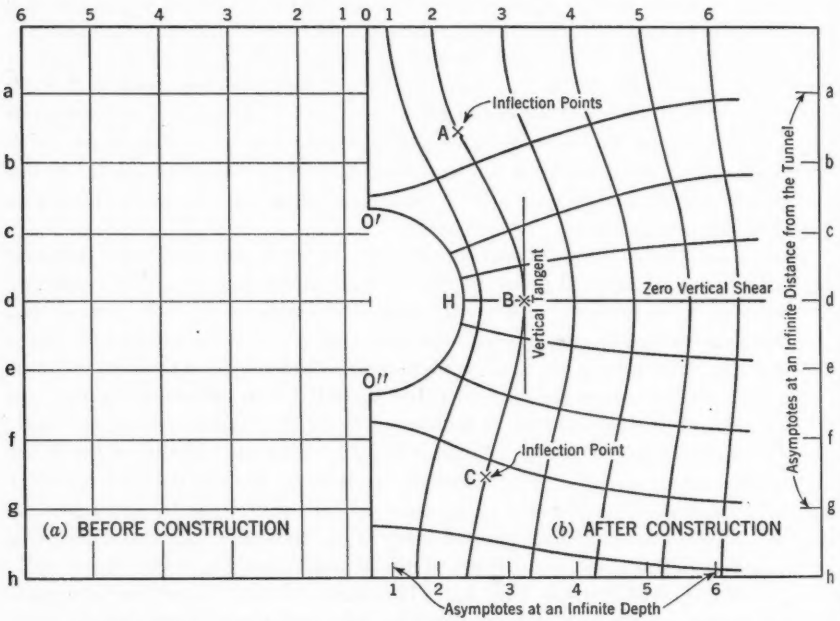

FIG. 15.—PATTERN OF PRINCIPAL STRESSES BEFORE (*a*) AND AFTER (*b*) CONSTRUCTION OF A TUNNEL IN ROCK, WITHOUT LINING

The vertical shearing stresses, which relieve the weight of the silt mass, become changed in sign at the horizontal line passing through the sides (haunches) of the tunnel H (Fig. 15) so that this horizontal line is the locus of zero vertical and horizontal shear. Mathematical analysis (which is beyond the scope of this paper) may show a more precise position of the locus. The principal stresses along the locus in question are vertical and horizontal; hence, the tangent to the distorted trajectory of the major principal stress is vertical.

The trajectory of the major principal stress at the center line of the hole consists of two vertical straight lines and a semicircumference belonging to the hole. All other trajectories of major principal stresses (for instance, the trajectories emanating from point 2, Fig. 15(*b*)) consist of four distinct parts: (*a*) From the boundary to which the trajectory is normal to the inflection point A; (*b*) from the inflection point A to the intersection with the locus of zero vertical shear (point B); (*c*) back to the inflection point C, and (*d*) finally to infinity. The vertical shear along the trajectory increases from zero at the

boundary to a maximum at the inflection point A. Another maximum value, but of the opposite sign, is found at the inflection point C. At the center line of the hole, O′ and O″ are considered inflection points.

Arching in Rock.—It has been suggested that an arch forms in the material above the tunnel. As far as rock or other homogeneous plastic material of considerable shearing strength is concerned, there is no such arch. The relief in pressure above the tunnel is due to the action of shearing stresses which transmit part of the weight of the rock mass close to the boundary to the lower strata. As the result of the action of the shearing stresses, straight trajectories of major principal stresses become distorted as in Fig. 15(*b*).

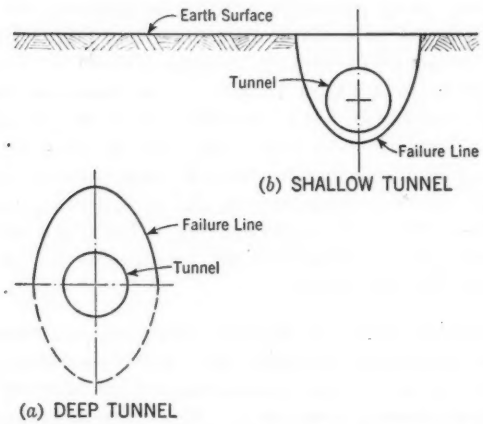

FIG. 16.—SCHEMATIC DIAGRAMS OF FAILURE ZONES AROUND TUNNELS

Case of Insufficient Shearing Strength of the Plastic Material Surrounding the Tunnel.—If a lateral support of a semi-infinite mass (such as a retaining wall) yields, a wedge separates from the remainder of the mass. In a similar way, if the lining of a tunnel is flexible and yields, there may be considerable settlement above the tunnel which is analogous to the yield of a lateral support. In both cases, a failure line (sliding surface) is formed. In the case of a tunnel, this failure line bounds a closed zone in which rock or clay material tends to descend toward the opening. J. R. Dinsdale has shown[12] how the material falling from the roof and sides of a mine tunnel was gradually replaced with logs until the final closed failure zone was reached. Fig. 16 shows schematically a closed and an open failure zone, the latter taking place if the tunnel is a relatively short distance underground. R. Fenner makes some simplifying assumptions and, using abundant mathematics, even determines the ratio of the axes of the elliptical failure line.[13] This ratio is given as $\tan\left(45° - \frac{\phi}{2}\right)$,

[12] "Ground Pressures and Pressure Profiles Around Mining Excavations—1," by J. R. Dinsdale, *Colliery Engineering*, December, 1935, Fig. 8, p. 409.

[13] "Untersuchungen zur Erkenntniss des Gebirgedruckes," by R. Fenner, *Glueckauf*, Vol. 74, 1938, pp. 681 and 705.

ϕ being the angle of internal friction of the material in which the tunnel is built. According to Mr. Fenner, in the case of a shallow tunnel, the failure line is parabolic. Of course, the question of the theoretical shape of the failure zones above a tunnel is subject to discussion. The writer believes, however, that the basic idea of a closed failure zone above a deep tunnel, or of an open failure zone in the case of a shallow tunnel, is sound. The same considerations as those for a hole pierced in rock may be applied to a closed failure zone. Thus, the distorted trajectories of major principal stress run around the closed failure zone, and the weight of the material above the zone is transferred by the shearing stresses to sections at and close to the bottom of the failure zone. The lining is loaded by the weight of the material inside the failure zone only.

Before applying these considerations to tunnels in silt of the Lincoln Tunnel type, it is necessary to determine whether a failure line due to downward motion of the silt material may be formed above a tunnel of this type. It should be realized also that, in a general case, shearing stresses above the tunnel are due to two causes—(*a*) consolidation of the silt layer of variable thickness, and (*b*) deflections of the lining. Even when no failure zone is formed, there are upward shearing stresses, the magnitude of which is controlled by the value of the vertical displacements due to causes (*a*) and (*b*).

Subaqueous Tunnels in Silt Constructed by the Shield Method.—The pressure on the lining of subaqueous tunnels in silt, constructed by the shield method, passes through the following stages:

(1) When the lining is shoved and the bulge is being formed, a frictional force along the shearing surfaces (Fig. 2(*a*)) acts downward, thus increasing the preconstruction weight of the overburden. This increase in weight lasts until the bulge starts moving downward. It is quite possible, therefore, that, on July 8, 1935 (see Fig. 7 and Table 1), there was an overload at the center line of the lining of 1.6 lb per sq in. (The lining is deflected during the shoving more than in the subsequent stages of the work when pressure and, hence, deflections are relieved by erosion, dredging, and upward shear and are perhaps somewhat redistributed.)

(2) Because of erosion and especially dredging of the bulge, the pressure on the lining decreases. At the same time two processes start—consolidation of the silt mass above the lining and healing of bonds along the sliding surfaces, as shown in Fig. 2. In stage 2, the pressure on the lining first decreases to its preconstruction value and afterward becomes less than that value. This statement is made with the understanding that a correction for compressed air has been introduced.

(3) Consolidation and healing of the mass proceed, and the pressure on the lining decreases. Examination of Fig. 3 shows that tunnels of the Lincoln Tunnel type are too shallow to develop a closed failure zone at this stage. In addition, it is possible that an open failure zone such as that shown in Fig. 16(*b*) cannot form since there are already sliding surfaces, as shown in Fig. 2. Examination of Fig. 7 reveals also that the shearing stress at the sides (haunches) of the tunnel practically equaled the shearing strength of the silt. Hence, although in a general case it is possible to decrease the pressure on the lining

by making it more flexible, in the case of the Lincoln Tunnel there was little chance to do so. The relieving shearing stresses at this stage were mostly due to differential settlement (that is, to differences in the thicknesses of the consolidating silt layer at the center and at the sides (haunches) of the tunnel). The question "For what period of time will this relief exist?" may be answered only on the basis of the existing data—for about 253 days in the case of the Lincoln Tunnel and for about 90 days in the case of the Detroit Tunnel.

(4) The final stage, if any, could be characterized by the tendency of the earth mass to return to the preconstruction stress condition. The record period in the case of the Lincoln Tunnel was too short, and there is no published evidence of such return. The Detroit Tunnel data cannot be applied to the Lincoln Tunnel unconditionally since the method of construction in both cases was not the same. The writer does not know whether or not, in a general case, the plastic mass, in which a circular tunnel is built, returns completely to its preconstruction-stressed state.

Vertical and Horizontal Silt Pressure on the Lining.—There was a relief in weight of the overburden in the case of the Lincoln Tunnel equal to about 10% at the sides (haunches) and to practically nothing at the center line, the average relief being about 6%. The diagram of actual vertical silt pressure may be obtained easily from Fig. 3(*c*) by introducing corrections from Fig. 7. The diagram in question is not a rectangle as is sometimes assumed.

In regard to the horizontal pressure on the lining, the writer believes that the Rankine formula is applicable—at least at the upper part of the tunnel. To be more precise, there is triangular lateral pressure distribution in the upper part of the lining. The question of lateral pressure is closely connected with that of the angle of internal friction in silt (or a similar value of the angle of repose). When the Holland Tunnel was designed, the angle of internal friction of 20° was assumed; and, using a certain conventional computation procedure, results very close to those measured during the construction of the Lincoln Tunnel were obtained. With an angle of internal friction of 9°, and using a somewhat different computation procedure, acceptable results may be obtained. In reality, neither 20° nor 9° is a correct value. The angle of internal friction of nonconsolidated plastic clays (and the Hudson River silt is very similar to such clay) is not far from zero. The writer believes firmly that this is true for the Lincoln Tunnel silt. Additional empirical formulas for the determination of the lateral pressure in the Hudson River silt may be proposed, for instance: "Compute the hydrostatic pressure at the given depth and add 10% for silt action." Such a recipe furnishes even better results than the formulas.

If another tunnel is ever built in the Hudson River silt, the lateral pressure may be computed in the foregoing conventional manner by assuming a 20° angle of friction, provided, however, that such a new tunnel is driven to the same depth and under the same loading conditions as the Lincoln Tunnel. In such a case, however, it is easier to scale the lateral pressure directly from Fig. 9.

Shearing Surfaces; Angle of Repose of the Silt.—As Mr. Bird rightly states, the straight-line surfaces in Fig. 2(*a*) are only crude approximations. The

statement which Mr. Drucker attributes to Jacob Feld,[6] M. Am. Soc. C. E.—namely, that the angle which the shearing surfaces make with the vertical equals the angle of friction—is also perfectly correct, provided, however, that the soil under consideration is cohesionless sand with an angle of friction of 30°. However, this condition is not true for the Hudson River silt. Some idea of the "angle of repose" of the Hudson River silt is afforded by the following fact concerning the organic silt in the Thames River in Connecticut (which is very similar to that of the Hudson River). During the construction of the first bridge at New London, Conn.:

> "The dredging was * * * performed as an independent preliminary operation, with a clam-shell dredge, and carried down 18 to 23 feet below the river bottom, the material standing on a slope of one to one * * *."[14]

In other words, the angle of repose of the silt in question is 45°. Obviously, this value is only apparent and is due to the cohesion of the material. The writer has had opportunities to observe the behavior of the Thames River silt when excavation for the piers of the highway bridge (opened in 1943) was in progress. Large silt blocks extracted from the bottom of the river maintained their shapes—sometimes with practically vertical faces.

Tangent to the Shear Diagram at the Center Line of the Tunnel.—The writer originally assumed that this tangent to the diagram of the relieving shearing stresses at the center line was horizontal. Whether or not this assumption is true can be determined only from a considerable number of observations. In any case, the writer does not insist on this horizontality, especially because in the diagram, Fig. 14, the tangent in question is oblique. It should be explained, however, that the angle in Fig. 14 varies according to the change in ratio of the vertical and horizontal scales of the drawing.

Compressed Air Action, Passive Resistance, and Soil Constant.—If a circular metallic tube of a certain thickness is subjected to internal pressure, stresses develop in the tube, the radial stress at the outside surface of the tube being zero, because of boundary conditions. If the tube is buried in earth, the tube and the surrounding earth mass work as a unit. The combined system "tube plus soil mass" may be visualized as a tube of a very large (in some cases infinite) thickness made of a nonhomogeneous material; and, if the tube proper is subjected to internal pressure, the entire mass of surrounding soil is stressed, the radial stress being zero only at the boundary of that earth mass (in some cases at infinity). At the outside surface of the tube proper, there is a radial stress. Since action and reaction are equal, the radial stress equals the stress in the earth mass at the given point.

If the soil mass surrounding the tube in question is loaded for the first time, the use of the "soil constant" is fully justified; but, if the soil mass is already heavily stressed, an additional stress increment would produce only a very restricted displacement. Stress-strain diagrams of a heavily loaded soil mass illustrate this fact clearly when a further increment of load produces a surprisingly small strain. Thus, in the design and analysis of earth structures,

[6] *Proceedings*, Brooklyn Engrs. Club, Vol. 22, No. 2, January, 1924, p. 33.

[14] *The Engineering and Building Record and the Sanitary Engineer*, October 11, 1890, p. 296.

the live load is not considered at all. The live load certainly produces stresses in the earth structure, but causes practically no deformations.

The so-called "soil constant" is a conventional "tool" used by some tunnel designers for convenience in computations. Deflection values computed using the "soil constant" are excessively large if the mass has been previously loaded. Therefore, the belief that passive resistance of a certain magnitude can be developed only by producing the displacement computed from the corresponding "soil constant" is decidedly erroneous.

Conclusion.—The writer greatly appreciates the valuable discussions by Messrs. Drucker and Bird which have offered the writer an opportunity to clarify several important points in the theory of tunnels. Many thanks are due to both discussers for their painstaking work. Many more field observations, analyses of data, and discussions by the profession are needed, however, before the problem of pressures on tunnels can be definitely solved.

AMERICAN SOCIETY OF CIVIL ENGINEERS

Founded November 5, 1852

DISCUSSIONS

DESIGN CONSTANTS FOR BEAMS WITH NONSYMMETRICAL STRAIGHT HAUNCHES

Discussion

BY AUGUST L. AHLF

AUGUST L. AHLF,[14] JUN. AM. SOC. C. E.[14a]—The discussion by Mr. Jameson, dealing with beams having haunches of infinite depth, is a welcome addition to the paper. This phase of the analysis of haunched beams is somewhat simpler than the case of beams with varying depth of haunch in that one set of variables, d_1 and d_2, are eliminated, leaving only the length of the haunches, a_1 and a_2, to be considered.

The general equations of column analogy as presented in the paper may be made to apply to the case where the beam has haunches of infinite depth. The expressions representing the constants of Eqs. 2, 4, and 6, respectively, will then be as follows: In Eq. 2—

$$C = 0.5 - a \ldots\ldots (54a)$$

in Eq. 4—

$$C = 0.5\,(0.5 - a)^2 \ldots\ldots (54b)$$

and in Eq. 6—

$$C = 0.333\,(0.5 - a)^3 \ldots\ldots (54c)$$

The values of the expressions $(C_1 + C_2)$ in Eq. 15 and $(-C_1 + C_2)$ in Eq. 16 may be obtained by computing the area and locating the center of gravity of the area of the moment diagram which lies between the haunches. As the depth of the beam (and hence the moment of inertia) is constant throughout this reach, these values may be computed from the geometrical properties of the moment diagram without any difficult integration. For the case of a uniform load or a concentrated load, Eqs. 49, 51, and 52 may be used if desired.

The author regrets that the scope of discussion did not permit Mr. Sherman to include a detailed illustration of how the Ruppel tables and the principle of

NOTE.—This paper by August L. Ahlf was published in October, 1944, *Proceedings*. Discussion on this paper has appeared in *Proceedings*, as follows: April, 1945, by Robert O. Jameson, John Sherman, Dale H. Rea, and I. B. Hosig.

[14] Engr., U. S. Bureau of Reclamation, Dept. of Interior, Denver, Colo.

[14a] Received by the Secretary May 21, 1945.

superposition could have been used to simplify the solution of nonsymmetrical haunched beams. A comparison of the relative accuracy and the amount of labor involved would have been of interest.

Mr. Rea has demonstrated ably the procedure to be followed in the column analogy solution of haunched beams by dividing the member into a number of segments. The close agreement between the results obtained by this approximate method and those obtained from tabular values is gratifying. The great number of beam segments chosen and the care with which Mr. Rea made the computations no doubt explain this agreement.

The truth of the statement—"the product of the carry-over factor away from the end and the stiffness factor at the end is constant for a given beam"—may be demonstrated by rearranging Eqs. 14*a* and 14*b* and equating:

$$r_1 K_1 = N = r_2 K_2 \ldots\ldots\ldots\ldots\ldots\ldots\ldots\ldots (55)$$

The term, "absolute carry-over moment," was used with deliberation. The carry-over factor was determined by dividing the induced or absolute carry-over moment by the applied moment represented by the absolute stiffness factor. It is important that the absolute stiffness factor and not the relative stiffness factor be used. The word, "absolute," was applied to both cases so that the numerator and denominator would agree in terminology.

The energy expended in the preparation of this paper is amply repaid by Mr. Hosig's statement that he "considers the tables a very valuable addition to his 'tool kit'"—even though only as a check for the results obtained by other, more laborious methods. After several hours have been spent in setting up the fundamental equations involving the slopes and deflections of a member, such as in the illustrative example, and in evaluating the resulting integrals, the values in Table 1 should give a convenient, accurate, and useful check of the results.

A discussion of the slopes, deflections, and curvatures of the haunched beam was avoided purposely. The primary objective of the paper was to present a rapid and accurate method by which the structural designer could obtain the stiffness factors, carry-over factors, and fixed-end moments for the nonsymmetrically haunched beam. It was presumed that an academic discussion was not required as a designer qualified to perform this type of analysis must be acquainted with the meaning of these terms.

Mr. Hosig's statement that there is an indication of error resulting from the viewpoint held by the writer is incongruous with his later statement that scattering values were checked by the classical method and that no errors were found.

The writer prefers to consider the phenomena of the induced or carry-over moment as actually existing in a structural frame. In the method of distributing fixed-end moments, each joint of the frame is considered to be held rigidly against rotation while the frame is subjected to loading. As each joint is released successively from restraint, the ends of the members, which comprise the joint, will be rotated because the unbalanced moment has been released. The opposite end of each member, still rigidly held, will have

moments induced or carried over to that end because of the rotation which the released end experiences. This procedure seems simpler than the consideration of each member as an isolated cantilever which is permitted to deflect and is then restored to its original position by the application of a force and a couple at the cantilevered end.

The statement that the induced moment can be no part of the applied moment is not consistent with structural theory. There are many charts and tables available whereby the design constants may be obtained for members with a haunch at only one end. The method presented is applicable, although not recommended, for this case. The procedure to be followed is the same as that outlined in Examples 1, 2, and 3. In this case, however, the length of the haunch at the small end should be considered equal to zero and the values of Table 1 under the heading of $a = 0$ must be used.

Corrections for *Transactions:* In October, 1944, *Proceedings*, in Table 1(*f*) and 1(*h*), page 1241, substitute the following values for $a = 0.2$:

d	Table 1(*f*)	Table 1(*h*)
1.0	0.0365	0.0469
1.2	0.0353	0.0451
1.4	0.0345	0.0437
1.6	0.0340	0.0426
1.8	0.0336	0.0418
2.0	0.0332	0.0412
2.2	0.0329	0.0407
2.4	0.0327	0.0405
2.6	0.0324	0.0400
2.8	0.0323	0.0399
3.0	0.0321	0.0395
4.0	0.0315	0.0387

On page 1243, line 3, change "rotate the free end" to "rotate the hinged end"; on page 1253, in the definition of Q_f, change "statical moment of load acting on analogous column" to "statical moment, about the center of the span, of the load acting on an analogous column."

The corrected forms of Examples 3*a* and 3*b* are as follows:

"EXAMPLE 3*a*

"Find the fixed-end moment for a triangular load totaling W pounds, having the small end of the load at end 1, for the beam shown in Fig. 4. (Values of A, e_a, L_1, L_2, and Q_a are as taken from Example 1.)

"*Load on the Analogous Column.*—From Table 1(*f*), using a_1 and d_1 to find C_1; and from Table 1(*h*), using a_2 and d_2 to find C_2—$C_1 + C_2 = 0.0329 + 0.0454 = 0.0783$. With these factors known, Eq. 15 becomes

$$P = \frac{0.0783\ W\ L^2}{E\ I_o} \qquad (34)$$

"*Statical Moment of Load.*—From Table 1(*g*), using a_1 and d_1 to find C_1; and from Table 1(*i*), using a_2 and d_2 to find C_2—$-C_1 + C_2 = -0.0047 + 0.0085 = 0.0038$. With these factors known, Eq. 16 becomes

$$Q_f = \frac{0.0038\ W\ L^3}{E\ I_o} \quad \ldots\ldots\ldots\ldots\ldots\ldots\ldots\ldots (35)$$

Then, by Eq. 17,

$$e_f = \frac{0.0038\ W\ L^3}{E\ I_o} \div \frac{0.0783\ W\ L^2}{E\ I_o} = 0.0485\ L \quad \ldots\ldots\ldots (36a)$$

and

$$e_f - e_a = (0.0485 - 0.0338)\ L = 0.0147\ L \quad \ldots\ldots\ldots (36b)$$

"*Fixed-End Moments.*—Applying Eq. 18*a* to determine the fixed-end moment at end 1,

$$\text{FEM} = \frac{0.0783\ W\ L^2}{E\ I_o} \div \frac{0.8036\ L}{E\ I_o}$$

$$+ \left(\frac{0.0783 \times 0.0147}{0.0455}\right)(-0.5338)\ W\ L = 0.0839\ W\ L \quad \ldots\ldots (37a)$$

Similarly, applying Eq. 18*b* to determine the fixed-end moment at end 2,

$$\text{FEM} = 0.0974\ W\ L + \frac{0.0783 \times 0.0147}{0.0455} 0.4662\ W\ L = 0.1092\ W\ L \ldots (37b)$$

"EXAMPLE 3*b*

"Find the fixed-end moment for a triangular load totaling W pounds, having the large end of the load at end 1, for the beam shown in Fig. 4. (Values of A, e_a, L_1, L_2, and Q_a are as taken from Example 1.)

"*Load on the Analogous Column.*—From Table 1(*h*), using a_1 and d_1 to find C_1; and from Table 1(*f*), using a_2 and d_2 to find C_2—$C_1 + C_2 = 0.0407 + 0.0356 = 0.0763$. Eq. 15 then yields:

$$P = \frac{0.0763\ W\ L^2}{E\ I_o} \quad \ldots\ldots\ldots\ldots\ldots\ldots\ldots\ldots (38)$$

"*Statical Moment of Load.*—From Table 1(*i*), using a_1 and d_1 to find C_1; and from Table 1(*g*), using a_2 and d_2 to find C_2—$-C_1 + C_2 = -0.0067 + 0.0060 = -0.0007$. With these factors known, Eq. 16 becomes

$$Q_f = \frac{-0.0007\ W\ L^3}{E\ I_o} \quad \ldots\ldots\ldots\ldots\ldots\ldots\ldots\ldots (39)$$

Then, as in Example 3*a*, Eq. 17 yields

$$e_f = \frac{-0.0007\ W\ L^3}{E\ I_o} \div \frac{0.0763\ W\ L^2}{E\ I_o} = -0.0092\ L \quad \ldots\ldots\ldots (40a)$$

and

$$e_f - e_a = (-0.0092 - 0.0338)\ L = -0.0430\ L \quad \ldots\ldots\ldots (40b)$$

"*Fixed-End Moments.*—Applying Eq. 18*a* to determine the fixed-end moment at end 1,

$$\text{FEM} = \frac{0.0763\ W\ L^2}{E\ I_o} \div \frac{0.08036\ L}{E\ I_o}$$

$$+ \frac{(0.0763 \times -0.0430)}{(0.0455)} (-0.05338)\ W\ L = 0.1334\ W\ L \ldots\ldots (41a)$$

Similarly, applying Eq. 18*b* to determine the fixed-end moment at end 2,

$$\text{FEM} = 0.0949\ W\ L + \frac{0.0763 \times -0.0430}{0.0455}$$

$$\times (-0.5338)\ W\ L = 0.0613\ W\ L \ldots\ldots\ldots\ldots (41b)"$$

AMERICAN SOCIETY OF CIVIL ENGINEERS

Founded November 5, 1852

DISCUSSIONS

CONSTRUCTION OF THE FLOW NET FOR HYDRAULIC DESIGN

Discussion

BY H. ALDEN FOSTER

H. ALDEN FOSTER,[6] M. AM. SOC. C. E.[6a]—The fact that so little discussion has been submitted on the paper might seem to indicate that there is not much general interest in the subject of flow nets as applied to hydraulic design. However, as noted by Professor Howe, the flow net has been used to good advantage in solving problems of two-dimensional flow. In the writer's opinion, the graphical method described in the paper does materially assist in the construction of the flow net; and, in many cases, the method should permit a much more precise determination of the velocity distribution, which, as a rule, is the primary purpose for which the flow net is constructed.

The extension of the graphical method to problems of three-dimensional flow has seemed to the writer to be logical, provided that the radius of curvature of the streamlines, in space, is not appreciably different from that for two-dimensional flow. Such an assumption is subject to verification by experiment. Unfortunately, there are few experimental data available on which to base a reliable test. The application of the graphical method to the experiments (8)[6b] by Cecil S. Camp, Assoc. M. Am. Soc. C. E., as noted by Professor Howe, indicates at least an approximate agreement when applied to a three-dimensional problem.

Essentially, a flow net for any particular hydraulic structure would be constructed only as a substitute for a model test. There is nothing to be determined by the flow net that cannot be learned with greater accuracy from a model test. However, model tests are often expensive and time consuming; and, in general, it should be possible to prepare a flow net at a considerable saving in cost and time. Even if a model test is to be conducted, it may be worth while to make a preliminary flow-net study as a guide to the construction

NOTE.—This paper by H. Alden Foster was published in May, 1944, *Proceedings*. Discussion on this paper has appeared in *Proceedings*, as follows: January, 1945, by J. W. Howe; and March, 1945, by Clarence S. Jarvis.

[6] Designing Engr., Parsons, Brinckerhoff, Hogan & Macdonald, New York, N. Y.

[6a] Received by the Secretary April 26, 1945.

[6b] Numerals in parentheses, thus: (8), refer to corresponding items in the Bibliography (see Appendix I of the paper), and at the end of discussion in this issue.

and testing of the model. Any device that would facilitate the preparation of the flow net should be worth consideration by the designer.

Mr. Jarvis seems to be under the impression that the writer's primary intention was to present a method for the design of "morning-glory" spillways. Actually, this problem was discussed only for the purpose of illustrating the application of the flow-net method to the more complicated conditions of three-dimensional flow when one boundary of the water passage is exposed to the atmosphere.

The writer is in general agreement with most of Mr. Jarvis' comments on morning-glory spillways. However, this subject is entirely beyond the scope of the paper. Consequently, it does not appear advisable to discuss the questions raised by Mr. Jarvis. In the writer's opinion, no adequate treatment of the complete theory of the design of such spillways has yet been published. He hopes, however, that the present paper may prove useful in the design of morning-glory spillways as well as in that of many other types of hydraulic structures.

Bibliography.—

(8) **"Tests of Circular Weirs,"** by Cecil S. Camp and J. W. Howe, *Civil Engineering*, April, 1939, p. 247. (*a*) Eq. 3, p. 248.

AMERICAN SOCIETY OF CIVIL ENGINEERS

Founded November 5, 1852

DISCUSSIONS

TRANSPORTATION OF SUSPENDED SEDIMENT BY WATER

Discussion

BY PAUL F. NEMENYI

PAUL F. NEMENYI,[56] ESQ.[56a]—The investigations made by Professor Vanoni represent a considerable advance in the study of sediment dynamics and of the relation of sediment dynamics to turbulence. Professor Vanoni's analysis of the deviations between the distribution of momentum transfer and sediment transfer in the cross section of a conduit seems particularly valuable. The highly controversial subject of secondary currents, too, has been advanced considerably by the author (see heading, "Discussion of Results: Secondary Flow Due to Suspended Load), by the phenomenon observed in connection with run 15.

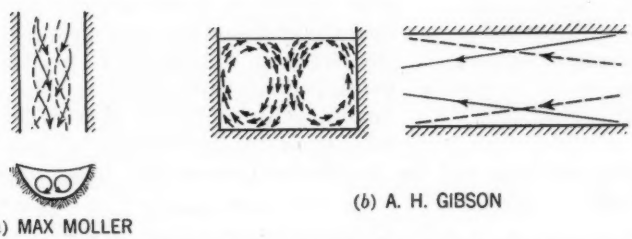

FIG. 18.—ORIGINAL OBSERVATIONS ON SECONDARY CURRENTS

The first observations on this subject were made by the German geophysicist, Max Möller,[38] and the American hydraulic engineer, the late F. P. Stearns,[37] M. Am. Soc. C. E., simultaneously and independently of each other

NOTE.—This paper by Vito A. Vanoni was published in June, 1944, *Proceedings*. Discussion on this paper has appeared in *Proceedings*, as follows: December, 1944, by Ralph W. Powell, and E. R. Van Driest; February, 1945, by Weston Gavett, and Berard J. Witzig; and March, 1945, by A. A. Kalinske.

[56] Asst. Prof., Mathematics Dept., The State College of Washington, Pullman, Wash.

[56a] Received by the Secretary March 2, 1945.

[38] "Studien über die Bewegung des Wassers in Flüssen mit Bezugnahme auf die Ausbildung des Flussprofiles," by Max Möller, *Zeitschrift für Bauwesen*, 1883, p. 201. A summary in English is given in *Hydraulic Laboratory Practice*, edited by J. R. Freeman, A. S. M. E., 1929, p. 70.

[37] "On the Current-Meter, Together with a Reason Why the Maximum Velocity of Water Flowing in Open Channels Is Below the Surface," by F. P. Stearns, *Transactions*, Am. Soc. C. E., Vol. XII (1883), pp. 331–338.

in 1882. Both writers agreed that secondary circulation consists of two perfectly symmetrical parts tending toward the middle of the open conduit at the top and tending outward at the bottom of the open conduit. Fig. 18(*a*) represents the Möller interpretation of this flow. The phenomenon was rediscovered, independently of both Messrs. Möller and Stearns, by A. H. Gibson,[39] in 1909 (see Fig. 18(*b*)), who found the order of magnitude of the cross-velocity component to be 5% of the longitudinal main velocity. Mr. Gibson's investigations seem to improve upon those of Messrs. Möller and Stearns both as to exactness and range of observations. Mr. Gibson found the surface convex whereas Mr. Möller thought it to be somewhat concave. There is a good theoretical reason to believe that in this point Mr. Gibson's observation is correct, because roughness protuberances, like any other obstacles, tend to produce a locally lowered average pressure. The theoretical explanations offered by Mr. Möller are "begging the question," whereas those by Mr. Gibson appear to be obscure.

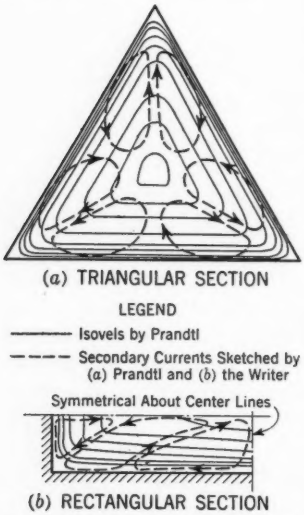
(a) TRIANGULAR SECTION
LEGEND
Isovels by Prandtl
Secondary Currents Sketched by (a) Prandtl and (b) the Writer
Symmetrical About Center Lines
(b) RECTANGULAR SECTION

FIG. 19.—SECONDARY CURRENTS IN CLOSED CONDUITS, ACCORDING TO THE PRANDTL HYPOTHESIS

The three independent investigators agree remarkably well, in assuming the simplest imaginable general pattern of secondary circulation. This very reassuring finding, which is generally accepted by most hydraulic engineers, is challenged by the more elaborate research of L. Prandtl[40] concerning turbulent flow in conduits. Although Mr. Prandtl's investigations refer mainly to closed conduits (see Fig. 19), their implications for open channels and rivers are obvious. Mr. Prandtl's starting point is the surprising shape of the "isovels" in a closed conduit with turbulent flow. The following translation (by the writer) will give an idea of the experimental facts and the hypothetical conclusions based upon them by Mr. Prandtl—

> "Instead of a velocity distribution having increasingly rounded (convex) isovels proceeding inward, as they are known in laminar flow, remarkable types of velocity distributions are found, as shown by the particularly surprising illustrations for the rectangle. For a long time no reasonable explanation was attainable. A paper concerning some old observations on helicoidal movements in straight channels gave a clue which led to an adequate explanation. The water in any conduit with a noncircular cross section has such a secondary movement that in any corner the secondary movement is directed along the bisectrix of the angle toward the corner, whereas, along the adjoining sides, the secondary movement is away from

[39] "Hydraulics and Its Applications," by A. H. Gibson, D. Van Nostrand Co., 3d Ed., 1925, p. 331, following the article "On the Depression of the Filament of Maximum Velocity in a Stream Flowing Through an Open Channel," by A. H. Gibson, *Proceedings*, Royal Soc. of London, Series A, Vol. 82, 1909, pp. 149–159.

[40] "Über die ausgebildete Turbulenz," by L. Prandtl, *Proceedings*, 2d International Cong. for Applied Mechanics, Zurich, 1927, p. 62.

the corner. These secondary streams, together with the turbulent pulsations, explain the observations well. The secondary streams are always carrying longitudinal momentum toward the corner, thus causing the unexpectedly high longitudinal velocities found there. However, how can the existence of the secondary streams be explained? There is no explanation unless the pulsatory, mixing movement along the isovels of the cross section—the 'asimutal' pulsation—is assumed to be more vigorous than that perpendicular to it along the velocity gradient. Indeed, if this is true, a simple consideration of the momentum distribution shows that the type of pulsations assumed to be particularly vigorous is connected of necessity with forces pointing toward the convex side of the isovels—forces which are particularly strong where the isovels have sharp curvatures. The question of why the pulsations are of the particular type assumed, however, is part of the 'great problem of turbulence' for which even a tentative solution, for the time being, is unattainable."

It is obviously impossible to draw a system of secondary streamlines for any cross section, such that each line is closed and, at the same time, is an orthogonal trajectory to the isovels. The best procedure to follow, therefore, is to start by tracing orthogonals to the system of isovels in the region where they have very sharp curvature and to consider these as part of the secondary streamlines. The remainder of the secondary streamlines, even if Mr. Prandtl's basic assumption is accepted as correct, will be based more or less upon conjecture.

Some uncertainty, however, is inherent in every theory that is merely qualitative. More serious than these uncertainties in practical application is the question as to the acceptability of the fundamental conceptions underlying the Prandtl hypotheses. For a statistically steady and permanent flow it is strictly meaningless to consider the steady secondary streams as caused by certain pulsations, and the shape of the isovels as caused by the secondary streams, because all are present at the same time and identically present in any cross section. The basic idea of causation, the explanation of the future from the present (or the present from the past), is inapplicable here. Therefore, in the background of Mr. Prandtl's too schematically expressed hypotheses one must seek an explanation as to the gradual development of the statistically steady, fully turbulent flow from laminar flow. If the investigator begins with laminar flow and assumes that with increasing average velocity the flow becomes turbulent gradually (an assumption which is by no means always justified) he can evolve a rational form to the Prandtl hypotheses. As soon as turbulence develops, comparatively strong pulsations along the originally laminar isovels may be assumed, which would indeed generate the secondary stream. The secondary stream, in its turn, starts to alter the isovels. With increasing turbulence, the "asimutal" pulsations (that is, pulsations favoring the isovels as orbits), and with them the secondary streams, increase and modify the isovels so long as, with fully developed turbulence, a statistical equilibrium is established. Stated in this way, the Prandtl hypothetical secondary currents, and the hypothetical prevalence of asimutal pulsations, would give a probable explanation for the surprising shape of the isovels, provided the turbulent régime develops gradually from the laminar régime. To the writer's knowledge, however, no direct experimental verification, even

of the existence of secondary currents, much less of the particular patterns assumed by Mr. Prandtl, is as yet available for any closed conduit.

For open channels, Mr. Prandtl did not indicate the pattern of secondary currents. The uncertainty of the practical application of his hypothesis to open channels is particularly great. In Fig. 20, the writer has applied the hypothesis tentatively to a broad, very rough channel and to a somewhat narrow channel—in one case tracing the hypothetical secondary circulations on the basis of the velocity measurements by H. Bazin and, in the other case, on the basis of Mr. Prandtl's isovels. In each case, there is a rather complicated pattern of circulation which is thoroughly at variance with the simple results obtained by Mr. Gibson and his precursors. However, in the latter example on the surface (Fig. 20(*b*)), and in the former example (Fig. 20(*a*)), both on the surface and at the bottom, the secondary currents are qualitatively the same according to both assumptions, so that only a more exact investigation can provide sufficient information for a decision between the conflicting possibilities.

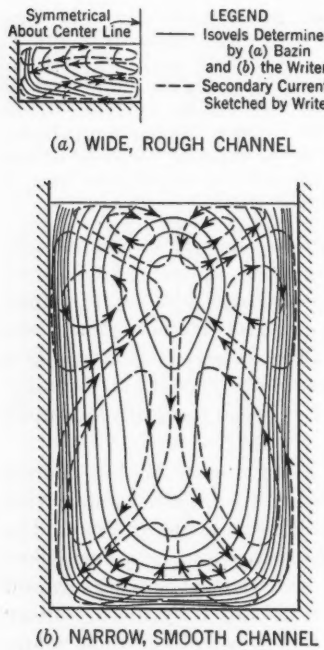
Symmetrical About Center Line
LEGEND
—— Isovels Determined by (a) Bazin and (b) the Writer
--- Secondary Currents Sketched by Writer
(a) WIDE, ROUGH CHANNEL
(b) NARROW, SMOOTH CHANNEL

FIG. 20.—SECONDARY CURRENTS IN OPEN RECTANGULAR CHANNELS, ACCORDING TO THE PRANDTL HYPOTHESIS

The latest information concerning secondary currents in a straight conduit containing homogeneous water comes from a very stimulating paper[57] by M. A. Welikanov, published in 1936. This work is a survey of fairly recent contributions of hydrologists and hydrodynamists of the U.S.S.R. to the understanding of river forms on a fluid dynamic basis. A considerable part of the paper deals with secondary currents in straight open channels.

Apart from somewhat questionable theoretical arguments Mr. Welikanov adduces the experimental results of Mr. Lossievsky in favor of the presence of steady secondary currents in any straight conduits with turbulent flow. Mr. Lossievsky found:

(1) For a broad rectangular cross section, the same result as Mr. Gibson;

(2) For rectangular channels with large ratio of depth to width, two secondary currents but with circulation opposite to the Gibson pattern;

(3) For intermediate depth-width ratio, a more complicated and rather unstable pattern of secondary currents, and

(4) For a strongly unsymmetrical cross section, one single stable secondary current.

[57] "Flussbettbewegungen und Geschiebefuhrung," by M. A. Welikanov, *Bulletin No. 6, D*, Fünfte Hydrologische Konferenz der Baltischen Staten, Helsinki, Finland, 1936.

Only item (2) is in direct contradiction to the expectation based on Mr. Gibson's results, whereas all four items (with the possible, but doubtful, exception of item (3)) are at variance with what one would expect on the basis of the Prandtl hypothesis.

A possible explanation of these contradictions is that Mr. Lossievsky failed to observe the entire pattern of secondary currents in the cross section and, on the basis of observations at the surface and the bottom, reached unwarranted conclusions; or that his results are thoroughly vitiated by the use of insufficiently long channels. Of course, it is also possible that Mr. Lossievsky's results are reasonably exact and that Mr. Prandtl's work, as well as that of Mr. Gibson, needs to be revised. Mr. Lossievsky's item (3) would be probable enough, provided that items (1) and (2) were correct. Indeed, an unstable, shifting pattern of flow can be expected under transitional conditions between two substantially different, distinct types of flow.

The great number of contradictions and discrepancies among the various investigations available on this subject suggests also the possibility that all the secondary currents are a mere consequence either of an insufficiently permanent régime of flow or of temperature influences or other nonhomogeneities in the force field. Professor Vanoni seems to be precisely of this opinion when he ascribes the interesting secondary circulations observed by him entirely to the presence of sediment. However, a simple theoretical consideration shows that, even in a perfectly homogeneous fluid, if the flow is turbulent, secondary currents of appreciable intensity will normally be present. Indeed, however questionable may be Mr. Prandtl's assumption that the pulsations favor everywhere the isovels as orbits, it is perfectly rational to assume that at most points of the cross section there will normally be a favored circle of curvature for the pulsations just as there is a favored direction of pulsations. A strictly isotropic pattern of turbulence is an exceptional (actually only an artificially produced) type of turbulence. On the average, straight pulsations are less exceptional; but still it is reasonable to assume that, unless the cross section is circular, in most points of the cross section there will be a favored circle of curvature for the pulsations. Wherever there is such a favored finite circle of curvature for the pulsations, Mr. Prandtl has shown convincingly that a permanent, steady momentum tending to generate secondary currents is present. The writer is convinced, therefore, that nonhomogeneities in the force field are not necessary conditions for the presence of secondary currents.

It must be admitted, however, that nonhomogeneity of the fluid can create substantially stronger secondary currents, at the same time that their pattern may be transformed. The first to observe this new type of secondary currents was Mr. Terada,[58] who showed that the particles of a fluid flowing in a very wide open flume, slightly and uniformly heated from below, move along a helicoidal curve (Fig. 21) so that the movement can be resolved into a straight flow along the channel axis, with secondary circulatory motions in the cross section. The regular striped clouds (popularly called "mackerel sky") were formerly considered "ripple" clouds and were attributed, in accordance with

[58] "Report of the Aeronautical Research Institute," by Terada, Tokyo Imperial Univ., Tokyo, Japan, Vol. III, 1928, and Vol. IV, 1929.

G. H. Darwin, to the rippling influence of a wind perpendicular to the stripes. Many hydrodynamists and meteorologists are of the opinion that this phenomenon may in most cases be due more probably to forced convection streams connected with wind parallel to the stripes—that is, to vortices with a longitudinal axis similar to those which were produced under laboratory conditions by Mr. Terada.

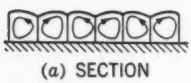

(*a*) SECTION

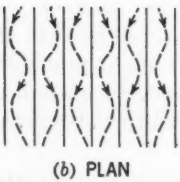

(*b*) PLAN

FIG. 21.—OBSERVATIONS OF SECONDARY CURRENTS, BY TERADA, IN AN OPEN, WIDE, AND STEEP CHANNEL HEATED FROM BELOW

Although Mr. Terada's paper[58] is not accessible to the writer, analogy with other convection phenomena makes it possible to infer that a vorticity with a longitudinal axis of this kind can be generated by convection in the nonturbulent as well as in the turbulent régime of flow.

In their brilliant vortex study,[59] M. Luntz and P. Schwartz remarked aptly that the Terada phenomenon is closely analogous to the vortices[60] in the fluid between two coaxial rotating cylinders discovered by G. I. Taylor—the nonhomogeneity of the centrifugal force field replaces the nonhomogeneity of the gravity force field conditioned by temperature differences in the Terada experiment.

In a paper by Hugh Casey,[61] there is a photograph which was made in a channel with turbulent flow and movable bed. No temperature influence was present in this case (at least not intentionally); yet the pattern of the secondary currents which is assumed by Mr. Casey (see Fig. 22) shows a surprising likeness

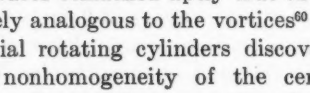

FIG. 22.—SECONDARY CURRENTS IN THE CROSS SECTION OF A BROAD CHANNEL, WITH MOVABLE BED, AS OBSERVED BY HUGH CASEY

to the convective secondary currents in the Terada study, of which Mr. Casey had no knowledge. Equally striking is the qualitative resemblance between these studies and Professor Vanoni's new observations. At the same time, it is important to observe that the number of the stripes is very different in the various cases; it is probably controlled primarily by the depth-width ratio of the flow.

Related to these phenomena, although somewhat less closely, are the longitudinal ridges observed in the African desert by R. A. Bagnold.[62] They differ from the stripes observed by Messrs. Casey and Vanoni in the essential fact that they are interrupted; the interruptions in the ridges observed by Mr. Bagnold are arranged in a more or less regular echelon-like pattern.

The foregoing leads to the decisive question of the rôle played by the secondary currents in the distribution of sediments in suspension and on the

[59] "Hydrodynamique du Cylindre Tournant," by M. Luntz and P. Schwartz, Paris, France, 1935.

[60] "Stability of a Viscous Liquid Contained Between Two Rotating Cylinders," by G. I. Taylor, *Philosophical Transactions*, Royal Soc. of London, Series A, Vol. 223, 1923, pp. 289–343.

[61] "Über Geschiebebewegung Mitteilung der Preussischen Versuchsanstaltfür Wasserbau und Schiffbau," by Hugh Casey, Heft 19, 1935, Fig. 8.

[62] "The Physics of Blown Sand and Desert Dunes," by R. A. Bagnold, William Morrow & Co., New York, N. Y., 1942.

bottom. Mr. Möller was the first to demonstrate the rôle played by secondary currents in the distribution of sediment, in the sorting of sediment in the cross section, and in the gradual alteration of the shape of the bed. There is much valuable material in Mr. Möller's observations and ideas; but it will have to be analyzed, in the light of modern concepts concerning turbulent flow, when knowledge of the secondary currents has become more accurate.

The effect of secondary currents in sediment flow has a twofold significance. First, if the magnitude of these secondary currents reaches a few per cent of the main longitudinal flow, these currents are capable, in their upward reaches, of carrying the finer particles of sediment directly although they may not be able to move the coarser sediment particles. It is necessary to emphasize this point, because John B. Leighly[63] denies the competence of the secondary currents to carry material even in curved rivers where the circulatory movement is very much stronger. Of course, the final decision concerning the relative importance of this effect must be postponed until more exact information is available, but it is obvious that the steady secondary currents constitute a ponderable factor in the analysis of suspension and distribution of finer particles. Second and even more important than this direct effect may be the indirect influence of the secondary currents on sediment distribution. If it is true, as Mr. Prandtl's studies indicate, that the longitudinal velocity distribution and the distribution of pulsations are inseparably interconnected with the steady secondary currents, then the distributions of the shearing stresses and of the Austausch coefficient are also linked, and thus even the phenomena at the bottom itself cannot be properly understood and analyzed without reference to the secondary currents.

For this reason, the writer believes that—in explaining the deviation of sediment distribution from the results of the simple theory—in addition to the two factors considered by Professor Vanoni, as a third, equally important factor the secondary currents (and, with them, the essentially three-dimensional character of the entire flow) should be taken into account.

This substantial deviation from a two-dimensional pattern of flow is probably the main reason also for the unsatisfactory agreement of the velocity distribution observed by Professor Vanoni with the theory advanced by Theodor von Kármán, M. Am. Soc. C. E. It would be quite justifiable to put the boundary of the profile a little below the top of the sand particles; but, even so, an appreciable discrepancy between theoretical and experimental velocity distribution would remain. It appears that there is no way to account for this discrepancy, except by studying the influence of the secondary currents and the entire essentially three-dimensional nature of turbulent flow in any open channel.

That such an approach is necessary follows immediately from scrutiny of Fig. 3. The substantial inadequacy of the assumption of a two-dimensional flow can be made particularly clear by drawing the distribution of velocities at the mid-channel vertical and at some near-by verticals—for example, at one sixth of the channel width from the middle on both sides.

[63] "Turbulence and the Transportation of Rock Debris by Streams," by John B. Leighly, *The Geographical Review*, Vol. 24, No. 3, 1934, p. 461.

If the foregoing reasoning is correct, the modification of any factor—the isovels, the pulsations, or the secondary currents—would influence all other factors and with them the sediment distribution and the bed shape. If the tentative experiments of Potapow can be accepted, it appears that the secondary currents are those elements that are most easily subject to deliberate modification; and thus the study of secondary currents may reveal a new method for the regulation of rivers. In the paper by Mr. Welikanov,[57] there is a short abstract of Mr. Potapow's experimental research which may be translated as follows:

> "The principle of the method is to arrange fixed leading walls in the rivers. To create a clockwise helicoidal movement, it is sufficient to divert the surface stream by the aid of surface screens toward the right. The bottom stream will then be diverted to the left, and a circulation pattern is produced which is maintained for a fairly long distance downstream, where it disintegrates gradually. Instead of surface screens, bottom screens may be used, arranged in the opposite direction; or both devices may be combined. The experiments of Mr. Potapow have established the following applications of these devices: (*a*) Through production of a double circulation [probably Mr. Welikanov means a reinforcement of the circulation according to Mr. Lossievsky's type (1) currents, previously mentioned herein], the axial strip of the bed can be deepened; (*b*) in a curve the existing circulation pattern can be reversed, bringing the scour to the convex side and making the concave side, on which the 'talweg' of the natural river was situated, shallower; (*c*) the increase of sand bars can be prevented through artificial diversion of the bed load from the bar threshold; and (*d*) in case of bifurcation the sediment can be directed, according to wish, into either branch. These four examples suffice to indicate the great importance of Mr. Potapow's results in various fields of hydraulic engineering."

To summarize:

1. The presence of nonhomogeneity in the fluid (caused either by temperature influence or by the presence of a dissolved or granular material) is by no means a necessary condition for the generation of steady secondary currents. The occurrence of such currents is normal, rather than exceptional, in turbulent flow.

2. The distributions of the longitudinal velocities, of the pulsations, of the steady secondary currents, and of suspended sediment (if suspendible material is present) are mutually and inseparably interconnected, so that an artificial change of any one of these factors would inevitably tend to modify all others.

3. Observations by Mr. Potapow suggest that an artificial modification of the secondary currents is easily practicable and that therefore these might be used as a steering effect to modify, or to stabilize, sediment distribution and bed formation.

4. From items 1 and 2, it follows that the three-dimensional nature of turbulent flow in an open channel is a major factor—probably the main factor—required to explain deviations of experimental findings from the two-dimensional von Kármán theory of velocity distribution and sediment suspension.

On the basis of the summary items 1 to 4, and supporting comment, the writer ventures to suggest that the greatest progress in turbulence research in

the near future is not to be expected from a more accurate and more detailed investigation of the turbulence tensor in some exceptionally simple cases (for example, the flow in a circular pipe). Still less can be expected from further study of such artificial cases as isotropic turbulence. Rather, the greatest progress will result from an improved and broadened study of the actual flow conditions in a variety of straight open channels and in a few straight closed conduits of noncircular cross section.

Even if, in the first stages, such a study were restricted to the investigation of the exact shape of the isovels and of the secondary currents (that is, even if no measurements of fluctuations are made at first), by implication it would afford a deepened insight into the three-dimensional mechanism of uniform turbulent flow, making possible a better hypothesis concerning the nature of pulsations than Mr. Prandtl could put forward without any reliable experimental facts concerning the secondary currents. Later, more exact pulsation studies and studies on the distribution of salinity, fine sediment, and other quantities subject to Austausch will make possible the checking and, if necessary, the correction of the hypothetical conclusions drawn from the first stage of the research.

As a beginning, therefore, the problem is to find a reliable picture of the three-dimensional distribution of the time averages of the velocity vectors. Since the secondary currents are comparatively small, this problem is rather difficult, challenging the ability of the best experimenter. Indeed, the contradictions presented by the various writers—all of whom were, in their time, able observers and experimenters—indicate the difficulty of obtaining more exact and more conclusive results concerning the steady secondary currents. The difficulties, of course, are mainly due to the fact that the turbulent pulsations disturb the recording of the steady components. Another difficulty is that, since the angle of the actual time-average velocity vector with the channel axis is rather small, any measuring device introduced into the liquid may vitiate the result. For these and other reasons, the writer's opinion is that the investigation in question will depend essentially upon the further development of purely optical techniques related to the one suggested by A. Fage and H. C. H. Townend.[64] In this method the extremely fine submicroscopic particles, which are present even in the purest drinking water, are observed by the aid of an ultramicroscope. If this or a similar optical method could be combined with a photographic technique to record time averages of velocity vectors, a basis for the first stage of the investigation would be presented.

Another method, simpler but probably less accurate, could perhaps be developed through improvements of Mr. Gibson's technique of working with weighted wax pellets. If very small (preferably streamlined) solid bodies can be made of exactly the same weight as the water displaced by them, and if their orbit and speed are recorded photographically, kinematographically, or by aid of Charles Camichel's[65] "chronophotographic" process, the solution of the problem may be possible.

[64] "An Examination of Turbulent Flow with an Ultramicroscope," by A. Fage and H. C. H. Townend, *Proceedings*, Royal Soc. of London, Series A, Vol. 135, 1932, p. 656.

[65] "Rapport des oeuvres effectuées dans les années 1932–35," by C. Camichel, Toulouse, France, 1935.

Those methods which restrict the study to the surface and the bottom (for example, the conventional use of silk threads and surface floats) have been tried and found insufficient. Only a study covering the entire cross section can lead to clarification of controversial points and to the attainment of new insight.

Of course, the greatest care is necessary in such investigations to establish a completely uniform régime of flow. The investigation of the fundamental questions of turbulent flow in an open channel presents a certain amount of additional difficulty compared to investigations in closed conduits. However, open channels have also certain practical advantages. The triangular cross section of an open channel affords excellent opportunities for the study of scale effects by the very simple device of varying the stages. On the other hand, the variation of stages in a nontriangular channel model makes possible the study of a large variety of geometrically dissimilar and, sometimes, even qualitatively very different cross sections. Thus studies of the few channel models indicated in Fig. 23 would give a very wide and highly instructive variety of flow patterns.

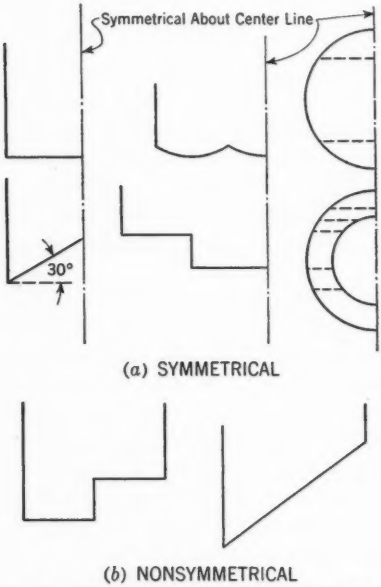

FIG. 23.—CROSS SECTIONS OF CHANNEL MODELS FOR PROPOSED INVESTIGATION

It is the writer's conviction that a research project along these or similar lines would clarify many problems which are essential to the understanding of turbulent flow in its relation to sediment propulsion, bed formation, and bed stabilization, and thus vital for river engineering. In addition, it may prove important for the most general and fundamental aspects of turbulence research.

The writer wishes to express his thanks to E. W. Lane, M. Am. Soc. C. E., of the Iowa Institute of Hydraulic Research, Iowa City, Iowa, for permission to use the results of an unpublished study that the writer made while he was a member of the staff of the Iowa Institute of Hydraulic Research.

AMERICAN SOCIETY OF CIVIL ENGINEERS

Founded November 5, 1852

DISCUSSIONS

CHARACTERISTIC REDUNDANTS USED FOR ANALYZING STATICALLY INDETERMINATE STRUCTURES

Discussion

BY JOHN B. WILBUR

JOHN B. WILBUR,[27] M. AM. SOC. C. E.[27a]—The discussion of this paper has been appreciated. The writer believes that the proposed method would have been more attractive to some if it had been interpreted in terms of the method of least work. The derivation in the paper might have ended with Section 2. The n characteristic forces $P_{a1}, P_{a2}, \cdots, P_{an}$ as defined in Eq. 5 then could have been taken as the n unknowns for a least work solution.

Let F_n denote the stress in any member of a truss due to the nth set of characteristic forces acting on the primary structure, and F_o equal the stress in any member of a truss due to the applied loads acting on the primary structure; then the n simultaneous equations resulting from a least work solution would be as follows:

$$\left.\begin{aligned}
\frac{\partial W}{\partial P_{a1}} &= \sum (F_o + F_1 + F_2 + \cdots + F_n) \frac{L}{A\,E} \frac{\partial F}{\partial P_{a1}} = 0 \\
\frac{\partial W}{\partial P_{a2}} &= \sum (F_o + F_1 + F_2 + \cdots + F_n) \frac{L}{A\,E} \frac{\partial F}{\partial P_{a2}} = 0 \\
&\cdots\cdots\cdots\cdots\cdots\cdots\cdots \\
\frac{\partial W}{\partial P_{an}} &= \sum (F_o + F_1 + F_2 + \cdots + F_n) \frac{L}{A\,E} \frac{\partial F}{\partial P_{an}} = 0
\end{aligned}\right\} \quad \cdots\cdots (85)$$

Because the characteristic redundants are orthogonal, however, $\sum \frac{F_m L}{A\,E} \frac{\partial F}{\partial P_{an}} = 0$

NOTE.—This paper by John B. Wilbur, Assoc. M. Am. Soc. C. E., was published in June, 1944, *Proceedings*. Discussion on this paper has appeared in *Proceedings*, as follows: September, 1944, by Charles A. Ellis; December, 1944, by Ralph W. Stewart, Myle J. Holley, Jr., M. W. Huggins, and Leon Beskin; and January, 1945, by Frederick S. Merritt.

[27] Prof., Structural Eng., Mass. Inst. Tech., Cambridge, Mass.

[27a] Received by the Secretary April 19, 1945.

when $n \neq m$; whence, Eqs. 85 reduce to

$$\left.\begin{aligned} \sum \frac{F_o L}{A E} \frac{\partial F}{\partial P_{a1}} + \sum \frac{F_1 L}{A E} \frac{\partial F}{\partial P_{a1}} &= 0 \\ \sum \frac{F_o L}{A E} \frac{\partial F}{\partial P_{a2}} + \sum \frac{F_2 L}{A E} \frac{\partial F}{\partial P_{a2}} &= 0 \\ \cdots\cdots\cdots\cdots\cdots\cdots\cdots\cdots\cdots & \\ \sum \frac{F_o L}{A E} \frac{\partial F}{\partial P_{an}} + \sum \frac{F_n L}{A E} \frac{\partial F}{\partial P} &= 0 \end{aligned}\right\} \quad \ldots\ldots\ldots\ldots\ldots\ldots (86)$$

Moreover, Eqs. 86 are not simultaneous in character since the first equation involves only P_{a1} as an unknown; the second equation, only P_{a2}; etc.

To illustrate this procedure, consider the analysis of the truss in Fig. 3(*a*) acted upon by the load. The characteristic loads as defined by Eq. 34 are computed as shown in the paper. Now, letting P_{a1}, P_{a2}, and P_{a3} equal X, Y, and Z, respectively, the F_o, F_1, F_2, and F_3 stresses are computed by statics, leading to the results shown in Fig. 10. Since $\frac{L}{A E}$ has the same value for all members, the working equations reduce to the following:

$$\left.\begin{aligned} \sum F_o \frac{\partial F}{\partial X} + \sum F_1 \frac{\partial F}{\partial X} &= 0 \\ \sum F_o \frac{\partial F}{\partial Y} + \sum F_2 \frac{\partial F}{\partial Y} &= 0 \\ \sum F_o \frac{\partial F}{\partial Z} + \sum F_3 \frac{\partial F}{\partial Z} &= 0 \end{aligned}\right\} \quad \ldots\ldots\ldots\ldots\ldots\ldots (87)$$

The required summations are obtained in Table 4.

TABLE 4.—EVALUATION OF SUMMATIONS OF EQS. 87

Bar	F = TOTAL STRESS = F_o	F_1	F_2	F_3	$F_o \frac{\partial F}{\partial X}$	$F_1 \frac{\partial F}{\partial X}$	$F_o \frac{\partial F}{\partial Y}$	$F_2 \frac{\partial F}{\partial Y}$	$F_o \frac{\partial F}{\partial Z}$	$F_3 \frac{\partial F}{\partial Z}$
L_oL_1	$+0.500\,P$	$-0.600\,X$	$-0.600\,Y$	$-0.600\,Z$	$-0.300\,P$	$+0.360\,X$	$-0.300\,P$	$+0.360\,Y$	$-0.300\,P$	$+0.360\,Z$
L_1L_2	$+0.250\,P$	$-0.849\,X$	0	$+0.849\,Z$	$-0.212\,P$	$+0.720\,X$	0	0	$+0.212\,P$	$+0.720\,Z$
L_2L_3	0	$-0.600\,X$	$+0.600\,Y$	$-0.600\,Z$	0	$+0.360\,X$	0	$+0.360\,Y$	0	$+0.360\,Z$
U_oU_1	0	$-0.600\,X$	$-0.600\,Y$	$-0.600\,Z$	0	$+0.360\,X$	0	$+0.360\,Y$	0	$+0.360\,Z$
U_1U_2	$-0.500\,P$	$-0.849\,X$	0	$+0.849\,Z$	$+0.424\,P$	$+0.720\,X$	0	0	$-0.425\,P$	$+0.720\,Z$
U_2U_3	$-0.250\,P$	$-0.600\,X$	$+0.600\,Y$	$-0.600\,Z$	$+0.150\,P$	$+0.360\,X$	$-0.150\,P$	$+0.360\,Y$	$+0.150\,P$	$+0.360\,Z$
U_3L_3	0	$-0.800\,X$	$-0.800\,Y$	$-0.800\,Z$	0	$+0.640\,X$	0	$+0.640\,Y$	0	$+0.640\,Z$
U_1L_1	$+0.667\,P$	$-1.933\,X$	$-0.800\,Y$	$+0.333\,Z$	$-1.290\,P$	$+3.735\,X$	$-0.533\,P$	$+0.640\,Y$	$+0.222\,P$	$+0.111\,Z$
U_2L_2	$-0.333\,P$	$-1.933\,X$	$+0.800\,Y$	$+0.333\,Z$	$+0.645\,P$	$+3.735\,X$	$-0.267\,P$	$+0.640\,Y$	$-0.111\,P$	$+0.111\,Z$
U_3L_3	$-0.333\,P$	$-0.800\,X$	$+0.800\,Y$	$-0.800\,Z$	$+0.267\,P$	$+0.640\,X$	$-0.267\,P$	$+0.640\,Y$	$+0.267\,P$	$+0.640\,Z$
U_oL_1	0	$+X$	$+Y$	$+Z$	0	$+1.000\,X$	0	$+1.000\,Y$	0	$+1.000\,Z$
L_oU_1	$-0.833\,P$	$+X$	$+Y$	$+Z$	$-0.833\,P$	$+1.000\,X$	$-0.833\,P$	$+1.000\,Y$	$-0.833\,P$	$+1.000\,Z$
U_1L_2	0	$+1.414\,X$	0	$-1.414\,Z$	0	$+2.000\,X$	0	0	0	$+2.000\,Z$
L_2U_2	$+0.417\,P$	$+1.414\,X$	0	$-1.414\,Z$	$+0.590\,P$	$+2.000\,X$	0	0	$-0.590\,P$	$+2.000\,Z$
U_2L_3	0	$+X$	$-Y$	$+Z$	0	$+1.000\,X$	0	$+1.000\,Y$	0	$+1.000\,Z$
L_2U_3	$+0.417\,P$	$+X$	$-Y$	$+Z$	$+0.417\,P$	$+1.000\,X$	$-0.417\,P$	$+1.000\,Y$	$+0.417\,P$	$+1.000\,Z$
$\Sigma =$	....	....	....	....	$-0.142\,P$	$+19.63\,X$	$-2.767\,P$	$+8.000\,Y$	$-0.991\,P$	$+12.38\,Z$

The equations to determine X, Y, and Z are:

$$\left.\begin{aligned} -0.142\,P + 19.63\,X &= 0; \quad X = +0.007\,P \\ -2.767\,P + 8.000\,Y &= 0; \quad Y = +0.346\,P \\ -0.991\,P + 12.38\,Z &= 0; \quad Z = +0.080\,P \end{aligned}\right\} \quad \ldots\ldots\ldots (88)$$

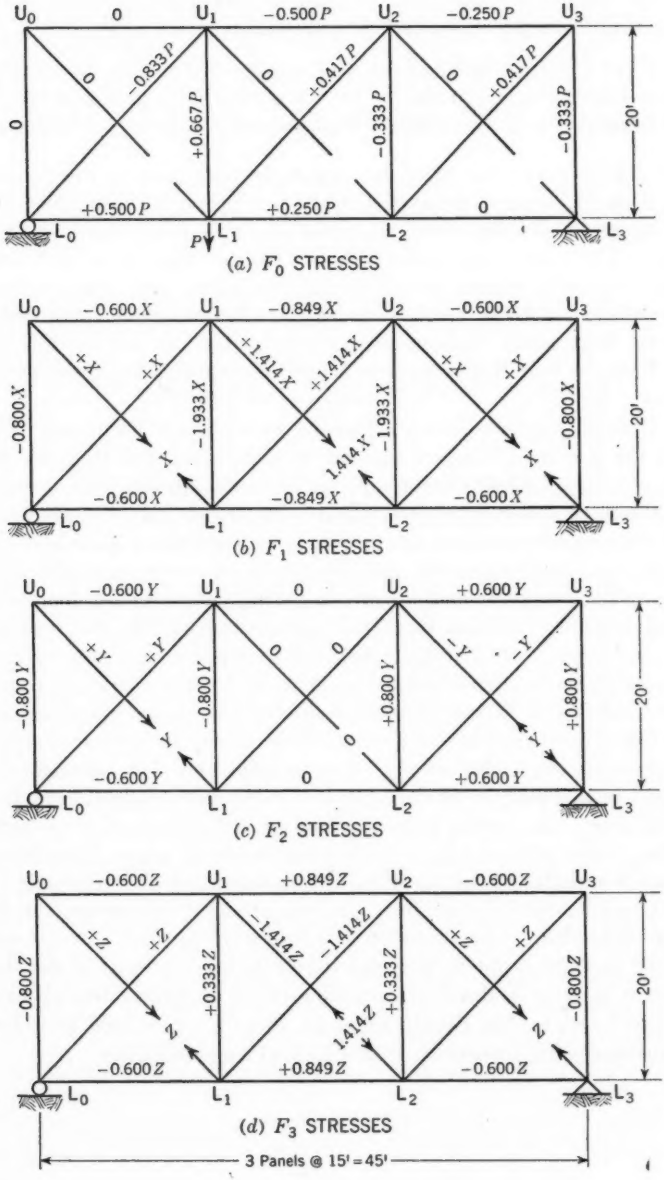
U0 0 U1 −0.500 P U2 −0.250 P U3
0 −0.833 P 0 +0.667 P 0 +0.417 P 0 −0.333 P +0.417 P −0.333 P
20'
+0.500 P +0.250 P 0
L0 P L1 L2 L3
(a) F0 STRESSES
U0 −0.600 X U1 −0.849 X U2 −0.600 X U3
−0.800 X +X +X −1.933 X +1.414 X +1.414 X −1.933 X +X +X −0.800 X
20'
−X 1.414 X −X
−0.600 X −0.849 X −0.600 X
L0 L1 L2 L3
(b) F1 STRESSES
U0 −0.600 Y U1 0 U2 +0.600 Y U3
−0.800 Y +Y +Y −0.800 Y 0 0 +0.800 Y −Y −Y +0.800 Y
20'
−Y 0 −Y
−0.600 Y 0 +0.600 Y
L0 L1 L2 L3
(c) F2 STRESSES
U0 −0.600 Z U1 +0.849 Z U2 −0.600 Z U3
−0.800 Z +Z +Z +0.333 Z −1.414 Z −1.414 Z +0.333 Z +Z +Z −0.800 Z
20'
−Z 1.414 Z −Z
−0.600 Z +0.849 Z −0.600 Z
L0 L1 L2 L3
(d) F3 STRESSES
3 Panels @ 15' = 45'

FIG. 10

Hence, the basic unknowns, X_a, X_b, and X_c (see Fig. 3(a)), are obtained by superposition from the characteristic redundants as follows:

$$\left.\begin{aligned} X_a &= +0.007\,P\ (+1) + 0.346\,P\,(+1) + 0.080\,P\ (+1) = +0.433\,P \\ X_b &= +0.007\,P\,(+\sqrt{2}) + 0.346\,P\ \ (0)\ \ + 0.080\,P\,(-\sqrt{2}) = -0.103\,P \\ X_c &= +0.007\,P\ (+1) + 0.346\,P\,(-1) + 0.080\,P\ (+1) = -0.259\,P \end{aligned}\right\} \quad (89)$$

In a minor way, the foregoing solution may answer the objections of Messrs. Ellis, Stewart, and Merritt that the method is too mathematical and too tedious to be of value, but the writer cannot actually hope to answer this criticism. The paper was presented in the belief that ideas that are new to structural engineers should be offered for discussion, even though their direct and immediate practical application may not be apparent—provided there is some hope that these ideas may eventually lead to worth-while methods. Messrs. Huggins and Holley have accepted the efforts of the writer from this viewpoint.

Mr. Beskin has contributed a learned and critical discussion which adds much to the general picture of the use of orthogonal functions in structural analysis, although he holds little hope for practical applications of this method in the analysis of statically indeterminate structures. He stresses the relation between the proposed method and methods for computing periods of vibration —actually the line of reasoning that led to the proposed method. An understanding of the proposed method of computing characteristic loads may help structural engineers wishing to extend their interests into the field of vibrations. Contrary to Mr. Beskin, the first sentence in Section 13 is correct, since the number of independent components of displacement is not necessarily equal to the number of independent redundant stress components, although equality happens to exist in the example chosen. By independent components of displacement, the writer simply refers to joint and chord rotations as commonly used in the analysis of rigid frames by the slope deflection method.

Summarizing, the writer believes that, once the characteristic forces corresponding to the redundants in an indeterminate structure have been determined, the remainder of the analysis, in terms of these characteristic forces, is simplified to an important degree. As indicated by the writer, the labor involved in determining the characteristic forces in the first place is such that the over-all method is not very promising in its present state of development. Perhaps it is possible to develop a simple method of determining characteristic forces, or perhaps, as Mr. Beskin suggests, these forces should be determined, in some instances, by inspection from physical considerations.

AMERICAN SOCIETY OF CIVIL ENGINEERS

Founded November 5, 1852

DISCUSSIONS

TRANSLATORY WAVES IN NATURAL CHANNELS

Discussion

BY J. H. WILKINSON

J. H. WILKINSON,[15] M. AM. SOC. C. E.[15a]—The comments and suggestions presented in the discussion of this paper are appreciated greatly. Mr. Weggel suggests that a correction factor provides a method for increasing the agreement between observed and computed velocities. This should be useful for predicting wave travel from data available on a given stream.

The writer is not entirely certain that, referring to the midpoint-of-rise and the midpoint-of-fall,

> "In the solitary wave of translation these points are the only parts of the wave that really travel as a wave front or movement of constant flow or wave height."

In connection with Wave 3, Fig. 2(*b*), if the increase in release at Norris Dam had stopped at 10:00 a.m., on December 12, a wave with $Z_2 = 6.0$ ft would have developed at the Norris gage. This phenomenon occurred in the case of Wave 5. Below the 6.0-ft stage, Wave 3 is practically identical to Wave 5. The portion of Wave 3 below the 6.0-ft stage travels as a wave front as much as does the portion of Wave 3 below the 8.0-ft stage. In a natural channel, the height of a wave varies with the characteristics of the river channel. Wave 3 rose 5 ft at the Norris gage, 5 ft at the Edgemoor gage, and 9 ft at the Wheat gage. At each station, the depth increased to that necessary to discharge the increased flow. Wave heights are constant only in a uniform channel.

When the midpoint-of-rise is used to determine the velocity of a wave in a natural channel, it is assumed that this is an identical point on the wave as it passes successive stations—that half the rise represents the same increase in discharge at successive stations. This is seldom exactly true.

NOTE.—This paper by J. H. Wilkinson, M. Am. Soc. C. E., was published in June, 1944, *Proceedings*. Discussion on this paper has appeared in *Proceedings*, as follows: January, 1945, by Harold A. Weggel, and W. M. Lansford; and February, 1945, by M. A. Churchill.

[15] Senior Hydr. Engr., TVA, Knoxville, Tenn.

[15a] Received by the Secretary May 7, 1945.

Professor Lansford presents experimental results which are in excellent agreement with computed velocities by Eq. 6 for the entire range of depths and flows. These experiments eliminate the uncertainties of variable channel areas and slopes and of local inflow. The results show that the approximate Eq. 2*b* cannot be depended upon for accurate results.

Mr. Churchill presents some interesting data on wave and water velocities for the lower Holston River. The high chloride concentration provides an excellent means of identifying the wave at successive stations and gives much more dependable results for water velocity than does the process of estimating the wave from measurements at four gaging stations as was the case on the Clinch River. Fig. 10 presents observed stages and discharges throughout both the falling and rising waves. The stage-discharge relation which exists at a gaging station under normal flow does not hold during periods of rapidly changing stage such as exist during the passage of a wave. Discharges can be approximated by the Jones formula,[16] but it seems impracticable to attempt to determine discharge throughout a wave.

The 5.7 ratio of wave to water velocity for the Watauga and South Holston rivers with a flow one third of the mean annual flow is slightly higher than that for the Clinch River, where the computed ratio for a corresponding flow is 3.8. Probably, the water velocity at gaging stations is somewhat higher than average for this flow.

Conversion of the wave velocity equation into the form of Eq. 7 simplifies the computation. The writer was fortunate in selecting a reservoir having a uniform variation in mean depth and results indicate that he was able to estimate, accurately, the effective mean depth of the reservoir.

---

[16] "A Method of Correcting River Discharge for a Changing Stage," by B. E. Jones, *Water-Supply Paper No. 375–E*, U. S. Geological Survey, 1915, pp. 117–130.

AMERICAN SOCIETY OF CIVIL ENGINEERS

Founded November 5, 1852

DISCUSSIONS

AMPLIFIED SLOPE DEFLECTION

Discussion

BY A. A. EREMIN, AND RALPH W. STEWART

A. A. EREMIN,[22] Assoc. M. AM. SOC. C. E.[22a]—An important advantage of the amplified slope-deflection method is that the moments in the members are computed in conjunction with the sketching of the axes of the sloped members, and the moments can be checked simply by inspection. In his illustrative example, Mr. Stewart treats members with constant sections. By application of the simple formulas, the method may be extended to the members with variable sections. In a member AB with variable section, the distances p and q to the centroids of $\frac{M_{AB}}{E\,I}$ and $\frac{M_{BA}}{E\,I}$ from ends A and B, respectively, are

$$p = c_1\,l \ldots\ldots\ldots\ldots\ldots\ldots\ldots\ldots\ldots\ldots (23a)$$

and

$$q = c_2\,l \ldots\ldots\ldots\ldots\ldots\ldots\ldots\ldots\ldots\ldots (23b)$$

The stiffness factors of beam AB are

$$K_{AB} = \frac{K}{1.5\,e_1} \ldots\ldots\ldots\ldots\ldots\ldots\ldots\ldots\ldots\ldots (24a)$$

and

$$K_{BA} = \frac{K}{1.5\,e_2} \ldots\ldots\ldots\ldots\ldots\ldots\ldots\ldots\ldots\ldots (24b)$$

in which $K = \frac{I}{l}$. The values of the coefficients c and e in Eqs. 23 and 24 may be computed by the moment-area method or may be obtained from diagrams such as those presented elsewhere by the writer.[23]

NOTE.—This paper by Ralph W. Stewart was published in September, 1944, *Proceedings*. Discussion on this paper has appeared in *Proceedings*, as follows: November, 1944, by Leon Beskin; February, 1945, by John E. Goldberg, and Camillo Weiss; and March, 1945, by William C. Spiker, Arthur B. McGee, and Jaroslav Polivka.

[22] Associate Bridge Engr., Bridge Dept., Div. of Highways, State Dept. of Public Works, Sacramento, Calif.

[22a] Received by the Secretary April 27, 1945.

[23] "Analysis of Continuous Frames by Graphical Distribution of Moments," by A. A. Eremin, Sacramento, Calif., 1943.

The sign convention for the algebraic distribution of moments in continuous frames is often a serious source of error. As stated by the author, the interpretation of signs is simplified considerably by sketching the slopes of the axes. However, considerable skill is required. The interpretation of signs can be simplified further by distributing moments graphically. The moment closing line, constructed graphically by "crosslines,"[24] is shown in Fig. 5. Results are

FIG. 5.—GRAPHICAL DISTRIBUTION OF MOMENTS

automatic and the signs cannot be misinterpreted. The resulting bending-moment diagram may be used directly for the design of the members.

In the realm of fine arts, the artist's message is broadcast through various mediums—oil, water color, stone, or marble. The artist selects the medium that best agrees with his temperament. Likewise, in the applied art of adapting the science of mechanics to the determination of stresses, various algebraic and graphic procedures of distributing moments are available. All methods based on the elastic theory are equally exact for practical purposes. Mr. Stewart is to be commended highly for his valuable contribution to moment-distribution methods. With the addition of the new concept of the railroad traverse line, the stress analyst has a wider range of choice in selecting a method to satisfy his personal requirements.

RALPH W. STEWART,[25] M. AM. SOC. C. E.[25a]—A number of questions about the paper have been raised by Mr. Beskin. His statement concerning the text following Eq. 7*b* has merit. The sentence he quotes should have an additional phrase as is indicated within the brackets:

> "It is well known to all users of the slope-deflection method that the final moment at the end of a beam for which the moments are not dominated by joint movements [or by the flexure of an adjoining span] is less than the fixed-end moment."

The other discussers apparently did not have Mr. Beskin's difficulties in applying signs. The paper states that any analyst can use his own system of signs and still take advantage of the interpretation of angle values—the basic idea of amplified slope deflection. Also, the statements regarding signs in the third and the last paragraphs of Mr. McGee's discussion should be noted.

The method followed by Mr. Beskin in Eqs. 16 and 17*a* involves the algebraic procedure of referring to Eq. 7*a* and transforming it by suitable substitu-

[24] *Proceedings*, Am. Soc. C. E., November, 1944, p. 1490.

[25] Bridge Engr., City of Los Angeles, Los Angeles, Calif.

[25a] Received by the Secretary April 30, 1945.

tions. The writer's aim is to avoid such algebraic procedures. The solution of Fig. 2 with one apparent unknown, as developed by Eqs. 18*a*, 18*b*, and a subsequent unnumbered equation, also involves what the writer considers algebraic work of an undesirable type—namely, substituting in Eq. 16 which, in turn, is obtained from Eq. 7*a*. Direct use of the elastic curve traverse offers a solution with one apparent unknown which avoids reference to previously established equations. The elastic curve traverse also reduces the problem to a simple reading of visible geometrical alinement and the direct application of basic mechanical laws. This fact is demonstrated by Fig. 6, in which the values of the Δ-angles are written on each side of joint A in terms of M_A. Each value will be M_A divided by the member stiffness. By geometry, θ_A will be one third of the beam angle Δ. Since the sum of the column moments must be 100 for shear equilibrium, the value of Δ_2 is $100 - M_A$. By simple angle summation from A downward: $\theta_D = -100 + \frac{13\,M_A}{6}$. By geometry the lower beam angle Δ is 3 θ_b as shown in Fig. 6. The lower column moment is known to be 100 since the horizontal footing reaction is 10 and the column height is 10. The equation for equilibrium of moments about joint D is written:

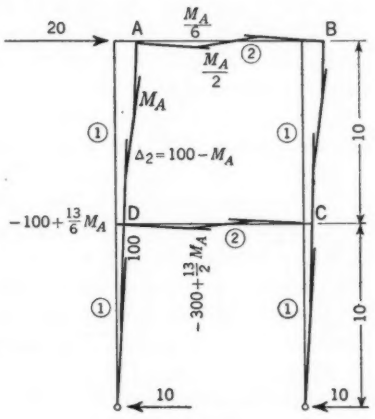

FIG. 6

$$100 + 100 - M_A - 2\left(-300 + \frac{13\,M_A}{2}\right) = 0 \ldots\ldots\ldots (25)$$

from which $M_A = 57.14$. Eq. 25 is shorter than the one following Eq. 18*b*; and, as the computation progresses, the physical significance of each term is shown by recording it in Fig. 6. Mr. Spiker has shown another, but longer, solution for Fig. 6.

As minor points, Mr. Beskin criticizes the use of the symbol Δ for angular change due to bending, as well as the use of the term "tapered beams." The term "tapered beams" has an excellent precedent.[26] The symbol Δ was selected because, in a number of treatises, it represents the angle between the tangents to a curve, and it seemed appropriate to extend its use to traverse diagrams which are solved largely as problems in geometrical alinement.

The writer is grateful to Messrs. Goldberg and Weiss for their comments. As Mr. Weiss suggests, the moment-area constants are the basis of the elastic curve traverse. If they are delineated as a traverse, the flexure of the structure can be visualized and the deformations due to flexure become easier to use than

[26] "Tapered Structural Members: An Analytical Treatment," by Walter H. Weiskopf and John W. Pickworth, *Transactions*, Am. Soc. C. E., Vol. 102 (1937), p. 1.

when pictured as areas. Such delineation also gives an opportunity to diversify and extend the use of moment-area constants. The object of the paper was to take advantage of this opportunity.

Mr. Polivka commented that "* * * the author's claim that the method reduces by one half the work of computation * * * if applied generally, cannot be upheld." The writer's claim was worded as follows: "* * * for many problems, the algebraic work required will be only one half that required by the procedure taught in current texts." It may be added that slope deflection, as amplified by the elastic curve traverse, will never, for any problem, involve more algebraic work than slope deflection as taught in current college textbooks.

The detailed equation given by Mr. Polivka, which he consolidates into Eq. 21*a*, represents either derivation of a formula by an algebraic procedure involving simultaneous equations as described by A. Amirikian,[21] M. Am. Soc. C. E., or handbook work which the writer wishes to avoid.

An important point which should not be overlooked is that the formulas derived by Mr. Amirikian are for frames composed only of members with constant cross sections. The introduction of tapering members would make no important changes in solutions which use the elastic curve traverse but it would have a serious effect on Mr. Amirikian's algebraic use of slope deflection.

The excellent and constructive work of Mr. McGee in presenting the complete detail of the solution for an unsymmetrical two-story frame with fixed-base columns is helpful. Following this step-by-step solution should clarify most of the situations which can arise in the general use of the method. As shown by Fig. 4(*c*), this problem involves eight unknown moments. The number of geometrical unknowns is six, comprising four joint rotations and two-story deflections. Only two unknowns (θ_1 and θ_2) appear in Fig. 4(*d*), the others having been eliminated in an easy manner so that only two simultaneous equations are needed for the solution.

Mr. Eremin offers suggestions regarding the extension of the method to structures having members of variable section. It is for such structures and also for such complicated conditions as "semirigid" joints that the use of an elastic curve traverse best shows its advantage.[7]

---

[21] "Analysis of Rigid Frames (An Application of Slope Deflection)," by A. Amirikian, Government Printing Office, Washington, D. C., 1942, p. 88.

[7] *Transactions*, Am. Soc. C. E., Vol. 107 (1942), p. 1028.

AMERICAN SOCIETY OF CIVIL ENGINEERS

Founded November 5, 1852

DISCUSSIONS

STRESSES IN THE LININGS OF SHIELD-DRIVEN TUNNELS

Discussion

BY LEON BESKIN, AND D. P. KRYNINE

LEON BESKIN,[24] ASSOC. M. AM. SOC. C. E.[24a]—The "basic principle" on which this paper is based has been used since the beginning of the twentieth century and is probably due to H. F. B. Müller-Breslau. It was taught by Bertrand de Fontviolant for at least twenty years before publication of his book on strength of materials.[25] The author has expended considerable energy on the redevelopment of conventional formulas for rings, which can be found in textbooks on stress analysis. These equations appear in various forms, such as the charts devised by Joseph A. Wise,[26] M. Am. Soc. C. E., and reproduced by Alfred S. Niles, Assoc. M. Am. Soc. C. E., and Joseph S. Newell.[27] Lieutenant-Commander Wise's formulas are more convenient than the author's expressions, which can be derived from them. Whereas Commander Wise uses a supporting fictitious shell, which has shearing reactions defined by a conventional beam distribution, the author deals with diaphragm reactions, in such a manner that the shell reactions vanish if the loads applied to the ring are in equilibrium. Influence factors are obtained in both methods.

A great advantage of the fictitious shell over the diaphragm is that the shell does not introduce any dissymmetry with respect to the load. Thus, the tables need be computed only for one half of a ring. It is a simple matter to transform Commander Wise's formulas into those of the paper. For instance, the function A_{Mr} is obtained by the superposition of the following loads on the

NOTE.—This paper by Anders Bull, M. Am. Soc. C. E., was published in November, 1944, *Proceedings*. Discussion on this paper has appeared in *Proceedings*, as follows: January, 1945, by J. A. Van den Broek; February, 1945, by Nathan D. Brodkin, M. A. Drucker, and Sigvald Johannesson; and May, 1945, by Jacob Feld.

[24] Design Specialist, Consolidated Vultee Aircraft Corp., San Diego, Calif.

[24a] Received by the Secretary March 24, 1945.

[25] "Resistance des Materiaux," by Bertrand de Fontviolant, J. B. Baillere & Fils, Paris, France, Vol. I, 1923, pp. 388 and 538; Vol. II, 1927, p. 628.

[26] "Analysis of Circular Rings for Monocoque Fuselages," by Joseph A. Wise, *Journal of the Aeronautical Sciences*, September, 1939, p. 460.

[27] "Airplane Structures," by Alfred S. Niles and Joseph S. Newell, John Wiley & Sons, Inc., New York, N. Y., 3d Ed., Vol. II, 1943, p. 272 et seq.

ring shown in Fig. 2; thus, for a load P_r at any point p:

$$P'_r = P_r \cos \alpha \quad \ldots\ldots (37a)$$

and

$$P'_t = P_r \sin \alpha \quad \ldots\ldots (37b)$$

At the invert joint A,

$$M = P_r r \sin \alpha \quad \ldots\ldots (38)$$

Defining W_1, W_4, and W_7 as the three coefficients of moment due to unit radial and tangential forces and unit moments—

$$A_{Mr} = - W_1(\alpha) + W_1(0) \cos \alpha + W_7(0) \sin \alpha - W_4(0) \sin \alpha \quad \ldots\ldots (39)$$

The values found by Commander Wise are:

$$\left.\begin{aligned} 2\pi W_1(\alpha) &= 0.5 \cos \alpha - (\pi - \alpha) \sin \alpha + 1 \\ 2\pi W_4(\alpha) &= 1.5 \sin \alpha - (\pi - \alpha)(\cos \alpha - 1) \\ 2\pi W_7(\alpha) &= 2 \sin \alpha + \alpha - \pi \end{aligned}\right\} \quad \ldots\ldots (40)$$

which, substituted into Eq. 39, yields the expression for A_{Mr} given by the author in Eqs. 8. The A-functions in this paper are no more informative than the charts presented by Commander Wise. In addition, the author's method is extremely sensitive to small computational inaccuracies, because the fictitious reaction is concentrated, instead of being distributed, as in the case of the Wise formulas. For instance, if applied forces are not balanced by a small couple, the total unbalance appears at the diaphragm location, so that the total error is repeated at each station, successively. When a shell is used as a fictitious support, the couple is absorbed by a constant shear flow and the error is distributed on the entire ring, instead of being concentrated at each section.

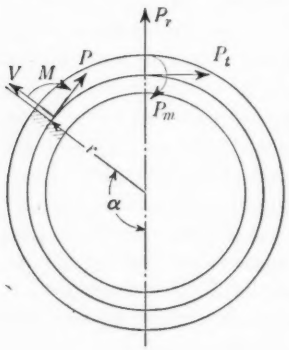

FIG. 24

The coefficients of moment can be established in a straightforward manner. The equations of equilibrium of a ring are:

$$\frac{dM}{d\alpha} = r V_p \quad \ldots\ldots (41a)$$

$$\frac{dV_p}{d\alpha} = P \quad \ldots\ldots (41b)$$

and

$$\frac{dP}{d\alpha} = - r V_s - V_p \quad \ldots\ldots (41c)$$

in which M, P, and V_p represent the moment and the axial and shearing forces at a section p; and V_s represents the shear from the fictitious shell. This

shear is defined by the conventional beam formulas applied to the shell:

$$V_s = -\left(\frac{P_m}{2\pi r^2} + \frac{P_t}{2\pi r}\right) + \frac{P_t}{\pi r}\cos\alpha - \frac{P_r}{\pi r}\sin\alpha \quad \ldots\ldots (42)$$

in which P_t, P_r, and P_m are the concentrated tangential and radial loads and the concentrated moment applied at the point $\alpha = \pm\pi$ in the shell (Fig. 24). Elimination of P and V_p in Eqs. 41 leads to:

$$\frac{dM}{d\alpha} + \frac{d^3M}{d\alpha^3} + r^2 V_s = 0 \quad \ldots\ldots (43)$$

Considering a tangential load P_t, the solution for M is the general antisymmetrical solution of Eq. 43, in which V_s has the value defined by Eq. 42, in which $P_r = P_m = 0$. For $\alpha > 0$:

$$M = r P_t \left[k \sin\alpha + \frac{\alpha}{2\pi}(1 + \cos\alpha) \right] \quad \ldots\ldots (44)$$

The constant k is defined by the condition of minimum strain energy which gives:

$$k = -\frac{\int_0^{\pi} \alpha (1 + \cos\alpha)\sin\alpha \, d\alpha}{2\pi \int_0^{\pi} \sin^2\alpha \, d\alpha} = -\frac{3}{4\pi} \quad \ldots\ldots (45)$$

Thus, the expression for M is:

$$M = r P_t \phi(\alpha) \quad \ldots\ldots (46a)$$

in which

$$\phi(\alpha) = \frac{1}{2\pi}\left[\alpha (1 + \cos\alpha) - \frac{3}{2}\sin\alpha \right] \quad \ldots\ldots (46b)$$

Applying Eqs. 41, V_p and P are obtained by differentiation:

$$V_p = P_t \phi'(\alpha) \qquad \text{with} \qquad \phi'(\alpha) = \frac{1}{2\pi}\left(1 - \alpha\sin\alpha - \frac{\cos\alpha}{2}\right) \quad \ldots (47a)$$

and

$$P = P_t \phi''(\alpha) \qquad \text{with} \qquad \phi''(\alpha) = -\frac{1}{2\pi}\left(\frac{\sin\alpha}{2} + \alpha\cos\alpha\right) \quad \ldots (47b)$$

Considering two loads $P_t = \pm P_r/d\alpha$, placed at a distance $r\,d\alpha$ from one another (Fig. 25(a)), which are equivalent to a load P_r, it appears that the coefficients for a unit load P_r are obtained by differentiating the coefficients corresponding to P_t; thus:

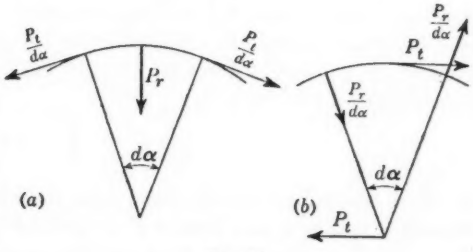

FIG. 25

$$M = r P_r \phi'(\alpha) \quad \ldots\ldots (48a)$$

$$V_p = P_r \phi''(\alpha) \quad \ldots\ldots (48b)$$

and

$$P = P_r \phi'''(\alpha) \ldots\ldots (48c)$$

Applied couples may be considered as the limit of two loads $\pm P_r/d\alpha$ and a load $P_t = P_r$ (Fig. 25(*b*)), since this combination of loads is equivalent to a couple, $P_m = P_r r$. Thus, combining Eqs. 46, 47, and 48:

$$M = P_m (\phi + \phi'') = P_m \psi \ldots\ldots (49a)$$

$$V_p = \frac{P_m \psi'}{r} \ldots\ldots (49b)$$

and

$$P = \frac{P_m \psi''}{r} \ldots\ldots (49c)$$

The A-constants in Table 1 are computed for very large increments (22° 30′); and the curves presented by Commander Wise do not always yield values of sufficient accuracy for practical use. Using the latter, the writer prepared[28] a table of ϕ-functions and ψ-functions for 5° increments of α, in which four ϕ-functions replace the author's six A-functions.

Adjusting for Polygonal Effect.—The adjustment proposed by the author in Section 8 can be avoided if the concentrated loads are replaced by uniformly distributed loads on an arc 2ϵ defined by the angles $\alpha - \epsilon$, $\alpha + \epsilon$. For instance, the coefficient A_{Mr} would be (the angle ω varying between $\alpha - \epsilon$, $\alpha + \epsilon$):

$$A_{Mr} = -\frac{1}{2\pi \times 2\epsilon} \int_{\alpha-\epsilon}^{\alpha+\epsilon} (\omega \sin \omega + 1 - \cos \omega)\, d\omega$$

$$= -\frac{1}{2\pi} \left(\alpha \sin \alpha \frac{\sin \epsilon}{\epsilon} + 1 - \cos \alpha \cos \epsilon \right) \ldots\ldots (50)$$

which yields values that differ but slightly from the values given by the formulas in Eqs. 8.

Symmetrical Loading.—The B-constants (see Section 12) require an extremely extended table if the functions are to be computed by small increments. The time saved by these coefficients is of relatively minor importance in any case.

Deflections of a Tunnel Lining.—The expressions given by the author contain two angles, α and β, and their computation by sufficiently small increments is a laborious operation. When a shell is used instead of a diaphragm, the method is greatly simplified. Coefficients of deflection can be defined by expressions of the type:

$$k_{(ti)(rj)} = \int_0^{2\pi} m_{ti}\, m_{rj}\, d\alpha \ldots\ldots (51)$$

in which the subscripts denote values caused, respectively, by a unit load P_t at point I and by a unit load of P_r at point J—that is, the first of two subscripts shows the location of the load and the second shows the nature of the load. Replacing coefficients m by the functions computed by Eqs. 46 to 49 and integrating, coefficients k are obtained. The deflections can be computed by

[28] "General Circular Ring Analysis," by Leon Beskin, *Aircraft Engineering* (publication pending).

means of unit dummy loads. Using radial and tangential dummy loads, the radial and tangential components of the displacement of a point B (designated d_{rb} and d_{tb}, respectively) are

$$d_{rb} = \frac{r^3}{E\,I}\left(\Sigma k_{(rb)(ti)}\,P_{ti} + \Sigma k_{(rb)(ri)}\right)P_{ri} \quad \ldots\ldots\ldots\ldots (52a)$$

and

$$d_{tb} = \frac{r^3}{E\,I}\left(\Sigma k_{(tb)(ti)}\,P_{ti} + \Sigma k_{(tb)(ri)}\right)P_{ri} \quad \ldots\ldots\ldots\ldots (52b)$$

The summations in Eqs. 52 are extended to all the loads on the ring. These displacements are relative and, to define absolute displacements, a point must be considered fixed. For instance, if the invert joint A is fixed, it is necessary to cancel its displacement d_{ra} which, under symmetrical loading, is expressed by Eq. 52*a* (except that subscript *b* becomes *a*). Adding $-d_{ra}$ to all the displacements, the final components of the displacement of point B (separated by the angle α from point A) are:

$$\delta_{rb} = d_{rb} - d_{ra}\cos\alpha \quad \ldots\ldots\ldots\ldots\ldots\ldots (53a)$$

and

$$\delta_{tb} = d_{tb} + d_{ra}\sin\alpha \quad \ldots\ldots\ldots\ldots\ldots\ldots (53b)$$

Coefficients k are functions only of the angle α between the point where the load is applied and the point where the deflection is calculated.

There are six different coefficients $k(\alpha)$:

$$\left.\begin{aligned}
k_{tt}(\alpha) &= \Gamma(\alpha) = \frac{1}{2\pi}\left[\cos\alpha\left(\frac{\pi^2}{6} - \frac{23}{8} - \frac{\pi\,\alpha}{2} + \frac{\alpha^2}{4}\right)\right.\\
&\qquad \left. + \frac{3}{2}\sin\alpha\,(\pi - \alpha) + \frac{\pi^2}{3} - 2 - \alpha\,\pi + \frac{\alpha^2}{2}\right]\\
k_{tr}(\alpha) &= \Gamma'(\alpha) = \frac{1}{2\pi}\left[(\pi - \alpha)\,(\cos\alpha - 1)\right.\\
&\qquad \left. - \sin\alpha\left(\frac{\pi^2}{6} - \frac{11}{8} - \frac{\pi\,\alpha}{2} + \frac{\alpha^2}{4}\right)\right]\\
k_{rr}(\alpha) &= -\Gamma''(\alpha) = \frac{1}{2\pi}\left[\frac{1}{2}(\pi - \alpha)\sin\alpha - 1\right.\\
&\qquad \left. + \cos\alpha\left(\frac{\pi^2}{6} - \frac{3}{8} - \frac{\pi\,\alpha}{2} + \frac{\alpha^2}{4}\right)\right]\\
k_{tm}(\alpha) &= \Delta(\alpha) = \Gamma(\alpha) + \Gamma''(\alpha) = \frac{1}{2\pi}\left[-\frac{5\cos\alpha}{2}\right.\\
&\qquad \left. + (\pi - \alpha)\sin\alpha + \frac{\pi^2}{3} - 1 - \pi\,\alpha + \frac{\alpha^2}{2}\right]\\
k_{rm}(\alpha) &= -\Delta'(\alpha) = \phi(\pi - \alpha)\\
&= \frac{1}{2\pi}\left[(\pi - \alpha)\,(1 - \cos\alpha) - \frac{3}{2}\sin\alpha\right]\\
k_{mm}(\alpha) &= \mathrm{E}(\alpha) = \Delta(\alpha) + \Delta''(\alpha)\\
&= \frac{1}{2\pi}\left[-2\cos\alpha + \frac{\pi^2}{3} - \alpha\,\pi + \frac{\alpha^2}{2}\right]
\end{aligned}\right\} \quad \ldots (54)$$

It is feasible then to prepare tables of deflection[28] coefficients from Eqs. 54.

Example.—To illustrate the foregoing argument the example given by Mr. Bull in Section 9 and Fig. 6 is solved by the Wise method. Since only four radial loads are applied, the adjustment for polygonal effect is not justified, and the comparison is made without adjustment (if necessary, the same adjustment can be made for both methods). The author's values are:

$$\begin{aligned}
\text{Thrust} \quad T &= -1.08317 - 1.77015 &&= -2.85332 \\
\text{Shear} \quad V &= -4.01595 + 5.05450 &&= +1.03855 \\
\text{Moment} \quad M &= -3.14551 + 2.79700 - 0.01644 &&= -0.36495
\end{aligned}$$

The values resulting from the use of the Wise method have been computed with coefficients read from the original graphs, Table 20(*a*),[26] and with coefficients interpolated from a seven-place table (see Table 20(*b*)).

TABLE 20.—SOLUTION OF AUTHOR'S EXAMPLE, SECTION 9, BY THE WISE METHOD

FORCE		UNIT COEFFICIENTS			TOTAL VALUES		
Fig. 6	Kips	*T*	*V*	*M*	*T*	*V*	*M*
(*a*) USING COEFFICIENTS READ FROM GRAPHS							
P_{r1}	+2	+0.325	+0.445	+0.145	+0.650	+0.890	+0.290
P_{r3}	+5	+0.125	−0.080	−0.045	−0.625	−0.400	−0.225
P_{r7}	−4	−0.145	−0.120	+0.040	+0.580	+0.480	−0.160
P_{r9}	−3	−0.225	+0.045	+0.075	+0.675	−0.135	−0.225
P_{r13}	−5	+0.020	−0.100	−0.010	−0.100	+0.500	−0.050
P_{r15}	+1	+0.420	−0.295	−0.000	+0.420	−0.295	−0.000
Totals	...	....	....	....	+2.850	+1.040	−0.370
(*b*) USING COEFFICIENTS READ FROM A SEVEN-PLACE TABLE							
P_{r1}	+2	+0.3255754	+0.4442074	+0.1457640	+0.6511508	+0.8884148	+0.2915280
P_{r3}	+5	+0.1248151	−0.0824400	−0.0457225	+0.6240755	−0.4122000	−0.2286125
P_{r7}	−4	−0.1464023	−0.1221527	+0.0408998	+0.5856092	+0.4886108	−0.1635992
P_{r9}	−3	−0.2280333	+0.0461712	+0.0750035	+0.6840999	−0.1385136	−0.2250105
P_{r13}	−5	+0.0231697	−0.1011569	−0.0077650	−0.1158485	+0.5057845	−0.0388250
P_{r15}	+1	+0.4241794	−0.2935702	−0.0003671	+0.4241794	−0.2935702	−0.0003671
Totals	...	....	....	....	+2.8532663	+1.0385263	−0.3648863

The author's values and the Wise values are seen to be in very close agreement; and the charts originally prepared by Commander Wise are shown to be sufficient for all practical purposes when only a few loads are applied on the ring.

The differences in signs result from different sign conventions. The change in diameter (see Section 15) can also be determined by means of a table[28] giving the coefficients k_{tr} and k_{rr} (functions $\Gamma'(\alpha)$ and $\Gamma''(\alpha)$).

Table 21 indicates that the agreement between both methods is excellent, which simply means that the numerical tables have been computed without error.

Comparison of Table 21 with Table 7 shows that the author's method necessitates more numerical computations than the method derived from Com-

mander Wise's concepts, because of the dissymmetry introduced by the diaphragm in Mr. Bull's method, which does not occur in the Wise method.

Another advantage resulting from Commander Wise's concepts appears from comparison of Tables 20 and 21 with the tables in the paper: The Wise coefficients have much smaller values than the author's coefficients, so that, for the same degree of final accuracy, less laborious computations are required.

TABLE 21.—COMPUTATION OF CHANGE IN DIAMETER

Forces	Angle	Kips	Function	Value	Product
P_{r7}, P_{r8}	90°	4 − 1 = 3	$\Gamma''(\alpha)$	+0.034160 × 2	+0.20496
P_{r1}, P_{r9}	45°	3 − 2 = 1	$\Gamma''(\alpha)$	+0.005140 −0.00245	+0.00269
P_{f3}	45°	5	$\Gamma'(\alpha)$	+0.016560 +0.018726	+0.17643
P_{f13}	90°	5	$\Gamma'(\alpha)$	0	0
Total coefficient	....	....	....	....	+0.38408
Author's value	....	....	....	+0.061890 +0.322171	(+0.384061)

For instance, the moment coefficients are approximately seven times smaller, and the deflection coefficients are five times smaller. This disparity may mean the difference between using a slide rule or a computing machine in many practical problems.

Finally, it can be remarked that, if the C-constants were calculated by 5° increments, it would be necessary to calculate 5,184 entries instead of the 72 entries required for the $\Gamma'(\alpha)$-functions and $\Gamma''(\alpha)$-functions.[28] Also, the interpolation in a table with two independent variables is extremely laborious.

Effects of Displacement.—Mr. Bull states in Section 17 that

> "* * * when the shearing stress at any point reaches a certain limit a slip takes place between the surface and the soil particles, or between the soil particles themselves, causing the stress at that point to be relieved suddenly."

The slip between the lining and the soil particles or between soil particles actually occurs under constant shearing stress (provided the normal force is not changed), which is practically independent of the rapidity of displacement and is equal to the product of the normal pressure and the coefficient of friction.

Tangential Forces.—It is very improbable (see Section 18) that the region between the lining and the soil is free from tangential forces. It is true that an arch effect exists near the shield, but this arch effect is certainly helped by the shears developed between the arch and the soil in front of the shield as well as by the shears between the arch and the soil that have already settled at some distance behind the shield. Thus, the equilibrium cannot be examined as a plane equilibrium in sections perpendicular to the direction of the tunnel—at least when the effect of tunneling is being felt. It is highly probable that a stress redistribution occurs when the shield has moved to some distance from a given section, since the aforementioned effects disappear, and a plane equilibrium reappears. The best assumption is that of the uniform equilibrium defined by Rankine's formulas, which imply the existence of shear in all directions, except the vertical and the horizontal. A state of equilibrium without

shear along the lining may be found, but that cannot be the condition assumed by the author because the normal component acting on the lining is not in equilibrium with the horizontal and vertical normal forces defined by Rankine's formulas. This is demonstrated by comparing Fig. 26(*a*), showing the loads on the lining, and Fig. 26(*b*), representing Mohr's circle of stress at any point

FIG. 26

of the lining (at an arbitrary scale). The maximum (vertical) and minimum (horizontal) pressures P_M and P_m are correlated by the formula,

$$P_m = P_M \tan^2\left(\frac{\pi}{4} - \frac{\phi}{2}\right) \quad \text{.....(55)}$$

In this case ϕ is the angle of friction. The author has used the conventional values $P_m/P_M = 1/3$, or $\phi = 30°$.

At points A and B (Fig. 26(*a*)), the normal stresses are represented by OA and OB; the shears are represented by AA′ and BB′ (see Fig. 26(*b*)). With the author's assumption that $\overline{AA'} = \overline{BB'} = 0$, Mohr's circles must be modified, so that their diameters end at point A or B. There are two possible Mohr's circles at each point. Near the crown, circle I must be chosen for reason of continuity; and, near the skewback, circle II must be chosen. Thus, neglecting the dead weight between points A and B, it appears that the pressures at point B are greater than the pressures at point A. This seems to indicate that there is an arch effect—a conclusion which contradicts the fact that the pressure at the skewback is defined without arch effect. The latter (arch effect) shows that the pressure distribution does not correspond to a possible equilibrium. Another aspect of this contradiction results from the inspection of the values of the vertical and horizontal pressures at points A and B (represented by OV_A, OV_B, OH_A, and OH_B, respectively). It appears that the vertical pressure, when moving along the lining, first decreases (points V_A); then, at some unknown arbitrary point, it jumps to the values represented by points V_B, instead of remaining constant and equal to P_M (point V). Such a state of stress appears extremely improbable. In addition, the reactions of the lining must be in over-all equilibrium with the loads above the lining. More precisely, a vertical elemental prism limited to the surface must be in equilibrium with the lining reactions and the shears along its vertical faces. The author has not attempted to show that this equilibrium is consistent with the lining reactions he has chosen, although proof is essential to give the method a sound

basis. Because of the aforementioned considerations, the method appears to be highly questionable. In addition, if considered approximate, the method is not conservative, since the vertical components of the lining reactions are smaller than the loads above the lining.

Soil Reactions Due to Settlement.—The author disregards tangential reactions, which must exist, since the displacement δ has the components $\delta \cos \alpha$ (normal) and $\delta \sin \alpha$ (tangential). For this reason, the directions of the forces F_1 to F_6 (Fig. 9) are incorrect, and the subsequent analysis is extremely questionable. Especially, the direction of forces F_5 and F_6 cannot be downward because the main component of displacement in the vicinity of these forces is tangential. Furthermore, the vertical component of the forces above the ring is determined by the dead weight—for example, if the direction of a force F_6 were downward, the soil reaction at point 7 would be decreased. On the basis of the foregoing reasoning, it is conclusive that Eq. 16 does not represent the soil reactions correctly.

It is impossible to obtain soil reactions on the segments near the crown since the ring settles as a whole and does not expand and since the section at its crown settles more than the other sections. The settled ring is obviously below the unsettled ring, and it is extremely probable that the maximum u (number of segments in which soil reactions are developed) is equal to 6, a fact confirmed by Table 14.

Specified Conditions.—Contrary to Eq. 22*c*, the horizontal pressure is equal to one third of the net vertical pressure (minus the hydrostatic pressure), plus the hydrostatic pressure:

$$p_H = \frac{0.100\, H_w + (0.125 - 0.063)\,(H_n - H_w)}{3} + 0.063\,(H_n - H_w)$$

$$= \frac{0.038\, H_n + 0.062\, H_w}{3} + 0.063\,(H_n - H_w) \ldots\ldots\ldots\ldots (56)$$

Eq. 56 defines a smaller pressure than does Eq. 22*c*, and the difference is especially important when H_w is small. Below the skewback, there is a vertical soil reaction, equal to one third of the net horizotnal pressure, thus, contrary to Eq. 22*a*:

$$p_v = \frac{0.038\, H_n + 0.062\, H_w}{9} + 0.063\,(H_n - H_w) \ldots\ldots\ldots\ldots (57)$$

Because of the foregoing, it is very dubious that the active forces are computed correctly. For example, if Eq. 22*c* is applied to a completely immersed material which has the density of water, a horizontal pressure greater than the hydrostatic pressure is indicated. This is an obviously incorrect result, since the material is in suspension and cannot produce an additional pressure. If Eq. 22*a* is applied to a case in which the water level is just above the point under consideration, it indicates a pressure practically equal to zero, which is also incorrect.

Perhaps these formulas can be used when crude methods of analyses are used, but not when a refined analysis is sought.

Active Forces.—The calculations indicated by the author can be simplified somewhat. For example, the tangential forces due to the lining weight, which are sinusoidally distributed, can be replaced by radial forces following a cosine distribution of the same amplitude, without introducing any additional bending in the lining. This fact can be shown by considering the differential equation of equilibrium of the ring. The radial forces can be divided into a constant pressure, producing thrust exclusively, and a variable pressure, giving bending moments and thrust.

Conclusions.—In this paper, applied active forces, as well as reactive forces, have been estimated by methods that cannot be considered satisfactory, and errors may result in the values of the final moments. There is no doubt that the author is entirely correct when he states that conventional methods are highly conservative, but it seems nonconservative to use the author's results without an additional factor of safety that would consider the inaccuracies of the method. Happily, it seems probable that errors in the basic data do not have an excessive influence on the final moments. For instance, a variation of the moment of inertia (or of the soil compression constant) in the ratio of 4 to 1 generally produces a variation of bending moments in a ratio of less than 2 to 1.

Thus, it is probable that the additional factor of safety would be so small that it could be omitted if the active forces were recomputed more conservatively. Because of the lack of precision in the basic data, the author's method seems too intricate. However, the numerical results presented may be considered a basis for estimating the reduction of moments due to the flexibility of the lining. This estimate can be made by computing the dimensionless coefficient $\frac{K r^4}{E I}$ and by using the results obtained by the author for the same value of this coefficient. For that purpose, it would be very helpful if the author would add to his data the values of the bending moments in the case where the flexibility of the lining is disregarded.

Notation.—The author specifies that the tangential component P_t is positive when directed upward. This is contrary to the conventional positive direction, which is either clockwise (or opposite), with reference to the center of the ring. Also, this convention is not consistent with the use of the author's tables, because they thus become restricted to the invert joint. If the tables are to be applied to other points, the sign convention must be changed so that the tangential component is positive when directed away from the diaphragm. Thus, when the diaphragm is moved, the sign of a given tangential force must be changed according to the location of the diaphragm. Such cumbersome notation, which is a source of error, should be rejected, and the signs in the tables corrected in order to make them consistent with the stipulation that positive tangential forces are clockwise.

D. P. KRYNINE,[29] M. AM. SOC. C. E.[29a]—In describing the present state of the art of designing and building shield-driven tunnels (circular in cross section),

[29] Research Associate in Soil Mechanics, Dept. of Civ. Eng., Yale Univ., New Haven, Conn.

[29a] Received by the Secretary May 16, 1945.

the author of this excellent paper presents Fig. 1 showing assumed vertical and horizontal pressures on the lining. Judging from the measurements of pressure on the lining of the Lincoln Tunnel in New York City,[30,31] the shape of the vertical downward pressure diagram seems to be qualitatively correct, whereas the shapes of other diagrams shown in Fig. 1 should be considered temporarily as approximations only, until more field measurements and analyses along these lines are available. Purely theoretical attempts of establishing the shape of such diagrams are not sufficient.

Eq. 15 and the "Soil Compression Constant."—In a general case, the value of K, termed the "soil compression constant," depends on the size and the shape of the plane area abutting the soil and displaced in a normal direction. According to Eq. 15, a given unit load $\frac{F}{A'}$ abutting a given soil (constant K) always produces the same displacement of ρ inches. It is a well-known experimental fact, however, that from the two areas loaded with the same unit load, the larger area will settle more than the smaller one.

In the particular case of a shield-driven tunnel, the value of K changes also according to where the load acting on the soil is applied. The value of K will be smaller in the upward direction than in the downward direction, especially if the tunnel is shallow. The value of K in a sidewise direction, perhaps, would be between the two; also it may be smaller than the other two. The writer cannot even imagine how the value of K in the case of a shield-driven tunnel could be determined experimentally. It is impossible to organize such a test and the value of K must be guessed.

Eq. 15 means implicitly that the soil mass obeys Hooke's law which, in general, is not the case.

Reversible and Nonreversible Displacements in the Soil Mass.—If a rigid loaded plate is placed on the surface of a previously unloaded soil, a displacement occurs which consists of a reversible and a nonreversible part, the reversible (elastic) part being generally much smaller than the nonreversible. Assume that the experimental plate is first loaded with a certain unit load and thereupon a new unit load of the same magnitude is superimposed on the given acting load. The additional displacement thus caused will be much smaller than that in the original case. The reversible (elastic) part of the displacement may be the same in both cases, but the nonreversible one will decrease substantially. This is an additional reason why the concept of the "soil compression constant" should be used with extreme care.

Stressed Condition of the Lining During and After Shoving.—If the tunnel is driven in a plastic mass (organic silt or plastic clay), the vertical diameter of the lining first increases, apparently due to shoving. In the case of the Lincoln Tunnel, this increase was about 0.4% of the diameter of the lining. It is not clear from the paper in what way the stresses caused in the lining by the shoving process should be estimated or computed. Apparently these stresses should be fully or partly superimposed on those caused by the loads, as in Fig. 1.

[30] "Lincoln Tunnel. The Field Measurements and Study of Stresses in Tunnel Lining," by G. M. Rapp and A. H. Baker, The Port of New York Authority, July, 1937 (lithoprinted).

[31] "Pressure on the Lining of Circular Tunnels in Plastic Soils," by D. P. Krynine, *Proceedings*, Am. Soc. C. E., May, 1944, p. 629.

Decrease in the Weight of the Lining.—Mr. Bull proposes using scaffolding in order to decrease the weight of the lining. Granted that the weight of the lining can be decreased in that manner, two conditions still remain: (*a*) The maximum acceptable deflections of the lining should be controlled by the shearing strength of the overburden; and (*b*) a rather heavy lining in soils possessing small shearing resistance still may be required to balance the effect of buoyancy. To clarify the statement made under item (*a*), the well-known trap-door experiment should be recalled. The bottom of a box filled with sand is provided with a horizontal trap door at the center. Some downward movement of the trap door causes the vertical pressure on it to decrease, but excessive downward movement of that door causes an increase in pressure.

The writer disagrees with the statement at the end of the paper:

> "There seems to be no good reason, however, for making material that is needed only during the erection of a tunnel an integral part of it, something that is being done in no other type of structure."

On the contrary, many types of foundations are built with excessive material which is useful only during the erection of the structure. One of such examples is the use of pre-cast concrete piles which are designed to furnish excess resistance to both handling stresses and driving stresses. A caisson (for instance, a metallic compressed air caisson) is nothing more than an excessively heavy shell of the structure, useful only during construction, but which, however, remains buried in the earth forever.

AMERICAN SOCIETY OF CIVIL ENGINEERS

Founded November 5, 1852

DISCUSSIONS

THE EFFECT OF BLANKETS ON SEEPAGE THROUGH PERVIOUS FOUNDATIONS

Discussion

BY HARRY R. CEDERGREN

HARRY R. CEDERGREN,[5] JUN. AM. SOC. C. E.[5a]—In presenting a mathematical analysis of seepage through impervious blankets, Mr. Bennett has defined one of the major problems encountered in the design of earth dams—the control of underseepage. The author has indicated the trend toward the use of graded filters and vertical drainage wells for the control of seepage and has discussed the value of impervious upstream blankets for reducing seepage quantities through pervious foundations. He has presented a mathematical analysis for determining the head loss through impervious blankets—evaluating the efficiency of the blankets in terms of head loss.

Undoubtedly, the formulas in the paper will find favor among engineers interested in obtaining quick evaluations of the general efficiency of proposed blanket designs. Such analyses should be particularly helpful for preliminary studies in which basic types of treatment and approximate costs of projects are being studied. In some cases, no further analysis may be required; however, in the preparation of final designs, more detailed analysis of the probable development of seepage pressures and gradients is often feasible. For this purpose many engineers make extensive use of the graphical flow-net[6,7] method. Although a moderate amount of study and practice is required for the development of skill in the construction of flow nets, the required effort is not out of proportion to the value. Frequent use of the flow net develops an understanding of seepage that often permits an engineer to detect inadequate designs quickly without detailed analysis, thus saving considerable time and expense.

NOTE.—This paper by Preston T. Bennett was published in January, 1945, *Proceedings*. Discussion on this paper has appeared in *Proceedings*, as follows: March, 1945, by Reginald A. Barron; and April, 1945, by V. A. Endersby.

[5] Engr., U. S. Engr. Dept., Eng. Div., Portland Dist., Portland, Ore.

[5a] Received by the Secretary April 23, 1945.

[6] "Seepage Through Dams," by Arthur Casagrande, *Journal of the New England Water Works Association*, June, 1937, pp. 131–172 (also reprinted in *Publication No. 209*, Graduate School of Eng., Harvard Univ., Cambridge, Mass., June, 1937; and in "Contributions to Soil Mechanics, 1925–1940," Boston Soc. of Civ. Engrs., Boston, Mass., 1940).

[7] "Theoretical Soil Mechanics," by Karl Terzaghi, John Wiley & Sons, Inc., New York, N. Y., 1943, pp. 235–247.

Furthermore, the flow net gives a graphical picture of the probable distribution of seepage pressures and gradients that is an important aid to the engineer in the design of water impounding structures.

As the author has stated, soil deposits are never uniform, and no seepage analysis is more dependable than the degree of accuracy of the conditions assumed in the analysis. Karl Terzaghi, M. Am. Soc. C. E., has stressed this limitation of soil mechanics analyses repeatedly and recommends[8] field observations during construction to determine the degree of safety of structures. Observation wells or piezometers at strategic points in earth dams and in dam foundations will permit the determination of actual pore pressures and thus will reflect the degree of safety of structures, both during and after construction. An adequate system of pore pressure measuring devices should be installed in all important earth dams, and reliable records of pore pressure data, together with pertinent information regarding the installations, should be made available to the engineering profession.

In evaluating the performance of an impervious blanket, or any other design feature relating to seepage control, the first consideration should be the safety of the dam. The safety of earth dams on pervious foundations depends in a large measure on uplift pressures in the vicinity of the downstream toe. The author has emphasized the value of downstream drainage systems for the control of uplift pressures downstream from dams, and his two examples (Figs. 4 and 5) show the beneficial influence of a pervious blanket installed beneath the downstream part of the dam. This type of drain increases the degree of safety of the structure but it may not be entirely adequate. Under the assumed condition that the soils are isotropic (horizontal permeabilities (k_I) equal to vertical permeabilities (k_{II}), Mr. Bennett's analysis indicates that the escape gradient at the downstream toe is 0.8 for the section in Fig. 4 without drainage and 0.20 for the section in Fig. 5, in which a gravel blanket has been provided beneath the downstream part of the dam. The former condition (Fig. 4) is decidedly unsafe and the latter may be considered barely adequate provided the soils are relatively free of stratification.

Before accepting a blanket design as adequate (for example, the section in Fig. 5), an investigation should be made to determine the probable degree of stratification of the foundation, since natural soil deposits are always more or less stratified and even moderate stratification can have an important influence upon uplift pressures. The effect of stratification can be demonstrated clearly with the aid of the flow net. For example, let it be assumed that all soils in the basic section given in Fig. 5 are moderately stratified and that all the horizontal permeabilities (k_I) are nine times the vertical permeabilities (k_{II}). The principal question to be answered is "What effect does this degree of stratification have upon uplift pressures at the downstream toe?" The results of a flow-net analysis of the basic section in Fig. 5, together with a number of modifications, are summarized in Table 1. The section given in Fig. 5 is designated "case 1," and modified sections are designated cases 2, 3, and 4, respectively. All flow nets were constructed by the Forchheimer graphical

[8] "Theoretical Soil Mechanics," by Karl Terzaghi, John Wiley & Sons, Inc., New York, N. Y., 1943, pp. 1–3.

method.[6,7] To show the influence of stratification, the original section with a 1,100-ft blanket upstream and a drainage blanket under the downstream half of the dam was analyzed for two conditions—namely, all soils homogeneous and isotropic ($k_I = k_{II}$) and all soils moderately stratified ($k_I = 9\,k_{II}$). To de-

TABLE 1.—EVALUATION OF THE BLANKET EFFICIENCY BY THE FLOW-NET ANALYSIS (BASIC SECTION OF FIG. 5, WITH MODIFICATIONS[a])

WITH UPSTREAM BLANKET						WITHOUT UPSTREAM BLANKET					
All Soils Isotropic ($k_I = k_{II}$)			All Soils Anisotropic ($k_I = 9\,k_{II}$)			All Soils Isotropic ($k_I = k_{II}$)			All Soils Anisotropic ($k_I = 9\,k_{II}$)		
Seepage[b]	Gradient[c]	Stability[d]	Seepage[b]	Gradient[c]	Stability[d]	Seepage[b]	Gradient[c]	Stability[d]	Seepage[b]	Gradient[c]	Stability[d]
(*a*) BLANKET DRAINAGE UNDER DOWNSTREAM HALF OF DAM											
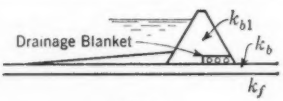 Case 1						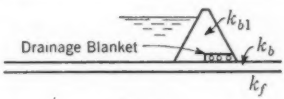 Case 2					
750	0.25	Barely adequate	1,100	1.0	Critical	1,400	0.41	Critical	1,900	1.73	Extremely critical
(*b*) FOUNDATION DRAINAGE											
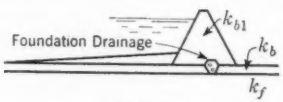 Case 3						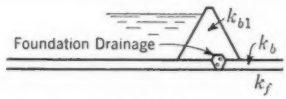 Case 4					
850	→0	Very safe	1,400	→0	Very safe	1,700	→0	Very safe	2,800	→0	Very safe

[a] In the diagrams: $k_{b1} = 0.25$ ft per day; $k_b = 5.0$ ft per day; and $k_f = 300.0$ ft per day. [b] Seepage quantity under the given permeability assumption, in cubic feet per day per foot of dam. [c] The discharge gradient at the downstream toe. [d] Comment on the degree of stability of the dam.

termine the benefit derived from the blanket, a similar analysis was made with the blanket omitted. This analysis indicated that the blanket reduced the seepage quantity and discharge gradients at the toe approximately 50%. The values obtained from the flow-net analysis of Mr. Bennett's section with homogeneous soils agree substantially with the results obtained from his formulas but indicate a slightly higher discharge gradient of 0.25 at the downstream toe. For the stratified condition, the discharge gradient is increased to 1.0 which represents a critical condition. The magnitude of the discharge gradient in this analysis varies approximately in proportion to the square root of the ratio of k_I to k_{II}; hence, the approximate gradient can be estimated for other degrees of stratification. The original design incorporating the 1,100-ft blanket (case 1, Table 1) may be considered barely adequate, provided the soil

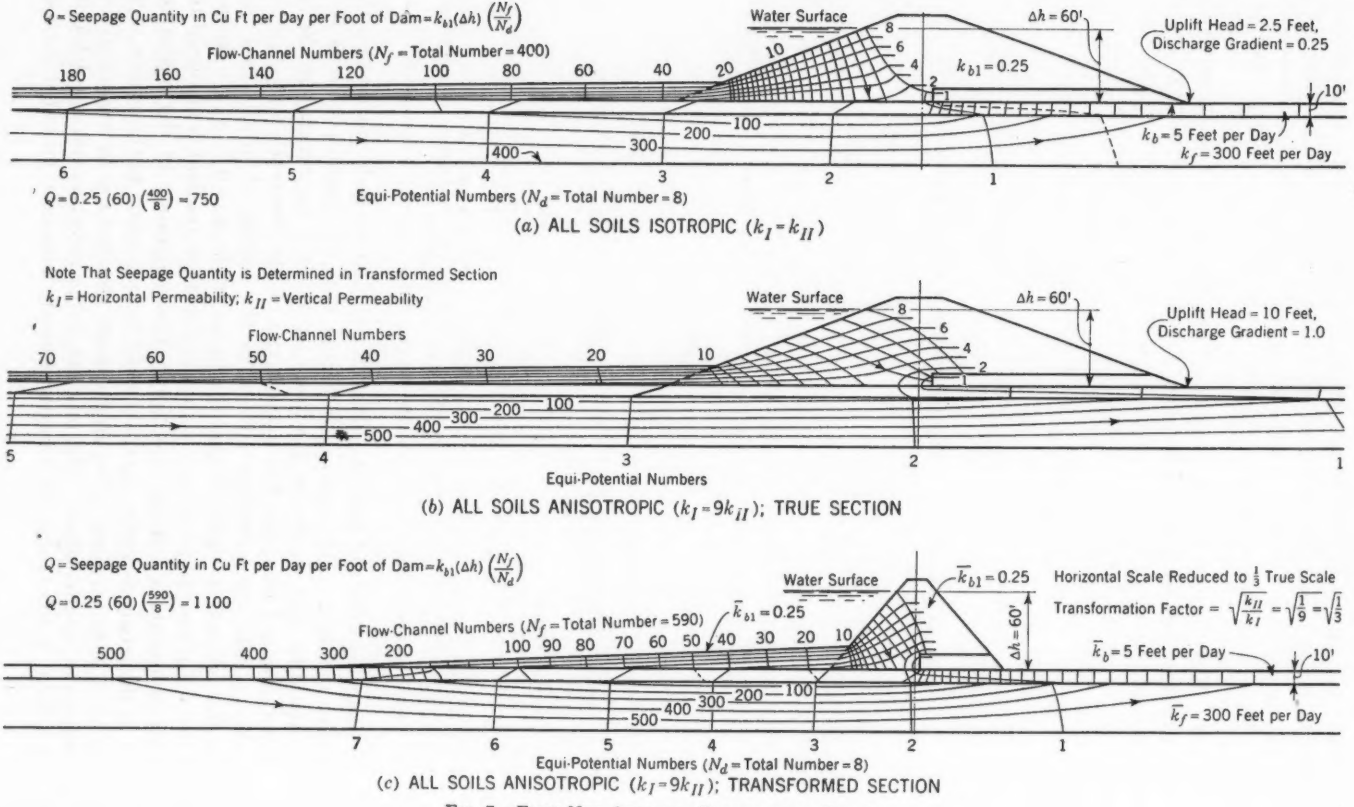
Q = Seepage Quantity in Cu Ft per Day per Foot of Dam = $k_{b1}(\Delta h)\left(\frac{N_f}{N_d}\right)$
Flow-Channel Numbers (N_f = Total Number = 400)
180 160 140 120 100 80 60 40 20
Water Surface
Δh = 60'
Uplift Head = 2.5 Feet,
Discharge Gradient = 0.25
k_{b1} = 0.25
k_b = 5 Feet per Day
k_f = 300 Feet per Day
10'
6 5 4 3 2 1
Q = 0.25 (60) $\left(\frac{400}{8}\right)$ = 750
Equi-Potential Numbers (N_d = Total Number = 8)
(a) ALL SOILS ISOTROPIC ($k_I = k_{II}$)
Note That Seepage Quantity is Determined in Transformed Section
k_I = Horizontal Permeability; k_{II} = Vertical Permeability
Flow-Channel Numbers
70 60 50 40 30 20 10
Water Surface
Δh = 60'
Uplift Head = 10 Feet,
Discharge Gradient = 1.0
5 4 3 2 1
Equi-Potential Numbers
(b) ALL SOILS ANISOTROPIC ($k_I = 9k_{II}$); TRUE SECTION
Q = Seepage Quantity in Cu Ft per Day per Foot of Dam = $k_{b1}(\Delta h)\left(\frac{N_f}{N_d}\right)$
Q = 0.25 (60) $\left(\frac{590}{8}\right)$ = 1 100
Flow-Channel Numbers (N_f = Total Number = 590)
500 400 300 200 100 90 80 70 60 50 40 30 20 10
$\bar{k}_{b1}$ = 0.25
Water Surface
$\bar{k}_{b1}$ = 0.25
Horizontal Scale Reduced to $\frac{1}{3}$ True Scale
Transformation Factor = $\sqrt{\frac{k_{II}}{k_I}} = \sqrt{\frac{1}{9}} = \sqrt{\frac{1}{3}}$
Δh = 60'
$\bar{k}_b$ = 5 Feet per Day
10'
$\bar{k}_f$ = 300 Feet per Day
7 6 5 4 3 2 1
Equi-Potential Numbers (N_d = Total Number = 8)
(c) ALL SOILS ANISOTROPIC ($k_I = 9k_{II}$); TRANSFORMED SECTION

FIG. 7.—FLOW-NET ANALYSIS; SECTION FROM FIG. 5

is essentially nonstratified, but it is not adequate if any appreciable degree of stratification exists. Omitting the blanket (case 2, Table 1) reduces the degree of safety by approximately 50%; hence, the blanket does definitely contribute to the safety of the structure, even though it may not be entirely adequate.

Examination of the flow nets for the original section with the 1,100-ft blanket (see Fig. 7) indicates that uplift pressures in the pervious substratum should be relieved by a suitable drainage system such as vertical drainage wells drilled to a substantial depth or a drainage trench excavated to the pervious substratum. The results obtained from flow-net analyses of the latter design are summarized in Table 1 under cases 3 and 4. Case 3 designates the section with a 1,100-ft blanket and with a drain excavated into the pervious substratum; case 4 is identical, except that the upstream blanket has been omitted. Flow nets drawn for the assumed conditions indicate that uplift pressures at the toe have been eliminated by the foundation drain and that the embankment is absolutely safe against blowouts, even with the blanket omitted. The data in Table 1 illustrate that the foundation drain increases the seepage quantity in varying amounts to a maximum of 47%; hence, the value of the lost water (if the structure is to provide storage) and the cost of removing seepage from developed lands on the back side of the structure must be considered in establishing the design.

Where conditions are favorable to the use of a positive cutoff, this alternative may be the most economical long-time solution. In many locations, however, pervious strata are so deep that a cutoff is impracticable; and, in such instances, some other method must be adopted for the control of underseepage. In preliminary studies of embankments incorporating upstream blankets, the method outlined by the author should be a valuable asset. In detailed design studies, many engineers will prefer a more general method that can be adapted to the analysis of a variety of methods of seepage control. For this purpose the graphical flow-net method offers advantages that should not be overlooked by the designing engineer.

FIG. 7.—FLOW-NET ANALYSIS; SECTION FROM FIG. 5

AMERICAN SOCIETY OF CIVIL ENGINEERS

Founded November 5, 1852

DISCUSSIONS

UTILIZATION OF GROUND-WATER STORAGE IN STREAM SYSTEM DEVELOPMENT

Discussion

BY IRVING B. CROSBY

IRVING B. CROSBY,[8] AFFILIATE AM. SOC. C. E.[8a]—The scope of this paper is deliberately restricted to the arid or semiarid regions of the United States west of the 97th meridian. The paper is largely confined to a discussion of the use of ground water for irrigation. This tends to give the impression that ground-water storage is more highly developed in the west than elsewhere and that the most important use of ground-water storage is for irrigation. Mr. Conkling also restricts his paper to ground-water storage in alluvium. It should be interesting and valuable, therefore, to cite some instances of the development of ground-water storage in other regions, for other purposes, and in other geological formations.

The use of ground-water storage for irrigation, its development, and climatic conditions are stressed by the author; but he includes little concerning the geologic conditions which make possible the accumulation and use of ground water in the valleys of the west. The two regions for which ground-water storage is discussed are the Great Plains and the "mountain and valley province." These two regions cover a vast area with widely varying conditions. Although the term, "mountain and valley province," is mentioned in connection with references to C. F. Tolman (8)[8b] and O. E. Meinzer (11), it does not appear to be used by them. Since there are already two classifications of ground-water provinces in the west, this attempt to introduce a different term is unfortunate and unnecessary. The region included in the author's term, "mountain and valley province," is subdivided into five provinces in Mr. Tolman's classification (8*b*). These are: (*A*) The Great Basin province covering parts of California, Nevada, Utah, and Idaho; (*B*) the Columbia Plateau province in Idaho, Washington, Oregon, and California; (*C*) the Great Valley of California;

NOTE.—This paper by Harold Conkling was published in January, 1945, *Proceedings*. Discussion on this paper has appeared in *Proceedings*, as follows: March, 1945, by Raymond A. Hill; April, 1945, by Clarence S. Jarvis, and John R. Charles; and May, 1945, by C. W. Sopp, and J. A. Bradley.

[8] Cons. Eng. Geologist, Boston, Mass.

[8a] Received by the Secretary April 24, 1945.

[8b] Numerals in parentheses, thus: (8), refer to corresponding items in the Bibliography (see Appendix of the paper), and at the end of discussion in this issue.

(*D*) the Coast Ranges of Central and Southern California; and (*E*) the northern Coast Ranges. The author's examples are largely from province (*D*), the Coast Ranges of Central and Southern California. The geologic conditions of this province are very different from those of other parts of the region and the attempt to lump these five ground-water provinces into one province oversimplifies the case.

Although the author's discussion of ground-water storage is restricted to alluvium, the principles he presents apply to pervious rocks and are important in many places. Some geologic formations, in addition to alluvium, in which ground-water storage may be significant are: (*a*) Very pervious sandstones, (*b*) beds of volcanic ash, (*c*) beds of fractured lava, (*d*) cavernous limestones, and (*e*) highly fractured zones in any type of rock. In the last three cases, in which the water occupies fractures and cavities rather than pores, wells for recharging the ground water may be important.

A peculiar case of underground storage in limestone was encountered by the writer in the West Indies. The water supply of Port Au Prince, Haiti, was formerly obtained entirely from springs at the base of Morne l'Hopital, a long limestone ridge which rises 3,000 ft directly behind the city. In 1938 and 1939 an investigation of possible additional water resources was made by the writer, acting as consulting geologist for the J. G. White Engineering Corporation, and it was decided to drive a tunnel into the mountain directly back of the city. A large flow of water was encountered 1,500 ft from the entrance, with a volume, at first, of 2.75 mgd. Later this volume gradually decreased to 1 mgd and became constant. Subsequent observations indicated that a large subterranean cavity filled with water had been tapped, that the large temporary flow was caused by the draining of this stored water, and that the smaller constant flow was the average yield resulting from rain on the mountain. During wet seasons this underground storage reservoir fills; the flow increases; and, during dry seasons, the reservoir is drawn down.

The two areas discussed in detail by the author—the Platte River Valley in the Great Plains and the valleys of the Coast Ranges in Southern California—are both outside the glaciated region, but similar conditions exist in the glaciated regions. In the valleys of Southern California the ground water occurs in alluvial fans at the base of the mountains. The alluvial material filling these valleys grades from very coarse gravel at the base of the mountains to finer sand at some distance but is all pervious in varying degree and is generally very thick. The alluvial fill of the valleys of the Great Plains, on the contrary, is generally thin.

Valleys with deep alluvial fill are common in New England and in other parts of the glaciated regions (52). In contrast with the unglaciated valleys, however, there is no regular gradation from coarse alluvium in the upper parts of the valleys to finer alluvium in the lower part. Because of the irregularities of glacial deposition, there may be an impervious dam of fine alluvium across a valley with basins of pervious gravel above and below it. The pattern of surface drainage is often very different from that of the buried preglacial valleys, and ground-water basins in the buried valleys may drain in different directions from surface streams. Therefore, it is more difficult to determine

the size of ground-water reservoirs in glaciated regions. Such reservoirs exist in many places, however, and are used for municipal and industrial water supplies. Generally, no attempt is made to recharge these ground-water reservoirs artificially, but one system which is so operated will be described briefly.

The first public water supply of the City of Cambridge (Mass.) was Fresh Pond in the western part of the city, and the pond is still used as part of the supply. Fresh Pond occupies a glacial kettle hole at the southern end of a glacial sand plain in a buried preglacial valley. No surface stream follows the entire length of this valley; but the upper part is occupied by the Mystic River, and the Charles River crosses the valley a mile south of Fresh Pond. The buried valley is filled with alluvium to a depth of about 170 ft. Immediately south of Fresh Pond is a glacial moraine which forms a ground-water dam and isolates the ground-water basin of Fresh Pond from the Charles River Valley. Another ground-water divide, a mile and a quarter north of the pond, separates the Fresh Pond ground-water basin from that part of the buried valley occupied by the Mystic River. Fresh Pond has an area of 85 acres and is 55 ft deep. The total surface drainage area tributary to it is 1.25 sq miles, but the area tributary to the sand plain is about 5 sq miles. Since 1887 there has been an additional water supply by conduit from Stony Brook Reservoir in Waltham, Mass.

In 1941 Cambridge needed additional water to supply war industries, and an investigation of ground-water possibilities was made by the writer who recommended that greater use should be made of ground-water storage, that Fresh Pond should be lowered much more in the summer to draw upon more ground-water storage, and that Fresh Pond should be filled in the spring to replenish the storage. Since then Fresh Pond has been drawn down in the summer, obtaining a large additional yield from the ground, and both pond and ground are filled in the spring by surplus water from Stony Brook which would otherwise be wasted over the dam.

Artificial recharge by water spreading is practiced at several plaecs in New Jersey, both in and outside the glaciated region. Artificial recharge has been practiced for more than 30 years at the Perth Amboy Water Works where rates of recharge ranging from 4,000 to 90,000 gal per acre per day have been measured. Ground-water recharge is also practiced in Long Island where it is recharged into glacial beds by means of wells and pits.

One of the most intensely developed rivers in the world is the Ruhr River in Germany. Although the climate is different, the geology somewhat different, and the water use very different, from the conditions in Southern California, there are interesting similarities in the developments. The Ruhr River flows west into the Rhine River at Duisburg-Ruhrort and has a drainage basin of 1,715 sq miles. The average natural flow before the construction of reservoirs or water works was 1,989 mgd, or 2,800 cu ft per sec. The Ruhr River is just outside the glaciated region, and it flows in an alluvial valley between low bluffs of slate and other relatively impervious rocks. The valley is floored with clay beneath which is a relatively thick layer of coarse, pervious gravel. This gravel layer forms a very long, narrow ground-water storage reservoir

in which the water table is frequently lower than the river. The river is then influent to the ground water. The Ruhr River cuts through the clay layer into the gravel, but the river bed is generally coated with sludge which hinders infiltration of river water into the ground.

The Ruhr River is the only source of water supply for the Ruhr industrial district, which includes a large area north of the Ruhr Valley. The total area served is 2,500 sq miles, with a population of 3,500,000. The average consumption, all obtained from the gravel, is 250 mgd, or more than the low-water flow of the river (53). This supply was obtained from ninety different water works. In 1929, the year of greatest consumption and lowest flow, 476 mgd were used. During September, 1929, no water flowed into the Rhine River from the Ruhr River.

An elaborate series of planned developments has been completed to use the limited water resources (54) to the greatest possible extent. Water is obtained from batteries of wells and from infiltration galleries near the riverbanks. To replenish the ground-water reservoir, river water is conducted to off-stream spreading grounds, which are basins excavated through the layer of clay into the gravel. These basins are floored with sand which is cleaned occasionally. Thus, there is an extensive underground reservoir protected from evaporation losses. The only loss is seepage through the gravel down the Ruhr Valley to the Rhine River. To develop the water resources further, a series of storage reservoirs was built on tributaries of the Ruhr River. Excessive deposition of sludge was caused by the reaction of the acid water from the Lenne River, which flows through an iron mining district, with the alkaline water from the Ruhr River, which comes from a paper mill district. To precipitate this sludge, a series of lakes was formed by low dams on the Ruhr River. The sludge is flushed out of the lakes during high water. This combined development of the surface and ground-water resources of the Ruhr River provides water supply, river regulation, navigation, water power, and recreation.

Another example of intensively developed ground-water storage is the water supply of the City of Haltern at the junction of the Stever and Lippe rivers in Germany. The Lippe River, the next large stream north of the Ruhr River, flows west and enters the Rhine River at Wesel. Salt springs and drainage from mines make the water of the Lippe River saline. The Stever River comes from the north and joins the Lippe River at Haltern. The Stever River Valley is filled to a depth of 400 ft with sand, whose grain size is 1 mm or less. The permeability of the sand is 340 ft per day at unit head. The drainage area of the Stever River is 395 sq miles. The annual precipitation on this area is 547,100 acre-ft and the annual runoff is 186,400 acre-ft (55). To obtain the maximum safe yield without drawing in saline water from the Lippe Valley, a dam with a sheet-pile cutoff was built on the Stever River, raising the water level 20 ft and forming two reservoirs (56). From these reservoirs, water is conducted to spreading grounds from which it seeps into the ground. The surface storage is 7,629 acre-ft, and the underground storage is estimated at 4,621 acre-ft. By making full use of the underground storage, an annual supply of 64,850 acre-ft, or 58 mgd, is available—even in extremely dry years. The water is obtained

by a battery of gravel-packed wells arranged in an east-west line across the valley.

These scattered examples of the uses of ground-water storage in the intensive development of stream systems show that the principle is not closely restricted by climatic or geologic conditions or by types of water use but that its application is feasible and valuable in a wide variety of conditions. By his detailed discussion of conditions and controlling factors in the semiarid western states, Mr. Conkling has made a valuable contribution to the subject.

Bibliography.—

(8) **"Ground Water,"** by C. F. Tolman, 1st Ed., McGraw-Hill Book Co., Inc., New York, N. Y., 1937. (*a*) p. 469. (*b*) p. 520.

(11) **"The Occurrence of Ground Water in the United States,"** by Oscar Edward Meinzer, *Water-Supply Paper No. 489*, U. S. Geological Survey, Government Printing Office, Washington, D. C., 1923.

(52) **"Ground Water in the Pre-Glacial Buried Valleys of Massachusetts,"** by Irving B. Crosby, *Journal of the New England Water Works Association*, September, 1939, pp. 372–383.

(53) **"Water Supply and Sewage Disposal in the Ruhr Valley,"** by K. Imhoff, *Engineering News-Record*, January 15, 1925, pp. 104–106.

(54) **"Die Stadtentwässerung in Deutschland,"** by J. Brix, K. Imhoff, and R. Weldert, Jena, 1934, pp. 455–477.

(55) **"Die Wasserversorgung des Industriesgebietes von Norden,"** by Schmick, *Das Gas und Wasserfach*, Jahrgang 75, No. 32, August 6, 1932, pp. 637–640.

(56) **"Der Stever-Staudamm bei Haltern (Westfalen),"** by E. Mattern, *Zentralblatt der Bauverwaltung*, May 6, 1931, pp. 269–272.

AMERICAN SOCIETY OF CIVIL ENGINEERS

Founded November 5, 1852

DISCUSSIONS

ECONOMICS OF PHOTOGRAMMETRY

Discussion

BY RAYMOND A. HILL, RAYMOND L. MOORE AND RALPH S. PEARSE

RAYMOND A. HILL,[3] M. AM. SOC. C. E.[3a]—Aerial mapping was a "child" of World War I; and, as described by the author, it has since grown to full stature even though most engineers have no appreciation of that fact. Those engaged in the photogrammetric field have suffered many disappointments because of the lack of interest shown by most engineers and because of the lack of understanding on the part of the few interested engineers. These disappointments should have been expected, however, because most engineers are not concerned with maps, and even those who use maps in their work often have no part in the preparation of maps. Hence, only a few engineers have had more than an academic interest in aerial surveys and photogrammetry, and it was not natural that all of them would turn from conventional methods and accept something which was new and untried. Furthermore, it must be confessed that even the small number of engineers who today rely greatly upon photogrammetry do so more because of faith in the result rather than because of understanding of a method that depends upon an optical illusion.

If a poll were taken of all members of the Society, the writer believes that a substantial number would be found to have no acquaintance with photogrammetry, that half of the membership would not distinguish between modern photogrammetry and aerial photography, and that half of the remainder would state that the same information could be obtained more cheaply and equally well by conventional ground methods. The author is thus to be commended for presenting, clearly and fairly, the distinction between the "child," aerial mapping, and the "adult," photogrammetry.

It is not likely that the majority of engineers will ever be interested more than academically in photogrammetry, any more than most engineers are concerned with developments in hydraulics, or in other specialties foreign to their own fields of endeavor. On the other hand, every engineer who uses

NOTE.—This paper by Leon T. Eliel was published in March, 1945, *Proceedings*.

[3] (Leeds, Hill, Barnard & Jewett), Los Angeles, Calif.

[3a] Received by the Secretary April 2, 1945.

maps should acquire an appreciation and understanding of both the advantages and the limitations of modern developments.

It should not be presumed from the statements of the author that aerial photography has been supplanted by photogrammetry. On the contrary, aerial photography probably has more applications to engineering problems than do the contour maps produced with a photogrammetric instrument. This is natural, because the relative positions of physical features and types of culture are generally more important than absolute elevations. Many illustrations may be cited: Changes along a shore line due to erosion or deposition; general routes for railroads, highways, and transmission lines; city planning, as distinguished from site planning; and general surveys, such as land and soil classifications, agricultural censuses, etc.

In most of the foregoing instances, the contact print from an aerial photograph presents, directly, more information than could be obtained by ground methods without excessive cost. When successive photographs are examined stereoscopically, the land form is clearly disclosed. The observer then has before him an accurate relief map on which is located every natural feature and all culture in the proper relationship.

Too little attention has been given to the interpretation of aerial photographs. Those in the industry, by reason of their own familiarity, took it for granted that any one could read an aerial photograph, not appreciating the fact that familiar objects viewed horizontally become strange when seen vertically. It should have been recognized that people must be taught how to read maps, even though maps have been in use for thousands of years. It is only natural that most people should look upon aerial photographs as interesting pictures and not as maps, because they have not been taught to interpret the shades and shadows which take the place of conventional symbols on a map.

Assembly of contact prints of aerial photographs into a mosaic produces a map that is frequently of great value in spite of inherent distortions. The accuracy of a mosaic, of course, depends upon the degree of control and the extent to which each part is brought to a common scale. A rough mosaic is little more than a rephotograph of overlapping contact prints placed in approximate relation one to another. A matched mosaic presents a better picture in that, to the eye, it has the appearance of a single photograph. For many purposes such a mosaic is ample, because the engineer who uses the map, as distinguished from the engineer who prepares the map, is generally most concerned with the relative position of natural features and cultures. Such mosaics are particularly valuable in general planning. They have been used extensively in flood control studies, in rerouting highways, in locating industries, and for many other purposes where a bird's-eye view of large areas was helpful.

The development of the controlled mosaic and the precise mosaic was in response to the demands of those who made maps rather than to satisfy the needs of those who used maps. Most of the former think in terms of the accuracy of the survey for which they are responsible; and, hence, they are

prone to demand comparable accuracy when aerial methods are used. Actually, the comparison should be on the basis of the finished and reproduced map. A ground survey may be made at an accuracy of 1:5,000, but no man can plot an observed distance on a map with one tenth of that accuracy. Furthermore, when a draftsman completes a map on tracing cloth, it is of little value until reproductions are made. Changes in humidity and temperature cause some distortion of the tracing even before prints are taken. Unless these prints are made entirely by a dry process, large distortions result; and, even under the best conditions, the map that is available to the user is neither true to scale nor free from distortion. It has been the writer's experience that a reproduction of a carefully made, matched mosaic can be used with confidence for almost all the purposes, excepting only elevations, for which any reproduction of any map at the same scale would be used.

Whenever either the absolute elevation or the relative elevation of features must be obtained from maps, the engineer responsible for the preparation of the map should ascertain whether photogrammetric methods should be used. As stated by the author, if the area is small, the answer is probably "no." Likewise, if the terrain to be mapped is open and relatively flat or if only a narrow strip of topography is needed, the answer is again "no." On the other hand, if a substantial area of broken terrain is to be mapped, the answer is probably "yes." In some cases, the nature of the cover will determine whether ground methods would be cheaper and faster or whether photogrammetric methods would be better. The writer could cite the case of one Army cantonment where the required contour map was prepared photogrammetrically because of the presence of a mantle of brush but where, otherwise, plane-table methods would have been more suitable.

In general, ground surveys, supplementing aerial photographs and matched mosaics, will usually be found most advantageous in the solution of specific engineering problems. On the other hand, photogrammetry will probably supplant ground surveys of large areas, and the future of photogrammetry is limited only by the extent of all the continents.

RAYMOND L. MOORE,[4] ESQ.[4a]—The multiplex "aero-projector" method is probably the most widely used of the three types of precision equipment described in the paper. The method is also the most recent addition to the field of photogrammetry although the spatial model was first constructed by dichromatic projection in 1858. Practical equipment for utilizing this principle in the production of topographic maps did not become available in the United States, however, until about 1935.

In general, the equipment of 1944 is similar to that of 1935, but vast improvements, both optical and mechanical, have been incorporated in later models. The most important change has been the result of improved lens design, not only in the projector unit but in the aerial camera itself, by increasing the effective field of coverage.

---

[4] Lt.-Col., Corps of Engrs., U. S. Army, Commanding Officer, 29th Engrs., Portland, Ore.

[4a] Received by the Secretary, May 11, 1945.

Early multiplex equipment was designed for aerial photography obtained with the multi-lens camera, of which the nine-lens tandem T-3A camera is probably the best known in the United States. Photography of this type necessitated two general projector designs—one for use with the vertical center chamber, and the other for use with oblique wing prints. Since distortion, displacement of images due to relief, and generally unsatisfactory quality were present in the oblique photographs, accurate mapping with these projectors was extremely difficult. The multi-lens camera is considered obsolete for general mapping purposes and it has been replaced by the so-called wide-angle, single-lens camera. This camera provides an effective field of coverage between 90° and 100°, depending upon the camera type; and the field of coverage for a single vertical photograph is about equal to the usable field of the older multi-lens cameras. Although most of the older normal-angle equipment is still being used, the newer wide-angle equipment is found in most multiplex mapping laboratories. This equipment makes possible aerial photography with most favorable base-altitude ratios—which results in greater contour accuracy and materially reduces the number of photographs required.

In comparing the relative merits of the different systems of photogrammetric plotting devices on a cost basis, it is necessary to examine the fields in which each system is used. Both the Brock equipment and the stereoplanigraph are suitable for the production of large-scale contour maps—a field in which the multiplex has not been used extensively. Sufficient mapping by both the Brock process and the stereoplanigraph has been published and tested to prove conclusively that exceedingly high standards of accuracy can be obtained. In this field the multiplex has not yet been used extensively enough to compete on a cost basis with the other methods.

Within the continental limits of the United States, more medium-scale mapping (that is, mapping on scales of 1:24,000 to 1:62,500) has been completed by multiplex than by either of the other two processes. Many factors have influenced the widespread acceptance of the multiplex method for this type of mapping. Multiplex maps have met rigid accuracy standards, and the comparatively low initial cost of equipment undoubtedly has been considered; but these factors alone do not entirely account for the popularity of the method. Availability of the equipment on the domestic market is a primary asset. Neither additional stereoplanigraphs, which are of foreign manufacture, nor Brock equipment, which was custom-built and not a standard commercial product, is available. Before the priorities of World War II made acquisition difficult, multiplex equipment was available to those organizations that had occasion to do topographic mapping and is the only precision plotting equipment that has been in actual production during the war.

The availability of photogrammetric operators has been a major problem of all agencies utilizing stereoscopic plotting equipment, since trained operators are not available and must be educated within the organization. As in all types of precision work, there are certain basic requisites of knowledge and aptitude that potential operators must possess. Only part of the people with this knowledge and aptitude will develop the acuity of vision necessary to become capable "photogrammetrists." Nevertheless, a larger percentage

capable of operating the multiplex will be developed than would be developed if the training were on other types of equipment. If candidates are selected carefully, the average operator will be able to draw contours on oriented models after about three months; he will become a reasonably skilled "phototopographer" in six months; and he may be expected to do satisfactory extension work in nine months or one year.

Inherent in the multiplex method are operational features which are not provided (or are difficult to execute) by the other types of equipment, the most important of which is the capability to "phototriangulate" or "bridge" field control both vertically or horizontally. Secondly, and of considerable importance in military mapping, contour plotting may progress simultaneously on a large number of stereoscopic models for later assembly into the finished map.

The cost of field control is a primary consideration in the planning of any mapping operation and may well be the deciding factor in determining which method, or methods, should be utilized. In general, the amount of field control is decreased as the scale of the map is reduced and the contour interval increased. Thousands of square miles of mapping have been produced by the multiplex method since 1936 with a publication scale of 1:24,000 and an average contour interval of 20 ft. For this type of mapping horizontal control is generally placed along the 7.5-min quadrangle with boundaries normal to the direction of the flight lines. Horizontal control, for the orientation of interior models, is obtained by "bridging" this control without the necessity for additional horizontal field control, although for this scale and contour interval it is still accepted practice to obtain a limited amount of vertical control on each interior photographic pair. Much work has been completed during this same period on standard quadrangle maps published on a scale of 1:62,500, with contour intervals averaging about 50 ft. Control lines are placed along the 15-min quadrangle borders crossing the flight lines; and, because of the greater contour interval, little or no vertical field control is required on the intermediate models. In planning projects of this type, both vertical and horizontal control bands are placed about 15 miles apart. Between these control bands the multiplex bridge, or "phototriangulation," produces adjusted positions and elevations upon which the intermediate models for drawing the topography are oriented.

Military and civilian practice differs somewhat inasmuch as time is frequently the paramount consideration in any military mapping project; and, for this reason, methods are frequently used which do not necessarily produce maps in a minimum number of man-hours. More frequently, the problem is the production of a map in the absolute minimum lapsed time even though the number of man-hours may be excessive. To produce a maximum amount of work in the minimum over-all length of time, control bridge work is conducted independently of contour mapping by an organized bridging section. Only the highest types of operators are assigned to this section. In general, the same type of equipment is used as that used in the plotting section, except that the multiplex bars are longer. In an emergency, projectors normally used in bridging work may be diverted to contour plotting, provided a sufficient number of additional operators are available.

The multiplex has been used to a limited extent in the field of reconnaissance mapping with highly satisfactory results. A brief description of a project recently completed will illustrate the potentialities of the method in this field. The topography of an area approximately 500 miles long and 10 miles wide was required for publication on a scale of 1:250,000, with a contour interval of 100 ft. The need for this work was urgent; the area was inaccessible; and part of the route was over terrain probably never before traversed by white men. There were available, within the area, seven control points of known geographic position and a few elevations of somewhat doubtful quality. Some additional elevations were secured by prorating known or assumed river grades. The longest single multiplex bridge extended 285 miles, and a single horizontal control point was available on each of the terminal models. This bridge did not run in a straight line but traversed river valleys and high mountain passes. Aerial photographs for the project were taken in the middle of the winter with the sun never more than 5° above the horizon. Although the multiplex work was completed in a remarkably short time, subsequent field work has indicated that this map is surprisingly accurate.

Although it was designed for the production of topographic maps, numerous other uses have been found for the multiplex. By a rather simple method it has been used in the production of mosaics. With the multiplex bridge adjusted for horizontal scale, sufficient planimetry to fix the orientation of each photograph is drawn for transfer to the mosaic base. With dianegatives substituted for diapositives, projection prints can be made directly below the projectors. These prints are both adjusted as to scale ratios and horizontalized; and they may be pasted down in the normal manner.

Unfortunately, many topographic maps are actually obsolete before they are published; and, to preserve their maximum usefulness, frequent revision of cultural detail may be necessary. This revision work will be a major mapping problem in some localities. For example, in California, several areas were mapped very accurately as recently as 1925. Because of development, cultural details in some of these areas have changed to such an extent that, without revision, an entirely erroneous picture of the terrain is presented. The work in some of these areas has been revised easily, and with utmost accuracy, by the multiplex method. After the war a large amount of map revision will be required where wartime activities have caused major cultural changes.

With large areas of the United States still unmapped, there is ample work to keep all types of plotting equipment in use for some years. It is obvious that, in particular instances, certain types of equipment are preferable to others. For some time after the war the popularity of the multiplex method will probably continue, if for no other reason than the availability of equipment and operators. In the field of large-scale mapping the method remains to be proved. It may be found that large-scale work by the multiplex method will be less economical in the long run and that this particular type of work should be left for instruments of greater precision. In the intermediate-scale field—which includes most of the mapping to be done in the continental United States—there is ample proof that the multiplex method can compete with other methods, both in economy and accuracy. Economy in field costs is possible because,

unlike the other methods, the multiplex does not require survey control on every stereoscopic model. When contour intervals of 50 ft or more are used, costs of aerial photography will be the same for the multiplex as for the stereoplanigraph, inasmuch as photographs for both methods will be taken close to the service ceiling of the aircraft employed, and this ceiling will be the deciding factor in determining the number of models and the unit area covered by each model.

A discussion of existing photogrammetric plotting devices should not be concluded without some mention of the K.E.K. Plotter (named for J. E. King, J. W. Elliott, and P. B. Kail) being used by the United States Forestry Service in the production of standard quadrangle maps in some parts of California. This plotter was developed by personnel of the Forestry Service and might be considered a much-refined and enlarged stereocomparagraph in which certain of the most undesirable characteristics have been eliminated. The principal improvements incorporated in the K.E.K. Plotter are: (1) An arrangement by which contours are drawn to correct orthographic scale, rather than on the conic projection (which is one of the principal disadvantages of the stereocomparagraph); and (2) a system of restitution by an appropriate inclination of the contact prints with respect to the operator's point of view. As with other devices, except the multiplex, vertical control is required on each model. Little information is available as to the amount of horizontal control necessary, but it is probably about the same as that required for the other processes. Comparatively low initial cost and portability may make the K.E.K. Plotter a most valuable instrument for some types of work.

RALPH S. PEARSE,[5] JUN. AM. SOC. C. E.[5a]—It is gratifying to find a paper on photogrammetry in the publications of the Society, since engineers are relying more and more on accurate, complete maps. Two additional methods should be included in this discussion. For example, the K.E.K. Plotter is an improved form of the stereocomparagraph incorporating the third dimension, together with an accurate means of correcting the photographs for tilt. A pair of contact prints are oriented and corrected for any tilt, the resulting model then being viewed through a stereoscope. A lens with a small dot in the center is suspended under each eyepiece of the stereoscope between it and the image. These dots fuse to form a floating mark with which the operator traces planimetric detail and contours. The pair of photo-tables on which the photos are fastened are raised or lowered, according to a varying scale, to compensate for the conic projection, thus allowing the floating mark to trace the contours directly to scale. The floating mark is connected to a pencil or pantograph which permits drawing the detail on to the map. A considerable amount of control is required for this method, at least two horizontal and four vertical points being needed for each pair of photographs. An accurate map may be obtained and the instrument may be moved easily from place to place. The cost of the K.E.K. Plotter is several hundred dollars—considerably less than that of either the multiplex or the stereoplanigraph.

[5] Photogrammetric Engr., U. S. Geological Survey, Arlington Va.

[5a] Received by the Secretary April 20, 1945.

The aerocartograph is an instrument quite similar to the stereoplanigraph, incorporating a similar optical-mechanical system for obtaining map detail from glass diapositives. There are three in the United States, but they are not much used. The advantages and disadvantages of this method over the other methods are similar to those of the stereoplanigraph.

Several items concerning the comparative economy of the multiplex and stereoplanigraph methods should be mentioned. The cost of $10,000 for one multiplex unit is extremely high, $5,000 or $6,000 being more nearly correct. In many instances, it has become the practice to equip one unit for bridging (described more fully in a later paragraph) and to streamline four or more units, thus reducing the cost of an average unit to $3,000 or $4,000.

The flying costs will be greater for the multiplex than for the stereoplanigraph because of the lower flying height, which necessitates more pictures and more flying to cover a given area. However, the cost of the flying, especially for extensive areas, is a minor item in the total cost of the finished map. With an increase in flying height, some detail is very likely to be sacrificed regardless of the magnification of the pictures in the plotting machine. In many instances, the detail thus lost is of minor importance or of no value at all. However, at other times this detail is of major importance, outweighing the cost of extra control and flying.

The multiplex adapts itself to bridging over an area of several consecutive models, since a number of stereoscopic models can be set up simultaneously. Thus, considerable horizontal control is eliminated. The stereoplanigraph can accomplish the same result if an adjacent model is set up on the established control, which is a system of "pass points." However, as the stereoplanigraph can accommodate only one stereoscopic pair at a time, a number of single models, requiring considerable time and repetition, must be set up and oriented.

The multiplex tracing table, or stand, is far from clumsy. Sliding on quartz feet, it moves smoothly and easily, being limited in speed only by the skill of the operator. Although the multiplex may require more models, the time of operation represents only from about 5% to 8% of the total time consumed. The increased flying height at which the pictures for the stereoplanigraph are taken necessitates a much more precise setup of the model to obtain the desired accuracy. With the multiplex, the average operator can place the floating mark in the model on the ground to an accuracy of ± 0.05 mm which, at a scale of 1:10,000, represents about 3 ft. Assuming the contour interval to be 20 ft, this is well within the accuracy of 90% of the contours in one half of an interval. In setting up a model in the stereoplanigraph, the floating mark would have to be set accurately to ± 0.025 mm—a very limited tolerance.

One distinct advantage of the multiplex is that the operator is working directly over the map and with a flip of a switch can see what he has drawn, whereas the stereoplanigraph requires an assistant whose job is to observe the actual drawing, the operator not being in a position to view his work readily. Although the multiplex system can be used by somewhat less skilled personnel with less training, it has proved highly desirable to utilize only the higher type of personnel—preferably operators with a working knowledge of topo-

graphic features. The stereoplanigraph has an advantage over the multiplex in that it can accommodate a wide range of scales from a given pair of photographs, whereas the range of the multiplex is very limited, the flight height depending on the scale and contour interval desired.

Two factors that have a tremendous bearing on the comparison of the two methods—photogrammetric versus ground—are the extent of the area and the scale. The multiplex is adaptable to scales from 1:2,500 to 1:24,000; the stereoplanigraph has a slightly wider range; and neither of them is as economical for small areas as for large areas—say, 60 sq miles or greater. Flying, sending control parties into the field, etc., to map only a few square miles by the multiplex or other photogrammetric method are not economical procedures under present conditions as compared with field or ground methods. In numerous instances, a planimetric base map has been prepared by the multiplex method and assigned to a field party for addition of the contours, especially in flat areas.

Another factor that is important in comparing the economies of the multiplex with those of the stereoplanigraph is the photographic laboratory and its skilled personnel. In connection with a large or medium sized multiplex organization, a complete photographic laboratory is maintained under the supervision of a highly trained laboratory photographer with several assistants. Since there is only one stereoplanigraph in the United States and since there is little likelihood of ever having many assembled in one place, it would appear that either economy or the advantage of a highly skilled photographer would have to be sacrificed unless photographic work of a similar nature were available to occupy part of the photographer's time.

To summarize: For small areas up to several square miles the ground method should be far more economical. In flat areas either the ground method or a combination of ground and photogrammetric methods should prove most satisfactory. Over extended areas, especially where the terrain does not permit easy access by foot, the photogrammetric method should be superior and more economical. As to which is the most suitable photogrammetric method, one must take into consideration the conditions pertaining to each particular assignment. The tremendous first cost of obtaining equipment, plus the training of personnel, must be considered along with the type and extent of mapping to be done before the most economical method can be ascertained. For example, the U. S. Geological Survey is engaged in a continuous and extensive mapping program where expensive equipment and trained personnel will be utilized over a long period of time; thus, the multiplex method combined with ground methods has proved the most economical. On the other hand, for a private company interested in a small local area on a job of short duration, the ground method, the stereocomparagraph, or the K.E.K. Plotter should prove more economical.

AMERICAN SOCIETY OF CIVIL ENGINEERS

Founded November 5, 1852

DISCUSSIONS

INTERRELATION OF CERTAIN STRUCTURAL CONCEPTS

Discussion

BY MAX W. STRAUSS

MAX W. STRAUSS,[10] JUN. AM. SOC. C. E.[10a]—In the "Introduction," the author makes the statement that "The method of moment distribution introduced by Hardy Cross,[2] M. Am. Soc. C. E., * * * is as good a method as can be devised." That this is open to question is suggested by the author himself by the fact that he introduces the concept of an exact carry-over factor. This concept is not a new one. The writer has seen it traced back to Maurice Lévy who developed it about 1880.[11] Since then it has frequently been employed by others. However, beyond implying this concept, the development of the thesis of the paper seems to fall short of its logical conclusion. For instance, if Eq. 1 is substituted in Eq. 9, the latter may be rewritten:

$$f_{AB} = \frac{1}{2 + \dfrac{K_{AB}}{\dfrac{K_{BJ}}{2 - f_{BJ}} + \dfrac{K_{BC}}{2 - f_{BC}} + \dfrac{K_{BH}}{2 - f_{BH}}}} \qquad (34)$$

Thus, to determine the carry-over factor for any span toward a joint, it is only necessary to know the carry-over factors away from that joint for all other spans. Starting at a fixed or free-end support, all other carry-over factors may be determined rather easily. This is the basic principle long advocated by R. C. Brumfield, M. Am. Soc. C. E.[12]

NOTE.—This paper by Camillo Weiss was published in January 1945, *Proceedings*. Discussion on this paper has appeared in *Proceedings*, as follows: May, 1945, by Ralph W. Stewart, and R. C. Brumfield.

[10] Stress Analyst, Consolidated-Vultee Aircraft Corp., San Diego, Calif.

[10a] Received by the Secretary April 30, 1945.

[2] "Analysis of Continuous Frames by Distributing Fixed-End Moments," by Hardy Cross, *Transactions*, Am. Soc. C. E., Vol. 96 (1932), p. 1.

[11] "La Statique Graphique et Ses Applications Aux Constructions," by Maurice Lévy, Gauthier-Villars & Co., Paris, France, 1886–1888.

[12] "Moving Loads on Restrained Beams and Frames," by R. C. Brumfield, *Proceedings*, Am. Soc. C. E., May, 1945, p. 627.

For continuous beams, Eq. 34 reduces to:

$$f_X = \frac{1}{2 + \frac{K_X}{K_{X-1}}(2 - f_{X-1})} \quad \ldots\ldots\ldots\ldots\ldots\ldots (35a)$$

which, for continuous beams of constant moment of inertia and equal spans throughout, becomes:

$$f_X = \frac{1}{4 - f_{X-1}} \quad \ldots\ldots\ldots\ldots\ldots\ldots\ldots\ldots (35b)$$

Because of the very rapid convergence, f_X approaches f_{X-1}; and, starting at either a free or fixed support, $f_X \approx f_{X-1} \approx 2 - \sqrt{3} = 0.268$. For all practical purposes, this convergence can be assumed to take place in three or four spans. The writer's attention has been called to a short table compiled by Bertrand de Fontviolant which illustrates this effect.[13]

Moment Transmission and Distribution.—Eq. 13 is an expression for the distribution of a moment applied externally at joint B to the various spans at that joint. The terms in the right-hand side of the expression are defined by Eqs. 11 and 12. Instead of an external moment, consider a moment in span BA at joint B, arriving from joint A, which is to be distributed to the other spans at joint B. This moment will be distributed to each span in the ratio of its distribution factor to the sum of the distribution factors of the receiving members. Thus,

$$M_r = M_s \frac{d_r}{1 - d_s} - M_s \frac{r_r}{R_s} \quad \ldots\ldots\ldots\ldots\ldots\ldots (36)$$

in which the subscripts r and s indicate the receiving member and the sending member, respectively.

Referring to Fig. 3, consider member AB loaded in such a manner that the fixed-end moments are FEM_{AB} and FEM_{BA}. Then the moment in span BJ at joint B is

$$M_{BJ} = \text{FEM}_{BA}\, d_{BJ} + \text{FEM}_{AB}\, d_{AB} f_{AB} \frac{d_{BJ}}{d_{BJ} + d_{BC} + d_{BH}} \quad \ldots\ldots (37)$$

Factoring out the moment split[12] for member BJ:

$$M_{BJ} = \frac{r_{BJ}}{R_{BA}} [\text{FEM}_{BA}\,(1 - d_{BA}) + \text{FEM}_{AB}\, d_{AB} f_{AB}] \quad \ldots\ldots\ldots (38)$$

Comparing Eq. 38 with Eq. 36:

$$M_{BA} = \text{FEM}_{BA}\,(1 - d_{BA}) + \text{FEM}_{AB}\, d_{AB} f_{AB} \quad \ldots\ldots\ldots (39a)$$

Similarly,

$$M_{AB} = \text{FEM}_{AB}\,(1 - d_{AB}) + \text{FEM}_{BA}\, d_{BA} f_{BA} \quad \ldots\ldots\ldots (39b)$$

Illustrative Problem.—To illustrate the foregoing, the writer has chosen a frame (see Fig. 6) that has been solved previously by the Cross method of

[13] "Resistance des Matériaux," by Bertrand de Fontviolant, J. B. Bailliere & Fils, Paris, France, 1923, p. 452.

successive approximations.[14] The expressions for the carry-over factor and the distribution factor are given in Table 3 as are the moments at the supports due to the various loads. A usual sign convention is followed. A positive moment indicates a clockwise resisting moment acting on the span and a negative moment indicates a counterclockwise resisting moment. Thus, a moment transmitted from one end of a span to the other will not change sign; but, in passing through a joint, a moment will change sign before it is distributed to the other spans.

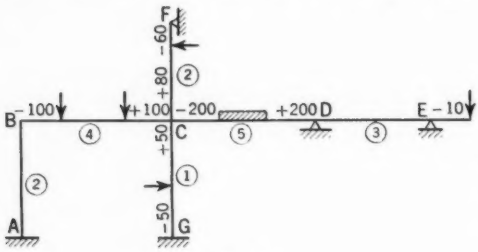

FIG. 6

The K-values are shown circled on each span in Fig. 6 and the fixed-end moments are indicated at the end of each span. Since $f_{BA} = \frac{1}{2}$, $r_{BA} = \frac{2}{1.5} = R_{BC}$, which results in $f_{CB} = \frac{1}{5}$ and $r_{CB} = \frac{4}{1.8}$. Similarly, $r_{CF} = \frac{2}{2}$ and $r_{CG} = \frac{1}{1.5}$, so that $R_{CD} = \frac{4}{1.8} + \frac{2}{2} + \frac{1}{1.5} = \frac{7}{1.8}$ and $f_{DC} = \frac{7}{23}$. Therefore, $r_{DC} = \frac{115}{39} = R_{DE}$ and $f_{ED} = \frac{115}{347}$. Beginning at the other end, $f_{DE} = 0$ and $r_{DE} = \frac{3}{2.0} = R_{DE}$, so that $f_{CD} = \frac{3}{16}$. Also, $r_{CD} = \frac{80}{29}$ and $R_{CB} = r_{CD} + r_{CG} + r_{CF} = \frac{80}{29} + \frac{1}{1.5} + \frac{2}{2} = \frac{385}{87}$ and $f_{BC} = \frac{385}{1{,}118}$. Therefore, $r_{BC} = \frac{4{,}472}{1{,}851} = R_{BA}$ and $f_{AB} = \frac{4{,}472}{12{,}646}$.

The moment splits (m) are obtained by Eq. 36. At a joint such as C, they are computed separately for each member acting as a transmitting member. Thus, for example, for the moment transmitted from joint B to joint C: $m_{CG} = \frac{r_{CG}}{R_{CB}} = \frac{1}{1.5} + \frac{385}{87} = \frac{174}{1{,}155}$; $m_{CF} = \frac{r_{CF}}{R_{CB}} = \frac{2}{2} \times \frac{87}{385} = \frac{87}{385}$; and $m_{CD} = \frac{80}{29} \times \frac{287}{385} = \frac{6{,}960}{11{,}165}$.

The distribution factors are obtained by Eq. 13. For example, $d_{CD} = \frac{1}{1 + R_{CD}/r_{CD}} = \frac{1}{1 + 7/1.8 \times 29/80} = \frac{144}{347} = 0.4150$.

Actual end moments of each loaded span due to the loads in the span are obtained by Eqs. 39; thus:

$$M_{BC} = -(100 \times 0.3556 + 100 \times -0.3343 \times 0.200) = -42.24$$
$$M_{CB} = +(100 \times 0.6657 + 100 \times 0.6444 \times 0.3444) = +88.76$$
$$M_{GC} = -(50 \times 1 + 50 \times 0.1003 \times 0.500) = -52.51$$

[14] "Analysis of Continuous Frames by Distributing Fixed-End Moments," by Hardy Cross, *Transactions*, Am. Soc. C. E., Vol. 96 (1932), Fig. 1, p. 5.

$$M_{CG} = + (50 \times 0.8997 + 50 \times 0) = + 44.98$$
$$M_{CF} = + (80 \times 0.8496 + 60 \times 1 \times 0.4248) = + 93.45$$
$$M_{CD} = - (200 \times 0.585 + 100 \times 0.6628 \times 0.3043) = - 137.17$$
$$M_{DC} = + (100 \times 0.3372 + 200 \times 0.4150 \times 0.1875) = + 49.28$$

These moments are distributed to the frame by the calculated carry-over factors and distribution factors as shown.

TABLE 3.—COMPUTATION OF FRAME CHARACTERISTICS AND MOMENTS IN FIG. 6

Member	$K = \frac{I}{L}$	$r = \frac{K}{2 - f}$	$R = \Sigma r_R$	$f = \frac{1}{2 + K/R}$	Moment Split = $\frac{r}{R_R}$			
	(1)	(2)	(3)	(4)	(5)	(6)	(7)	(8)
Point A—								
AB	....	....	....	....	....	....	....	....
Joint B—								
BA	2	1.3333	2.4160	0.3536 = f_{AB}	....	1.0000	....	....
BC	4	2.4160	1.3333	0.2000 = f_{CB}	1.0000	....	....	....
Joint C—								
CG	1	0.6667	5.9808	0.4614 = f_{GC}	....	0.1507	0.1181	0.1714
CB	4	2.2222	4.4253	0.3444 = f_{BC}	0.3716	....	0.3935	0.5714
CF	2	1.0000	5.6475	0.4248 = f_{FC}	0.1672	0.2260	....	0.2572
CD	5	2.7586	3.8889	0.3043 = f_{DC}	0.4612	0.6233	0.4884	....
Point F—								
FC	....	....	....	....	....	....	....	....
Point G—								
GC	....	....	....	....	....	....	....	....
Joint D—								
DC	5	2.9486	1.5000	0.1875 = f_{CD}	....	1.0000	....	....
DE	3	1.5000	2.9486	0.3314 = f_{ED}	1.0000	....	....	....
Joint E—								
ED	....	....	....	....	....	....	....	....

TABLE 3.—(*Continued*)

Member	$d = \frac{1}{1 + R/r}$	Actual Moments at Joints, Due to Loads in the Given Span					
		BC	CF	GC	CD	Joint E	Total
	(9)	(10)	(11)	(12)	(13)	(14)	(15)
Point A—							
AB	....	+21.12	+3.68	+1.67	−7.84	−0.06	+18.57
Joint B—							
BA	0.3556	+42.24	+7.35	+3.34	−15.67	−0.12	+37.14
BC	0.6444	−42.24	−7.35	−3.34	+15.67	+0.12	−37.14
Joint C—							
CG	0.1003	−13.38	−11.03	+44.98	+23.51	+0.18	+44.26
CB	0.3343	+88.76	−36.77	−16.71	+78.37	+0.61	+114.26
CF	0.1504	−20.06	+93.45	−7.52	+35.29	+0.27	+101.43
CD	0.4150	−55.32	−45.65	−20.75	−137.17	−1 .06	−259.95
Point F—							
FC	....	0	0	0	0	0	0
Point G—							
GC	....	−6.69	−5.52	−52.51	+11.76	+0.09	−52.87
Joint D—							
DC	0.6628	−10.37	−8.56	−3.89	+49.28	−3.31	+23.13
DE	0.3372	+10.37	+8.56	+3.89	−49.28	+3.31	−23.13
Joint E—							
ED	....	0	0	0	0	+10.00	+10.00

Conclusions.—In view of the obvious similarity of the Cross method to the method of successive approximations and the fact that the Cross method is derived from the basic slope-deflection equations, it seems fair to question the

author's assertion that the Cross method is based on a concept of "restraint" whereas the slope-deflection method is based "on relations governing deformations comprising the geometry of flexure." Actually, use of the Cross method is equivalent to solving the simultaneous slope-deflection equations by successive approximations. On the other hand, the method indicated by the author is truly based on the concept of "restraint." By recognizing that "restraint" is a function solely of the structure and is entirely independent of the loading and by proper evaluation of "restraint," a method is provided for the distribution of moments in a framework of restrained beams by a single operation.

AMERICAN SOCIETY OF CIVIL ENGINEERS

Founded November 5, 1852

DISCUSSIONS

COLUMN FORMULAS

Discussion

BY LEON BESKIN

LEON BESKIN,[17] ASSOC. M. AM. SOC. C. E.[17a]—That a column formula may be used as a curve on a graph, a set of precomputed values in a table, or as an algebraic expression, solved mathematically for each case that occurs in practice, is obvious. Nearly all structural designing departments plot column formulas instead of using them in their mathematical form, even if specifications give column strengths in terms of a mathematical expression. The author makes the point that, if this is so, an otherwise acceptable formula should not be rejected merely on the ground that it is complicated, since a graph of the formula is as easy to apply as the most elementary empirical expression. This seems to imply that the author proposes first to adjust a formula to fit experimental results and then to plot the resulting expression. This proposal seems to eliminate all interest in the formula since it is more straightforward to use an averaged curve of experimental results, directly without bothering with its mathematical expression.

Mathematical column formulas may be useful, however, when materials with different characteristics (such as aluminum alloys or concrete) are being considered. Graphical representation of a formula then involves a set of curves that can be applied to any material of the group. In this case it may be convenient to derive a formula in which the strength or the modulus of elasticity, or both, appear explicitly. Given the material to be used, it is then a simple matter to plot an acceptable column curve. In about 1934 the French Air Department introduced the following expression:

$$\sigma = \frac{1 + \frac{3\sqrt{3}}{2}\lambda^3_o}{1 + \lambda^2_o\left(1 + \frac{3\sqrt{3}}{2}\lambda^3_o\right)} \qquad (45)$$

NOTE.—This paper by William R. Osgood was published in December, 1944, *Proceedings*. Discussion on this paper has appeared in *Proceedings*, as follows: February, 1945, by L. E. Grinter, George Winter, and Jonathan Jones; March, 1945, by Edward Godfrey; and May, 1945, by Ralph E. Spaulding, and James H. Cissel.

[17] Structures Engr., Consolidated Vultee Aircraft Corp., San Diego, Calif.

[17a] Received by the Secretary April 23, 1945.

Eq. 45 is valid for $\lambda^2_o > \frac{1}{3}$, whereas, for $\lambda^2_o < \frac{1}{3}$, σ is assumed equal to unity. The value of σ is asymptotic to the Euler value $\sigma = \frac{1}{\lambda^2_o}$ for infinite values of λ_o, is equal to 1, and has a derivative equal to zero, for $\lambda^2_o = \frac{1}{3}$, so that the conditions of continuity, monotony, and continuity of the derivative are satisfied. The same result is obtained when, for a wide class of aluminum alloys, a straight line or a Johnson parabola, tangent to the Euler curve and corresponding to the block strength for $\lambda_o = 0$, is used.

The curves resulting from Eq. 45 do not satisfy the author's condition of extrapolation, and it is not necessary that they do so since the Euler curve in one case and the limiting value $\sigma = 1$ in the other are so defined that errors in extrapolation are normally avoided. There seems no doubt that the condition of possible extrapolation is unnecessary if the entire range of possible slenderness ratios is covered by a formula (or by several formulas). One such limitation may be defined as the Euler formula, whereas, for small slenderness ratios, a "cutoff" constant value may be used.

Furthermore, a system of several formulas satisfying the conditions of continuity, monotony, and continuity of the derivative as a whole can always be replaced, either exactly, or within the desired degree of accuracy, by a unique formula satisfying the same conditions so that the condition of a unique formula has no mathematical significance. Consequently, there is no practical, mathematical, or logical objection to the use of a limited number of simple formulas, instead of one complicated formula covering the entire range of possible slenderness ratios. An engineer can memorize simple formulas and compute allowable stresses on the slide rule, or by any other method best suited to his immediate needs, whereas a complicated formula leaves the practical engineer no choice but to plot a graph. Since that is his only choice, the best possible graph is that plotted directly from test data.

The writer cannot sense the importance of the condition stated in the "Introduction" that "An empirical [column] formula * * * should be one that expresses theoretically possible relations." The "theoretically possible relations" referred to by the author seem limited exclusively to the condition defined by the Euler formula. If a given empirical formula is claimed to be valid only for stresses less than the Euler values, that formula is absolutely legitimate as soon as it has been shown to fit the experimental results. In addition, if the formula is represented by a curve tangent to the Euler curve, it satisfies the condition of continuity of the derivative; but this condition is not important, since the stress-strain curve is never considered necessary to satisfy it. Since the column curve is a function of the stress-strain curve, it is possible that none of these curves satisfies the condition of continuity.

Thus, of all the conditions expressed by the author, the condition of monotony appears to be the only justifiable one. Incidentally, a decreasing function is always a monotonically decreasing function, because the concept of monotony is broader than the concept of the decreasing function. Mathematically, the word "monotonic" means "not decreasing or not increasing as

the independent variable increases."[18] When Mr. Osgood refers to a "monotonically decreasing function" in the "Synopsis," it is understood to mean that the dependent variable "stress" does not decrease as the independent variable "slenderness ratio" increases.

As stated by the author, the derivation of a column formula from a stress-strain curve is a difficult task. The double-modulus theory, which has been used for a long time, involves a basic error in theory, in that it presupposes a theoretically straight column. When a column with some initial curvature or eccentricity is considered, the double-modulus theory cannot be applied, and then the single-modulus theory appears to be more representative of both the theoretical picture and the actual facts.

A so-called "theoretical" formula, derived from an empirical stress-strain curve, cannot be considered theoretical, according to the precise meaning of the word as used by physicists. A formula of "correct form" (see "Introduction") cannot be devised without introducing at least one observed constant of the structure, and one observed constant related to the material. A formula of correct form should contain at least the slenderness ratio and one constant related to the strength of the material in compression (for a slenderness ratio of zero). In addition, since the author's opinion is that the "correct form" implies that the curve must be asymptotic to that of the Euler formula, the modulus of elasticity of the material must appear explicitly in the formula.

In the "Introduction," the author declares that "It would be very hard to justify more than two constants of the material in any practical column formula." All the formulas that he indicates, with the sole exception of the Rankine formula, contain two dimensionless constants. If only two constants of the material, one of them being the modulus of elasticity, were to be used, a single dimensionless constant, related to the ratio between the yield point (or the ultimate strength) and the modulus of elasticity, would be sufficient to define a column formula. The occurrence of two dimensionless constants in nearly all formulas shows that at least three constants of the material must be considered. Possibly, these constants could be taken as the average modulus of elasticity before the yield point, the average modulus of elasticity after the yield point, and the yield strength of the material. In the relation between free length and actual length (Eq. 2), the constant k may be different from the theoretical values such as $k = \frac{1}{2}$ for fixed ends, when the material is not in the elastic range, because of the important effect of initial eccentricities. In addition, when the ends are restrained elastically, the constant k is a function of the moduli of elasticity of both the support and the beam, and varies with the load when the column is not in the Euler range.

In the text following Eq. 2, the author states that the arbitrary constant S "* * * should be taken as a compressive secant yield strength." A yield strength defined by an arbitrary value of the permanent strain could be used as well as the secant yield strength. It would be interesting to learn if the author has a definite reason for using the secant yield strength rather than some other constant of the same nature.

[18] "Webster's New International Dictionary of the English Language," G. & C. Merriam Co., Springfield, Mass., 2d Ed. (unabridged), 1939, Vol. I, p. 1588.

A better choice for the constant S seems to be the intercept, S_o, of the column curve with the axis, σ. This choice eliminates one constant from all the dimensionless equations summarized by the author, with the exception of the two formulas (Eqs. 15 and 18) derived by means of the double-modulus theory. Eqs. 15 and 18 are not practical since they give an infinite column load for a slenderness ratio of zero. When the value of S is assumed equal to that of S_o, the various nondimensionless equations are transformed as follows:
The Rankine formula (Eq. 3*a*)—

$$\sigma = \frac{1}{1 + \lambda^2_o} \quad \ldots\ldots (46)$$

the secant formula (Eq. 7*a*)—

$$\cos \frac{\lambda_o \pi \sigma}{2} = \frac{.1}{\frac{1 - C}{\sigma} + C} \quad \ldots\ldots (47)$$

the Aarflot formula (Eq. 9*a*)—

$$\sigma = \frac{1}{C \lambda^2_o + \sqrt{1 + (1 - C)^2 \lambda^4_o}} \quad \ldots\ldots (48)$$

the Ylinen formula (Eq. 11*a*)—

$$\lambda^2_o = \frac{1 - \sigma^n}{\sigma} \quad \ldots\ldots (49)$$

the author's formula (Eq. 13*a*)—

$$\sigma = \frac{1}{1 + C \lambda_o + \lambda^2_o} \quad \ldots\ldots (50)$$

the parabolic formula (Eq. 20*a*)—

$$\sigma = 1 - \frac{1}{n + 1} \left(\frac{n}{n + 1} \right)^n \lambda^{2n}_o \quad \ldots\ldots (51)$$

and the Kreüger formula (Eq. 21*a*)—

$$\sigma = \frac{1 - \lambda^2_o C^2}{1 + (1 - 2 C) \lambda^2_o} \quad \ldots\ldots (52)$$

Experiments show that, when the shape of the cross section of a column is modified for a constant value of the slenderness ratio, the ultimate load is also changed. The constants which appear in the formulas are thus shown to be related to the shape of the cross section, as well as to the material—a fact that is easily explained when the influence of an initial curvature or eccentricity is considered.

Regrettably, the dimensions of the constants in Eqs. 3 to 21 are not the same throughout all the formulas. In the following tabulation, dimensionless constants are denoted by zero, and S represents a constant of the dimension of a stress:

Constant	B	C
The Rankine formula, Eq. 3	0	....
The secant formula, Eq. 7	$1/S$	0
The Aarflot formula, Eq. 9	0	0
The Ylinen formula, Eq. 11	$(1/S)^n$	....
The author's formula, Eq. 13	0	0
The author's formula, Eq. 15	$(1/S)^{n-1}$	....
The author's formula, Eq. 18	$(1/S)^{n-1}$	....
The hyperbolic formula, Eq. 20	S	....
The Kreüger formula, Eq. 21	$1/S$	$1/S$

In the "Summary," the author indicates that "The column formulas in Sections II to V, inclusive, apply for all values of the ratio of slenderness * * *." For very small slenderness ratios, Eqs. 15 and 18 are exceptions to this statement. When these formulas are used, a "cutoff" must be made for the strength corresponding to very short columns, which violates the author's principle that column formulas must be valid for all slenderness ratios. Incidentally, it would be interesting to know how two column equations have been derived from the same basic assumptions; that is (see paragraph containing Eqs. 18), "* * * derived by the double-modulus theory from a stress-strain curve of the form of Eq. 17."

Both the secant formula, when $C > 0$, and Eq. 13 give values less than those of the Rankine formula. This indicates that these formulas have only a limited usefulness, since, as noted by the author in the "Introduction," "* * * the [Rankine] formula gives lower values of the average stress than the mean of the average stresses found in tests of most materials." This fact disqualifies all column curves below the Rankine curve.

Both the secant formula and the Ylinen formula are extremely difficult to apply since the stresses are not given explicitly in terms of the slenderness ratio. Consequently, since the formulas cannot be used directly, tables must be compiled for the computation, which makes these formulas impractical.

From the foregoing, it can be stated that only the Rankine, Aarflot, parabolic (including the Johnson parabolas and the straight line), and Kreüger formulas are of practical value in the design of columns. The remaining formulas cannot be recommended, because they do not fit experimental results, and because they do not define the strength as an explicit function of the slenderness ratio.

AMERICAN SOCIETY OF CIVIL ENGINEERS

Founded November 5, 1852

DISCUSSIONS

COMPUTING COAGULANT REQUIREMENTS IN SLUDGE CONDITIONING

Discussion

BY PAUL D. MCNAMEE

PAUL D. MCNAMEE,[17] ESQ.[17a]—The question, "How much coagulant is necessary to condition a sewage sludge for filtration?" would rate $64 on any quiz program. As a rule, fresh solids require less coagulant than do digested solids, whereas activated sludges require the highest dose. Without running actual filter tests, it is hazardous even to venture a guess as to the actual amount of coagulant required by a particular sludge. The common procedure is to add varying amounts of coagulant and then to compare filter yields or filtration times. Mr. Genter has presented a simple method for calculating coagulant requirements which should prove helpful to all persons engaged in the filtration of sludge. Eq. 6 appears to hold for all types of sludge; but, as Mr. Genter has stated, it may have to be modified somewhat when more results are available for comparison. To date, Eq. 6 has had limited application and it will be necessary to apply it to many other sludges before its true worth can be evaluated.

An equation of this type establishes the optimum dose required and gives the operator a definite value at which to aim. In actual practice it is often difficult to attain theoretical values; but, as Mr. Genter has stated, the use of such an equation does show when something is wrong. Mr. Genter's basic data showed that the Washington, D. C., plant used more coagulant than is indicated by Eq. 6. Laboratory tests at the plant verify this conclusion. At the Washington, D. C., plant, there has been some difficulty in maintaining a constant flow of elutriated solids to the sludge meter, which in turn controls the ferric chloride doser. In other words, the ferric chloride is discharged every time the sludge meter makes a certain number of revolutions, and the sludge meter will revolve with a full or a partial load. If the operator regulates the discharge for a partial load and then receives a full load, the sludge will be

NOTE.—This paper by A. L. Genter was published in March, 1945, *Proceedings*.

[17] Chief Chemist, District of Columbia Sewage Treatment Plant, Blue Plains, Washington, D. C.

[17a] Received by the Secretary March 29, 1945.

underconditioned, which causes the filters to become clogged with slime. This necessitates shutting down the filter and washing the cloth. To keep the filters running, it is necessary for the operator to set the dose for a full load, with the result that the sludge is overconditioned when a partial load is received. The trouble is caused by small pieces of wood and trash that find their way to the plant. The plant itself has no screens; the sewage is screened at the main sewage pumping station. The bottleneck in the plant for this material occurs at the sludge pumps that handle digested and elutriated sludge. A single stick will become lodged in a pump and a mat of fine material is built up which eventually clogs the pump. An extremely small amount of trash can cause considerable trouble. For example, if just one sizable stick escapes in every 4,000,000 gal of sewage treated, sufficient interference has been created to require thirty pump cleanings per day. Various steps have been taken to remedy this condition, such as increasing the size of the pumps and lines, but the condition, although relieved, still exists. A different type of coagulant doser would eliminate the overdosing, but additional screening facilities are needed for final solution of the problem.

With the present setup, it is necessary to overcondition the sludge by a definite percentage even if straight digested sludge is being filtered. Thus, the saving in coagulant by elutriation under present conditions is higher than the theoretical saving since the same percentage increase is three times more for the digested, than for the elutriated, sludge in terms of ferric chloride.

Eq. 6 is divided into two parts: One part determines the ferric chloride required to satisfy the alkalinity of the solution, and the other part determines the amount of coagulant actually needed to coagulate the sludge. The first part is based on well-known and established facts. Although there are many theories in chemistry, there are but a few fundamental laws. The first part of Eq. 6 is based on the law of combining weights, which is well established. If any fault is found with Eq. 6, it will probably involve the second part where Mr. Genter was limited to eight sewage sludges for the derivation. The ferric chloride requirements are shown to be a function of the ratio of volatile matter to mineral matter in the sludge. This condition is somewhat difficult to explain since the determination of volatile matter complicates the picture. The volatile matter is generally taken as a measure of organic matter, although this assumption is only approximately true. Considerable inorganic material is changed by ignition into other forms—with corresponding changes in respective weights. Compounds such as sulfates break down with the loss of sulfur dioxide; carbonates lose carbon dioxide; and other compounds may sublime. The true organic content of a sample, therefore, would probably be lower than the volatile content. This fact does not invalidate Eq. 6, but it does make the use of Eq. 6 more difficult since the operator does not know just how much true organic matter is measured or to what extent the volatile loss may have included inorganic substances capable of reacting with coagulant. The fact that Mr. Genter's ratio of volatile matter to mineral matter does show such remarkable agreement with coagulant requirements must mean that the mineral-matter conversion factor measured by the volatile test is fairly constant for the different sewage sludges.

Breaking down the coagulant requirements of a sludge into two components as Mr. Genter has done affords a clear-cut picture of the value of elutriation. Not only can it be seen at a glance which sludges lend themselves to elutriation but also it is possible to calculate the exact savings of coagulant that can be realized. Eq. 6 should prove helpful to any person estimating the value of elutriation.

In the case of partial dosing to produce partial coagulation, the writer believes that it is a question either of the mixing or of the contact of the ferric chloride itself with the sludge, rather than a question of the precipitation of ferric hydroxide by partial alkalinity neutralization. In running batch samples, the stirring is usually fairly constant. When a strong solution of ferric chloride is added to a sample, there will be a zone where all the alkalinity is satisfied and the local sludge particles are in contact with more ferric chloride than is necessary to condition them. The resulting sample contains conditioned and unconditioned sludge. In the case of sludges with high alkalinity, more ferric chloride is precipitated before it can come in contact with a sludge particle and the percentage of sludge conditioned is not directly proportional to the percentage increase in dosing.

Mr. Genter's paper certainly supplies "food for thought." It is probably the first attempt to correlate the coagulant requirements of all types of sewage sludges with certain sludge characteristics. It was known that, with well-digested sludges, where the volatiles are low and more or less constant, the coagulant requirements vary almost directly with the alkalinity; but this relationship did not hold when other types of sludge were considered. By introducing the ratio of volatile matter to mineral matter, Mr. Genter has correlated the other sludges. A study of Eq. 6 will prove worth while. For instance, if the operator is interested in discovering how the thickness of the sludge will change coagulant requirements, it is only necessary for him to select a given alkalinity value and plot the X-values for different sludge concentrations. About ten times as much coagulant is required for a 1% sludge as for a 10% sludge to satisfy the first or X-part of the equation. If for no other reason than curiosity, all operators who filter sludge should try to apply Eq. 6 to the particular sludge with which they are dealing.

AMERICAN SOCIETY OF CIVIL ENGINEERS

Founded November 5, 1852

DISCUSSIONS

ORGANIZATION, FINANCING, AND ADMINISTRATION OF SANITARY DISTRICTS

PROGRESS REPORT OF THE COMMITTEE OF THE SANITARY ENGINEERING DIVISION

Discussion

BY I. VERNON WERBIN

I. VERNON WERBIN,[3] ASSOC. M. AM. SOC. C. E.[3a]—The United States Supreme Court in the case of Brush vs. Commissioner of Internal Revenue (300 U. S. 352) makes the following comment concerning the confusion that exists in the court decisions of the various states as to whether certain functions are governmental or proprietary (see page 362):

> "There is probably no topic of the law in respect of which the decisions of the state courts are in greater conflict and confusion than that which deals with the differentiation between the governmental and corporate powers of municipal corporations. This condition of conflict and confusion is confined in the main to decisions relating to liability in tort for the negligence of officers and agents of the municipality. In that field no definite rule can be exacted from the decisions."

This case is an income tax matter. Under the tax law as it then existed the salaries of officers of municipalities engaged in a government function were exempt from tax and the question before the Court was whether the engineer of the New York Water Supply system was engaged in a governmental function. The Court in its opinion stated (pages 370–371):

> "We conclude that the acquisition and distribution of a supply of water for the needs of a modern city involve the exercise of essential governmental functions, and this conclusion is fortified by a consideration of the public uses to which the water is put. Without such a supply, public schools, public sewers so necessary to preserve health, fire departments, street sprinkling and cleaning, public buildings, parks, playgrounds and

NOTE.—This report was published in February, 1945, *Proceedings*. Discussion on this paper has appeared in *Proceedings*, as follows: May, 1945, by C. Maxwell Stanley.

[3] Attorney and Eng. Expert, New York, N. Y.

[3a] Received by the Secretary May 9, 1945.

public baths could not exist. And this is equivalent, in a real sense, to saying that the city itself would disappear."

It can be said with equal truth that modern cities would disappear in the absence of a proper sewerage system. The Court further stated (see page 372) that the fact that the government makes a charge for the service does not make it a proprietary one.

"What the city is engaged in doing in that respect is rather rendering a service than selling a commodity."

The same may be said of a sanitary system.

The committee's report states (see Section 15, Item (*a*)): "Under the proprietary powers, the district would be financed by users and not by property."

From the fact that a sanitary system may be considered a proprietary function, it does not necessarily follow that the system must be financed exclusively by users. The construction and operation of the subway system in New York, N. Y., has been held to be of a proprietary character. Nevertheless, its huge deficits are financed from the general tax fund.

The comments of the New York Court of Appeals, in its decision wherein it was determined that the construction and operation of the subway system was of a proprietary character, indicate the basis of this determination. The opinion (matter of Rapid Transit Railroad Commissioners, 197 N. Y. 81) states:

"1. Was the action of the city in building the subway, governmental or proprietary in character?

"The city owns the subway, and it is a railroad corporation as far as the construction, operation and leasing thereof is concerned. It was not required but simply permitted, to build and operate the road. It is authorized to lease its railroad, either for 'a specified sum of money or a specified proportion of income, earnings or profits,' or it may operate the road itself and charge such rates of fare for transportation of persons and property as may be fixed by its own boards and officers. In other words, the subway is a business enterprise of the city, through which money may be made or lost, the same as if it were owned by an ordinary railroad corporation. It was built by and belongs to the city as a proprietor, not as a sovereign."

The construction and operation of the subway system was deemed to be proprietary because the project was a business enterprise. Of course, railroad business is usually conducted by private corporations, and it is truly a business enterprise. The same can hardly be said of a sanitary system. Few individuals or corporations, if any, would undertake to supply sanitary facilities as a business enterprise. The prospect of making any money would be practically nil. The object of such a system is primarily to protect the public health, and when a branch of the government undertakes to perform this function, it would seem to be purely a governmental one. The United States Supreme Court decision in the Brush case, involving a water supply system, is equally applicable to the construction and maintenance of a sanitary system—that the government is "rather rendering a service than selling a commodity."

AMERICAN SOCIETY OF CIVIL ENGINEERS

Founded November 5, 1852

DISCUSSIONS

A PLAN FOR A MOVABLE DAM

Discussion

BY JAY L. SOUTHWORTH

JAY L. SOUTHWORTH,[6] ASSOC. M. AM. SOC. C. E.[6a]—The dam described in this paper is worthy of consideration both as a movable and an emergency dam. As an emergency dam, it would afford a fast remedy in case of accident to the miter gates. As a movable dam, it would greatly reduce the cost of maintenance of the gates and lock chamber. It is particularly adapted to a lock which has a shallow breast wall as illustrated. This construction should prevent silt from depositing to a harmful depth on the structure in its supine position. For a lock with a breast wall of sufficient height, it would be more economical to use the Lockport (Ill.) type of emergency dam[7] which is similarly placed between the two upper breast walls.

The dam should be designed to withstand the warping stresses resulting from the dynamic effect of the swirl of water under high velocity. In actual experience, this swirl of water has been caused by one upper operating gate leaf hanging by its anchorage in a diagonal obstructive position after the other gate leaves have been swept clear away.

The writer is not convinced of the necessity for an emergency dam in any lock. Since 1925, the hydraulic system for emptying and filling lock chambers has been so improved that the surge—the principal cause of lock gate damage in the past—has been sufficiently reduced so that the danger is practically removed. In thirty years of operation, the emergency gates of the Panama Canal have not been used as such. There has been no occasion to test them. Since the lock gates in the old Welland Canal between Lake Erie and Lake Ontario in Canada were damaged at the rate of two or three accidents per year for a long period, metal horns were provided at great expense at the miter ends of the new Welland Canal lock gates to prevent damage by absorbing the shock

NOTE.—This paper by Isaac DeYoung was published in February, 1945, *Proceedings*. Discussion on this paper has appeared in *Proceedings*, as follows: May, 1945, by C. L. Hall, C. E. Meyerdick, and Ralph R. Leffler.

[6] Civ. Engr., Federal Power Comm., Washington, D. C.

[6a] Received by the Secretary May 9, 1945.

[7] "Engineering Features of the Illinois Waterway," by Walter M. Smith, *Transactions*, Am. Soc. C. E., Vol. 98 (1933), Fig. 11, p. 328.

of a blow from a moving vessel. Today operators have been trained to use extreme care in moving vessels through a lock.

Inasmuch as the structure described can be used at great saving in ordinary gate and lock chamber maintenance, necessity seems to have been the "prime mover" in this unique conception. This type of dam would supplant the elaborate and unwieldy emergency structures that have been in vogue at Sault Sainte Marie, Mich., and other places in the past.

AMERICAN SOCIETY OF CIVIL ENGINEERS

Founded November 5, 1852

DISCUSSIONS

ANALYSIS OF STATICALLY INDETERMINATE STRUCTURES USING REDUCED EQUATIONS

Discussion

BY JAROSLAV POLIVKA

JAROSLAV POLIVKA,[11] M. AM. SOC. C. E.[11a]—The results of analyses of a two-hinged arch of parabolic, circular, and elliptical shape, with a variable moment of inertia, I, are presented in this excellent paper. Tables and graphs are included showing clearly the effect of the variation of I, and the effect of the shape upon the horizontal reaction H. With this evidence, Dean Johnson arrives at the conclusion that H can be found with sufficient accuracy from three types of average influence lines, referring to three general types of two-hinged arches. The author discusses the correlation of error resulting from average values and the "correspondence of ordinates"; and he expresses this error in a novel manner by means of "difference terms."

Furthermore, the author defines the limitations of the method of using typical average values or reference curves. He states that such reference curves will not apply to rigid-framed bents and other similar structures, solved as two-hinged arches, because of the lack of "correspondence of ordinates." Finally, he concludes that such average reference curves will not necessarily give close approximations to redundant reactions for structures in which small deformations produce large changes in reactions—as, for example, those produced by the moments at the abutments of a restrained arch.

The author derives the "reduced equation" (Eq. 10) from the "classic equation" (Eq. 9) by eliminating the variable term $E\,I$. This is possible [12,13] by making $E\,I$ proportional to $\frac{1}{\cos\phi} = \sqrt{1 + \left(\frac{dy}{dx}\right)^2}$, in which $\frac{dy}{dx} = \tan\phi$. Eqs. 16 used to determine the influence line for H in the case of a parabolic

NOTE.—This paper by Lee H. Johnson, Jr., was published in November, 1944, *Proceedings*. Discussion on this paper has appeared in *Proceedings*, as follows: February, 1945, by Josef Sorkin; and May, 1945, by I. Oesterblom, and Leon Beskin.

[11] Lecturer, Univ. of California Eng. Dept., Cons. Engr., Berkeley, Calif.

[11a] Received by the Secretary April 6, 1945.

[12] "Der elastische Bogen berechnet mit Hilfe der graphischen Statik," by W. Ritter, Albert Raustein, Zurich, Switzerland, 1886.

[13] "Anwendungen der graphischen Statik," by W. Ritter and C. Culmann, Albert Raustein, Zurich, Switzerland, 1906, Vol. 4, pp. 124 and 245.

arch has been derived by W. Ritter as follows:

$$H = \frac{x\,(L - x)\,(L^2 + L\,x - x^2)}{2\,L^3\,m} \ldots\ldots\ldots\ldots\ldots\ldots (46)$$

in which

$$m = \frac{4}{5}\,h\left(+\frac{3\,I}{2\,A\,h}\right) \ldots\ldots\ldots\ldots\ldots\ldots (47)$$

The second term in Eq. 47 is an expression of rib shortening; and, for $x = \frac{L}{2}$ (or for $j = 1$ in the paper), Eq. 46 yields:

$$H_{\max} = \frac{25\,L}{128\,h} \ldots\ldots\ldots\ldots\ldots\ldots (48)$$

The effect of a variation in the thickness of the ribs is obtained by expressing the variation in simple terms which allow easy integration—a procedure which has been proposed by several writers.[14,15] The new version of the reduced equation should be a great help in the design of two-hinged arches with variable moments of inertia because the conventional methods involve a great many cumbersome computations.

[14] "Beitraege zur Theorie der vollwandigen Bogentraeger ohne Scheitelgelenk," by Max Ritter, W. Ernst & Son, Berlin, Germany, 1909.

[15] "Neuere Methoden zur Statik der Rahmentragwerke und der elastische Bogentraeger," by A. Strassner, Vol. 2, W. Ernst & Son, Berlin, Germany, 1921.

AMERICAN SOCIETY OF CIVIL ENGINEERS

Founded November 5, 1852

DISCUSSIONS

HYDRAULIC MODEL INVESTIGATION OF MITER GATE OPERATION

Discussion

BY MAURICE N. AMSTER

MAURICE N. AMSTER,[7] ASSOC. M. AM. SOC. C. E.[7a]—Quite appropriately, Mr. Soucek emphasizes the necessity for giving full consideration to the limitations involved in applying the test results to the design of other gate operating machines. More than one of the discussers overlooked the limiting nature of the writer's statement (see heading, "Application of Test Results to Other Miter Gates") that the test data "probably" could be applied to other miter gates having "the same kinematic cycle."

A specific limitation mentioned by Mr. Soucek is the fact that no tests were made of the effect of speed variation at low submergences. In the case of a miter gate of the same length, operated on the same kinematic cycle but with a submergence lower than that of the "base conditions," the only strictly applicable test results would be found in Fig. 6(*b*), and these would apply only for an operating time of 2 min. The effect of geometric disproportionality is small, however, and the speed-torque relations shown in Fig. 6(*a*) can be applied with reasonable reliability provided that the ratio of length of gate leaf to submergence is not too far from unity.

The test results presented by Mr. DeYoung in Fig. 11 are interesting and provide a basis for estimating loads on other gates operated with similar kinematic cycles. The angular position at which peak load occurs is close to that at which peak load was observed in the model tests of single-leaf operation. However, the kinematic cycle of the cable-and-drum mechanism described by Mr. DeYoung is so unlike that of the crank-and-strut mechanism used in the Panama Canal locks that the significance of the agreement between results in the two cases is doubtful. The diagram presented by Mr. DeYoung in Fig. 12 is quite convenient for some purposes.

NOTE.—This paper by Maurice N. Amster was published in March, 1944, *Proceedings*. Discussion on this paper has appeared in *Proceedings*, as follows: June, 1944, by Edward Soucek; September, 1944, by Isaac DeYoung, and F. W. Edwards; and March, 1945, by William A. Tripp.

[7] Engr., Air Products, Inc., Chattanooga, Tenn.

[7a] Received by the Secretary May 12, 1945.

Professor Edwards presents interesting extrapolations of the test results. The range of operating times tested with the model, like other phases of the model tests, was confined to the contemplated range of prototype values. It is regrettable that the model-test schedule could not be extended to cover more generalized studies.

As Professor Edwards states, the model study did not include any variation of the kinematic cycle except speed. The writer's conclusion that low speeds are best at the extremes of travel was based on the fact that peak loads occur near those positions. It is quite evident that a uniform speed throughout the leaf movement, for example, would produce even greater peak loads. The ideal load would be a uniform one, and this would be approached, not by increasing the relative speed near the recessed position, where a slight peak already exists, but by decreasing the relative speed near the mitered position. The degree to which this can be achieved in practice is limited by mechanical and structural design features and by space limitations. Dead-center recessed and mitered positions are desirable because they prevent gate-leaf overtravel in case of limit-switch failure.

Mr. Tripp contends that the model-test results are substantially in error because of improper consideration of the chamber lengths and the influence of the lock culverts. Mr. Tripp's statements regarding the effect of gate movement show clearly that he has applied steady-flow formulas to transient phenomena, which fact alone invalidates his views. Mr. Soucek describes accurately the nature of the gate loads when he states that they "are principally due to water-level variations which are transient in character and local in extent—surges induced by the gate movement—and therefore not related in any simple manner to the adjacent water-surface areas." However, since Mr. Tripp obtains results differing so greatly from those reported, and in consideration of the danger that his method of computation might be adopted by others, a detailed examination of the differences and the reasons therefor appears advisable. Accordingly, it will be shown that:

1. The gate loading cannot be computed on the basis of surface areas;
2. The effect of the 200-ft downstream chamber length is relatively small;
3. The culverts have negligible effect upon the critical gate load;
4. The loads for the "base conditions," although somewhat severer than the normal operating loads, may occur frequently in the prototype locks; and
5. The "base conditions," as applied, are logical criteria for design of the prototype operating machines.

Fig. 13 shows the effect of variation in the upstream chamber length between the limits of 300 ft and 1,105 ft for both the opening operation and the closing operation. The peak torque reached in the opening operation is critical for design. In these tests, the downstream chamber length was held constant at 200 ft, but it is theoretically evident, and was shown by similar tests, that the effect of length changes is about the same for an upstream chamber as for a downstream chamber. These tests show clearly that changes in the chamber

length had no significant effect for lengths exceeding 625 ft and therefore that the gate loading cannot be computed on the basis of surface area. The theoretical basis for this result is quite simple. The wave velocity is expressed by

$$c = \sqrt{g\,y} \qquad (8)$$

in which c is the wave velocity; g is the gravitational acceleration; and y is the depth. Thus, $c = \sqrt{32.2 \times 82.5}$, or about 50 ft per sec. The peak opening

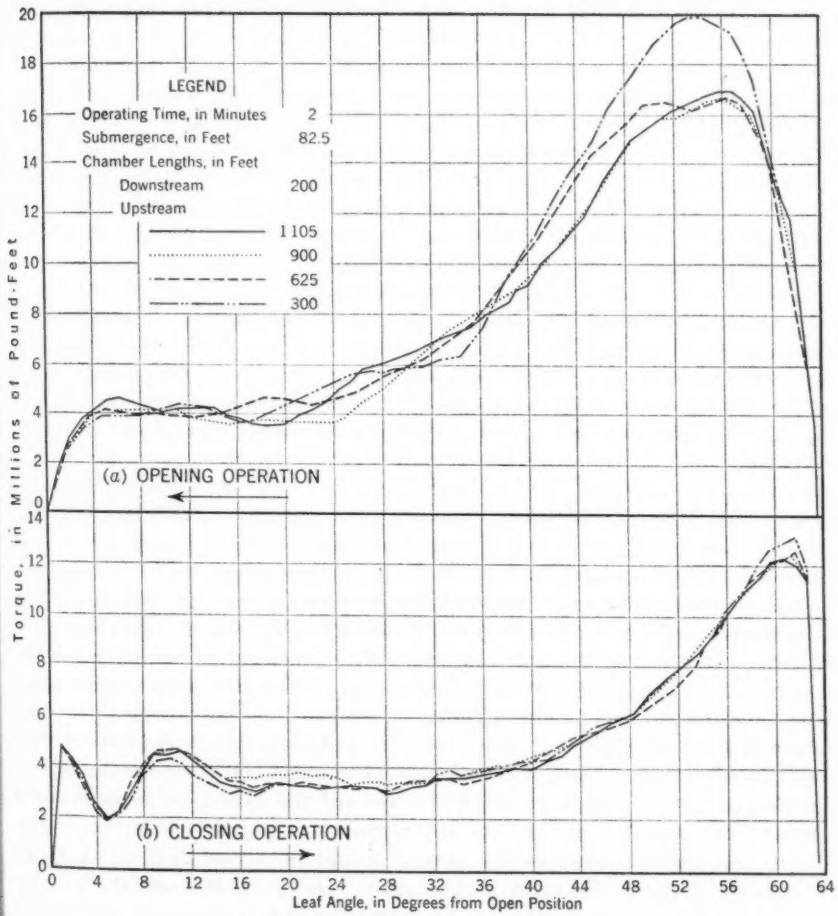

FIG. 13.—VARIATION OF CHAMBER LENGTH

torque occurs about 20 sec after operation begins; therefore, in order for the peak torque to be affected by the waves generated at the instant operation begins, these waves must encounter a reflecting surface no farther than about 500 ft from the gate. Since the torque remains at or near its peak value for a few seconds, it was stated conservatively (and it was shown by the tests) that lengths exceeding 625 ft have no effect upon the peak torque.

The fallacy in computing the operating loads on the basis of surface area, as suggested by Mr. Tripp when he mentions "* * * a definite volumetric change, which must be distributed over the free surface of the lock chambers * * *," is evident when it is considered that consistent application of that theory would indicate zero loads in the operation of a gate separating two areas of infinite extent.

As shown in Fig. 13, a reduction in upstream chamber length from 625 ft (the approximate limit of significant length effect) to 300 ft increased the peak opening torque from about 17,000,000 lb-ft to about 20,000,000 lb-ft; an increase of less than 10% in torque corresponds to a decrease of 52% in upstream chamber length within the effective range. Any reasonable method of extrapolating these results—even Mr. Tripp's computation procedure—would show that a decrease of 68% in chamber length would not increase the torque to the extent indicated by Mr. Tripp in his discussion. Even when one of the two chambers is only 200 ft long, it requires about 8 sec for a wave to travel the length of the short chamber and back. Thus, the reflected wave that is effective at the instant of peak torque originates from a slow gate movement occurring early in the cycle and produces a correspondingly small effect.

In making a substantial allowance for the effect of culvert discharge upon the gate operating load, Mr. Tripp again ignores a transient phenomenon that makes the effect of the culverts negligible. Tests of an intermediate gate at one of the existing locks showed that the duty cycle was absolutely unaffected by the position of the culvert valves (that is, whether they were closed or open). Since this result differs so greatly from Mr. Tripp's belief, some explanation of the reason is necessary. If a gate were operated under the base conditions—that is, with a 1,105-ft length of chamber upstream and a 200-ft length downstream—the throttling effect of the small port-and-lateral capacity in the short chamber would so restrict the culvert flow that little effect would be expected. Therefore, a condition more favorable to free flow through the culverts will be considered—opening of a single gate with chamber lengths of more than 1,000 ft both upstream and downstream and with culvert valves open. Since the gate leaves are accelerated continuously during the interval prior to occurrence of peak torque—a time of about 20 sec—the conditions will not be affected by reflections from the chamber ends and there will be an approximately uniform slope upward toward the gate from a point about 1,000 ft upstream and an approximately uniform slope downward toward the gate from a point about 1,000 ft downstream. At the instant of peak torque, the culvert discharge due to the average head on the system would be about 25% of that due to consideration of the head at the gate. However, the actual discharge is much smaller. It is impossible to determine the "equivalent unthrottled length" of the manifold system without considering the theory of hydraulic manifolds, but since only an approximate answer is sought, it will be assumed that the manifold system of the two 1,000-ft chambers has an "equivalent unthrottled length" of only 1,000 ft rather than the total culvert length of 2,000 ft. It is evident that the length cannot be assumed much shorter, because a shorter length would include so few ports and laterals that these rather than the culvert area would govern the rate of flow. With an "equiva-

lent unthrottled length" of 1,000 ft, even if head losses that oppose the flow are ignored, the acceleration of the culvert flow would be approximately 0.016 ft per sec per sec at the instant of peak torque. The approximate mean acceleration from the start of gate operation to the instant of peak torque would be 0.008 ft per sec per sec, and the velocity of flow would be approximately 0.16 ft per sec. It appears that the velocity computed on the basis of steady flow corresponding to the head at the gate, disregarding friction losses, would be about 8.0 ft per sec—fifty times as great as the effect obtained by consideration of transient conditions. Of course, one simplifying assumption after another has been used in the preceding evaluation of the effect of the culverts for the transient conditions; however, any reasonable adjustment of these assumptions may be made without effect upon the principal conclusion—that the observed lack of appreciable effect of culvert discharge is consistent with theoretical considerations. A short loop culvert or an opening in the gate, of course, would have a pronounced effect.

It was not intended to convey the impression that the results for "base conditions" represent the average operating load. It is true that when two consecutive gates 200 ft apart are swung simultaneously the load is distributed to two sets of gate machines and is not critical. However, such operation will not be as general as would be inferred from Mr. Tripp's comments; it will occur only where it is desired to maintain two barriers against the upper pool. In other locations, it is contemplated that a single gate will be operated, with chamber lengths of more than 1,000 ft both upstream and downstream. Whether culverts are open or closed, the peak opening torque will be some 2,000,000 or 3,000,000 lb-ft less than the value obtained with the "base conditions" used in the model tests when no extraneous factors enter the problem. However, one normal condition, the presence of a large ship in either of the chambers between which the gate is located, will create a peak torque closely approximating that of the "base conditions." Occurrence of unexpected surges is another factor that makes it necessary that the design load exceed the usual operating load by a reasonable amount. Since the main purpose of the paper was to illustrate the application of model test data in design, it was not considered necessary to explain in detail all factors affecting selection of the base conditions, any more than it is felt necessary to defend the selection of a conservative unit stress in the design of an important structure subject to variable and uncertain loads. However, Mr. Tripp's claim that the base conditions were unduly conservative makes it clear that some of the additional factors considered in establishing the base conditions should have been explained for the benefit of those who are not familiar with the actual operating conditions.

The peak-torque values found in the model tests for "base conditions" were used as criteria for the design of the mechanical components of the gate operating machines because, as stated in the preceding paragraph, it is entirely possible and very likely that these values will occur in normal operation of the lock gates. However, the power of the driving motors was not controlled by the peak-torque requirements. During the part of the gate movement at which the peak torque occurs, the motors are loaded to approximately 180%

of their full-load torque rating. It was also intended that, in the event of motor failure, one of the two motors for the machine of each gate leaf be capable of operating the gate leaf under otherwise favorable conditions, although the single motor would be considerably overloaded.

In conclusion, it is interesting to observe that transient conditions closely analogous to those affecting the peak opening torque exist in the field of electrical engineering. This is true not only of the wave conditions in the lock chambers but also of the inertial effects that make the discharge through the culverts insignificant.

The writer wishes to thank Messrs. Soucek and G. D. Smith for their assistance in the preparation of the text of this closure. The interest taken by all discussers is also appreciated.

AMERICAN SOCIETY OF CIVIL ENGINEERS

Founded November 5, 1852

DISCUSSIONS

LOCK MANIFOLD EXPERIMENTS

Discussion

BY RALPH W. POWELL, AND EDWARD SOUCEK AND E. W. ZELNICK

RALPH W. POWELL,[22] M. AM. SOC. C. E.[22a]—As the authors state, the theoretical treatment of the pressures in manifolds has been very unsatisfactory. As one who, in the past, perhaps has helped to produce this situation, the writer feels moved to make another attempt to clarify the underlying hydraulics of the problem. Discussion will be limited to the case of a single port.

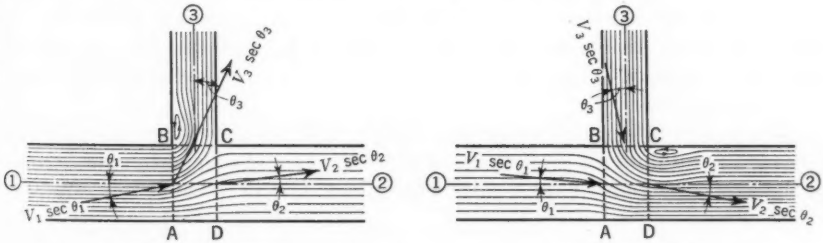

FIG. 22.—DIAGRAMS OF IDEALIZED FLOW

Fig. 22(*a*) is a diagram of a single manifold port with liquid entering through pipe 1, and leaving through pipe 2 and branch 3. The total pressure on section CD must exceed the total pressure on section AB by the loss of momentum per second, in the axial direction, of the liquid in the space ABCD. Since the liquid flowing into branch 3 will not cross section BC at right angles, it will carry away some of the momentum. The neglect of this condition vitiated the writer's former treatment.[23] Taking this fact into account,

$$\gamma A_c (Z_2 - Z_1) = \frac{\beta_1 Q_1 \gamma V_1}{g} - \frac{\beta_2 Q_2 \gamma V_2}{g} - \frac{\beta_3 Q_3 \gamma V_3 \tan \theta_3}{g} \quad \ldots (21)$$

NOTE.—This paper by Edward Soucek and E. W. Zelnick was published in October, 1944, *Proceedings*. Discussion on this paper has appeared in *Proceedings*, as follows: March, 1945, by J. Pietrkowski; April, 1945, by John S. McNown, F. W. Edwards, and W. M. Lansford; and May, 1946, by Robert F. Kreiss, and Ralph G. Berk.

[22] Associate Prof. of Mechanics, Ohio State Univ., Columbus, Ohio.

[22a] Received by the Secretary April 27, 1945.

[23] Discussion by R. W. Powell of "Hydraulics of Sprinkling Systems for Irrigation," by J. E. Christiansen, *Transactions*, Am. Soc. C. E., Vol. 107 (1942), pp. 245–247.

in which θ_3 is the mean angle that the liquid crossing section BC makes with the axis of pipe 3, and β_1, β_2, and β_3 are the momentum factors in the respective pipes for correcting for the nonuniform velocity distribution. The other symbols are defined in the paper.

Eq. 21 reduces to

$$\frac{\Delta Z}{(V_1)^2/2\,g} = 2\left[\beta_1 - \beta_2\,(1 - P_d)^2 - (P_d)^2\,\frac{\beta_3\,A_c}{A_p}\tan\theta_3\right] \ldots\ldots (22)$$

Assuming that β_1 and β_2 are both unity, letting $\beta_3\,\frac{A_c}{A_p}\tan\theta_3 = \psi$ and equating to the value given by Eq. 2:

$$\psi = \frac{\beta_3\,A_c}{A_p}\tan\theta_3 = \frac{1 - k_d}{P_d} \ldots\ldots (23)$$

When P_d is small, the foregoing assumptions are probably nearly correct; but, for larger values of P_d, the factor β_2 will be much larger than unity.

Using Eq. 23 and the data given or cited in the paper, the writer attempted to find the value of θ_3. About his only conclusion was that θ_3 approached 90° as P_d approached zero and that it also depended very much on the value of A_c/A_p. In fact, for any given value of P_d, when the side branch was made smaller with respect to the main pipe, θ_3 was increased enough that ψ remained more nearly the same for different values of A_c/A_p than did $\beta_3 \tan\theta_3$. In any given case, assuming a reasonable value of β_3, such as 1.05, an entirely reasonable value of θ_3 could be computed, but no law for forecasting the value could be deduced.

The case of inflow is shown in Fig. 22(*b*). The total pressure on section AB exceeds the total pressure on section CD by the gain in momentum per second, in the axial direction, of the liquid in the space ABCD. Thus:

$$\gamma\,A_c\,(Z_1 - Z_2) = \frac{\beta_2\,Q_2\,\gamma\,V_2}{g} - \frac{\beta_1\,Q_1\,\gamma\,V_1}{g} - \frac{\beta_3\,Q_3\,\gamma\,V_3\tan\theta_3}{g} \ldots (24)$$

which, assuming that β_1 is unity, reduces to

$$\frac{\Delta Z}{(V_2)^2/2\,g} = 2\left[\beta_2 - (1 - P_i)^2 - \beta_3\,(P_i)^2\,\frac{A_c}{A_p}\tan\theta_3\right] \ldots\ldots (25)$$

or letting $\frac{\Delta Z}{(V_2)^2/2\,g} = J$:

$$\frac{J}{2} = \beta_2 - (1 - P_i)^2 - (P_i)^2\,\psi \ldots\ldots (26)$$

In Eqs. 24, 25, and 26, β_2, β_3, and θ_3 are all unknown, and there seems little chance of determining them short of laborious experiments. By plotting J against P_i as in Fig. 7(*d*) and extending the curve back to $P_i = 0$, the value of β_2 can be estimated for small values of P_i. For Port VII the value of β_2 seems to be 1.12 and for the other ports it varies from 1.03 to 1.18. The data of Itaru Naramoto and Taijiro Kasai[24] gives, as nearly as can be estimated:

[24] "On the Loss of Energy at Impact of Two Confined Streams of Water," by Itaru Naramoto and Taijiro Kasai, *Memoirs of the College of Engineering*, Kyushu Imperial Univ., Fukuoka, Japan, Vol. VI, 1931–1932, p. 189.

$\beta_2 = 1.06$. The foregoing are for low values of P_i; when P_i becomes large, Ports I, II, III, VI, and VII show that the value of β_2 must increase, because otherwise the values of tan θ_3 become negative.

Table 5 gives a possible set of values for Port I. The values of P_i and J are scaled from the plotted values given in the authors' original paper. Only sixteen of the thirty points have been included, but they are distributed throughout the range of the experiment. Values of β_2 have been assigned arbitrarily, but in such a way as to give a smooth curve when plotted against P_i. The value of β_3 was taken as 1.00, and $A_c/A_p = 36/12.25 = 2.94$. The resulting values of θ_3 seem to be reasonable. Unfortunately, the writer has not been able to devise any equation that will forecast the values of β_2 and ψ or θ_3. For ports of the same proportions as those used by the authors, designs may be based on experimental results. For other proportions, new model tests will be needed.

TABLE 5.—COMPUTATIONS FOR INTAKE PORT I

P_i (1)	J (2)	β_2 (3)	ψ (4)	θ_3 (5)
0.047	0.21	1.040	12.3	76°.6
0.088	0.34	1.040	4.9	59°.0
0.140	0.50	1.040	2.55	40°.9
0.152	0.53	1.040	2.42	39°.5
0.190	0.64	1.040	1.77	31°.0
0.240	0.80	1.040	1.07	20°.0
0.266	0.89	1.040	0.79	15°.1
0.320	1.03	1.040	0.62	11°.9
0.388	1.17	1.041	0.54	10°.4
0.429	1.32	1.043	0.31	6°.0
0.489	1.44	1.050	0.29	5°.6
0.567	1.69	1.087	0.171	3°.3
0.627	1.94	1.130	0.053	1°.0
0.668	2.06	1.170	0.067	1°.3
0.739	2.26	1.245	0.086	1°.7
0.768	2.45	1.290	0.019	0°.4

EDWARD SOUCEK,[25] ASSOC. M. AM. SOC. C. E., AND E. W. ZELNICK,[26] JUN. AM. SOC. C. E.[26a]—As the principal conclusions of the paper appear to have been accepted by all who discussed it, this closure will be confined to a brief comment on each discussion and to clearing up a few minor points concerning which some difference of opinion appears to exist.

Mr. Pietrkowski enlarges upon the suggestion that the theoretical treatment adopted in the paper is related to the analysis of flow in side channel spillways. In his problem, the lateral discharge is out of the channel rather than into it. Although the basic principles are the same in the two cases, the direction of flow requires consideration as it appears that the conditions necessary for $k_d = 1$ cannot be obtained whereas $k_i = 1$ is quite possible. This point will be considered further in connection with Professor McNown's discussion. Mr. Pietrkowski's references concerning the conditions under which Bernoulli's theorem may be applied will be valuable to those who wish to explore the limitations of this important principle.

Professor McNown's study of the manifold problem is lucid and comprehensive; for research purposes, it may well supplant the brief theoretical study which appeared in the paper. For use in design, either treatment can be considered merely to support the observation that the characteristics of any port and culvert combination are expressible in terms of P_d and P_i. Professor McNown suggests clarification of the statement that "* * * Bernoulli's theorem is not applicable to the phenomenon under consideration, although a

[25] With Office, Chf. of Engrs., Washington, D. C.
[26] With The Panama Canal, Balboa Heights, Canal Zone.
[26a] Received by the Secretary May 15, 1945.

modified energy equation might be used." Bernoulli's theorem with a head-loss term is probably satisfactory for the analysis of discharge manifolds—tests of Boulder Dam penstocks were analyzed in this manner by the U. S. Bureau of Reclamation.[7] In intake manifolds or side channel spillways where flows from sources of differing energy content converge and mix in the culvert or channel as the case may be, Bernoulli's theorem would have to be modified by weighting the head from the two sources in proportion to the respective discharges, even if energy losses did not occur. In the side channel spillway, the energy of the flow received laterally is properly considered to be lost; with vanes to direct the inflow, a large part of the energy could be retained. Closely analogous conditions occur in an intake manifold. In connection with use of the energy principle for discharge manifolds, the Oakey-A curve indicates an energy gain in the direction of flow. The consistency of the A, B, C, and D curves makes experimental error an extremely unlikely explanation of the phenomenon. Professor McNown's other suggestion—that the lateral bleeds away enough low velocity water to increase the energy content of the remainder—seems more logical. However, there is another possibility—that in some manner mechanically similar to that in which water does work on a turbine blade, the lateral discharge actually yields a portion of its energy to the conduit flow. If future research should indicate that this is the correct explanation, it would be preferable to use the momentum principle for both intake and discharge manifolds.

Professor McNown stated that the mention of $k_d = 1$ has no practical significance. The remark in the paper was applied to insertion of values in Eq. 2 and Eq. 3, and consequently no practical significance was indicated. It is clear from the text that values of $k_d = 1$ were not anticipated. Moreover, the statement pertained equally to k_i and k_d; $k_i = 1$ is decidedly significant. It is well, however, that Professor McNown has clarified the matter. Mr. Pietrkowski has used $k_d = 1$ for analysis of a side spillway but, if the weir is constructed with side-walls so as to deflect the flow at right angles to the channel axis as assumed in the derivation, k_d will have a value less than unity. Conversely, if the weir is sharp-edged, the flow will not be diverted at right angles to the channel axis and a basic condition of the derivation—loss of momentum by the lateral flow—will not result. In either case, a rise in water levels substantially less than twice the difference in velocity heads may be anticipated.

It appears that Professor McNown may overestimate the significance of the correspondence of his c (= constant)-curves with the Enger-Levy curve. The theoretical bases for this curve involves flow through a longitudinal slit in a pipe. Although the substantial correctness of the curve is indicated by tests,[10] the agreement is not so close as to warrant adoption of the c (= constant)-curves at this time. The Oakey curves show a more rapid drop in the relative pressure rise for high values of P_d than do the most nearly comparable c (= constant)-curves. The Bureau of Reclamation curve corresponds quite

[7] "Model Studies of Penstocks and Outlet Works," *Bulletin 2*, Pt. VI, Boulder Canyon Project Final Repts., Bureau of Reclamation, U. S. Dept. of the Interior, 1938.

[10] "Pressures in Manifold Pipes," by M. L. Enger and M. I. Levy, *Proceedings*, A.W.W.A., May, 1929, p. 659.

closely to the curve for $k_d = 0.3$ over a rather wide range. Of course, it is not necessary to determine the mathematical nature of the pressure-change curves, as they may be determined experimentally. Discharge from a longitudinal slit in a pipe—the basis for the Enger-Levy curve—is a phenomenon closely related to flow from a discharge manifold, but there are significant differences. Some of these were revealed in 1931 in discussions of a paper by Jakob Kunz.[27] The jet discharged from a continuous longitudinal slit suffers no loss of momentum in the direction parallel to the pipe axis but each element retains a longitudinal velocity component equal to the pipe velocity at the point of issue. The normal component of velocity appears to take place at the expense of pressure head only (it is assumed that the slit is at an extremity of a horizontal diameter). Shock loss is conspicuously absent. Under these conditions, there is every reason to expect that the pressure changes would occur in accordance with Bernoulli's theorem, although the momentum principle was used in deriving the curve. In a discharging manifold, shock loss (or unbalanced port pressure if the momentum principle is used) is the essence of the problem. Despite these minor differences of opinion, Professor McNown's basic ideas are accepted and endorsed—especially appreciated is his thorough treatment of the energy concept which was merely suggested in the paper. Although it is quite generally realized that the momentum and energy principles are but different statements of Newton's Second Law of Motion, statements that one or the other is exclusively applicable are fairly common. No statement in the paper was intended to suggest exclusion of the energy principle but the clarification suggested and largely supplied by Professor McNown was highly desirable.

Professor Edwards' discussion is most welcome; it was he who initiated the test program in the face of considerable evidence that the theory could not be developed in time for use on the Third Locks Project. As he states, the studies and tests did much to expedite the design and testing of complete lock models. The characteristic curves for Ports I to VI, inclusive, were much better defined than those for Port VII as shown in Fig. 21 by Mr. Berk but the verification tests were made for Port VII only. It is for this reason that Port VII is presented in detail. The port described by Professor Edwards has several desirable characteristics, the foremost of which are its high capacity, a relatively constant discharge coefficient over a considerable range of P_d, and elimination of an undesirable velocity component—lack of the latter characteristic to some extent defeats the purpose of the bottom-filling system of the original Panama locks. The similarity of the ports used in the MacArthur Lock and the one described by Professor Edwards has been noted. There is little doubt that this port shape is largely responsible for the quiet filling conditions in the MacArthur Lock—in addition to its other advantages, the flattened jet has a large surface area which is conducive to a high rate of energy dissipation and tends to minimize surface disturbances.

The curves introduced by Professor Lansford provide some basis for the analysis of flow from a perforated pipe but should eventually be supplemented by tests on a larger scale which will enable calculation of the pressure gradients.

[27] "Jets from Manifold Tubes," by Jakob Kunz, *Transactions*, A.S.M.E., 1931, APM-53-14, p. 181.

Although Fig. 18 shows the "great effect the ratio of the kinetic energy to the potential energy has upon the flow through a manifold orifice in a pipe," it is not evident upon inspection that the data corroborate a functional relationship between the discharge coefficient and the ratio P_d. Starting with the basic orifice equation, successive transformations show that such is the case (Z_1 and H_d are equivalent).

$$C_d = \frac{Q_3}{A_p \sqrt{2\,g\,Z_1}} = \frac{P_d\,Q_1}{A_p \sqrt{2\,g\,Z_1}} = \frac{P_d\,A_c\,V_1}{A_p \sqrt{2\,g\,Z_1}} = \sqrt{\left(\frac{A_c}{A_p}\right)^2 (P_d)^2 \frac{(V_1)^2}{2\,g\,Z_1}} \quad . \quad (27)$$

Since A_c/A_p is a constant for any orifice and pipe combination, and as Fig. 18 shows that $(V_1)^2/(2\,g\,Z_1)$ is a function of P_d for each of the orifices tested, it follows that C_d for each orifice is expressible as a function of P_d alone. This experimental support of the theory presented in the paper is greatly appreciated.

The tests reported in the paper would be of little value if they did not lead to a method of designing manifolds. Mr. Kreiss has contributed a very practical means of applying the theory. In Eq. 18, the quantity $N\,A_3$ is the gross area of the ports downstream from the section at which the energy head is determined. In a simple manifold, for example, a lock culvert with wall ports, the energy head producing discharge is simply the gross head minus entrance losses. A few preliminary calculations will indicate whether or not friction losses are significant in any particular case—Fig. 20 serves as a guide for estimating the effect of friction losses. It should not be overlooked that calculations similar to those in Table 2 must be made in the preparation of Table 4. Thanks are due to Mr. Kreiss for undertaking this task and for presenting data on several more ports. It is gratifying to learn that he has made additional tests which tend to confirm the value of single port data in the design of manifolds.

Mr. Berk's comments are particularly interesting because they illustrate an error that is very likely to occur if it is forgotten that the characteristic curves are for a particular port and culvert combination—not for the port alone. Under the heading, "Single Port Tests: Limitations," it was stated that "The data are based on tests of ports of particular sizes, shapes, and lengths—attached to a conduit of a particular size and shape." Elsewhere in the paper, the effects of conduit area and conduit velocity were mentioned. Eq. 27, applicable to Professor Lansford's data, further shows that the culvert size has an important effect upon discharge coefficients.

The concept of a "port and culvert combination" clarifies the questions raised by Mr. Berk. The verification tests were based upon ports of the same size as the one used in single-port tests of Port VII; therefore, as Mr. Berk indicates, scale effects were not investigated. However, the phenomena considered are essentially dynamic in character and there is little question that Froude's law is applicable. The inconsistencies which Mr. Berk believes to exist are entirely due to incomplete geometric similarity in his comparisons. All data are based on a 6-in. square conduit. The values of C which would be used "in calculating the performance of a prototype lock manifold, with ports which should necessarily be much larger than the test ports" are the

same as those obtained in small-scale model tests, but the characteristic curves would have to be based on complete geometric similarity. The culvert size and shape must not be ignored. In some cases, allowance for departures from geometric similarity could be determined by interpolation based on diagrams similar to Fig. 21.

Although Mr. Berk's conclusion regarding the value of small-scale tests must be rejected, his sincere discussion goes far toward clarifying the concept of the "port and culvert combination." Table 1 shows that Ports I to VI, inclusive, are all geometrically dissimilar. Even if the lengths of Ports I to III, inclusive, had been proportional to the heights and widths, the fact that all ports were attached to a 6-in. square conduit would prevent correspondence of the characteristic curves. Similar reasoning is applicable to Ports IV to VI, inclusive. Although interpolation in Fig. 21 between the curves for the round-cornered ports would be more difficult and less reliable than for the square-cornered ports, it would suffice for some purposes. For precise results, additional single port tests might be necessary.

The conclusions were limited specifically to the applications of single port test data. Although "definite information for solving the practical problem of designing a prototype manifold larger in size than the test models and with port shapes other than square cornered" is much to be desired, it is far beyond the scope of the paper. Mr. Berk raised the interesting question of scale effects, but this too is beyond the scope of the paper. However, there is much reason to believe, from the ever-increasing number of model-prototype comparisons, that scale effects would be very small in the present case. As explained in the paper, the allowances for conduit friction are independent of scale effect, so one important source of error in model indications has been eliminated.

Professor Powell has extended the analysis to cover momentum coefficients and angularity of velocities. It is unquestionable that a complete understanding of the mechanics of manifold hydraulics must be developed along these lines. Fortunately, design of manifolds need not await the isolation and analysis of these factors as their effects may be grouped together and determined experimentally. Table 5, prepared by Professor Powell, appears to indicate reasonable variation in angles and momentum coefficients for Port I although, as he states, determination of exact values would require "laborious experiments."

In closing, it should be emphasized that the use of characteristic curves for study of any port-and-culvert combination is simply a convenient method of reducing the number of variables. The fact that the characteristic curves may be plotted in terms of P_d and P_i is not a fortunate accident but has the same physical basis as the dimensionless representation of pressure variations in a bend. The ratios P_i and P_d establish the arrangement of stream paths and these patterns remain essentially unchanged by variations in the absolute values of the several variables if proportionality is maintained. One additional point which may merit mention is the fact that an entire lateral in a bottom-filling lock can be treated merely as a port on the longitudinal culvert. The interest shown in the paper is sincerely appreciated.

AMERICAN SOCIETY OF CIVIL ENGINEERS

Founded November 5, 1852

DISCUSSIONS

FLOW IN A CHANNEL OF DEFINITE ROUGHNESS

Discussion

BY JOE W. JOHNSON AND E. A. LEROUX

JOE W. JOHNSON,[26] ASSOC. M. AM. SOC. C. E., AND E. A. LEROUX,[27] ESQ.[27a]—The author is to be congratulated for a splendid experimental investigation which is a welcome contribution toward a better understanding of the problem of channel roughness. Similar investigations in the University of California Fluid Mechanics Laboratory at Berkeley were made with water in both open and closed channels, and with air in closed channels. Various types of artificial roughnesses were used. Experiments by V. J. Skoglund[28] were made with water in rectangular channels roughened by 60° V grooves transverse to the direction of flow. The grooves were 0.060 in. apart with an average depth of 0.0125 in. The hydraulic radius was varied from 0.030 ft to 0.230 ft. Later experiments were made by J. E. Ogden[29] using this same apparatus but with a groove spacing one half that used by Mr. Skoglund; that is, the roughness grooves were 0.030 in. center to center. Tests were made with the hydraulic radius of the channel equal to 0.019 ft. The results of experiments in a a triangular open channel with the roughness formed by attaching sand grains of constant mean diameter to the channel walls have been published by T. DeF. Rogers.[30]

Other open-channel experiments were made by M. E. Fuller and R. E. Graham, Juniors, Am. Soc. C. E., in a rectangular flume 9½ in. by 9½ in. in cross section and 70 ft long.[31] The type of roughnesses included the following combinations: (*a*) Smooth sides and bottom coated with enamel; (*b*) sides

NOTE.—This paper by Ralph W. Powell was published in December, 1944, *Proceedings*.

[26] Asst. Prof., Div. of Mech. Eng., Univ. of California, Berkeley, Calif.

[27] Graduate Student, Univ. of California, Berkeley, Calif.

[27a] Received by the Secretary May 14, 1945.

[28] "Effect of Roughness on the Friction Coefficient of a Closed Channel," by V. J. Skoglund, *Journal of the Aeronautical Sciences*, Vol. 4, November, 1936, pp. 28–29.

[29] "Artificial Roughness," by J. E. Ogden, Univ. of California Fluid Mechanics Laboratory, Berkeley, Calif., 1944 (unpublished report).

[30] "Friction in Hydraulic Models," by Thomas DeF. Rogers, *Civil Engineering*, June, 1939, p. 367.

[31] "A Study of the Distribution of Frictional Energy Losses in Open Channels," by M. E. Fuller and R. E. Graham, thesis submitted to the Univ. of California, Berkeley, Calif., in partial fulfilment of the requirements for the degree of Bachelor of Science, 1942 (unpublished).

and bottom covered with a 90-lb Flintkote roofing paper with rough side exposed; (*c*) enameled sides with bottom covered with the roofing paper; (*d*) enamel sides with ½-in. mesh hardware cloth tacked over the roofing paper on the bottom. These roughnesses are not "definite" in the sense implied by the author; hence, the results are not summarized herein.

Of particular value in connection with a discussion of the author's data are the results of various investigations on roughnesses, rectangular in cross section. Although most of these data have been discussed elsewhere,[32] a summary (Table 3) in terms of the author's notation is necessary for comparative purposes. For each of the roughnesses tested by the various experimenters, the data in Table 3 include the following terms (see Fig. 12): Center-to-center spacing, s, of the roughness battens; the batten height, h; the batten

TABLE 3.—SUMMARY OF INVESTIGATIONS ON RECTANGULAR ROUGHNESSES, UNIVERSITY OF CALIFORNIA

Roughness (see Fig. 13)	Dimensions (Inches)			$\frac{t}{h}$	$\frac{s}{h}$	k (ft)	$\frac{k}{h}$	n_b
	h	t	s					
				(*a*) W. TRIPP AND F. JONASSEN				
....	1/8	1/2	5/8	4	5	0.000652	0.0625	....
1	1/8	3/16	5/16	1.5	2.5	0.00176	0.069	....
2	1/8	1/8	5/8	1	5	0.0264	2.53	....
3	1/8	1/8	1 1/4	1	10	0.0575	5.52	....
4	1/8	1/8	2 1/2	1	20	0.0364	3.49	....
5	1/8	1/8	5	1	40	0.0155	1.49	....
				(*b*) C. A. SMITH, JR., AND C. WARREN				
A	1/8	5/32	5/16	1.25	2.5	0.0022	0.21	0.0112
B	1/8	5/32	5/8	1.25	4	0.0432	4.15	0.0185
C	1/8	5/32	1 1/4	1.25	10	0.0525	5.04	0.0200
D	1/8	5/32	2 1/2	1.25	20	0.0313	3.00	0.0170
E	1/8	5/32	5	1.25	40	0.0125	1.20	0.0149
				(*c*) J. W. JOHNSON				
A	1/4	1	2	4	8	0.0202	0.97	0.0163
B	1/4	1	4	4	16	0.1297	6.23	0.0244
C	1/4	1	8	4	32	0.0698	3.35	0.0208
D	1/4	1	2 1/2	4	10	0.0500	2.40	0.0194
E	1/4	1	5	4	20	0.1185	5.69	0.0236
F	1/4	1	3	4	12	0.1050	5.04	0.0229
G	1/4	1	6	4	24	0.0940	4.51	0.0223
H	1/4	1	3 1/2	4	14	0.1255	6.02	0.0240
I	1/4	1	4 1/2	4	18	0.1270	6.10	0.0240
				(*d*) E. A. LEROUX				
J	1/4	3/4	1 1/2	3	3	0.0176	0.846	0.0158
K	1/4	3/4	3	3	12	0.0925	4.44	0.0222
L	1/4	3/4	6	3	24	0.0549	2.64	0.0198
M	1/4	3/4	2 1/4	3	10	0.0641	3.08	0.0204
N	1/4	3/4	4 1/2	3	18	0.0840	4.03	0.0219
O	1/4	3/4	9	3	36	0.0163	0.783	0.0177
P	1/4	3/4	3 3/4	3	15	0.0870	4.18	0.0222

[32] "Rectangular Artificial Roughness in Open Channels," by J. W. Johnson, *Transactions*, Am. Geophysical Union, Hydrology Section, 1944.

width, t; the width-height ratio, t/h; and the spacing ratio, s/h. The observations of W. Tripp[33] and F. Jonassen[34] were similar to those of Mr. Skoglund, except that air was used in wooden rectangular conduits roughened by saw cuts transverse to the direction of flow (Fig. 13). The investigations by C. A. Smith, Jr., and C. Warren, Juniors, Am. Soc. C. E., and by the writers were made in a wooden flume $9\frac{1}{2}$ in. by $9\frac{1}{2}$ in. in cross section and 70 ft long.[35] In the experiments by Messrs. Smith and Warren the roughness was formed by saw cuts made in removable planks fastened to the flume bottom. Different spacing ratios (s/h) were made by removing alternate ridges between saw cuts (see Fig. 13). It is of interest to note that the average value of Manning's n for the enameled surface was 0.0091, whereas the value of n for the bottom after all roughness ridges had been removed was 0.0104. In the writers' experiments the roughness was made by nailing redwood strips to the bottom of the flume transverse to the direction of flow. Strips 1 in. by $\frac{1}{4}$ in. were used for roughnesses in the Johnson experiments; whereas $\frac{3}{4}$-in. by $\frac{1}{4}$-in. strips were used by Mr. LeRoux (Fig. 13).

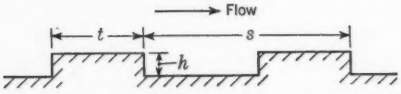

FIG. 12.—DESIGNATION OF DIMENSIONS OF RECTANGULAR ROUGHNESS

The method of calculating the hydraulic radius, Manning's n, and the equivalent sand roughness in the experiments of Messrs. Smith and Warren, and of the writers, have been described elsewhere;[32] however, because of differences in the experimental equipment and the method of analysis of the data a brief review is of interest. In the author's experiments both the bottom and sides of the flume were covered by roughness battens, and the results were analyzed with G. H. Keulegan's formulas as the basis. In the writers' experiments only the channel bottom was roughened. The side-wall effect first was "eliminated" by the method suggested by H. A. Einstein,[36] Assoc. M. Am. Soc. C. E., and then the hydraulic radius of the bed, R_b, Manning's n of the bed, n_b, and the equivalent sand roughness of the bed, k, were computed, the latter term being computed by the Nikuradse equation:

$$\frac{1}{\sqrt{f}} = 2 \log_{10} \left(\frac{2 R_b}{k} \right) + 1.74 \ldots\ldots\ldots\ldots\ldots\ldots (19)$$

in which

$$f = \frac{8 g R_b S_e}{V^2} \ldots\ldots\ldots\ldots\ldots\ldots\ldots\ldots\ldots (20)$$

and S_e is the slope of the energy grade line.

The data in Table 3 are of value in giving a more complete picture of the relation of relative roughness to spacing than that given by the author in

[33] "Friction Losses in an Artificially Roughened Rectangular Channel," by W. Tripp, *Journal of the Aeronautical Sciences*, November, 1936, pp. 10–11.

[34] "Artificial Roughness," by F. Jonassen, Univ. of California Fluid Mechanics Laboratory, Berkeley, Calif. (unpublished).

[35] "Friction Losses in Artificially Roughened Channels," by C. A. Smith and C. Warren, thesis submitted to Univ. of California, Berkeley, Calif., in partial fulfilment of the requirements for the degree of Bachelor of Science, 1943 (unpublished).

[36] "Formulas for the Transportation of Bed-Load," by H. A. Einstein, *Transactions*, Am. Soc. C. E., Vol. 107 (1942), pp. 575–577.

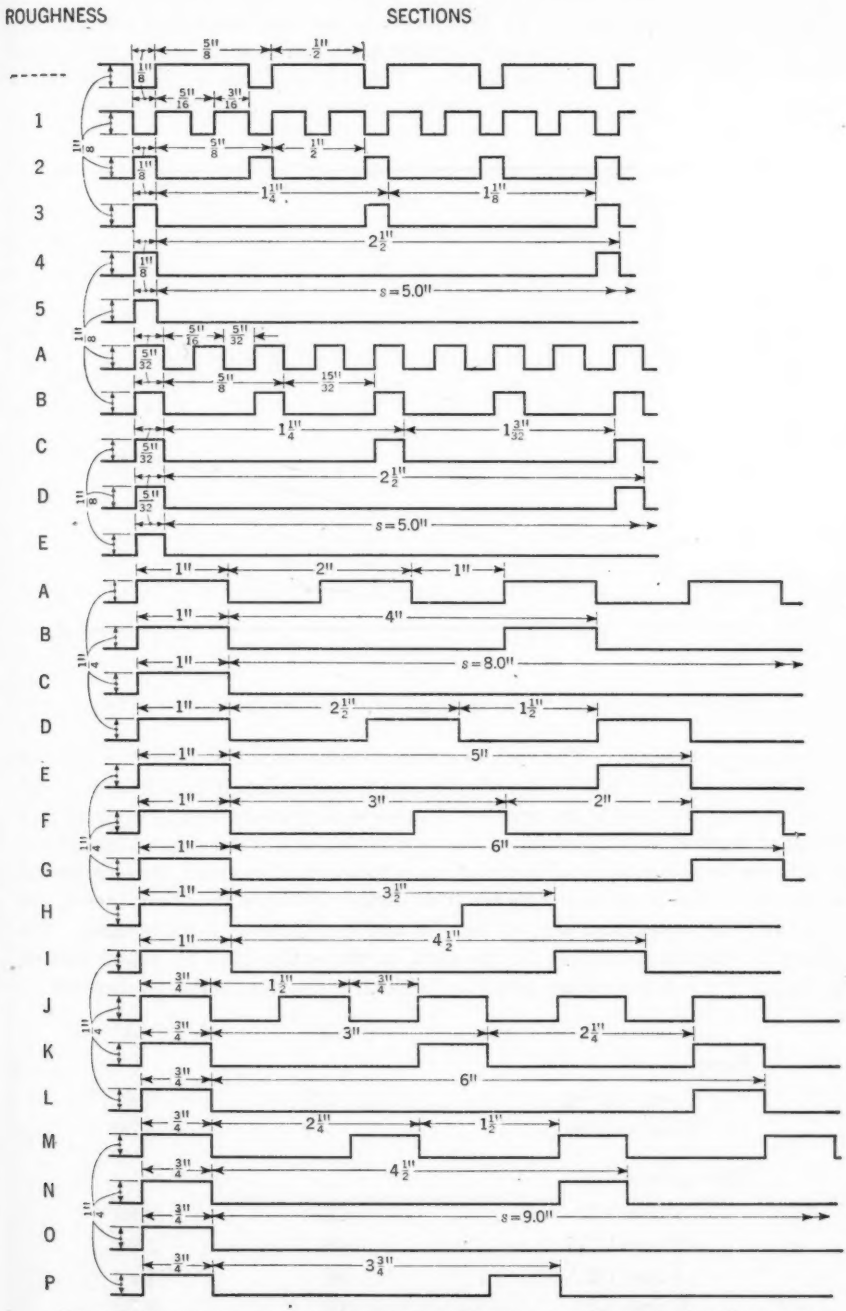

FIG. 13.—VARIOUS RECTANGULAR ROUGHNESSES TESTED AT THE UNIVERSITY OF CALIFORNIA (NOTE SCALE CHANGES)

Fig. 10. Fig. 14 shows a plot of these data and indicates that the author's data and Bazin's results probably are not part of the same curve but appear to be branches of two separate curves. The author has called attention to the uncertainty of a single curve. Fig. 14 indicates that the width-height ratio, t/h,

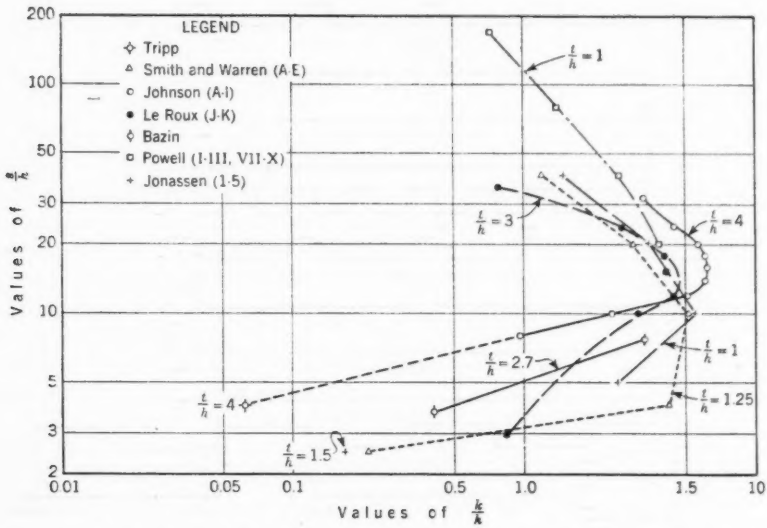

FIG. 14.—RELATION OF RELATIVE ROUGHNESS TO SPACING FOR VARIOUS DATA

may be of importance. The various curves indicate that the maximum relative roughness occurs in the vicinity of s/h equal to approximately 15 instead of 12. The value of the maximum relative roughness appears to be approximately a constant regardless of the value of t/h. On either side of the point of maximum roughness there is considerable variation in the curves; however, for a particular value of s/h, the roughness appears to be larger with the smaller values of t/h.

It is to be noted that the values of k and n_b (Table 3) are averages. The values of relative roughness for the data of the author and H. Bazin plotted in Fig. 14 are not the values given in Table 2. The appropriate values are:

Roughness	s/h	k/h
Bazin—		
Close spacing	3.7	0.41
Wide spacing	7.7	3.36
The author—		
III and VII	20	3.89
II and VIII	40	2.60
I and IX	80	1.40
X and XI	160	0.72

The author previously has converted the values of ϵ in Table 2 to the corresponding values of the Nikuradse k.[37]

It is important to note that in the author's experiments the water depth was measured from the water surface to the flume bed without battens in place; whereas, in the writers' experiments, the depth was measured to the top of the battens. At small depths of flow relatively large differences in the results from the two experiments may occur if comparisons are attempted. The author has recognized the uncertainty in determining the true depth and has suggested that the problem be given further study.

[37] Discussion by R. W. Powell of "Rectangular Artificial Roughness in Open Channels," by J. W Johnson, *Transactions*, Am. Geophysical Union, Section of Hydrology, 1944.

AMERICAN SOCIETY OF CIVIL ENGINEERS

Founded November 5, 1852

DISCUSSIONS

SIMULTANEOUS CONSOLIDATION OF CONTIGUOUS LAYERS OF UNLIKE COMPRESSIBLE SOILS

Discussion

BY HAMILTON GRAY

HAMILTON GRAY,[23] ASSOC. M. AM. SOC. C. E.[23a]—The discussions may be classified into two types. Those in type 1 suggest certain approximate solutions that can be applied with less expenditure of time than the rigorous solutions and for which the degree of approximation may be fairly high, at least within certain limits. Type 2 involves the application of the solutions to various foundation problems. Both types of discussion are valuable contributions to the subject.

There is no reason for applying involved and time-consuming analyses to engineering problems unless no simpler mode of attack will suffice. Exact methods of analysis may be useful from either of two standpoints: (*a*) As the only available rational attack on a problem, or (*b*) as a check on the degree of approximation in simpler methods of analysis.

Mr. Barber illustrates that, if preferred, compressions may be expressed in terms of strain rather than in terms of void-ratio changes. This is wholly a matter of personal taste since some engineers prefer pressure, void-ratio curves whereas others favor curves showing percentages of compression as functions of the pressure. In either case the results of the analysis are identical.

Mr. Barber's statement regarding the computation of the resultant consolidation on the basis of compressions rather than of thicknesses merits comment. Computation on the basis of thicknesses requires the use of the formula:

$$U_r = \frac{U_1 + \nu U_2}{1 + \nu} \qquad (43a)$$

which indicates the extent to which the transfer of stress from fluid to solid phase has occurred. Eq. 43*a* may be termed the "resultant degree of consolida-

NOTE.—This paper by Hamilton Gray, Jun. Am. Soc. C. E., was published in February, 1944, *Proceedings*. Discussion on this paper has appeared in *Proceedings*, as follows: June, 1944, by Edward S. Barber, and Jacob Feld; and September, 1944, by George W. Glick.

[23] Asst. Prof., Civ. Eng., New York Univ., New York, N. Y.

[23a] Received by the Secretary April 28, 1945.

tion" by virtue of the definition of "degree of consolidation" given in Eqs. 9 and 10. Computation on the basis of compressions utilizes the expression:

$$U_r = \frac{U_1 + \frac{\mu}{\sigma} U_2}{1 + \frac{\mu}{\sigma}} \qquad (43b)$$

Eq. 43*b* indicates what portion of the resultant ultimate compression has occurred, based on the assumption that the pressure, void-ratio curves are linear in the pertinent pressure range. This may be called the "resultant relative compression." From a practical standpoint, Eq. 43*b* is required for estimating the actual settlements. Only if $\frac{\mu}{\sigma} = \frac{a_2}{a_1} = 1.0$ will Eqs. 43*a* and 43*b* give identical results. The distinction between these two formulas should have been treated in the paper. For the example in the paper Eqs. 43 do not give very different results. This is illustrated in Fig. 13 which also reveals that, if the

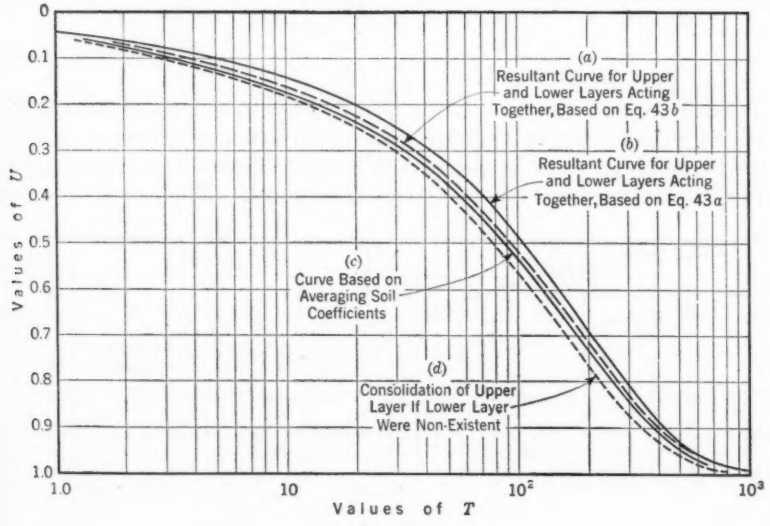

FIG. 13

compressibility of layer I were to be ignored completely, a fairly close approximation to the exact result would be obtained.

Fig. 14 illustrates the situation in which the positions of the two layers which were considered in the paper are interchanged. Under these conditions, the agreement between Eq. 43*a* and Eq. 43*b* is less close, and neither of the two approximate solutions suggested in connection with Fig. 13 seems to yield as reliable results. Table 8 is included to clarify the differences that are reflected by the curves in Figs. 13 and 14. Fig. 15, based on case D, is analogous to Fig. 5 which is based on case C.

Table 8 also illustrates typical numerical values for the pertinent physical constants. In this connection, it is of interest to note that the actual time required to achieve 50% of the ultimate resultant consolidation or settlement is greater for case C than for case D—in case C consolidation of layer I is

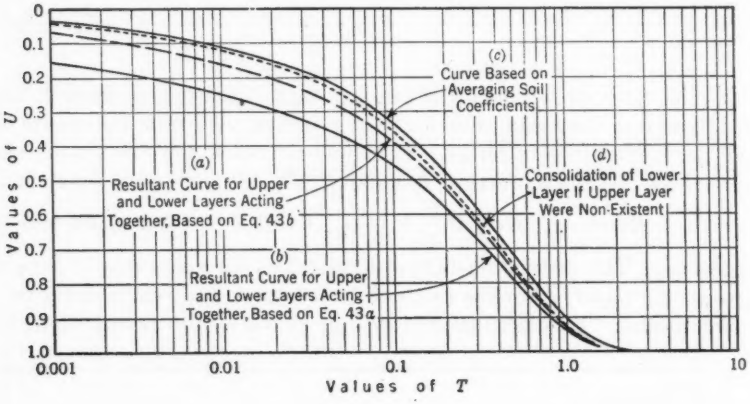

FIG. 14

retarded by layer II as indicated in Fig. 7, whereas in case D layer II drains relatively rapidly and in addition exerts only a minor influence on layer I. If the thinner layer in each case is neglected, a moderately close approximation to the actual behavior of the two layers is obtained. This phenomenon seems

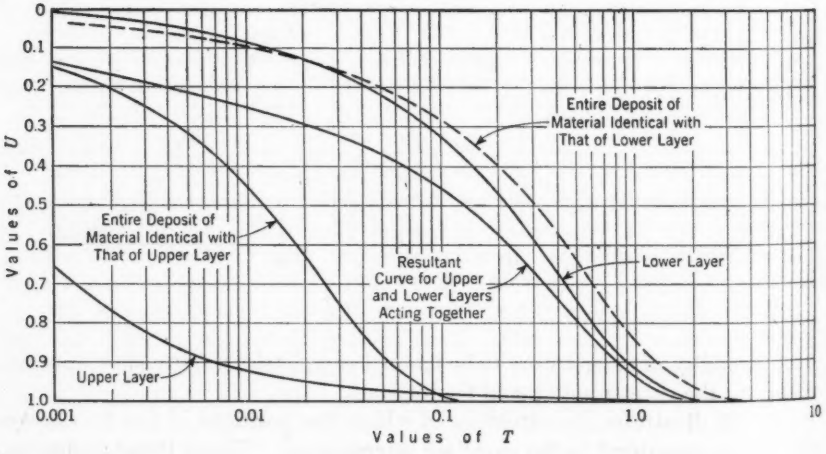

FIG. 15

to be due to the great difference in the consolidation characteristics of the two layers. In cases A and B discussed by Mr. Barber, layers I and II would each consolidate at the same rate if they were not contiguous, since the ratio, t/T, is the same for each. Consequently, ignoring one or the other of these layers will

not give a close approximation of the exact behavior when the layers are contiguous.

TABLE 8.—Typical Values of Physical Constants

Description	Case C	Case D	Key
Layer II—			
k_{s2} (cm per sec)	1×10^{-8}	1×10^{-7}	
h_2 (ft)	20	5	
e_2	1.5	1.5	
a_2 (cm² per g)	5×10^{-4}	2×10^{-4}	
c_2 (cm² per sec)	2×10^{-5}	5×10^{-4}	
Layer I—			
k_{s1} (cm per sec)	1×10^{-7}	1×10^{-8}	
h_1 (ft)	5	20	
e_1	1.5	1.5	
a_1 (cm² per g)	2×10^{-4}	5×10^{-4}	
c_1 (cm² per sec)	5×10^{-4}	2×10^{-5}	
Ratios—			
$\nu = h_2/h_1$	4.0	0.25	
k_{s1}/k_{s2}	10.0	0.10	
a_1/a_2	0.40	2.5	
c_1/c_2	25	0.04	
μ	5.0	0.20	
$T = t\, c_1/(h_1)^2$ (yr)	$0.68\, t$	$0.0017\, t$	
t	$1.47\, T$	$590\, T$	
t_{50} (yr)	138	103	
σ	2.0	0.5	

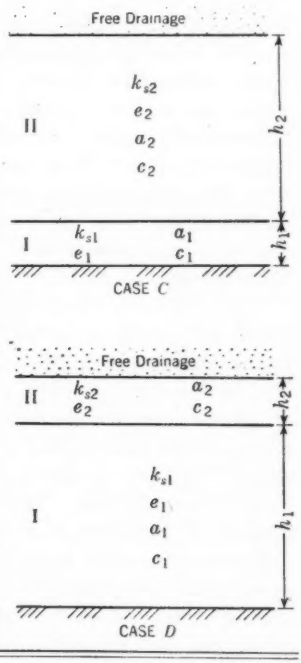

As Mr. Glick states, when $\sigma = 1$ it can be shown that, if the thickness, h_2, of layer II be multiplied by $\mu = \sqrt{\frac{c_1}{c_2}}$ so as to yield $(h_2)' = \mu\, \nu\, h_1$, it is possible to obtain the following expressions for the resultant consolidation:

$$U_r = \frac{U_1 + \mu\, \nu\, U_2}{1 + \mu\, \nu} = 1 - \frac{8}{\pi^2} \sum_{n=0}^{n=\infty} \frac{1}{(2\, n + 1)^2}\, \epsilon^{-N' T'} \quad \ldots\ldots (44a)$$

and

$$U_r = \frac{U_1 + \mu\, \nu\, U_2}{1 + \mu\, \nu} = 1 - \frac{8}{\pi^2} \sum_{n=0}^{n=\infty} \frac{1}{(2\, n + 1)^2}\, \epsilon^{-N''' T'} \quad \ldots\ldots (44b)$$

in which

$$N''' = (2\, n + 1)^2\, \pi^2 \quad \ldots\ldots (45a)$$

and

$$T' = \frac{c_1\, t}{(1 + \mu\, \nu)^2\, (h_1)^2} \quad \ldots\ldots (45b)$$

and N' is given by Eq. 14. Since the right-hand sides of Eq. 44*a* and Eq. 44*b*, respectively, are identical with the expressions for the degree of consolidation of homogeneous layers (thickness, $h_1 (1 + \mu \nu)$, consolidation coefficient, c_1, and drained, respectively, at one face and at both faces), the transformation, $z' = \mu z$, applied to dimensions, Z, in layer II makes it possible to consider the two layers as a single homogeneous stratum. When μ is equal to unity, there does not appear to be any analogous transformation that may lead to a simplification of the general problem.

For practical applications, the various approximate solutions or modifications outlined by Messrs. Barber and Glick are very valuable, provided one knows the extent to which the approximate results differ from those which are theoretically exact. In some cases two or more approximate approaches are suggested, and it then becomes important to know which method is best—from the standpoint of accuracy as well as from that of time. In many cases an inspection of the relative consolidation characteristics of the pertinent strata will give some indication of the reliability to be expected from one or another of the suggested methods of approach.

Mr. Feld has described numerous cases, both natural and man made, to which the methods outlined in the paper may be applied. It is of great help to the engineer to be able to analyze actual field conditions in terms of an idealized situation, especially if, at the same time, he does not lose sight of the differences between actual conditions and assumed conditions. Mr. Feld emphasizes this fact, which the writer had in mind when he suggested that the results obtained in the paper should be verified by observations before being used with confidence. In many instances it is possible to explain discrepancies between a theoretical approach and the observed behavior on the basis of differences between actual and assumed conditions. The writer would disagree with one of Mr. Feld's statements since he believes that the influence of surface evaporation upon the consolidation of a soil deposit can be analyzed by appropriate methods.

The writer wishes to express his thanks to the discussers for their worthwhile comments on this paper.

AMERICAN SOCIETY OF CIVIL ENGINEERS

Founded November 5, 1852

DISCUSSIONS

CONVERSION OF KINETIC TO POTENTIAL ENERGY IN FLOW EXPANSIONS

Discussion

BY BORIS A. BAKHMETEFF, AND E. R. VAN DRIEST

BORIS A. BAKHMETEFF,[32] M. AM. SOC. C. E.[32a]—Professor Kalinske's paper marks a serious advance in the science of fluid mechanics. It reveals facts, relating to turbulence in "form resistance" patterns, wholly unknown before and which substantially further present-day knowledge in this obscure and generally uncharted realm. The most significant result is the disclosing of the quantitative inner relations between the over-all energy loss E_r, occurring in the course of expansion, and the turbulent energy E_t, apparent and measurable in the turbulent fluctuations. Although the paper deals with flow expansions only, the facts, as established, seem to be typical in all probability of other "form" or "local" resistances.

The aforesaid terms are meant to designate the concentrated losses of energy known to accompany the abrupt variations of flow geometry, such as the losses in bends, knees, valves, back of bluff bodies, etc. It is generally recognized that the generic cause conducive to "form" losses is "separation," with the highly strained and labile "discontinuity sheets" serving as seats of concentrated turbulence engendering activity. It is accepted further that the turbulent eddying composite, featured by the energy E_t, represents the final phase of a complex process by the force of which flow energy is withdrawn from the store inherent to the streaming, and is subjected to "conversion" into vortical eddying form. It has been surmised, finally, that, in the course of the cyclic deformations of the free discontinuity sheet which accompany "transition" from the laminar to the turbulent regimen, only a portion of the used up flow energy reappears in the ostensible turbulent manifestations, and that the remainder of such energy is dissipated in loco in the process of conversion, constituting what may be termed a "conversion loss."[33] However,

NOTE.—This paper by A. A. Kalinske was published in December, 1944, *Proceedings*. Discussion on this paper has appeared in *Proceedings*, as follows: February, 1945, by F. T. Mavis; and May, 1945, J. C. Stevens.

[32] Prof., Civ. Eng., Columbia Univ., New York, N. Y.

[32a] Received by the Secretary May 5, 1945.

[33] "The Mechanism of Energy Loss in Fluid Friction," by Boris A. Bakhmeteff and William Allan, *Proceedings*, Am. Soc. C. E., February, 1945, pp. 143–147.

all prior inferences regarding the possible energy balance in the turbulent process were necessarily conjectural, as no factual evidence existed to permit reliable quantitative interpretations. It is only now, in the light of Professor Kalinske's findings, that the actual situation has been ascertained reliably.

It would seem that the situation is best illustrated by expressing the different pertinent quantities in terms of the initial kinetic energy E_{m1}, at the mouth of the small conduit. In fact, since the denominator in Eq. 7 may be represented with sufficient approximation by

$$E_{m1} - E_{m2} = E_{m1}\left[1 - \left(\frac{D_1}{D_2}\right)^4\right] \quad \ldots\ldots\ldots\ldots\ldots\ldots (8)$$

the over-all relative loss E_r/E_{m1} may be expressed by

$$(1 - \eta)\,[D_1 - (D_1/D_2)^4] \quad \ldots\ldots\ldots\ldots\ldots\ldots (9)$$

—or, for the 2.75-in. to 4.75-in. expansion, by $0.89\,(1 - \eta)$. The data required for the calculations may be taken from Tables 2 and 4, as well as from Fig. 4. One also finds therein the information for establishing the ratio $E_t\,(\max)/E_{m1}$ of the maximum measured turbulence energy to the initial E_{m1}, and with this the final ratio of $E_t\,(\max)/E_r$. The values are assembled in Table 7.

TABLE 7.—VALUES OF ENERGY RATIOS

Flow (cu ft per sec)	30° EXPANSION			180° EXPANSION		
	$\frac{E_r}{E_{m1}}$	$\frac{E_t\,(\max)}{E_{m1}}$	$\frac{E_t\,(\max)}{E_r}$	$\frac{E_r}{E_{m1}}$	$\frac{E_t\,(\max)}{E_{m1}}$	$\frac{E_t\,(\max)}{E_r}$
0.082	....	....	....	0.425	0.090	21%
0.147	0.365	0.115	31%	0.470	0.095	19%
0.210	0.474	0.105	22%	0.506	0.082	16%

With all possible allowances for experimental uncertainties devolving (as the author states) from the colossal observational difficulties, the order of magnitude is established beyond doubt. The turbulent energy E_t at its maximum is but a small portion of the total loss E_r. No wonder the author is prompted to refer to the turbulence created as a "kind of by-product," attributing the major loss to the intense and variable local shearing stresses, set up on the outside of the high velocity jet. The description fits the rather striking circumstances, provided the wording is not misinterpreted. The fact is, of course, that the mechanism of energy loss is an entity, a composite whole, no constituent portion of which should be considered separate and alone. Turbulence is engendered ultimately for the very reason that separation originates intensive local stresses, initially of viscous nature. In the inevitable sequence of events, these local stresses lead to vehement deformations, transforming the discontinuity sheets into eddying patterns, with the latter in turn breaking up into inordinate turbulent "swarming." In other words, the first and the last phases in this process, characterized respectively by the highly strained viscous sheets and by the ostensible turbulent fluctuations, constitute

inseparable links of an organic whole. In this light, the findings of the paper, in so far as the small numerical ratios of E_t/E_r are concerned, could be qualified as having disclosed the surprisingly low efficiency of energy exchange in the turbulence producing mechanism.

In reflecting on these properties, one gains the impression that perhaps the feature of having relatively small manifestations reflect the presence of momentous processes, deeply affecting the essence of things, is rather typical of turbulence phenomena in general. For instance, consider the case of so-called established turbulence, in uniform motion in conduits. The measured turbulent energy in pipes, etc., constitutes on the average only a few per cent of the kinetic energy of the main motion. Nevertheless, the transverse mixing, concomitant to such turbulence, increases the stress structure, and with that the over-all energy loss, to many hundreds if not thousands of times the shearing forces and the losses, which would prevail if the motion at the same flow rate were to remain laminar. Again in this case, the measurable E_t is only a part of the total energy E_r withdrawn from the flow and spent on conversion.[34] In fact, the writer feels that the possible (E_t/E_r)-ratios in uniform motion, when actually measured, may prove to be even lower than the values shown in the paper for flow expansions.

In uniform motion the production of turbulence and all other features of the energy spending process unfold in equal measure in each of the successive cross sections. In other words, all the functions of the energy-loss mechanism are uniformly distributed along the length of the conduit. In the case of form resistances, on the other hand, the consecutive functions, started by separation, unfold in successive fashion over a certain distance range along the axis. Naturally one is tempted to seek, in the factual evidence presented in the paper, possible clues which would help to disclose, even if conjecturally, the physical nature of the energy-loss mechanism. Note, in this connection, that in Fig. 4, for the 180° expansion, turbulence reaches its maximum in the very first measured station at a distance of about 0.55 ft from zero. It is true that, in the case of the 30° and particularly with the 15% expansion (see Table 2), the locus of maximum E_t is shifted somewhat downstream. This could be explained, however, by the fact[35] that, in divergent cones, the separation is somewhat delayed. These facts are quite significant. Obviously, in the initial stage of separation, when the live jet first comes into contact with the "roller," friction in the discontinuity sheet is viscous, so that the shearing stresses are shaped by the Newton law $\left(\frac{\mu\, du}{dy}\right)$. Furthermore, as these viscous discontinuity sheets are highly unstable, the rolling up process to form eddying patterns is begun almost at once. In other words, the over-all distance from the beginning of separation to transition must be rather short. Beyond the transition reach, where the turbulent regimen has established itself, the high local stress may continue by force of convective transverse mixing. The

[34] "The Mechanism of Energy Loss in Fluid Friction," by Boris A. Bakhmeteff and William Allan, *Proceedings*, Am. Soc. C. E., February, 1945, p. 151.

[35] "Versuche über die Strömungsvorgänge in erweiterten und verengten Kanälen," by H. Hochschild, *Forschungsarbeiten des Vereines Deutscher Ingenieure*, Heft 114, 1912.

pertinent question however is whether, in this post-transition stage, there is any further production of turbulence, in the sense of further investment of flow energy into vortical turbulent form; or, perhaps the conversion process, with the inherent concentrated absorption of flow energy, is confined to the short pre-transition stage. Within the latter, of course, flow energy is spent by way of viscous deformation in accordance with the generic Stokes formulation $\mu \zeta^2$, in which ζ denotes vorticity. The abrupt drop of the energy line in Fig. 6 would seem to point in the direction of the latter hypothesis. If such is the case, and if no further turbulence is engendered beyond the transition reach, then subsequent losses of flow energy would occur by reason of the transverse turbulence mixing. The dynamics of this particular loss, concomitant to "turbulent diffusion," have been discussed elsewhere.[36] In uniform flow such diffusion loss is comparatively low. The rather gentle slope of the total energy lines in Fig. 6, beyond the first abrupt drop, seems to point toward analogous conditions in the case of flow expansions.

Another point, to which the writer would like to draw attention, is the prevailing custom of qualifying the losses in flow expansions, as losses of kinetic energy. Actually, in a closed conduit the mean velocities U_1 and U_2 in the initial and final sections are prescribed by continuity. Accordingly, except for the secondary effect of local velocity distributions, the corresponding kinetic energies of the average flow are predetermined and cannot be either increased or reduced. What is actually lost is pressure, for the eventual gain in potential energy, which theoretically should accompany the reduction in velocity, is consummated only partly, to the extent of $\eta (E_{m1} - E_{m2})$. One may take account of what happens by resorting to the basic Euler equation

$$\frac{dp}{ds} = -\rho \frac{d}{ds}\left(\frac{u^2}{2}\right) - F_r \qquad (10)$$

featuring the dynamic balance along a filament s. The eventual pressure increase developing from the inertial force, $-\rho u \frac{du}{ds}$, is reduced to the extent of the resultant friction traction F_r, forthcoming from the high local stresses. Note, in particular, that the F_r resultant is determined not by the absolute value of the local stress but by the transverse gradient of the latter; and, of course, it is typical of separation sheets to evidence highly concentrated stress changes. If and when separation (which is the source of high local shear) can be reduced by that or other means, the process of restoring pressure is correspondingly remedied. The paper indicates certain means to that effect, cited by H. Peters.[5] The writer would like to supplement the reference by drawing attention to some earlier research by K. Andres[37] and by H. Hochschild.[35] Both of these exceptionally complete and valuable monographs on flow expansion deal in detail with the physical and dynamical features of the phenomenon.

[36] "The Mechanism of Energy Loss in Fluid Friction," by Boris A. Bakhmeteff and William Allan, *Proceedings*, Am. Soc. C. E., February, 1945, p. 153.

[5] "Conversion of Energy in Cross-Sectional Divergences Under Different Conditions of Inflow," by H. Peters, *Technical Memorandum No. 737* (Translation), National Advisory Committee for Aeronautics, 1934.

[37] "Versuche über die Umsetzung von Wassergeschwindigkeit in Druck," by K. Andres, *Forschungsarbeiten des Vereines Deutscher Ingenieure*, Heft 76, 1909.

In particular, the Andres experiments reveal the extent to which pressure restoration is affected by the degree of turbulence in the oncoming streaming. Restoration is at its lowest when the initial flow is smooth and the inherent turbulence intensity small. The higher the disturbances, imposed by artificially increasing the turbulence, the smaller will be the effects of the forthcoming separation and with that the higher the rate of the gained pressure. At the time when the Andres report was written (1909), the science of fluid mechanics was in its infancy and the aforesaid results might have appeared paradoxical. At present, one sees at once the analogy with the well-known effect of a turbulent boundary layer delaying separation and thus reducing the form resistance of an immersed sphere or of a cylinder. The best remedy for counteracting pressure losses, as found by Mr. Andres, was to impose a rotary motion on the expanding jet. Through such means he raised the restoration rate to more than 90%. A similar effect is achieved, of course, by removing the reversed flow film next to the solid boundary, by artificial suction.[38]

The Hochschild experiments are especially valuable in that they offer detailed velocity and pressure distribution profiles in the diverging sections. Characteristic is the lack of symmetry in the expanding flow, and the fact that the actual expansion of the jet extends in many instances far beyond the end of the diverging tube. On the whole, the different Hochschild diagrams, featuring the energy distribution in flow expansions, complement most usefully the over-all flow pictures presented in Figs. 1 and 2.

The sole intention prompting these remarks is to possibly add toward clarifying the different topics, presented in pioneer fashion in Professor Kalinske's excellent paper. Indeed, the engineering profession is deeply indebted to the author for a contribution which raises so many new and fascinating questions to be attacked by future research.

E. R. VAN DRIEST,[39] ASSOC. M. AM. SOC. C. E.[39a]—The chief advantage of this paper is that it gives a quantitative description of the distribution of turbulence in, as well as the variation of pressure along, a fluid as it moves through an expanding conduit. Such information is of great concern to the fluid flow analyst.

The author's findings concerning the relative amounts of molecular internal energy and turbulence energy are very interesting and prompt one to calculate the rise in temperature if no turbulence energy appeared. For the high flow through the sudden expansion, a simple calculation leads to a temperature change of about 0.0004 F. The measurement of such a small change would require a most sensitive thermocouple. Although the author states that temperature changes are to be neglected during the expansion process, these changes do occur for a real fluid in spite of the incompressibility.

That turbulence is a by-product of shearing action is a fact that all fluid technicians should know. It is only through shear that instability of flow and

[38] For reference to Ackeret's work on diffusers and other experiments on boundary layer control, see "Applied Hydro- and Aeromechanics," based on lectures by L. Prandtl, by O. G. Tietjens, McGraw-Hill Book Co., Inc., New York, N. Y., 1934, p. 81.

[39] Asst. Prof., Mech. Eng., Mass. Inst. Tech., Cambridge, Mass.

[39a] Received by the Secretary May 9, 1945.

resulting turbulence arise. The effect of turbulence on shaping the ensuing velocity distribution by diffusion is well exemplified by the change in the distribution through the transition region in flow along a flat plate.

Although, as the author states, it was not the purpose of the paper to present further pressure-loss data, nevertheless, owing to its practical importance, it may be of interest to compare the efficiencies of the energy conversion as computed from the author's data with efficiencies determined by other experimenters. The conventional efficiency formula is

$$\eta = \frac{p_2 - p_1}{\frac{\gamma \bar{U}^2_{m_1}}{2g}\left[1 - \left(\frac{A_1}{A_2}\right)^2\right]} \qquad (11a)$$

which differs from Eq. 7 in that the velocity distribution is assumed uniform across the initial and final sections. For sudden expansions, Eq. 11*a* becomes (upon insertion of the Borda loss formula):

$$\eta = \frac{2}{1 + \frac{A_2}{A_1}} \qquad (11b)$$

From the very comprehensive paper by G. N. Patterson,[40] the writer has replotted, in Fig. 7, data obtained by H. Peters and A. H. Gibson. Calculated

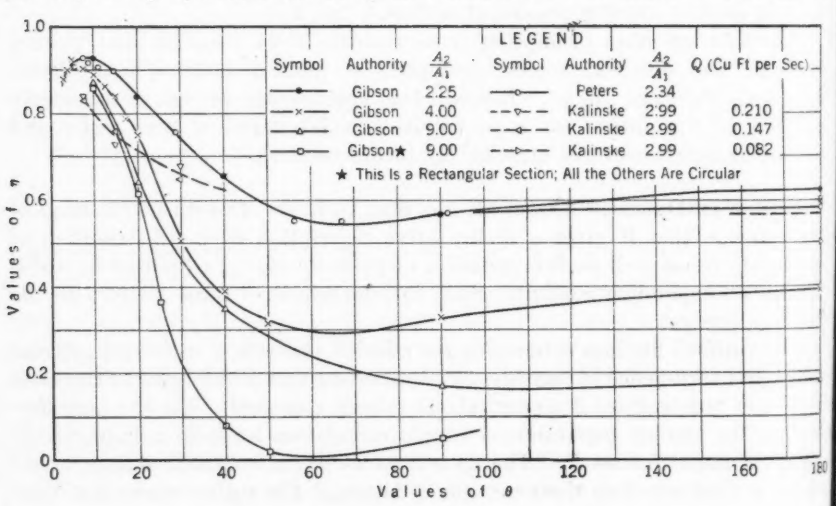
LEGEND
Symbol Authority $\frac{A_2}{A_1}$ Symbol Authority $\frac{A_2}{A_1}$ Q (Cu Ft per Sec)
Gibson 2.25 Peters 2.34
Gibson 4.00 Kalinske 2.99 0.210
Gibson 9.00 Kalinske 2.99 0.147
Gibson★ 9.00 Kalinske 2.99 0.082
★ This Is a Rectangular Section; All the Others Are Circular
Values of η
Values of θ
1.0
0.8
0.6
0.4
0.2
0
0 20 40 60 80 100 120 140 160 180

FIG. 7

efficiencies are plotted in Fig. 7, using Eq. 11*a* and the author's data in Table 3 and Fig. 5. It is seen that the author's efficiency data are somewhat higher in general than would be expected from Eq. 11*b* (with which the Peters and Gibson results agree well) and somewhat lower than the test data of Messrs. Peters and Gibson at small angles of divergence.

[40] "Modern Diffuser Design," by G. N. Patterson, *Aircraft Engineering*, September, 1938, p. 267.

Dimensional analysis shows that

$$\eta = f\left(\frac{\bar{U}_{m1} D_1 \rho}{\mu}, \frac{A_2}{A_1}, \theta\right) \ldots\ldots\ldots\ldots\ldots\ldots (12)$$

if the density ρ and the viscosity of the fluid are assumed to be effective. In Eq. 12, D_1 is the diameter of the small pipe and θ is the total angle of divergence. However, Mr. Gibson[41] stated that he found no systematic variation of his results with the Reynolds number, which was always greater than about 50,000 in his experiments. It is probably true that the variation of the author's data with discharge is also not an effect of the Reynolds number which was greater than 50,000 for the two highest discharges.

The writer is very happy to have assisted in the development of the photographic technique used in these studies and to have helped in the collection of some of the turbulence data.

Corrections for *Transactions:* In December, 1944, *Proceedings*, pages 1552, 1553, and 1555 (Figs. 1 and 2), change the lower abscissa caption to read: "Mean Square Velocity Fluctuation, in (Feet per Second)^2." On pages 1557 and 1558 (Figs. 3 and 4), change the inner ordinate caption by deleting "in Foot-Pounds per Second" after values of $\frac{E_t}{E_m}$. On page 1564, in conclusion 4, omit "rate of."

[41] "On the Flow of Water through Pipes and Passages Having Converging or Diverging Boundaries," by A. H. Gibson, *Proceedings*, Roy. Soc. of London, Series A, Vol. 83, 1910, p. 366.

AMERICAN SOCIETY OF CIVIL ENGINEERS

Founded November 5, 1852

DISCUSSIONS

STABILITY AND STIFFNESS OF CELLULAR COFFERDAMS

Discussion

BY ROBERT F. LEGGET, D. P. KRYNINE, J. J. POLIVKA, AND KARL TERZAGHI

ROBERT F. LEGGET,[13] M. AM. SOC. C. E.[13a]—The use of steel sheet piling has increased so rapidly in the past twenty years, for both temporary and permanent civil engineering works, that the written records of the profession still contain all too few discussions of the many complex factors that must be considered in the design of structures consisting of this versatile rolled steel section. Professor Terzaghi's paper, therefore, has a double value: (*a*) It assembles much useful information on actual experience with cellular cofferdams in connection with a very thorough design study; and (*b*) it inevitably mentions some of the general characteristics affecting the use of steel sheet piling for other types of structures. Although discussion of these wider implications of the paper is not in order at this time, it is to be hoped that critical study of the paper will direct increased attention to these other points and thus lead, even if indirectly, to improvement of the art.

Professor Terzaghi is unusually forthright in condemning the application of the results of laboratory soil tests to the design of cellular steel pile structures, and he emphasizes the corresponding importance of observations on actual structures. The soundness of this empirical approach, especially in view of the many variable factors, will not be questioned at this stage in the development of steel piling design. However, some simple laboratory soil testing may provide useful and practical design information—such as how to determine the type of fill material and the degree of its conformity with the assumptions as to its properties made by Professor Terzaghi, as well as how to determine the friction between fill material and the surface of the steel piling.

Since this friction (admittedly an important factor in design) is a variable, the statement (see heading, "Part I. Practical Considerations: Deflection of

NOTE.—This paper by Karl Terzaghi was published in September, 1944, *Proceedings*. Discussion on this paper has appeared in *Proceedings*, as follows: December, 1944, by G. G. Greulich, and Raymond P. Pennoyer; February, 1945, by Dean P. Tsagaris; March, 1945, by R. T. Colburn, A. F. Hedman, and Adolph J. Ackerman; April, 1945, by Savile Packshaw, and Martin W. Lautz; and May, 1945, by J. S. Miller.

[13] Associate Prof., Civ. Eng., Dept. of Civ. Eng., Univ. of Toronto, Toronto, Ont., Canada.

[13a] Received by the Secretary May 2, 1945.

Cellular Cofferdams") that the "* * * elastic properties [of a cellular cofferdam] can be compared to those of a composite construction material such as reinforced concrete" is somewhat puzzling. Possibly, the author intended such a comparison to demonstrate the differences between the two combinations of materials. Some elaboration of the statement would be welcome.

Another frictional force, that developed in the interlocks of the steel sheet piling, is clearly one of the most important factors involved in the stability of cellular structures. It cannot be calculated on the basis of any theory in view of the many practical variables—the type of lock, the limits of clearance between the jaws of locks in contact, the nature of the material (if any) plugging the locks, and the relative position of "mating" locks (as determined by the way they are held by either the soil or the rock into which they have been driven). In view of the emphasis given in the paper to lock friction (see conclusion 3), it would be of great interest to know whether any experimentally determined values of lock friction have been developed for any type of steel pile or, alternatively, whether the author believes that such values could be obtained.

Lock friction is even more important than this paper would suggest; for, in the case of straight walls of deep-arch, steel sheet piling which retain lateral loading, the degree to which lock friction is developed determines whether the piles must be considered acting as individual units or, alternatively, whether the wall can be regarded as made of "interlocked units"—the lock friction exceeding the shear stress developed longitudinally in the lock. In some countries other than the United States, deep-arch piles have been developed which do give an "interlocked section modulus." In consequence, double-wall cofferdams have been used generally there instead of the cellular type of structure, which appears to be confined almost exclusively to American practice. Although it is probably outside the province of the paper, an economic comparison of the two types of piles would be of interest.

In view of this wider significance of lock friction, the author's condemnation of the practice of lubricating the interlocks of steel sheet piling will be most heartening to all who have had to argue about this matter with enthusiastic pile driving foremen. Unfortunately, his reasoned arguments will provide little useful "ammunition" for such on-the-job discussions; but they should go far toward clarifying not only this point but also many others in the minds of all those responsible for the design of structures of steel sheet piling.

D. P. KRYNINE,[14] M. AM. SOC. C. E.[14a]—Few formulas are as accurate as the Rankine formula as applied to cohesionless masses, such as cohesionless sand or gravel. If there are claims that actual pressures in a cohesionless mass are not in accordance with the Rankine formula, such claims possibly may be based on the fact that the formula in question has been used incorrectly. In particular, the value of C given by Eq. 20 is the ratio between the minor and the major principal stresses at a point of a cohesionless mass just immediately preceding the failure of that mass by shear, but, in a general case, the

[14] Research Associate in Soil Mechanics, Dept. of Civ. Eng., Yale Univ., New Haven, Conn.
[14a] Received by the Secretary May 7, 1945.

value of C given by Eq. 20 is not the ratio between the horizontal and the vertical pressure at the point in question.

Internal Shear in the Fill of a Cofferdam on Rock.—If the shear failure is expected to occur along a vertical plane, such as plane gh in Fig. 7(*b*), this direction is not a principal one because, by definition, there are no shears along principal axes. Hence, to compute the horizontal pressure on the plane of expected failure such as section gh in Fig. 7(*b*), Eq. 20 cannot be applied.

The well-known Mohr's circle can be applied for finding the ratio C between the horizontal and vertical pressures at a point on plane gh (Fig. 7(*b*)) at a depth Z from the top of the fill, just immediately prior to failure by shear. Simply draw a horizontal line and a circle of arbitrary radius with its center O on that horizontal line (Fig. 25). Draw a line tangent to a circle that will describe an angle ϕ intersecting the horizontal at point E, as shown in Fig. 25. Furthermore, draw both the diameter through the point of tangency B and the vertical line AEC. Then the ratio of the distances EF and EG is the ratio of the principal stresses at the given point as determined by Eq. 20. Distance AB is proportional to the normal pressure on the plane of failure (section gh in the given case, Fig. 7(*b*)), and distance CD is proportional to the pressure on the plane perpendicular to that plane of failure—that is, in the given case, the horizontal plane. Hence, the ratio of both distances AB and CD multiplied by γZ (which is the vertical pressure at the given point), is the horizontal pressure on plane gh at the given point. Simple algebra shows that the value of C for the plane of expected failure gh is

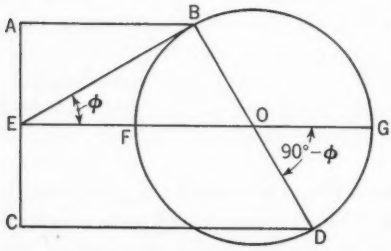

FIG. 25.—RANKINE FORMULA REPRESENTED GRAPHICALLY

$$C = \frac{\cos^2 \phi}{2 - \cos^2 \phi} \quad \ldots\ldots\ldots\ldots\ldots\ldots\ldots\ldots\ldots\ldots (41)$$

If the angle of friction equals 30°, the value of C given by the Rankine formula, if correctly interpreted, is 0.6, and not $(0.577)^2 = 0.33$, as determined by Eq. 20.

Recomputation of the Selected Example.—The factor of safety with respect to shear in the example immediately following Eq. 20 is $G_s = 0.87$. In the numerical formula for this factor of safety the value of $(0.577)^2$ must be replaced by 0.6, as explained in the preceding paragraph, which furnishes a corrected value of the factor of safety $G_s = 1.59$. Neglecting the friction in the locks—that is, dropping the value of 0.3 in the numerical formula in question—the factor of safety would be $G_s = 1$.

Perfect Safety of Plane gh (*Fig. 7(b)*) *with Respect to Shear.*—It will be assumed that Eq. 19*b* for the factor of safety G_s, with respect to shear, is correct except for the value of C which should be computed by Eq. 41. Consider a fill material weighing $\gamma = 110$ lb per cu ft with the angle of friction ϕ

varying from 30° to 40°. Let $\gamma_w = 62.5$ lb per cu ft and $f = 0.3$. Then for $\phi = 30°$:

$$G_s = 2 \times \frac{110}{62.5} \times \frac{b}{H} \times 0.6 \times (0.577 + 0.3) = 1.85 \frac{b}{H} \ldots\ldots (42a)$$

Similarly, for $\phi = 40°$,

$$G_s = 1.65 \frac{b}{H} \ldots\ldots (42b)$$

Since Eq. 42*b* is less favorable than Eq. 42*a*, compute the values of the safety factor for $\phi = 40°$, as follows:

Ratio $\frac{b}{H}$	Safety factor G_s
0.85	1.4
1.00	1.65

Hence, under the given assumptions, plane gh is always safe with respect to shear. It is no miracle and no paradox, therefore, that many cofferdams wide enough, but with factors of safety of 0.6 or 0.7 incorrectly calculated, stand safely. Their true factor of safety with respect to shear certainly is greater than 1.

These considerations do not mean, however, that a shear failure cannot occur in a cellular cofferdam. They mean simply that under the given assumptions shear cannot occur along plane gh (Fig. 7(*b*)).

Phenomenon of Internal Shear in a Cofferdam on Rock.—In 1935, R. P. Pennoyer, Assoc. M. Am. Soc. C. E. (10*c*),[14b] called the attention of the profession to the possibility of internal shear along the vertical plane gh (Fig. 7(*b*)). Professor Terzaghi also considers this plane dangerous with respect to shear. The writer, however, visualizes the possibility that internal shear can occur in a still different way. When the cofferdam begins to tip, it comes from the initial position ABCD into some other position AB′C′D (Fig. 26(*a*)). As the

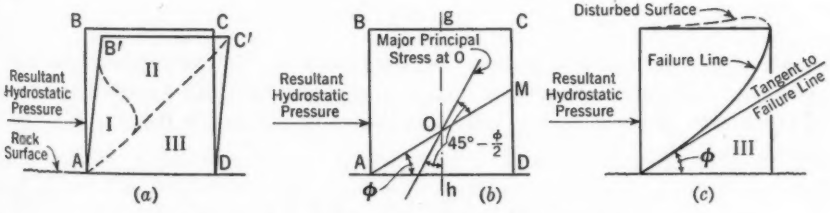

FIG. 26.—INTERNAL SHEAR IN A CELLULAR COFFERDAM

tipping of the cofferdam progresses, the density within the compressed zone I (and perhaps the size of this zone) increases until a certain critical density has been reached. Zone I then bursts and pushes zone II upward. To bring this picture back to the Rankine formula, it should be remembered that at any point O of a mass (Fig. 26(*b*)) there are actually two directions of maximum

[14b] Numerals in parentheses, thus: (10*c*), refer to corresponding items in the Bibliography (see Appendix I of the paper), and at the end of discussion in this issue.

shear—not one. Each of these makes an angle $45° - \frac{\phi}{2}$ with the direction of the major principal stress. It follows that, if point O (Fig. 26(*b*)) is located in plane gh, there is, at that point, another possibility of shear along plane AOM making an angle ϕ with the horizon. The hydrostatic pressure pushes the mass up along a plane AM making an angle ϕ at point O (Fig. 26(*b*)) with the horizon, to meet the inside wall of the cofferdam, MC. The actual failure probably occurs as shown in Fig. 26(*c*). An observer standing at the top of the cofferdam possibly would report that, in the case of shear failure, all sand grains and all rocks and pebbles of the mass were moving. In reality there is probably a zone of quiet marked III in Fig. 26(*a*) and 26(*c*). A simple inspection of Fig. 26(*c*) shows that, to offer due resistance, the failure line must be sufficiently long. In other words, a guarantee against possible shear failure is the widening of the cofferdam.

Overturning of the Cofferdam on Rock.—Unless a shear failure in the fill occurs, the cofferdam is exceedingly stable with respect to overturning. If there is no water outside the cofferdam the fill material is pressed against the outside wall by the active pressure $\frac{1}{2} \gamma C H^2$, the value of C being smaller than that at the plane gh (Fig. 7(*b*)). To be conservative, it will be assumed that C may be computed using Eq. 20. If there is water outside the cofferdam, the pressure of the fill material, in addition to active pressure, is applied against the outside wall by the full hydrostatic pressure due to flexibility of the sheet piles. To start overturning, friction between the fill material and the outside wall must be overcome. The situation is very similar to that of a man who wants to lean to the right but cannot do so because his left leg is deep in a sticky swamp; the first thing for him to do is to pull his leg out of that swamp. In the case of the cofferdam, the friction is tantamount to a vertical force acting downward at the outside wall. Neglecting the weight of the cofferdam entirely, the factor of safety with respect to overturning would be:

$$G_s = \frac{(\frac{1}{2} \gamma C H^2 + \frac{1}{2} \gamma_w H^2) b \tan \delta}{\frac{1}{6} \gamma_w H^3} \quad \ldots\ldots\ldots\ldots (43a)$$

in which the term $\tan \delta$ denotes the coefficient of friction between fill and sheet-pile enclosure. Assuming, furthermore, that the width b is some fraction of the height H, such as $b = a H$, and the value of $\tan \delta = 0.4$, Eq. 43*a* may be rewritten thus:

$$G_s = 1.2 a \left(\frac{\gamma C}{\gamma_w} + 1 \right) \quad \ldots\ldots\ldots\ldots\ldots\ldots (43b)$$

For current values of a, C, γ, and γ_w, this safety factor is always greater than 1.4. It should be recalled that Eqs. 43 were developed neglecting the weight of the fill inside the cofferdam completely, so that at least a value of 1.4 should be added to the value of the factor of safety computed as recommended in the paper. In the example selected to illustrate this procedure a total of $2 + 1.4 = 3.4$ should be computed, which is very close to 3.8 as determined by the usual gravity wall method.

Sliding of the Cofferdam on Rock.—Fig. 7(*a*) is of rather academic interest and perhaps should have been omitted. It is questionable whether the boundary corrections should be introduced in this diagram since discontinuity of stresses (but not of strains) is acceptable. Corrected as it is, the area shown in Fig. 7(*a*) is less than the value of F as given by Eq. 1. This fact implies the necessity of correcting the ordinates at the middle of the diagram and thus changing the given value of the angle of friction. Finally, boundary corrections, if any, should be extended through the diagram to meet somewhere at the middle of the curve and not be connected to the curve at some arbitrary points. What is important, however, is not the diagram but that "There seems to be no record of a failure by sliding" as Professor Terzaghi states (see heading, "Part II. Design of Cellular Cofferdams: General Considerations"), and this apparently settles the question of sliding.

Conclusion.—The designer of a cellular cofferdam on rock must ensure close cooperation between the sheet-pile enclosure and the inside fill, making them work together and preventing their possible separation by internal shear. Attention should be paid to: (*a*) A good packing of the gravel and sand fill inside the cofferdam in order to increase the horizontal pressure and (*b*) a good interlock arrangement. The size of sheet pile should be selected properly and the cofferdam should be given ample width, the latter item being of extreme importance. To design and analyze such structures good engineering judgment and vast experience in the given field combined with clear understanding of statics are needed. A great number of cellular cofferdams have been constructed successfully in the United States—incomparably more than in other countries. It is obvious therefore that American engineers have demonstrated fully their ability to design and to build these structures, both permanent and temporary.

J. J. POLIVKA,[15] M. AM. SOC. C. E.[15a]—In the field of cellular cofferdams this excellent paper is a valuable contribution to engineering knowledge. In July, 1944, the writer had the opportunity to make some preliminary studies on cellular cofferdams in the Kaiser Shipyards at Richmond, Calif. These cofferdams had been constructed in February–March, 1945, for the U. S. Maritime Commission, preliminary to deepening the existing concrete-lined basins. In many respects the basins resembled graving docks, 100 ft by 590 ft in plan, and originally were built behind the protection of a cofferdam made with part of the rock excavation (37).

Semicircular walls were built consisting of a series of cellular cofferdams, each 40 ft in diameter and 51 ft in average depth, connected by short arcs of 9-ft radius (Figs. 27 and 28). Since the cofferdams rest on a rock foundation, a fill approximately 10 ft deep was placed before driving sheet piles (Fig. 29).

---

[15] Lecturer, Univ. of California, Cons. Engr., Kaiser Co., Berkeley, Calif.

[15a] Received by the Secretary May 9, 1945.

Studies and tests were made to determine:

(*a*) The relation between the overturning moment and the weight of the fill for different ratios H/r;

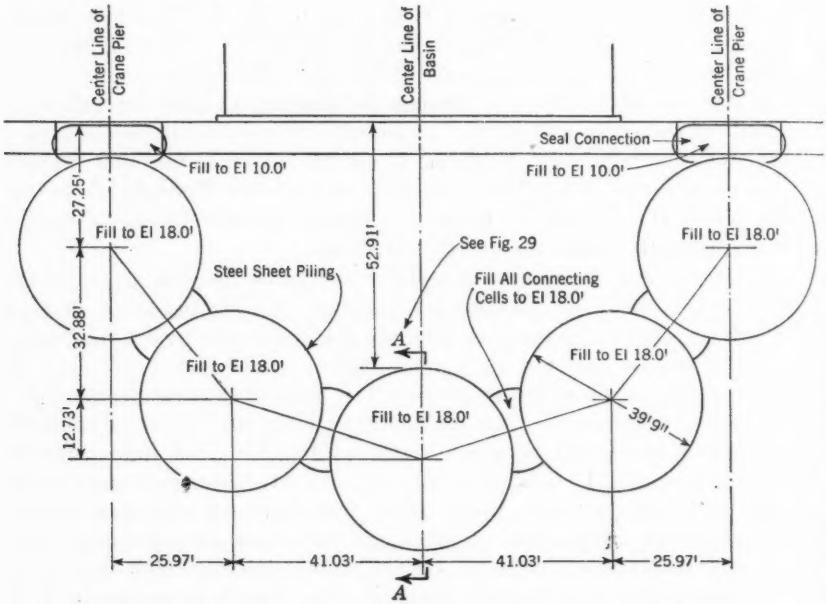

FIG. 27.—PLAN OF CELLULAR COFFERDAM, KAISER SHIPYARD, RICHMOND, CALIF.

FIG. 28.—VIEW OF CELLULAR COFFERDAM

(*b*) The effect of the arch-web sheet piles on the safety of a cellular cofferdam; and

(*c*) The effect of the arch-shaped wall of the cofferdam cells upon the stability.

(*a*) *Relation Between the Overturning Moment and the Weight of the Fill for Different Ratios H/r.*—The results of the investigations under item (*a*) are in good agreement with the author's shear theory of the cofferdam presented in

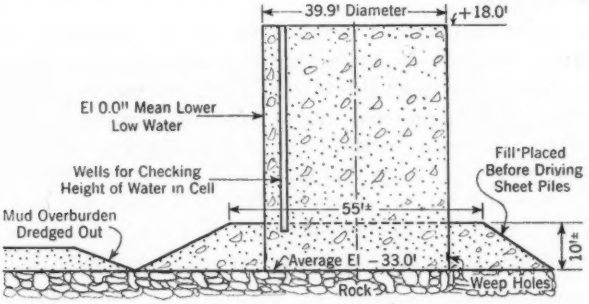

FIG. 29.—SECTION A-A OF CELLULAR COFFERDAM (SEE FIG. 27)

this paper. Fig. 30 shows some of the test installations. The standard formula for the pressure on a solid retaining wall, assuming that the full weight of the fill is acting, cannot be applied to a cofferdam consisting of a steel shell and containing more or less cohesive, plastic fill, with a variable degree of water saturation. This fact can be demonstrated by simple and inexpensive tests on small specimens made of thin sheet metal, thus simulating the cofferdam by a continuous smooth shell without irregularities of interlock. The minimum interlock strength of the sheet piles in the prototype is from 8,000 lb per lin in. to 12,000 lb per lin in. which, in the case of a $\frac{3}{8}$-in. web, is equal to from 21,333 lb per sq in. to 32,000 lb per sq in. In practical cases the stress ordinarily does not reach 50% of the latter values so that the effect of the interlock can be neglected. In the writer's investigations, the specimens simulating the cofferdams were made of plain sheet metal, 0.004 in. thick (see Fig. 30).

TABLE 2.—RELATION BETWEEN THE OVERTURNING MOMENT AND THE WEIGHT OF THE FILL FOR DIFFERENT RATIOS H/r

Specimen No.	Radius r (in.)	Ratio H/r	Weight W (lb)	Overturning moment M (lb-in.)	M/W	Overturning moment[a]	V (lb)
1	3.5	1.72	12.0	17.7	1.5	17.5	3.2
2	3.0	2.00	8.8	12.5	1.4	12.6	2.7
3	2.5	2.40	6.1	8.1	1.3	8.2	2.1
4	2.0	3.00	3.9	5.0	1.3	4.9	1.5
5	1.5	4.00	2.2	2.6	1.2	2.6	1.1
6[b]	1.5	4.00	2.4	3.1	1.3	3.2	1.4

[a] Computed by Eqs. 5 and 6. [b] Special shape; see text.

With height (H) equal to 6 in. and with radii varying from 1.5 in. to 3.5 in., most of the ratio values of H/r occurring in practice were represented. The greater stiffness of the shell can possibly affect the result of test to a certain extent. A very fine sand was used as fill, for which, approximately, $\phi = 26.5°$ and $\gamma = 90$ lb per cu ft.

Table 2 shows the values of the weight and overturning moment of individual specimens as determined by measurements. It also shows the overturning moments computed from the total average shearing resistance exerted by the fill on the shell.

The shear resistance against overturning can be computed from the frictional resistance obtained by measuring the vertical force, V, necessary to overcome the friction between the fill and the inner surface of the cylindrical shell. The shear or sliding force acting upon the inner surface of the cylindrical shell can also be computed on the basis of a theory of arching as presented by the author in 1943 (17*a*). Applying this theory (which was originally developed for the yielding of a rectangular base) to a segment of a circle, representing the base of a circular cofferdam, the vertical stress σ_v on a horizontal section at the depth z below the surface of the fill is

$$\sigma_v = \frac{\frac{r}{2}\left(\gamma - \frac{2c}{r}\right)}{K \tan \phi}(1 - e^{-n}) + q\, e^{-n} \quad \ldots\ldots (44)$$

in which

$$n = \frac{z}{r} K \tan \phi \quad \ldots\ldots (45)$$

and, in addition to the notation of the paper: K is a coefficient $= \sigma_h/\sigma_v = 1$; q is the additional unit load upon the fill; e is the base of Napierian logarithms; and c is cohesion in Coulomb's equation. The horizontal pressure exerted by the fill upon the unit length of the cofferdam is

$$\sum_h = \int_0^H \sigma_h \, dz \quad \ldots\ldots (46)$$

and the force, v, which it is necessary to apply in a vertical direction to overcome the friction between the fill and the inner surface of the circular cofferdam, per unit length of the circumference, is

$$v = \sum_h \times \tan \delta \quad \ldots\ldots (47)$$

in which δ is the angle of the wall friction. The total force V is then

$$V = 2\pi r v \quad \ldots\ldots (48)$$

It has been found that the vertical force V computed from Eqs. 44, 46, and 47 agrees with the results of tests. For sand as fill material, the cohesion, c, is equal to zero, and Eq. 46 has the simplified form

$$\sum_h = \sum_v = r\gamma \int (1 - e^{-z/(2r)})\, dz = r\gamma A \quad \ldots\ldots (49)$$

assuming that $K \tan \phi = \frac{1}{2}$.

The term A can be computed by Simpson's rule or by substituting the irregular area with the base $b = (1 - e^{H/(2r)})$ and the height H by a triangle and a parabolic segment:

$$A = \frac{b\,H}{2} + \frac{2}{3} H\, b_0 \quad \ldots\ldots (50)$$

in which $b_0 = b' - \frac{b}{2}$, the dimension b' being the value of b for $z = \frac{H}{2}$.

This method of determining the value of V will be demonstrated for a case in which the ratio H/r is equal to 1.72 (Table 2). Assuming further

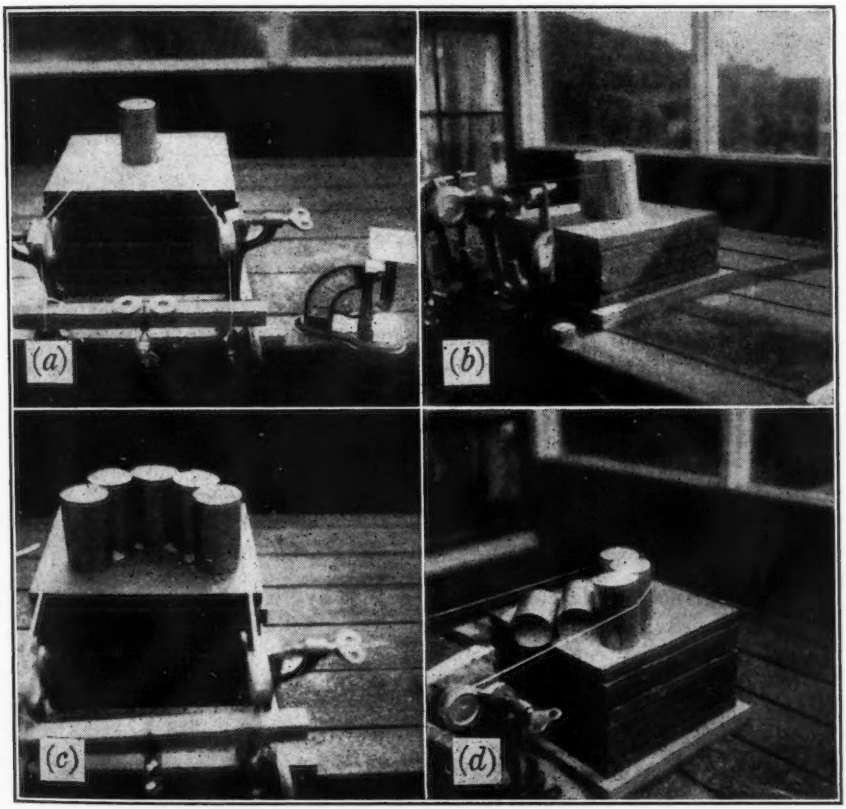

FIG. 30.—LABORATORY DEVICES FOR STUDYING CELLULAR COFFERDAMS

that the fill material is cohesionless ($c = 0$), the angle of internal friction $\phi = 26.5°$ ($\tan \phi = 0.5$), the wall friction (friction between the fill and the sheet piles of the cofferdam) $\tan \delta = 0.4$, the unit weight of the fill $\gamma = 0.052$ lb per cu in., and no additional load upon the fill ($q = 0$), the following values are obtained: $b = 0.57876$; $b' = 0.34929$; and $b_0 = 0.34929 - 0.28938 = 0.05991$. The term $A = \frac{5.665 \times 0.1 \times 6}{1.72} = 1.976$, or, from the simplified Eq. 50, $A = 0.57876 \times \frac{6}{2} + 4 \times 0.05991 = 1.976$. The exponential values can be arranged as shown in Table 3.

The total horizontal pressure of the fill on the linear unit of the circumference of the cofferdam, by Eq. 49, is $\Sigma_h = 3.5 \times 0.052 \times 1.976 = 0.3596$ lb; the elemental vertical force (Eq. 47) is $v = 0.3596 \times 0.4 = 0.1438$ lb; and the total vertical force is $V = 2 \times 3.1416 \times 3.5 \times 0.1438 = 3.16$ lb. The measured value was 3.2 lb, so that the agreement with the test is good. The values of V for other specimens were computed similarly (see Table 2).

TABLE 3.—COMPUTATIONS FOR ARCHING EFFECT IN THE FILL

z/r	n (Eq. 45)	e^{-n}	$e^{-n}\,z$	$1 - e^{-n}$	$(1 - e^{-n})\,z$	A (Eq. 50)
tan ϕ	0.5	0.95123	0.475	0.04877	0.025	....
0.1	0.05	.....	.....	.....	.....	....
0.5	0.25	0.77880	3.925	0.22120	0.575	.....
1.0	0.50	0.60653	7.371	0.39347	2.129	2.111
1.5	0.75	0.47237	10.053	0.52763	4.447	.....
2.0	1.00	0.36788	12.143	0.63212	7.357	7.353
2.5	1.25	0.28650	13.771	0.71350	10.729	.....
3.0	1.50	0.22313	15.039	0.77687	14.461	14.437
3.5	1.75	0.17377	16.026	0.82623	18.474	.....
4.0	2.00	0.13534	16.795	0.86466	22.705	22.521

The small differences between the computed and measured values may be explained as follows:

(1) Inaccuracy in the measuring devices;

(2) A slightly higher value of the coefficient of friction between the fill and the wall ($\tan \delta = 0.41 - 0.43$) as introduced in the analysis (0.4);

(3) Variable value of the coefficient K, assumed in the analysis to be equal to 1, but increasing to $K = 1.5$ for higher elevations (38).

If an external couple created by external hydrostatic pressure tends to overturn the circular cell, this external couple will be resisted by the skin friction (friction between the fill and the shell). At the critical instant the internal couple of the force V in the formula

$$M_i = V\,d_0 \qquad (51)$$

will balance the external couple; that is, $M_e = M_i$. Thus the overturning moment of a cellular cofferdam can be determined readily if the values V and d_0 are known. The value V is given by Eqs. 47, 48, and 49, and the lever arm d_0 of the internal forces V can be determined under the assumption that the intensity of the friction between fill and shell follows a straight line, as shown in Fig. 31. In that case,

$$d_0 = r\,\frac{\int_0^{\pi} \sin^2\phi\,d\phi}{\int_0^{\pi} \sin\phi\,d\phi} = \frac{\pi\,r}{2} = 1.57\,r \qquad (52)$$

The values of the overturning moment computed by Eqs. 51 and 52 differ only slightly from the measured values (see Table 2). Table 2 contains also a specimen with folded shell (Fig. 32) which was included in the tests in order

to determine the effect of the increased surface (circumference) of the shell upon the overturning moment. Such a case occurs when sheet piles with arched webs are used. The base of specimen No. 6, Table 2, was 7.6 sq in., and its circumference was 10.5 in.—12.5% greater than that of specimen No. 5.

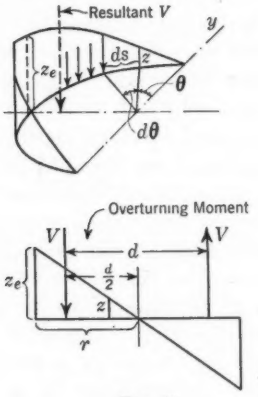

FIG. 31

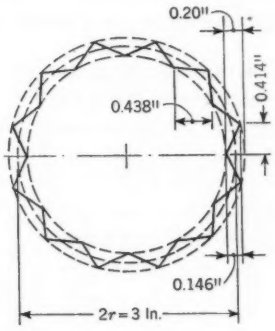

FIG. 32.—FOLDED SHELL TYPE OF COFFERDAM

It might be of interest to compare the values of overturning moment which resulted from the tests with those obtained by applying Eq. 17 to a continuous shell. Such a continuous shell simulates a sheet-pile wall without any slippage in the interlock joints. The use of Eq. 17 for this special case may be questioned, because it is necessary to substitute $f = 1$ in Eq. 17 in order to express the condition of unyielding interlocks of the cofferdam. Eq. 17 becomes then

$$S = \tfrac{1}{2}\,\gamma\, C\, H^2\,(\tan\phi + 1) \ldots\ldots\ldots\ldots\ldots\ldots (53)$$

In accordance with Eq. 21, the coefficient of earth pressure, C, is greater than $\tan^2(45° - \phi/2)$. Substituting the values of the tested specimens: $\gamma = 0.052$ lb per cu in., $\phi = 26.5°$, $H = 6$ in., and assuming $C > 0.383 = 0.4$, the average shearing resistance becomes $S = \frac{1}{2} \times 0.052 \times 0.4 \times 6^2 \times 1.5 = 0.562$ lb per inch of width of the neutral plane. According to the author, the critical overturning moment may be expressed as an internal couple of the shearing resistance S; that is:

$$M_e = S\,(2\,r)\,d'_0 \ldots\ldots\ldots\ldots\ldots\ldots\ldots\ldots (54)$$

The lever arm d'_0 will be smaller than $\frac{2}{3}\,b$ (Figs. 7(*b*) and 7(*d*)). Assuming that $d'_0 = \dfrac{4\,r}{\pi}$ (which is the distance of centroids of two semicircles), the overturning moment equals

$$M_e = \frac{8}{\pi} S\, r^2 = 1.43\, r^2 \ldots\ldots\ldots\ldots\ldots\ldots\ldots (55)$$

Table 4 shows the values of overturning moment computed from Eq. 55 as compared with test results and values obtained from Eqs. 51 and 52. A better agreement between the measured overturning moments and their values

calculated from Eq. 17 (Col. 3, Table 4) would be obtained by a variable coefficient of earth pressure, C, decreasing with an increasing ratio H/r, as shown in Col. 4, Table 4.

(*b*) *The Effect of Arch-Web Sheet Piles Upon the Safety of a Cellular Cofferdam.*—It should be emphasized that all investigations by the author regarding the shearing resistance on vertical sections through the fill in the cells and the lock friction are valid only for cellular cofferdams with straight-web sheet piles. If arch-web sheet piles are used, the total tension in a lock, expressed by Eq. 14*a*, will produce considerable deformation in the cofferdam shell. In the lower parts of the cofferdam the deformation may be beyond the elastic limit, resulting in an increase of 10 in. or more in the diameter of the cell. The bulge in such a case is quite noticeable. Any deformation of a structure beyond the elastic limit can be classified as failure, although several cofferdams of this type did not collapse, and served the purposes for which they were built. The total resistance against slippage in the lock will increase with bulging of the shell, since the total resistance against slippage increases with the increasing radius, as expressed by Eq. 14*b*.

TABLE 4.—COMPARISON OF OVERTURNING MOMENTS

Specimen No.	Overturning Moment in Inch-Pounds, Obtained from:			C
	Tests (1)	Writer (2)	Author (3)	(4)
1	17.7	17.5	17.5	0.40
2	12.5	12.6	12.9	0.39
3	8.1	8.2	8.9	0.37
4	5.0	4.9	5.7	0.35
5	2.6	2.6	3.2	0.33

In the case of the cofferdam in the Kaiser Shipyards, the maximum tension in the locks, computed by Eq. 13, is $t_{max} = r \gamma C H = 20 \times 110 \times 0.5 \times 41 = 45{,}100$ lb, or in sheet piles with $\frac{3}{8}$-in. web: $\frac{45{,}100}{0.375 \times 12} = 10{,}020$ lb per sq in. If arch-web sheet piles were used (for example, M112), the eccentricity of the interlock will produce bending of the sheet piles in a horizontal direction. The additional stress computed from the standard formula is so high $\left(\frac{45{,}100\ (1\frac{11}{32} - \frac{3}{16})}{0.28} = 185{,}531 \text{ lb per sq in.}\right)$ that the eccentricity ($1\frac{11}{32}$ in. $-\frac{3}{16}$ in.; see e in Fig. 33) will gradually decrease as the arch-web sheet piles stretch. In any case, the combined stress in the sheet piles will reach the yield point and cause permanent deformation as described previously.

The answer to the questions as to the approximateness of Eq. 13, and the nature of the two-dimensional stress conditions, can be attempted theoretically, considering the cellular cofferdam as a thin shell restrained at the bottom along its circumference. The results of any theoretical investigation of a problem, in which so many uncertain and indeterminate values are involved, must be approached with extreme caution. The analytical solution indicates deformation and stress distribution very similar to observations on actual cofferdams.

The horizontal force $P_s = Q_0$ (see Fig. 8) which is applied at the lower edge of the sheet piles in order to maintain equilibrium, and the restraining

moment M_0 may be calculated (39) from the equations:

$$Q_0 = -\frac{\gamma\, r\, H\, h_2}{\sqrt{12\,(1-\nu^2)}}\left(2\,\beta - \frac{1}{H}\right) \ldots\ldots\ldots\ldots\ldots (56a)$$

and

$$M_0 = \frac{\gamma\, r\, H\, h_2}{\sqrt{12\,(1-\nu^2)}}\left(1 - \frac{1}{\beta\, H}\right) \ldots\ldots\ldots\ldots\ldots (56b)$$

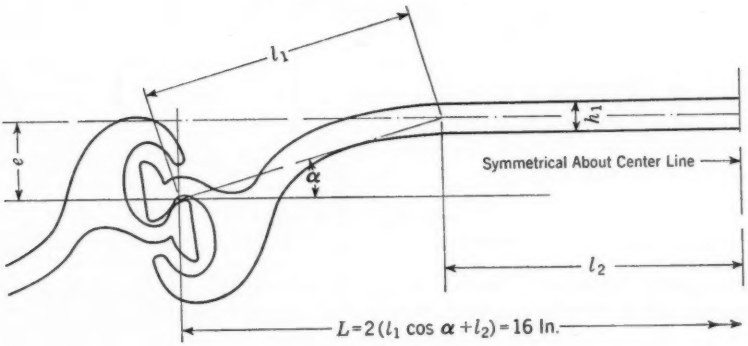

FIG. 33

in which h_2 is a "theoretical thickness" of sheet piles derived from the section modulus S; thus,

$$h^2{}_2 = \sqrt{\frac{6\,S}{12}} = 0.7071\,\sqrt{S} \ldots\ldots\ldots\ldots\ldots (57)$$

In Eqs. 56, furthermore, ν is Poisson's ratio for steel = 0.25; and β is computed from

$$\beta^4 = \frac{3\,(1-\nu^2)\,h_1}{r^2\,h^3{}_2} \ldots\ldots\ldots\ldots\ldots (58)$$

In Eq. 58, h_1 is the actual web thickness of sheet piles. The values $N_{z'}$ and $M_{z'}$ for any depth $z' = H - z$ are expressed (39) by:

$$N_{z'} = -E\,\frac{h_1\,w}{r} = \gamma\, r\, H\left[1 - \frac{z'}{H} - \theta\,(\beta\, z') - \left(1 - \frac{1}{\beta\, H}\right)\zeta\,(\beta\, z')\right] \ldots (59a)$$

and

$$M_{z'} = -D\,\frac{d^2w}{dz^2} = \frac{\gamma\, r\, H\, h_2}{\sqrt{12\,(1-\nu^2)}}\left[-\zeta\,(\beta\, z') + \left(1 - \frac{1}{\beta\, H}\right)\theta\,(\beta\, z')\right] \ldots (59b)$$

in which

$$\theta\,(\beta\, z') = e^{-\beta z'}\cos \beta\, z' \ldots\ldots\ldots\ldots\ldots (60a)$$

and

$$\zeta\,(\beta\, z') = e^{-\beta z'}\sin \beta\, z' \ldots\ldots\ldots\ldots\ldots (60b)$$

The preceding values can be applied only for straight-web sections (see Table 5).

For arch-web sections, such as Carnegie Steel sections M112 and M113, or Inland sections (see Fig. 33) a modification of the formulas is necessary, expressing greater elastic displacements in circumferential direction due to bending of sheet piles. This effect can be attained theoretically by introducing

TABLE 5.—CHARACTERISTICS OF STRAIGHT-WEB SHEET PILES

No.	Section	Cross-section area A (sq in.)[a]	Section modulus S (in.^{3})[a]	Weight (lb)[a]	h_1 (in.)	h_2 (in.)	β (in.$^{-1}$)
A	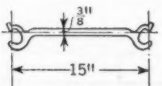	9.1	3.0	31	0.375	1.225	0.0563
B	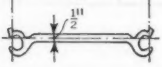	10.3	3.1	35	0.5	1.245	0.0598

[a] Per linear foot of wall.

an imaginary modulus of elasticity, E_1, for calculating elastic elongations in a circumferential direction, which is considerably smaller than the modulus of elasticity, E_2, expressing the stress-strain ratio in vertical direction of the sheet pile.

The ratio $\frac{E_1}{E_2}$ $\left(\text{equal to } \frac{1}{100} \text{ approximately for section M112}\right)$ can be calculated under the assumption that the elastic displacement (expansion) of an arch-web sheet pile considered as an elastic bent is equal to the elongation of an imaginary straight-web sheet pile having a modulus of elasticity, E_1.

The computations confirm the fact that arch-web sheet piles must be avoided for cofferdams having a lateral (horizontal) tension (from two-dimentional stress condition). For cellular cofferdams only straight-web sheet piles should be used (see Table 5).

In all literature pertaining to cellular cofferdams to which the writer has had access, there was no statement to the effect that, for cellular cofferdams where a circumferential tension can occur, it is inadvisable and even dangerous to use arch-web sheet piles. Examination of the literature has shown that in very many cases the use of the arch-web sheet piles resulted in bulging or failure.

KARL TERZAGHI,[16] M. AM. SOC. C. E.[16a]—The discussion of this paper has been eminently constructive; any one who faces the problem of designing a cellular cofferdam will find in the discussions an inexhaustible source of information and guidance. Therefore, the profession as a whole is indebted to the discussers for the generosity with which they contributed from the store of their experience.

One of the principal theses of the paper is that the customary stability computations of cellular cofferdams based on the gravity concept need to be

[16] Cons. Engr. and Lecturer, Graduate School of Eng., Harvard Univ., Cambridge, Mass.

[16a] Received by the Secretary May 22, 1945.

supplemented by an inquiry into the stress conditions in the fill constituting the body of the cofferdam. This conclusion was forced upon the writer by the results of observations made on a large cofferdam during 1941 and 1942. According to the gravity concept, the dam should have been stable; yet the observations left no doubt that the dam would be unable to stand the unbalanced horizontal pressures unless the shearing resistance of the earth in the cells was increased by artificial methods. These methods were adopted and their effect actually demonstrated the efficacy of the procedure.

Some of the discussions revealed the fact that the engineers on the staff of the Tennessee Valley Authority (TVA) arrived at similar conclusions at an earlier date. The TVA engineers checked all their designs for what they called "internal shear," and for this purpose they used a method similar to the one proposed by the writer. This is more than a mere coincidence. It indicates that the time was ripe for this new development, and the writer acknowledges with pleasure that the credit for the corresponding modification of the design procedure belongs to the TVA engineers.

Mr. Greulich expresses the opinion that the inward deflection of a cellular cofferdam is associated with an important increase of the resistance against sliding in the interlocks of the cross-walls, equivalent to the introduction of stay rods from the inner top to the outer base of the cell. The lock friction as such, because of the hoop tension in the walls of the cells, has the mechanical effect of stay rods, because it counteracts the distortion of the cross-walls. However, it seems doubtful that the inward deflection of the cofferdam is associated with an increase of the lock friction. If such an increase occurs, it can scarcely be evaluated rationally.

Commenting on the depth to which the sheet piles for cofferdams on deep sand strata should be driven, Mr. Greulich contends that $H/2$ would be ample. His argument is that the sand in the cells can grip only one side of the sheet piles whereas when driven into the sand the piling is gripped on both sides. This argument can be accepted for the outer row, but it does not apply to the inner row. On the inner side of the inner row the water percolates through the sand in a vertical upward direction (see Fig. 9(*c*)). This process reduces the skin friction very considerably. An extreme possibility for this reduction was demonstrated by the following incident. An excavation was made by dredging in dense sand between sheet piles for a small dry dock in the vicinity of Hamburg, Germany. Prior to pumping, 1,500 wood piles were driven between 12 ft and 15 ft into the sand. No deeper penetration by driving could be obtained without breaking the piles. The pile cutoff was a short distance above grade. When the water level was lowered within the sheet-pile enclosure by about 8 ft, the piles began to rise one by one; yet the seepage pressure was not important enough to cause the sand to boil. It merely reduced the total skin friction of the pile to less than the hydrostatic uplift.

The total seepage pressure which acts on the sand adjoining the inner side of the inner row of sheet piles depends on details of stratification which are unknown. Hence, in some instances, a penetration of $H/2$ may be more than ample and in others not enough.

At the end of his discussion, Mr. Greulich requests an amplification of conclusion 2 of the paper and he also comments on conclusion 5. Conclusion 2 refers to the distribution of the soil pressure over the base of cellular cofferdams with conventional dimensions. According to the results of the analysis given in the paper, the application of an unbalanced horizontal force on such a cofferdam has very little, if any, effect on the distribution of the pressure on the base. In other words, the pressure distribution remains practically uniform. The entire overturning moment is transferred through skin friction on to that part of the sheet piles which is located below the base of the cofferdam. In conclusion 5 the writer implied that the ratio between the horizontal and the vertical pressure in the fill in the cells is greater than the Rankine value. Hence, the Rankine value is not on the conservative side as suggested by Mr. Greulich.

In several paragraphs of his discussion Colonel Pennoyer expresses the opinion that the paper involves an attempt to supersede the design method based on the gravity concept by proposing a standard ratio between width and height. Thus, he states:

> "* * * the writer feels that Professor Terzaghi has oversimplified the problem by assuming a cell width of 0.85 H and a conversion factor of 0.4 to develop the bursting pressures."

This, and many other similar passages in Colonel Pennoyer's discussion, indicate that the paper was not explicit enough to eliminate the possibility of misunderstandings in the minds of at least some readers. To clarify the issue, the following synopsis of the basic reasoning is submitted.

The stability and stiffness of cellular cofferdams depend on a great number of factors including the foundation conditions and the shearing resistance of the fill occupying the cells. Even under the simplest conditions, involving a cofferdam filled with sand and gravel resting on a solid foundation, theory alone cannot be relied upon because one of the most important factors—the ratio between horizontal and vertical pressure in the soil which occupies the cells—cannot be computed. This fact has been known ever since the first measurement of the side pressure in grain bins was made. Therefore, the designer depends to a certain extent on data derived from experience.

During the twenty years since 1925 a great number of cellular cofferdams have been built which have the following features in common: The sheet piles are driven through sand to bedrock; the cells are filled with sand or sand and gravel; the cofferdams are acted upon by one-sided water pressure; and the average (not the maximum) width of the cofferdams is roughly equal to 0.85 H. Since all these cofferdams gave satisfactory service, they constitute useful precedents and prototypes. To apply the experiences incorporated in the prototype to the design of cellular cofferdams to be built under different conditions of foundation and loading, the writer investigated the influence of several commonly encountered deviations from the prototype on stiffness and stability. If these influences are clearly recognized, the dimensions and proportions of the prototype can be changed in accordance with the findings. No claim is made that all the conceivable deviations from the prototype are

covered, because such an attempt would obviously transcend the scope of a single paper. For the same reason, the discussions are limited strictly to cellular cofferdams filled with sand. As a matter of fact, cellular cofferdams filled with other soils are rather exceptional, as demonstrated by the construction record of the Dravo Corporation and the TVA.

Cellular cofferdams are commonly considered major structures and the uncertainties involved in their design are generally recognized. Hence, it goes without saying that no responsible engineer will consider the design of such cofferdams a routine problem under any except very simple conditions. Every scrap of available information should be utilized; and every known theoretical approach, including the stability computation based on the gravity concept, should be made before final decisions are reached. The design of the Kentucky cofferdam described by Messrs. Tsagaris, Colburn, and Hedman is an outstanding example. If two different approaches lead to different results, the more unfavorable one will be accepted.

Colonel Pennoyer comments on the writer's assumption that the soil fails along a vertical plane and calls the assumption fallacious. He further states:

> "What actually happens is that the entire mass of confined soil changes shape simultaneously. This action can best be described as a universal plastic flow, or distortion * * *."

The writer's concept of the process of failure is essentially identical with that described by Colonel Pennoyer, and the equations which were derived by the writer are merely mathematical expressions of the stress conditions required for producing this type of failure. Since the original explanation of the physical meaning of the equations was apparently not explicit enough to avoid a misunderstanding, the following discussion is presented in the hope of clarifying the issue. Fig. 34 is a vertical section through a mass of soil confined between two straight rows of sheet piles, not interconnected by cross-walls. The soil is assumed to adhere to the piles, and the resistance of the sheet piles against bending at ground level in the plane of the drawing is assumed negligible.

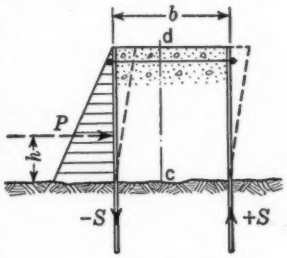

FIG. 34

As soon as a horizontal force P is applied at an elevation h above the ground surface, the outer row of sheet piles is pulled by a force $-S$, and the inner row is pushed down by the same force S. The force S is equal to the overturning moment $M = P\,h$ divided by the distance b between the two rows. The horizontal force P produces a change of shape as described by Colonel Pennoyer. As soon as the horizontal force exceeds a certain critical value, the distortion increases at a constant rate and the cofferdam fails by tilting forward more and more—whereby the cross section of the dam changes from a rectangle into a parallelogram with equal area. Since there are no cross-walls, the failure by plastic flow starts simultaneously at every point in the confined mass of soil. The failure occurs by shear along an infinite number of vertical planes. According to the theory of plastic materials, failure occurs

as soon as the total shearing force on any vertical section such as cd becomes equal to the shearing resistance on this plane; and, according to the laws of mechanics, the shearing force is equal to S.

If the dam shown in Fig. 34 is reinforced by cross-walls consisting of sheet piles, the presence of these walls complicates the process of failure to some extent. Instead of starting at every point at the same time, the plastic flow spreads from the neutral plane toward the walls. However, the laws that determine the conditions of failure are identical with those cited previously.

Colonel Pennoyer maintains that, if the coefficient of lock friction of 0.3

> "* * * was assumed analogous to the coefficient of friction of steel on steel, the statement would seem fallacious. Interlocks of sheet piling are designed * * * with emphasis on reducing the area of contact between surfaces to a minimum * * *. There is no relation between the frictional value of two pieces of steel in what amounts to line contact and the coefficient of friction of steel on steel times a tension force per unit of length, when no area of contact can be assumed."

The value of 0.3 assumed by the writer really is nothing more than the coefficient of friction of steel on steel. According to sources available to the writer (40), the coefficient of friction for metal on metal, dry, ranges from

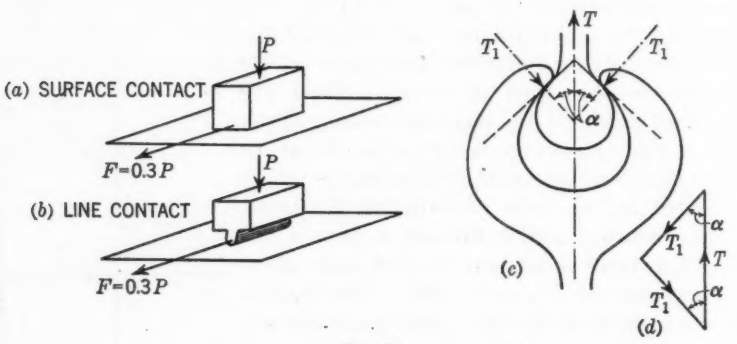

FIG. 35

0.15 to 0.20 and for metal on metal, wet, it is 0.30. To these values may be added the results of some tests performed by the writer who found that, for steel on smooth glass, dry, f equals from 0.20 to 0.22 and that, for steel on smooth glass, wet, f equals from 0.32 to 0.47 (16). In the walls of a cofferdam, the locks are wet or moist. Tests have shown that a trace of moisture is sufficient to produce the full "antilubricating" effect of water. Therefore, it seemed justified to assume $f = 0.3$.

Figs. 35(a) and 35(b) represent two different test arrangements for making a friction test. One involves a surface contact and the other what appears to the unaided eye as a line contact. Experience has shown that both test arrangements lead to the same result. Even if the two surfaces touch each other at what appears to be only a point, the result is no different. In other

words, the coefficient of friction, $f = F/P$, is independent of the area of contact. This is quite generally regarded as one of the fundamental laws of physics.

Fig. 35(c) illustrates the influence of the shape of the lock on lock friction. It represents a section through a fictitious lock. If T is the lock tension per foot of length, the pressure on the two contact lines combined is equal to $\frac{T}{\cos \alpha}$, and the lock friction is $F = \frac{0.3\ T}{\cos \alpha}$ per foot of length. For $\alpha = 45°$, $F = 0.42\ T$. If $\alpha = 0°$, the lock friction assumes the smallest value that can be obtained without the aid of a lubricant—that is, $0.3\ T$. There seems to be no fallacy involved. The computation of the lock friction for the Kentucky cofferdam was made on the basis of a coefficient of friction of 0.3. Considering the customary shape of the locks, the value of 0.3 seems to be conservative.

Colonel Pennoyer describes an arching phenomenon which he observed in 1932 on a cellular cofferdam of the diaphragm type, After the sand was washed out under the fill of the cell, the fill was found to arch over the cavity. This observation led Colonel Pennoyer to conclude that arching may quite generally lead to the formation of a "bottom," or of "bottoms," in the cell, and he discusses the mechanical implications of the phenomena. Since the writer has noticed similar phenomena in grain and coal bins, he was interested in the mechanical prerequisites for such arch formation. Therefore, in 1918, he made several experiments involving the pressure conditions in bins filled with sand (41). The bottom of the bin was mounted on a platform scale. The side pressure of the sand on the walls of the bin was measured by horizontal friction tapes installed at different depths below the top. The tests were made with both dense and loose sand. The bin was filled while the bottom was held in its original position; and, after the bin was filled, both side and bottom pressures were measured. The next step was to lower the bottom of the bin by increments and to observe the effect of this operation on the pressures. The test results are illustrated by Fig. 36. The abscissas of the curve C_1 represent the unit pressure on the side-walls at different depths below the top of the bin. The unit pressure increased steadily from the top down. As soon as the bottom of the bin was allowed to descend, the pressure on the bottom and on the lower part of the side-walls decreased, whereas the pressure on the upper part of the side-walls remained unchanged. Finally, the pressure distribution on the side-walls became that shown by curve C_2. At this stage a slight amount of cohesion would have sufficed to keep the sand in the bin without any bottom support. This was the action that occurred in the cofferdam cells inspected by Colonel Pennoyer. The yield of the bin bottom in the experiment was produced in nature by the escape of the sand which originally occupied the space beneath the fill. However, under normal conditions the base of the fill remains intact; and, as a consequence, the distribution of the pressure on the walls of the cells is shown in Fig. 36 by curve C_1 and not by curve C_2.

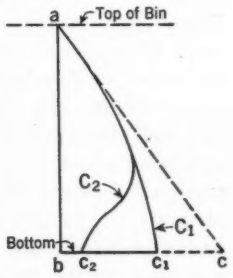

FIG. 36

Colonel Pennoyer remarks that he will continue to use the Rankine conversion factor until something better is available. Since the cells of a cellular cofferdam are essentially bins, the following data may be of interest. In 1920 the writer determined, by small-scale experiments, the ratio between the horizontal pressure in dense sand and the corresponding vertical pressure. In these tests the friction tape method was used and a value of 0.42 was obtained. The Rankine conversion factor for this sand was 0.22 (16). In 1929 direct measurement was made of the pressure exerted by loose sand on to the walls of a prismatic reinforced concrete container 7 ft high with a base 14 ft by 14 ft. The results of the observations furnished a value of 0.405 against a Rankine conversion factor of 0.31 (25) for the ratio between horizontal and vertical pressure. The lateral pressure exerted by completely submerged glacial till with an effective grain size of 0.019 mm was found equal to the sum of the full hydrostatic pressure of the water and the lateral pressure of the fill, computed on the basis of the submerged unit weight and a conversion factor of 0.38. The Rankine conversion factor for this material, computed on the basis of the results of friction tests, was 0.22 (42). These test results suggest that the value of 0.4 proposed by the writer may be much closer to the real ratio between the horizontal and the vertical pressure in sand enclosed in the cells of a cellular cofferdam than the Rankine conversion factor.

In discussing cofferdams on deep sand strata, Colonel Pennoyer refers to his own paper published in 1935 (29). Since this paper had escaped the writer's attention, he appreciated the reference and studied the paper with interest. The paper contains empirical values for the required sheet-pile penetration, together with other information. For water-bearing sand, the value is given as 30% to 40% of the unbalanced hydrostatic head. The writer has observed that the values in Colonel Pennoyer's paper are quite generally accepted in practice. However, he also noticed that blowouts are quite common, which induced him, about 1920, to make an inquiry into the causes.

The first step was to determine the hydraulic head required to produce a blowout under a straight row of sheet piles embedded in perfectly homogeneous sand. Both theory and experiment showed that the blowout does not occur until the hydraulic head approaches a value somewhat less than three times the depth of sheet-pile penetration. The grain-size characteristics of the sand are irrelevant (16); yet several instances have come to the writer's attention in which the sand began to boil on the inner side of single sheet-pile cofferdams at a head which ranged between $1\frac{1}{2}$ and $2\frac{1}{2}$ times the depth of sheet-pile penetration. Lazarus White, M. Am. Soc. C. E. (6), even describes a serious blowout in an open cut near the intersection between Canal Street and West Street in New York, N. Y. In this case the depth of sheet-pile penetration was equal to the full depth of the cut.

When several records of this nature were assembled, the reasons for the apparent incompatibility between test results and experience became quite plain. A blowout occurs as soon as the upward "drag" exerted by the water percolating through the sand along the inner face of the buried part of the sheet piles becomes equal to the submerged weight of the sand through which it percolates. The tests were made with perfectly homogeneous sand and the

theory was developed for similar materials. However, in nature, sand strata are never even approximately homogeneous. By theory it can be shown that the drag depends to a large extent on the variations of the permeability of the sand in both horizontal and vertical directions, other factors being equal. By properly changing the permeability pattern for a sand adjoining a row of sheet piles, one can regulate the critical head within very wide limits. Hence, in nature too, the hydraulic head required to produce a blowout at a given sheet-pile penetration may vary between wide limits, and the real value cannot be ascertained by any practicable procedure before the sheet piles are driven and an unbalanced head is established.

A second factor that needs to be considered is the effect the seepage pressure or upward "drag" has on the bearing capacity of the inner row of sheet piles and on the resistance of the sand against a lateral displacement of the buried, lower part of the piles. Colonel Pennoyer mentions an instance in which a single sheet pile, driven 25 ft into sand, sustained a load of 47 tons. The piles previously mentioned in connection with Mr. Greulich's discussion would probably have sustained a load of 80 or 100 tons each because they were driven into hard sand. However, while the water level within the cofferdam was being lowered 8 ft by pumping, the sand loosened its grip on the piles to such an extent that the piles floated out of the sand. Hence, when evaluating the bearing capacity of the sheet piles of the inner row, the reducing effect of the "drag" on the skin friction must be considered. The results of load tests can be very misleading.

The mechanical effects of the "drag" must also be considered in the computation of the passive resistance of the sand adjoining the inner face of the buried part of the inner row of sheet piles. Lowering the water level adjoining the inner face of the cofferdam reduces this resistance very considerably as illustrated by Fig. 37, representing two vertical sections through a single-wall

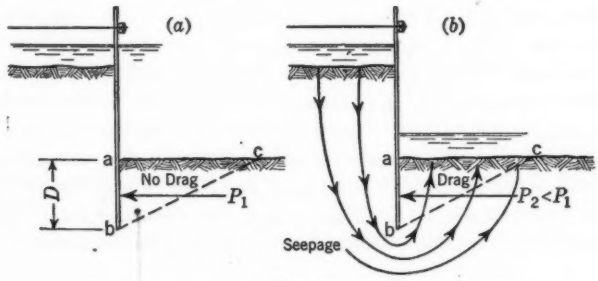

FIG. 37

cofferdam. In Fig. 37(*a*), the water level is at the same elevation on both sides of the sheet-pile enclosure. On this assumption, the passive resistance of the sand on the right-hand side of the buried part of the sheet piles can be computed by Rankine's equation:

$$P = \tfrac{1}{2} D \gamma' \tan^2 \left(45 + \frac{\phi}{2} \right) \ldots\ldots\ldots\ldots\ldots\ldots (61)$$

in which γ' is the submerged unit weight of the sand. If the water level within the cofferdam is lowered by pumping the water down to the level indicated in Fig. 37(*b*), the sand within the sliding wedge abc is acted upon not only by the simple hydrostatic uplift associated with submergence in still water but also by the seepage pressure or upward "drag" of the water which percolates through the wedge from below. This drag reduces the passive resistance of the sand considerably. The loss of resistance due to drag can be estimated by the flow-net method (17). In Colonel Pennoyer's computation of the passive resistance of the sand adjoining the inner face of a sheet-pile cofferdam (29), the drag has been disregarded. Therefore, the real passive resistance is smaller than the resistance indicated by Colonel Pennoyer's equations.

Considering all these facts and the inevitable uncertainties resulting from the unknown details of stratification of natural sand layers, the writer felt compelled to recommend a sheet-pile penetration of $2H/3$ instead of the customary $0.3H$ to $0.4H$.

In two places Colonel Pennoyer calls the reader's attention to various omissions in the writer's paragraphs on breakwaters. The design of cellular breakwaters has been treated so ably and comprehensibly in older publications that there was no incentive for discussing any aspect of this subject except the one that had not received any attention—the possibility of a base failure due to spontaneous liquefaction of underlying strata of loose sand. The writer's remarks on this subject were prompted by the spontaneous and complete subsidence of a breakwater on sand off the Atlantic coast of South America during a heavy storm. There are so many failures due to sponteneous liquefaction of masses of loose sand on record that this danger should not be ignored.

Mr. Tsagaris presents a brief review of the methods used in the design of the cellular cofferdams for the TVA. He points out that the possibility of a failure due to internal shear has received serious consideration, and comments on the writer's neglect of the tension contributed by the connecting arcs to the tension in the locks of the main cells. The reason for this omission will be given in the writer's comments on Mr. Hedman's discussion.

Mr. Colburn describes the Kentucky cofferdam, the highest cellular cofferdam which has ever been built. His account of the drainage provision on this and some of the other TVA cofferdams deserves special attention. An attempt to measure the tension in the sheet-pile enclosure of two of the cells of the Chickamauga cofferdam by strain gages was unsuccessful. The observations disclosed a very erratic distribution of the tensile stresses over the sheet piles.

More reliable information on the pressure acting on the walls of the cells can be obtained by pressure cells inserted into some of the sheet piles as shown in Fig. 38(*a*). A box composed of two channels is welded to a pile. The cells are $\frac{3}{8}$ in. thick and have a diameter of about 7 in. They fit into circular holes in the sheet piles and are seated on the outside of the web of the inner channel. The strain gage chambers project into the box and the cables are also installed in the box. The minimum requirement for obtaining fairly consistent results is the equipment of three sheet piles with five cells each.

These piles should be placed at the three-quarter points of the main arc on the inside of the cofferdam at the junction of the cofferdam with the connecting arcs.

Sheet piles to which cells are attached should not be driven because the impact of the hammer is likely to injure the cells. In order to incorporate a cell pile (unit B in Fig. 38(*b*)) into the sheet-pile enclosure of a cell, the pile is

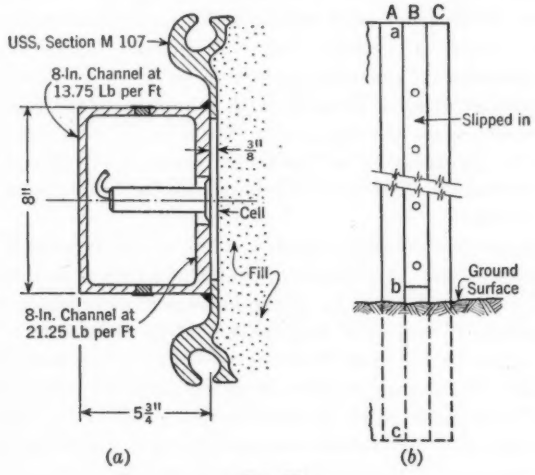

FIG. 38

made of two pieces. First the lower part bc is driven to the required depth by means of a follower; then the next pile (unit C) is driven to full depth; the upper part of unit B is pulled; and finally the section containing the cells is slipped into place.

The cells register the sum of the earth and the water pressure which acts on the face of the cell. The water pressure alone is measured independently. If the fill consists of sand, reliable values can be obtained by means of observation wells with a small diameter.

Deflection observations on the Kentucky cofferdam showed that one of the cells deflected slightly outward with a rising river. This observation calls attention to the fact that the movement of every dam due to a change of the unbalanced head is equal to the difference between two movements in opposite directions. If the head increases, all the cells tilt inward with reference to their base on account of the increase in the overturning moment. At the same time, the base tilts outward due to the increase of the water load on the area outside the cofferdam. If the water is retained by a flexible cofferdam on a relatively unyielding foundation, the inward tilt prevails. On the other hand, a fairly rigid cofferdam on a yielding base must be expected to tilt outward. For similar reasons, the rise of the water level behind a relatively rigid storage dam on a less rigid foundation causes a tilt in an upstream direction. Such an upstream tilt was expected, and subsequently observed, on a concrete dam resting on a thick stratum of clay in northeastern Russia (43).

Before construction began, it was computed that filling the reservoir would cause a 0.75% tilt of the dam and powerhouse in an upstream direction. Since the turbine shafts had to be installed before the reservoir was filled, they were mounted with a 0.75% tilt toward the downstream side. While the reservoir was being filled for the first time, the shafts moved into an almost vertical position.

The Kentucky cofferdam rested on a limestone base. Hence, the outward tilt due to a rise of the river level undoubtedly was very small compared with the inward tilt of most of the cells; yet it might have been important enough to produce a measurable outward deflection of those cells which, for some reason, retained their original position with reference to the base.

Mr. Colburn expresses the opinion that the reactive pressure of the fill in the cells prevents a relaxation of the lock tension even though the bursting pressure may decrease. There is no doubt in the writer's mind that this assumption is justified.

Mr. Hedman gives a detailed account of the methods used in the design of the Kentucky cofferdam. He remarks that the writer's statement regarding the effect of seepage on the tension in the locks is contradictory to subsequent statements regarding the effect of seepage on sliding resistance. The apparent contradiction is due to the fact that the writer's first statement was inadequately qualified. Furthermore, Mr. Hedman does not agree "that the unit weight of the fill in a moist state should be used in Eq. 3." This objection is justified. The effect of the air content on the unit weight of a drained soil can be disregarded only if the effective grain size is equal to, or smaller than, about 0.05 mm.

Mr. Hedman presents a résumé of the procedure for determining the lock stresses:

> "This stress was found to be equal to 9,500 lb [per lin in.]—more than 50% higher than would have been the case if the author's suggested empirical formula, Eq. 28*f*, had been used."

The major part of the difference is due to the fact that the TVA computation was based on the assumption of complete saturation of the fill in the cells, whereas the writer's equation presupposes fairly complete drainage. The fill in the cells of most or of all the TVA cofferdams was deposited by the hydraulic method during a low-water stage. On this condition, Eq. 28*f* should be modified in such a way as to comply with the state of full saturation. The modified equation furnishes, for the interlock stress in the main cells, a value of about 8,120 lb per lin in. against the value of 7,280 lb per lin in. given by Mr. Hedman.

To the value of 7,280 lb per lin in. was added 2,220 lb per lin in. for the tension contributed by the connecting areas. This supplementary force was computed on the assumption that the sand pressure on the connecting arcs increased like a hydrostatic pressure in direct proportion to depth. However, considering the slenderness ratio of the columns of sand adjoining the connecting arches, the bin effect must be very important. In 1918 when the writer made his bin tests, he tried to destroy the bin effect by various means, such as pounding the sides of the container, but he did not succeed. He also

poured the sand into water and afterward drained it through the perforated bottom of the bin; yet the bin effect persisted. Hence, it can be counted upon. If the bin action is taken into account, the contribution of the connecting arches to the tension in the main cells will probably be found to be rather unimportant and well within the range of error associated with the estimate of the bursting pressure exerted by the sand in the main cells. There is no doubt, however, that the junction between the main cells and the connecting arches is a delicate detail, and the attention which is received in the TVA design was fully justified.

Commenting on the effect of a berm on the lock tension in the cross-walls, Mr. Hedman points out correctly that the writer's statements concerning this effect require qualification. These statements are not valid unless the cells are filled while the water level in the river is fairly close to its highest position. The influence of the river stage when the cells are filled is strikingly demonstrated by the difference between the deflections of the Kentucky cofferdam which was filled at low water and those of the cofferdams on the west shore of the Hudson River in New York City which were filled while the water level was close to the high-water mark.

Considered as a whole, the procedure for designing the Kentucky cofferdam, as described by Mr. Hedman, is an outstanding example of sound engineering. This procedure discloses a thorough grasp of all the theoretical principles involved combined with mature judgment, and it deserves the attention of every engineer who faces the problem of designing a cellular cofferdam.

Mr. Ackerman presents a significant résumé of the practical considerations that enter into the selection of the type of cellular cofferdams under given conditions of foundation and exposure. Attention is called to his remarks on the benefits derived from the use of portable templates. The writer agrees with Mr. Ackerman that it might be preferable to refer to the cellular cofferdams as plastic and not as composite structures because the reactions of these cofferdams to external forces are decidedly those of plastic materials.

For comparison, Mr. Packshaw discusses the conditions required for the stability of double-wall sheet-pile cofferdams. The stability computation which he presents conveys a clear conception of the factors that determine the stability of these structures. Since, even in the United States, the double-wall type of cofferdam is far more frequently used than the cellular type, his contribution will be welcomed by many readers.

Mr. Lautz assumes that the excess of the normal pressure over the Rankine pressure on the vertical shear plane or planes is chiefly due to the horizontal load imposed upon the outside of the cofferdam. The bin tests which were described in the writer's comments on Colonel Pennoyer's discussion suggest that this excess is chiefly due to the fact that the fill is deposited within a laterally confined space. According to the results of bin tests, the normal pressure on every vertical section through the cells is much greater than the active Rankine pressure even before horizontal forces have been applied.

Example 1 in Mr. Lautz's discussion illustrates the application of the cellular cofferdam method to the construction of a dock-wall. The cells of this wall contain soft silt and clay in an undisturbed state. In this state

clays and silty clays possess a remarkable degree of rigidity although their water content may be very high. Quite recently the writer examined a stratum of clay with a liquid limit of about 40% of the dry weight. The water content of the clay in its natural state was about 60%. Nevertheless, the clay contained hair cracks and was decidedly brittle. By kneading, it was transformed into a thick, viscous liquid. The rigidity of undisturbed clay, combined with an increase of the lock friction in the cross-walls and the low intensity of the unbalanced horizontal forces, accounts for the absence of noticeable deflections. The cells of the cofferdam for the intake system in Detroit, Mich. (Example 3), also chiefly contained soft clay in an undisturbed state. However, in contrast to the dock-wall, the cofferdam was acted upon by clay and water pressure combined. Hence, in spite of its ample dimensions, it required supplementary support.

Mr. Miller's discussion ranks among the most noteworthy contributions to this subject because it is based on extensive and varied experience in the design and construction of cellular cofferdams. Mr. Miller takes exception to the writer's statement concerning the influence of the outer row of sheet piles on the percolation of water through cells filled with clay or other soils with a low permeability. This influence has been the topic of several good-natured verbal controversies between Mr. Miller and the writer with the result that both parties remained utterly unconverted. The writer's arguments in favor of his thesis appear in "Part I. Practical Considerations" under the heading, "Permeability of Cellular Cofferdams and of Their Sheet-Pile Enclosures." Mr. Miller's confidence in the efficacy of weep holes is somewhat at variance with the results of the observations of the TVA engineers described in the discussions of Messrs. Tsagaris, Colburn, and Hedman.

Professor Legget comments on the writer's mildly skeptical remarks regarding the practical value of laboratory tests in connection with the design of cellular cofferdams. The principal benefit to be derived from these tests is that they give the engineer a firsthand knowledge of the character and the properties of the materials involved in the design. The benefits derived from such knowledge are important enough to justify a considerable amount of testing.

In the course of his discussion, Professor Legget requests an amplification of the writer's comparison of cellular cofferdams with structures made of composite materials. When making this comparison, the writer merely wished to emphasize that the distribution of the external forces acting on the two constituents of the dam—the steel and the soil—is governed by the stress-deformation characteristics of the two materials involved. The analogy cannot be extended further.

Commenting on lock friction, Professor Legget presents a list of all those variables which are likely to influence the friction value, and he raises the question as to whether or not reliable values could be obtained by experimental methods. In the writer's opinion, the lock friction can be resolved into two parts. One part is determined by the coefficient of friction of metal on metal and by the orientation of the surfaces of contact with reference to the direction of the pull. It has been referred to as the basic part of the friction. The

second part is caused by the effect of one of several of the factors enumerated by Professor Legget. All these factors tend to increase the lock friction to some extent. Hence, the basic value determines the lower limit for the lock friction. The writer estimated that the basic value for the coefficient of lock friction is $\frac{0.3}{\cos \alpha}$ (see Fig. 35(*c*)). The data and considerations which led to this value are treated previously in the writer's comments on Colonel Pennoyer's discussion.

A more accurate basic value could be obtained by friction tests with specimens cut out of new steel sheet piles. Some information on the difference between the real and the basic values of the lock friction for the buried part of sheet-pile enclosures could be obtained by friction tests on specimens cut from sheet piles after they have been pulled. To preserve the state of contamination of the lock with soil particles, two sheet piles should be clamped together securely and pulled in a single operation. When cutting the test specimen from the pair, special precautions should be taken to prevent a slippage in the locks prior to the test.

Professor Legget also raises the question as to how much reliance can be placed on the lock friction in straight rows of sheet piles composed of deep arch sheet piling. In such rows, the tension in the locks is at least theoretically equal to zero. Hence, the basic value for the lock friction is also equal to zero and the resistance against slippage in the locks is entirely due to those factors which produce lock friction in excess of the basic value in the driven part of the sheet-pile enclosures of cellular cofferdams. Nevertheless, in Germany the manufacturers of deep arch sheet piling with locks in the neutral plane claimed that the weakening effects of the lock can be disregarded, and the moments of resistance contained in their catalogs were computed on the assumption that the locks do not exist. In design practice, it was customary to distinguish between the sheet piles driven into sand and those driven into clay. For sheet piles in sand, it was considered safe to ignore the presence of the locks, whereas the moment of resistance of sheet piles in clay was reduced by one third of the value obtained for jointless piling. The writer has never had much confidence in this procedure; yet it is conceivable that the mere process of driving sheet piles into the soil may create various sources of considerable friction. Hence, if in those parts of the steel skin of a cellular cofferdam which is located below the original ground surface or dredging line, the real lock friction may be greater than the basic value.

Professor Krynine furnishes convincing proof that shear failure on vertical planes is inevitably preceded by, and associated with, a considerable increase of the normal pressure on these planes. At the instant of failure the normal pressure is much higher than the value computed on the basis of the Rankine conversion factor $\tan^2\left(45 - \frac{\phi}{2}\right)$. This is a noteworthy contribution to the clarification of the theoretical issues involved in the cofferdam problem. The Mohr diagram which is used to support the argument serves its purpose to perfection.

Professor Krynine also calls attention to the possibility of a failure along shear planes other than vertical ones. However, the writer doubts whether

these other planes can possibly be oriented as indicated in Fig. 26(*c*). A failure along such planes requires that the major principal stress be oriented as indicated in Fig. 26(*b*) and in Fig. 39(*a*). Such orientation of the major principal stress would be associated with a distortion of the body abcd in Fig. 39(*a*) into the shape a_1b_1cd. A deformation of this kind involves an outward tilt which is incompatible with the nature of the problem. To

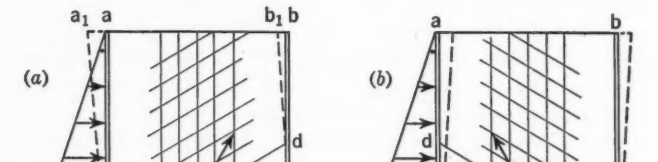

FIG. 39

account for the inward tilt of the cells, it is necessary to assign the orientation indicated in Fig. 39(*b*) to the shear planes. One set of shear planes is vertical whereas the other slopes at an angle ϕ toward the inside of the cells. Failure occurs simultaneously on the vertical and the inclined planes. Hence, for estimating purposes, it seems justifiable to evaluate the factor of safety with respect to failure by internal shear on the basis of the stress conditions on vertical planes.

Mr. Polivka describes the small-scale model tests made preliminary to the design of a cellular cofferdam in the Kaiser Shipyards at Richmond, Calif. The model cells were no more than 6 in. high. They consisted of cylinders made of plain sheet metal, 0.004 in. thick, filled with very fine sand. The results of tests on such cells cannot be correlated with the author's theory of internal shear, because the walls were incapable of distortion comparable to that in cells with walls containing locks. This difference is crucial.

In his mathematical interpretation of the test results on the basis of the general bin theory, Mr. Polivka assigned a value of 26° 30′ to the angle of internal friction ϕ of the sand and a value of $K = 1$ to the ratio between the horizontal and the vertical pressure in the sand. The value of ϕ appears to be rather low. Reliable values can be obtained only by an appropriate shear box apparatus or a triaxial compression device. The smallest value that was ever obtained by either one of these devices ranges from 27° to 28° 30′ (44)(45). The tests were made on Ottawa standard sand—a very uniform sand consisting of almost perfectly spherical quartz grains with a smooth surface. The normal values for loose sand range between 32° and 34°. The value $K = 1$ was derived from trap-door experiments and is not applicable to the case under

consideration. The experimental values obtained from bin tests are mentioned previously in the writer's comments on Colonel Pennoyer's discussion. They are approximately equal to 0.4.

To establish an equation for the resistance of the model cells against shear along vertical sections, Mr. Polivka introduced a value of $f = 1$ into Eq. 17. This does not seem permissible, because the equation thus obtained applies to walls with locks, if the coefficient of lock friction is equal to unity. If the walls are continuous (such as is the case for model cells), Eq. 17 cannot be used.

In the last part of his discussion Mr. Polivka describes the practical implications of making the walls of cellular cofferdams of arch-web sheet piles such as the Carnegie M112 and M113 sheet piles and their equivalents. In cofferdams local stressing of the steel beyond the yield point can scarcely be considered a failure. However, the excessive increase of the diameter of the cells which results from the low value of the "equivalent modulus of elasticity," E, of arch-web sheet piles is a very undesirable feature. Since it involves an important lateral stretching of the fill in the cells, it is associated with an equally important decrease of the horizontal pressure in the fill, which in turn reduces the lock friction in the cross-walls and the resistance of the fill against deformation. Hence, the writer agrees with Mr. Polivka that the straight-web sections are preferable.

Bibliography.—

(6) **"Cofferdams,"** by Lazarus White and Edmund A. Prentis, Columbia Univ. Press, New York, N. Y., 1940.

(10) **"Gravity Bulkheads and Cellular Cofferdams,"** by Raymond P. Pennoyer, *Civil Engineering*, Vol. 4, 1934, pp. 301–305. (*a*) Eq. 13, p. 303. (*b*) p. 305. (*c*) Eq. 12, p. 303. (*d*) Fig. 4, p. 304. (*e*) Fig. 1, p. 301.

(16) **"Erdbaumechanik auf bodenphysikalischer Grundlage,"** by K. Terzaghi, F. Deuticke, Vienna and Leipzig, 1925, pp. 128–131.

(17) **"Theoretical Soil Mechanics,"** by Karl Terzaghi, John Wiley & Sons, Inc., New York, N. Y., 1943. (*a*) p. 66.

(25) **"Large Retaining-Wall Tests: I—Pressure of Dry Sand,"** by Karl Terzaghi, *Engineering News-Record*, Vol. 112, 1934, pp. 136–140.

(29) **"Design of Steel Sheet-Piling Cofferdams,"** by Raymond P. Pennoyer and George Hockensmith, *Civil Engineering*, Vol. 5, 1935, p. 19.

(37) **"Shipyard Uses Basins Instead of Ways,"** *Engineering News-Record*, Vol. 129, No. 9, August 27, 1942, p. 57.

(38) **"Stress Distribution in Dry and Saturated Sand Above a Yielding Trap-Door,"** by K. Terzaghi, *Proceedings*, International Conference on Soil Mechanics, Cambridge, Mass., Vol. 1, 1936, pp. 307–311.

(39) **"Theory of Plates and Shells,"** by S. Timoshenko, *Engineering Societies Monographs*, McGraw-Hill Book Co., Inc., New York, N. Y., 1940, p. 410.

(40) **"Smithsonian Miscellaneous Collections,"** Smithsonian Institution, 8th Revised Ed., Washington, D. C. Vol. 88, 1933, p. 204.

(41) **"Die Erddruckerscheinungen,"** by K. Terzaghi, Österreichische Wochenschrift für öffentlichen Baudienst, 1919.

(42) **"Large Retaining Wall Tests: V—Pressure of Glacial Till,"** by Karl Terzaghi, *Engineering News-Record*, Vol. 112, 1934, p. 503.

(43) **"Some Features in Connection With the Foundation of Svir III Hydro-Electric Power Development,"** by H. Graftio, *Proceedings*, International Conference on Soil Mechanics and Foundation Eng., Cambridge, Mass., Vol. I, 1936, pp. 284–290.

(44) **"Shearing Properties of Ottawa Standard Sand,"** by D. W. Taylor, *Proceedings*, Conference on Soils and Foundations, Corps of Engrs., U. S. Army, Boston, Mass., 1938.

(45) **"Stress-Deformation Characteristics of Cohesionless Soils from Triaxial Compression Tests,"** by J. D. Watson, thesis submitted to Harvard Univ., Cambridge, Mass., in 1940, in partial fulfilment of the requirements for the degree of Doctor of Engineering.